A DETAILED STUDY OF THE SCALE INHIBITOR PHASE ENVELOPE OF PPCA IN THE CONTEXT OF PRECIPITATION SQUEEZE TREATMENTS

By

Nazia Mubeen Farooqui

Thesis Submitted for the degree of

Doctor of Philosophy in Petroleum Engineering

School of

Energy, Geoscience, Infrastructure & Society

Heriot-Watt University

Edinburgh, Scotland, UK

May 2015

ABSTRACT

Scale formation in the oilfield is considered to be one of the major problems associated with oil and gas production. This mineral scaling problem relates directly to the water produced in hydrocarbon production and the worldwide industry produces more than 10 times the volume of water than oil. Barium sulphate and calcium carbonate scales are the most common mineral scales found in oilfield operations. The formation of these scales may result in the blockage of tubulars or safety valves, the failure of ESPs (electrical submersible pumps) and in the blockage of rock pores (in the near wellbore formation), which will greatly reduce the well production. The most effective way to prevent the scale formation is to treat the near wellbore region of the producer wells with chemical scale inhibitors (SI). Chemical scale inhibitors are widely applied in the oil industry to prevent downhole scale formation in so-called squeeze treatments. A successful squeeze treatment can be defined by two attributes; one it must prevent scale crystal growth at sub-stoichiometric concentrations between 2–20 ppm and it must interact with the formation in such a way to give low concentration returns to provide longer squeeze lifetime, typically in the range of 3-12 months. Scale inhibitors are generally either phosphonate species or they are polymeric and both of these SIs can be applied as adsorption or precipitation squeeze treatments, depending on the mechanism of SI retention in the formation.

Phosphino Poly-Carboxylic Acid (PPCA) is a well-known industry standard polymeric scale inhibitor which is often applied in precipitation squeeze treatments. In these, the PPCA forms a sparingly soluble complex with calcium ions, denoted PPCA_Ca. The research on PPCA precipitation processes described in this thesis aims to fully develop its potential to provide reliable and long-lived squeeze lifetimes. The objectives of this research are as follows:

1. To develop the full understanding of the Phase Envelop of PPCA.
2. To define the important role of the molecular weight (MW) and molecular weight distribution (MWD) of PPCA in the return curve in precipitation squeeze treatments.
3. To understand the dynamics of PPCA precipitation treatments in sand-pack floods carried out over a range of flow rates.

4. The development of a retention model based on the MWD of the precipitate/supernatant/stock for polymeric scale inhibitors.

Static and dynamic lab tests were carried out at realistic reservoir conditions in order to understand the phase behaviour of PPCA, the solubility of the precipitated PPCA_Ca complex and why/how the precipitated polymeric species performed better than the stock. All of the parameters governing the phase behavior have been studied and reviewed as they relate to the MWD of PPCA in precipitation or phase separation squeeze treatments. These processes rely upon the interaction of the inhibitors with metal cations such as calcium (Ca^{2+}), pH and temperature.

The non-equilibrium dynamic sand-pack floods suggest that the reduced flow rate leads to higher effluent concentrations and vice-versa. The static and dynamic results from this work will be used to develop improved models of coupled adsorption/precipitation and inhibition efficiency (IE) for polymeric scale inhibitors. These models will be incorporated into future field squeeze design models for adsorption/precipitation (Γ/Π) processes using polymeric scale inhibitors such as PPCA. It is believed that these results are the most detailed to be published in the literature on the PPCA system applied as a precipitation processes and that they are of particular significance and application for all polymeric scale inhibitor precipitation squeeze treatments.

DEDICATION

This thesis is dedicated to my Parents, and my Abbu.

ACKNOWLEDGEMENT

There are a number of people without whom this thesis might not have been written, and to whom I am greatly indebted.

First and foremost, I offer my gratitude and appreciation to my supervisor Prof. Ken Sorbie who has given me chance and showed his trust on to me that I will survive through this journey. He has lovingly challenged and supported me throughout the whole of this work - knowing when to push and when to let up. I am fortunate to have been able to work with him. His kindly but rigorous oversight of this thesis constantly gave me the motivation to perform to my maximum ability. Thank you very much Ken.

I offer special thanks to those who supported me in the mechanics of producing this thesis. Lorraine, for lab training and also helped me to get 'unstuck' with this research on many occasions, Heather for all the admin assistance, team Tom-Tom for building sand-pack rig and bringing joy to labs, Wendy for ICP analysis, Will for sand-pack training, Ivan and Oscar for interesting talks. I would like to thanks my former Ph.D. colleagues Mohammed Murtala, Scott, Jamal and Cyril for being the best moral supporter in the office during the first year of my PhD. I would like to place special thanks to Eric for his time, encouragement, guidance and expertise throughout this project; and Mike's critics are always helpful to see the way forward. Finally, I would like to thank all the members of the Flow Assurance & Scale Team (FAST) for making my stay at Heriot-Watt, memorable, for my lifetime.

I would like to express my sincere thanks to Dr. Myles Jordan, who provided insight and expertise that greatly assisted my research.

I am very thankful to Prof. Russell Howe from the University of Aberdeen and Prof. Sebastian Geiger from Institute of Petroleum Engineering of Heriot-Watt University, for agreeing to examine this thesis. Their time invested in reading and evaluation of this thesis was invaluable.

Special thanks to the sponsors of FAST 4/5 project, for their exquisite attention to detail and for their demands for high excellence. I would like to extend my appreciation to the Warwick University, UK for doing GPC analysis on my samples and Federal University of Rio de Janeiro, Brazil for the collaboration of knowledge exchange program.

There are people in everyone's lives who make success both possible and rewarding. My husband, my friend, Asad Nazir, 'rescued' me at those times when I was almost defeated by the technology. I am tremendously appreciative of the support you gave me; in willingly accompanying me on a journey of exploration that we knew would be immensely challenging and painful in parts. I will never forget our long rides and the long walks, when it is needed most; thanks for being there always on my side and reminding those words "no one said it was going to be easy".

I would like to thank especially my mother Shaheen Zafar, and father Mohammad Mubeen Farooqui for their love and unconditional support throughout my life. Thanks to both of you for believing in me and making me tough, responsible and confident, for giving me strength to reach for the stars and chase my dream.

When I have started this journey, there is one special person who stands at my back on which I can blindly lean upon. Yes my brother, Amir Farooqui. My special thanks go to him, for providing encouragement at those tough times when it seems impossible to continue and push me hard enough to go through it.

I would like to have a special word of thanks to my sister Rubeena Aslam, who is being the best entertainer, the best mentor and my best friend throughout my life who has been listened to me tirelessly irrespective of the time zone difference and offered encouragement when it was most needed.

I am thankful to my sister-in-law, Naziya Amir, who is being very supportive, and encouraging through my ups and downs during this journey. I hope to return the favour when she writes her own doctorate thesis. Ayesha, my niece, being my best mate in the evenings, when I came home tired, the way she greets me puts all my worries away. Mostly I have forgotten about how hard my day was. My sincere thanks offered to my brother-in-law Mohammad Aslam, my niece Alisha Aslam and nephew Abdul Mohi, who contributed all the cheerful moments, to bring the smile out of me.

I would like to place a special thanks to my extended Pakistani family and my Abbu, for their love and support to this wonderful journey. I would like to convey my gratitude, to all my school friends, Edinburgh family, college mates and my well-wishers helped me, cajoled, and prodded me when I needed it the most. Sheema madam, my special thanks goes to her for all her prayers for me. Thanks to all my uncles and aunties and my cousins for the encouragement during this process and over the years.

Finally, I would like to thanks to myself for being stubborn to make it happen. I am privileged to be a part of such an exciting path and witnessed that the journey was beautiful. This makes me what I am today, and I am honoured for this.

Above all thanks to God, the Divine who continues to make the impossible possible.

ACADEMIC REGISTRY
Research Thesis Submission

Name*:*	Nazia Mubeen Farooqui		
School/PGI:	School of Energy, Geoscience, Infrastructure & Society		
Version: *(i.e. First, Resubmission, Final)*	Final	Degree Sought (Award **and** Subject area)	Thesis Submitted for the degree of Doctor of Philosophy in Petroleum Engineering

Declaration

In accordance with the appropriate regulations I hereby submit my thesis and I declare that:

1) the thesis embodies the results of my own work and has been composed by myself
2) where appropriate, I have made acknowledgement of the work of others and have made reference to work carried out in collaboration with other persons
3) the thesis is the correct version of the thesis for submission and is the same version as any electronic versions submitted*.
4) my thesis for the award referred to, deposited in the Heriot-Watt University Library, should be made available for loan or photocopying and be available via the Institutional Repository, subject to such conditions as the Librarian may require
5) I understand that as a student of the University I am required to abide by the Regulations of the University and to conform to its discipline.

* *Please note that it is the responsibility of the candidate to ensure that the correct version of the thesis is submitted.*

Signature of Candidate*:*		Date:	

Submission

Submitted By *(name in capitals):*	Nazia Mubeen Farooqui
Signature of Individual Submitting:	
Date Submitted:	

For Completion in the Student Service Centre (SSC)

Received in the SSC by *(name in capitals):*			
Method of Submission (Handed in to SSC; posted through internal/external mail):			
E-thesis Submitted (mandatory for final theses)			
Signature:		Date:	

List of Contents

List of Figures

List of Tables

List of Publications

1. Phase Behaviour of Polyphosphino Carboxylic Acid (PPCA) Scale Inhibitor for Application in Precipitation Squeeze Treatments Chemistry in the Oil Industry XlII: Oilfield Chemistry –New Frontiers RSC Conference, Manchester, UK, 4-6 Nov 2013

2. Polyphosphino Carboxylic Acid (PPCA) Scale Inhibitor for Application in Precipitation Squeeze Treatments: The Effect of Molecular Weight Distribution- NACE Corrosion Conference and Expo, San Antonio, TX, 9-13 Mar 2014

3. Oilfield Scale Inhibitors for Application in Precipitation Squeeze Treatments: Solubility of the Ca_PPCA Complex - SPE 169792, SPE Aberdeen Conference, 14-15 May 2014

4. Polymeric Scale Inhibitor for the Application of Precipitation Squeeze Treatment: The Molecular Weight Distribution Effect on the Inhibition Efficiency Performance- Rio Oil and Gas Expo and Conference, Rio de Janeiro, Brazil, 14-18 Sep 2014

5. Study of Ca_PPCA complex of the Polymeric Scale Inhibitor for Precipitation Squeeze Treatment- Oil Field Chemistry Symposium 2015, Geilo Norway, 22-25 March 2015

6. The Effect of Molecular Weight Distribution on the Inhibition Efficiency Performance of Polymeric Scale Inhibitors during Retention- NACE Corrosion 2015 Conference and Expo, Dallas, TX, 15-19 Mar 2015

7. Molecular Weight Effects in Polymeric Scale Inhibitor Precipitation Squeeze Treatments", SPE European Formation Damage Conference, Budapest Hungary, 3-5 June 2015

8. The use of PPCA in Scale Inhibitor Precipitation Squeezes: Solubility, Inhibition Efficiency and Molecular Weight Effects- J. SPE Production and Operations (in press)

9. The Solubility and Dissolution of PPCA_Ca complex in Precipitation Squeeze Processes- SPE Scale Conference, Aberdeen, 11-12 May 2016 (to be published)

Nomenclature

(r_n)	Rate of Dissolution
[Ca^{2+}]	Calcium Concentration
[SI]	Scale Inhibitor Concentration (ppm active)
AMPS	2-acrylamido-2-methypropane sulphonic acid
B/D	Barrels per day
Cs	Solubility of the inhibitor calcium complex
DETPMP	Diethylene-triamine-pentakis (methylene phosphonic Acid) - Penta Phosphonate
DW	Distilled Water
EABMPA	Ethanolaminebis (methylene phosphonic acid) – Di – Phosphonate
EDTMPA	Ethylene-diamine-tetra (methylene phosphonic acid) – Tetra-Phosphonate
ESEM	Environmental Scanning Electron Microscopy
FW	Formation Water
HEDP	1-Hydroxyethylidene-1,1-di-phosphonic acid –Di-phosphonate
HMDP	Hexamethylene-diamine-tetrakis (methylene phosphonic acid) - Tetra Phosphonate
HMTPMP	Bis-hexamethylene-triamine-pentakis (methylene phosphonic acid) - Penta Phosphonate
HPAA	2-HydroxyPhosphono Acetic Acid
HSB-SW	High Salinity Brine – Sea Water
ICP	Inductive Coupled Plasma Spectroscopy
IE	Inhibition Efficiency
M/L	Moles per Litre
m/V	Mass to Volume
MAT	Maleic acid ter-polymer (a green SI)
MeOH	Methanol
MIC	Minimum Inhibition Efficiency
M_n	Average Number Molecular Weight
M_w	Average Molecular Weight
MWD	Molecular Weight Distribution
MW	Molecular Weight
NFFW	Nelson Forties Formation Water

NSSW	North Sea Sea Water
NTP	Nitrilotris (methylene phosphonic acid) – Tri – Phosphonate
OMTHP	Octamethylene-tetraamine-hexakis (methylene phosphonic acid) – Hexa Phosphonate
PAA	Poly Acrylic Acid
PBTC	2-phosphonobutane-1,2,4- tricarboxylic acid
PF	Post Flush
PFC	Phosphorus Functionalized Copolymer
pH	$-Log_{10}[H^+]$ ($[H^+]$ in moles/L)
pKa	$-Log_{10}$ Ka
PMAA	Poly Meta Acrylic Acid
PMPA	Phosphino-methylated-polyamine acid- Poly Phosphonate
PPCA	Phosphino Polycarboxylic Acid
ppm	Parts per million (mg/L)
PTFE	PolyTetra Fluoro Ethylene (Teflon)
PV	Pore Volume
PVS	Poly Vinyl Sulphonate
RT	Room Temperature
SFSW	Sulphate Free Sea Water
SI	Scale Inhibitor
SI_Ca	Scale Inhibitor _Calcium complex
SI_PPCA	Scale Inhibitor_Phosphino polycarboxilic Acid
SP	Sand-Pack
SPPCA	Sulphonated Phosphino Polycarboxylic Acid
SW	Sea Water
T	Temperature (^OC)
TDS	Total Dissolved Solid
UV	Ultra Violet Spectroscopy
VS-Co	Vinylsulphonate Acrylic Acid Co-polymer

Terminology

Phase Line or Phase Boundary	A line on the Phase Envelope which defines where the 2 phases appear
Phase Envelope	The Phase Envelope shows a graphical representation of fluid phase behaviour in terms of a temperature, pH, [SI] and [Ca^{2+}]

CHAPTER 1- **INTRODUCTION**

1.1 The problem of Oilfield Scale

The formation of the mineral scale in oilfield production systems is one of the major problems in the oil industry (Vetter, 1976; Weintritt, 1967; Charleston, 1970). These mineral scales found in oil fields form by either direct precipitation from naturally occurring waters from the reservoir (e.g. calcite, $CaCO_3$) or as a consequence of the produced water becoming supersaturated with scaling ions when two incompatible brines comingle downhole (e.g. barite, $BaSO_4$). Whenever an oil or gas well produces natural waters, there is the likelihood of mineral scale forming (Crabtree et al, 1999). The most common scales encountered in North Sea offshore operations are the carbonate and sulphate salts of calcium, barium and strontium. These scales or salts are then free to precipitate and may result in greatly reduced well performance as rock pores, tubular, casing, perforations, pumps, valves and topside machinery become choked by a build-up of insoluble inorganic precipitate. The formation of the scales at different places subsequently reduces the recovery of oil from the reservoir. This can be dramatic and immediate and the cost to the operator can be enormous. For example, in one of the wells in the Miller field in the North Sea, the engineers observed production fall from 30,000 B/D [4770 m^3/d] to almost zero in just 24 hours (Brown, 1998).

Over the past few years, a variety of techniques like chemical treatments, mechanical intervention, the application of electrical and magnetic fields etc., have been used to try to prevent the formation of oilfield scale. However, to date, the methods considered to be the most effective for controlling oilfield scale are chemical and mechanical methods and these are commonly used in the oil industry. Overall, the preference in the industry has been to use chemical scale control rather than mechanical since it is a preventative measure, and in general, it is cheaper and more convenient to apply in offshore and deep water fields.

The scales formed are mostly inorganic solids which have low solubilities. The three important techniques which are used to remove these scales once formed are removal using acids, scale dissolver or sequestrants. Acidizing is one of the widely applied approaches used to treat calcium carbonate scales but this method is insufficient to remove insoluble barium sulphate scales (Bonnett et al., 1991; Smith et al., 1968;

Vetter, 1975; Vetter et al., 1987; Vetter and Kandarpa, 1979). Scale dissolution is another chemical technique, in which EDTA is commonly applied as a scale dissolver sequestrant chemical. Although, this method enhanced productivity of oil in a few cases (Charleston, 1968; Shaughnessy and Kline, 1983), in most cases the rate of dissolution of the scale is very slow (Carrell, 1987; Mazzolini et al, 1990; Vetter, 1972; 1986). The most effective preventative measure in dealing with most mineral scale problems is to use chemical scale inhibitor which prevents or retards the formation of the mineral scale crystals by slowing the nucleation and/or crystal growth stages of scale formation.

The most effective method to use the chemical inhibitor for the protection of surface equipment, topsides and also downhole is known as a squeeze treatment. This chemical treatment, if successful, will protect the well from deposition in the tubing and from formation damage. In a squeeze treatment, a scale inhibitor slug is injected or squeezed into the near-well rock formation. Once the chemical has been placed in the rock formation it is over-flushed by a volume of injection fluid and the well is then shut-in for a period of hours to allow the inhibitor to interact with the formation either through adsorption or precipitation, in the rock matrix. When the well is put back onto production, produced water will pass through the pores, where the chemical inhibitor has been retained dissolving or desorbing some of it into the flowing mobile aqueous phase. In this way, the produced water in the early stages should contain enough inhibitor to prevent scale formation. Later, the concentration of inhibitor may fall below the minimum inhibitor concentration (MIC) level, and at this point the well should be re-squeezed. When the scale inhibitor concentration drops below its MIC level, the inhibitor no longer prevents scale deposition (Crabtree et al, 1999; Todd et al, 2010).

This thesis will focus on the interaction of scale inhibitor with the formation matrix in precipitation/re-dissolution processes, which occur in precipitation squeeze treatments using the polymeric scale inhibitor- phosphino polycarboxylic Acid (PPCA).

1.2 Research Outline:

This study consists of the following areas of research:

Chapter 1 briefly reviews the basic problem of oilfield scale and the various approaches to scale control. This chapter also explains the main objectives of the study as well as obtaining the thesis outline.

Chapter 2 describes the squeeze process itself together with the use of polymeric scale inhibitors. This includes a detailed discussion of the current literature relating to the mechanisms behind precipitation squeeze treatments along with the factors affecting the precipitation and retention of the inhibitor.

Chapter 3 explains the experimental methodology used to study the governing factors responsible for the phase separation/precipitation mechanisms for PPCA. This work includes:

1. Precipitation and re-dissolution tests for phase separation.
2. Beaker tests for static adsorption and compatibility experiments to show whether pure adsorption and/or coupled adsorption/precipitation are occurring.
3. Inhibition Efficiency (IE) tests were used to establish the MIC of different fractions of the polymeric scale inhibitor including the Stock PPCA solution and also the Supernatant and Precipitated samples of PPCA.
4. Wet Chemical Analysis was used to estimate the polymeric content present in different fractions of the scale inhibitor and compared it with ICP which measured Phosphorus (P) values.
5. Solubility experiments were used to understand the mechanism behind the re-dissolution of SI_Ca precipitate complexes.

Chapter 4 presents results of our study of the phase envelope of PPCA and identifies and discusses the factors responsible for PPCA phase behaviour. To improve our understanding of the precipitation processes for PPCA, the PPCA phase envelope was scanned in four different ways:

i. by coupled adsorption and precipitation experiments,
ii. by estimating the stoichiometry of the PPCA_Ca complex
iii. by inhibition efficiency testing, and
iv. by wet chemical analysis

Chapter 5 describes the detailed solubility behavior of the PPCA_Ca complex which plays an important role in precipitation squeeze treatments. This chapter presents results

on the rate of dissolution of the precipitation complex. It is also shown that the solubility of the precipitated PPCA_Ca complex becomes lower as it is exposed to successive fresh supernatant brine and the behavior is very unlike that expected from a "solubility product" model.

Chapter 6 attempts to examine molecular weight for different fractions of polymeric scale inhibitor- PPCA. This will examine the effect of various parameters like pH, temperature, concentration of calcium and SI on MWD. It will also re-discuss the issues of the previous experimental results of chapter 4 and 5 in terms of MWD of polymeric scale inhibitor PPCA.

Chapter 7 presents results on PPCA precipitation sand pack floods at various flow rates. These results showed that the bulk observations on the solubilities of the various MW fractions of the PPCA carried through to the dynamic sand pack tests.

Chapter 8 compares the results of Chapters 4, 5 and 6 of PPCA with other polymeric scale inhibitors, SPPCA and PFC. This chapter will compare the mechanisms/theory studied for PPCA and shows that the theory will also applicable for other polymeric inhibitors. For this research, SPPCA and P-copolymer (denoted PFC) are the sulphonated polymeric scale inhibitors used to confirm the hypothesis.

Chapter 9 gives the summary and overall conclusions of the above experimental chapters. This will also present recommendations for future research in this related work. The field significance of certain factors, in particular molecular weights, is discussed in terms of their effect on both the retention and inhibition mechanisms.

In the Appendices, the following subjects have been presented in order to support the discussion and finding in the main chapters of this thesis:

- Appendix A: General equipment and apparatus

CHAPTER 2- **LITERATURE REVIEW**

2.1 Scale Inhibitors

Scale inhibitors (SI) are chemicals which have been applied in oilfields (and other industrial systems) for many years to prevent or drastically reduce the formation of mineral scale deposits, such as calcium carbonate or barium sulphate, in the production system. Initially, scale control is required in the production facilities; however, sea water injection and produced water reinjection also lead to scale formation which must be controlled. However, the most effective approach to the problem of barium sulphate scale is prevention at the early stages of its formation and subsequent crystal growth. Thus scale inhibitors are species which prevent or significantly retard nucleation or crystal growth at sub-stoichiometric concentrations.

In this chapter, some of the main aspects of SI inhibition and retention mechanisms are reviewed, particularly as they apply in squeeze treatments. This review contexts the present study which focuses on the basic mechanism of how polymeric scale inhibitors, such as PPCA, function in SI precipitation squeeze processes.

2.2 Mechanisms of Scale Inhibition

The most important property of a scale inhibitor is that it prevents or delays crystal growth at threshold concentrations. This means that it must be effective at sub-stoichiometric levels. Primarily it follows nucleation inhibition, and then crystal growth will occur until the supersaturation of the system is completely released (Nancollas and Liu, 1975). Many workers (Van der Leeden and Van Rosmalen, 1988; Graham et. al., 1992; Breen et. al., 1990; Graham, 1994) have studied the mechanism of threshold scale inhibition and numerous scale studies have also been conducted with in the FAST group (Boak, 1996; Shaw, 2012; Shaw et.al. 2010a, 2010b, 2014, 2015).

In order to describe the mechanism, it is known that the inhibitor molecules adsorb at the active growth sites known as kinks, which may be crystal defects, thus preventing further crystal growth by interference with the growth process. The important of such defects on crystal growth is that, when an ion settles on a flat crystal surface, it may only be in contact with a single surface atom. However, if it settles in a corner, formed by a kink, it now interacts with several atoms and the attraction is consequently much

stronger. Adsorption of inhibitor species at such crystal defects then prevents further growth from these preferential growth sites. Coupled with this, the morphology, tendency to agglomerate and the potential of the electric double layer (the zeta potential) of the growing nucleons are also altered by the adsorption of inhibitor molecules at the growth sites.

Naono (1967) postulated another mechanism for the inhibition of the growing nucleon in which adsorption of the inhibitor resulted in the increase in the energy barrier for thermodynamically stable crystal growth. In this system, free energy of nucleation is described as a function of cluster radius for nucleation. The favourable free energy function due to the release of the supersaturation is countered by the free energy requirement for the formation of a surface. At the point where the resultant free energy is maximum, critical clusters are formed which have an equal probability to grow further or dissociate. Clusters larger than the critical cluster radius tend to grow, since the surface energy term becomes less important (Nancollas, 1985).

To summarize the above two mechanisms by which scale inhibitors work to reduce nucleation, crystallisation and the subsequent growth of scale deposits, are as follows (Yuan et al., 1998):

a. Nucleation Inhibition: In the earliest stages of formation, SIs disrupts the thermodynamic stability of the growing nucleons. This mechanism of inhibition then involves endothermic adsorption of inhibitor species, causing dissolution of the barium sulphate embryo crystals.

b. Crystal Growth Retardation: At this later stage of crystal growth, the SI retards the growth processes of the growing crystals (for heterogeneous crystal growth). This mechanism of inhibition then involves irreversible adsorption of inhibitor species at the active growth sites of barium sulphate crystals, resulting in their blockage. Indeed, the SI molecules may become incorporated into the growing crystal lattice which further distorts the morphology of these crystals.

All scale inhibitors show the ability to work through *both* nucleation and crystal growth mechanisms. However, most SI species work predominantly through one or other of these mechanisms to achieve scale inhibition.

2.3 Types of Scale Inhibitor

The most commonly used scale inhibitors for the control of barium sulphate ($BaSO_4$) scale formation downhole are phosphonates and polymers. Most polymeric SIs are poly carboxylate based polymers with relatively low average molecular weights, typically with $M_w < 10^4$. These types of inhibitors tend to perform better over a range of pH and temperature conditions. The most important property of the scale inhibitor is that it is able to control the scale formation at sub-stoichiometric (threshold) concentrations. The threshold concentration level at which the SI performs at a specified level is referred to as minimum inhibitor concentration (MIC). Gill (1996) reviewed the early years of application of chemical scale inhibition in the oilfield. The key function of the scale inhibitor was identified as preventing scale deposition either through nucleation inhibition or crystal growth inhibition or even by scale dispersion (Yuan et al., 1998). Phosphonates and polymers are the two main generic types of scale inhibitors which are commonly used throughout the oil industry. In the broader view, polymers are good nucleation inhibitors and dispersants and phosphonates tend to be better crystal growth retarders. However, both types of SI act through both of these mechanisms to some extent (Graham et al., 2003; Sorbie and Laing, 2004; Boak et al., 1999).

Several authors have noted that polymeric SIs are favoured in terms of environmental friendliness of the products, but in terms of IE, phosphonates SIs are often comparatively better inhibitors (Taj et al., 2006; Jordan et al., 1995; Inches et al., 2006). This improved performance of phosphonates is mainly because of the presence of the phosphonate functionality (usually as an amino phosphonate), which yields the best IE and SI retention results (Singleton et al., 2000) despite the fact that these products are less environmentally acceptable (Fleming et al, 2001). Davis et al (2003) studied some polymeric SIs containing phosphonate end-capped moieties, which improved the IE but decreased the biodegradability of the polymer. PMPA is an example of a poly-phosphonate SI which has significantly better IE and retention properties compared to other polymeric SIs (Singleton et al., 2000). However, PMPA has an extremely high phosphorus content, at a level comparable with phosphonate SIs and, indeed, it is currently thought that PMPA is not in fact polymeric in nature at all.

2.3.1 Phosphonate Scale Inhibitors

Phosphonate SIs (e.g. DETPMP- penta phosphonate shown in Figure 1) forms a class of high performing inhibitors which mainly work through a crystal growth mechanism. However, it is known that phosphonates tend to have a lower "cut off" temperature. This means phosphonate performs quite poorly at low temperature and work best above a 'switch on' temperature. However, polymeric scale inhibitors are less sensitive to temperature. Similarly, PPCA and non-polymeric, mono-phosphonated, carboxylated species such as HPAA and PBTC also have crystal growth inhibition qualities, although probably not as good as highly phosphonated species. For this reason, selected phosphonated and/or carboxylated SIs can be used synergistically to improve their crystal growth inhibition properties (Shaw and Sorbie, 2014).

The primary bonding mechanism for the phosphonate group appears to be ionic interaction between the PO_3^{2-} group and the Ba^{2+} ions of the crystal growth sites (van der Leeden and van Rosmalen, 1988; van der Rosmalen et al., 1980). This is supported by the fact that the optimum pH for scale inhibitor performance is reached when the pKa value for $PO_3H^- \equiv PO_3^{2-}$ is exceeded. The performances of the SI could be increased at lower pH, by incorporating the groups like –OH, $-CO_2H$ and $–NH_3^+$ which will interact with SO_4^{2-} ions on the crystal surface through hydrogen-bonding (van der Leeden and van Rosmalen, (a-1988), (b-1988); van der Rosmalen et al., 1980). With these chemistries, the IE performances enhanced at slightly lower pH values, for both the phosphonates and the polyphosphonates. These groups are also available for possible co-ordination to Ba^{2+} ions aiding the surface adsorption.

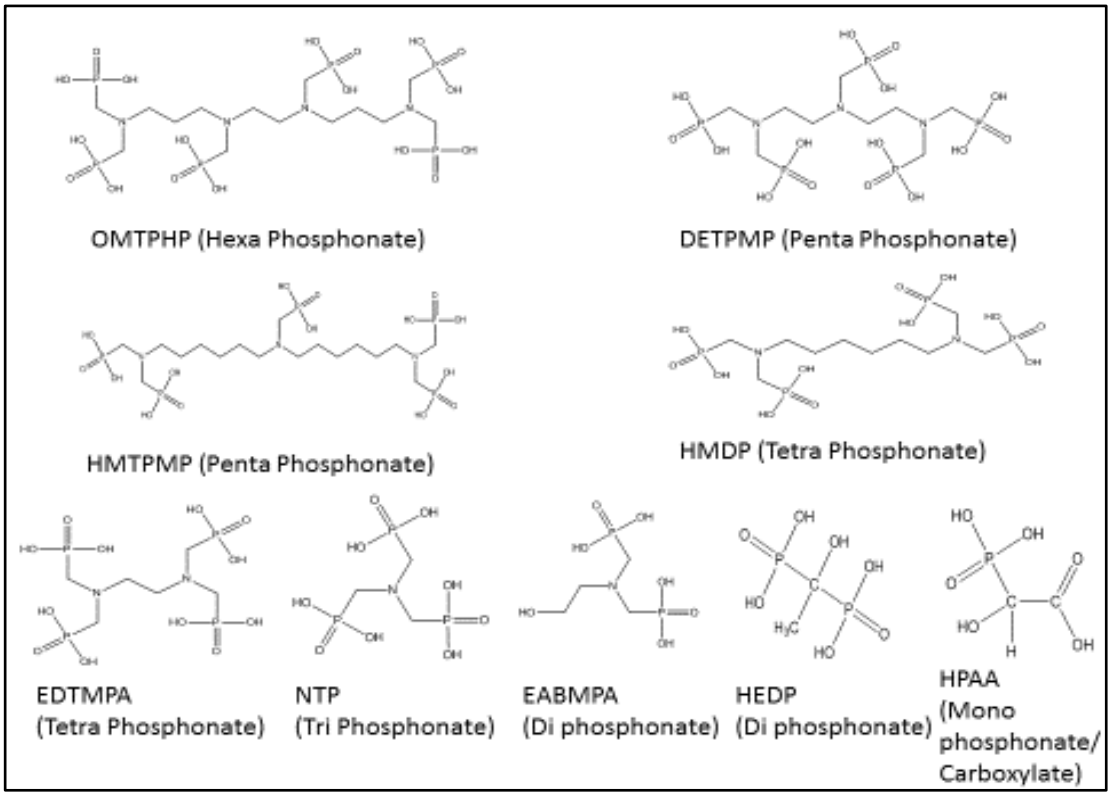

Figure 1: Chemical Structure of Phosphonate Scale Inhibitors

2.3.2 Polymeric Scale Inhibitors

Polymeric SIs worked mainly by nucleation inhibition, although as noted above, they also show some (poorer) crystal growth retardation. A practical observation supporting this is that the IE of most polymers is high at early times in these tests but tends to be lower at 24 hours (where crystal growth mechanisms are more dominant). Researchers (Graham et al., 2003; Shaw et al., 2010b) have found that PPCA is principally a nucleation inhibitor, which is effective over longer residence times although it is gradually consumed with in the growing crystal lattice. The inference is that, this species is less effective at adsorbing onto, and thus completely blocking, active growth sites on the crystal surface. However, adsorption of the PPCA inhibitor onto the initial crystallites makes it a very effective growth retardant during the early crystal growth period. Similarly, this is also true for PVS, polymeric SI that has the least crystal growth inhibition properties. PVS is generally in a highly dissociated state (due to the low pKa of the sulphonate groups) with weak metal binding, which means that it plays a less effective role in the crystal growth mechanism. In order to inhibit barium sulphate crystal growth, SI (phosphonate or polymeric) must be able to incorporate into the

growing scale lattice in combination with Ca^{2+}. It is known that sulphonate groups do not bind to Ca^{2+} or Mg^{2+} cations because these functional groups are highly dissociative, i.e. they have very low K_a values (Graham et al., 2003). Sorbie and Laing (2004) reported the mean pKa values for PVS = ~3 and for DETPMP = ~4.5. Thus, sulphonated homo-polymers and co-polymers such as PVS, SPPCA and VS-Co have good nucleation inhibition properties and less good crystal growth properties.

Carboxylated species, particularly polycarboxylates such as PPCA and maleic acid ter polymer (MAT- a green SI) are generally regarded as having crystal growth properties in-between those of sulphonated polymers (such as PVS) and conventional phosphonate SIs. These differences can be explained on the basis of the binding constants of the functional groups sulphonate, carboxylate and phosphonate with Ca^{2+} cations. At any selected pH and temperature, Ca^{2+} and Mg^{2+} bond strongest to phosphonate groups (large binding constants, like those quoted for DETPMP above), followed by carboxylate (moderate binding constants), followed by sulphonate (extremely weaker binding constants). The performances of the polycarboxylate inhibitors in terms of IE can be helped because of the many bonds between the inhibitor and the surface in the polymeric species. Thus both dissociated and un-dissociated acid groups can co-ordinate to the surface. It follows that co-polymers such as VS-Co (vinylsulphonate acrylic acid co-polymer) will operate via both nucleation inhibition and crystal growth inhibition mechanisms. Phosphonates and sulphonated polymers may also be used synergistically in blends, to yield better IE, since both mechanisms of scale inhibition can operate effectively simultaneously (Shaw and Sorbie, 2014; 2014).

SPPCA – Sulphonated Phosphino PolyCarboxylic Acid

SPPCA monomer structures: Acrylic Acid and AMPS (2-acrylamido-2-methylpropane sulphonic acid). Structure same, as PPCA but sulphonated – some of the carboxylate functional groups will be replaced by AMPS side chains. This replacement may be ~50%, but depends upon the synthesis.

P-Functionalised Co-Polymer (PFC)

This is a sulphonated polycarboxylate polymer containing phosphorus. The exact molecular structure is not known (has not been disclosed to FAST) – hence in this thesis, it is given the generic name: “P-Functionalised Copolymer”, and is named as such throughout (sometimes abbreviated PFC). This Product was supplied to FAST for laboratory IE testing/evaluation.

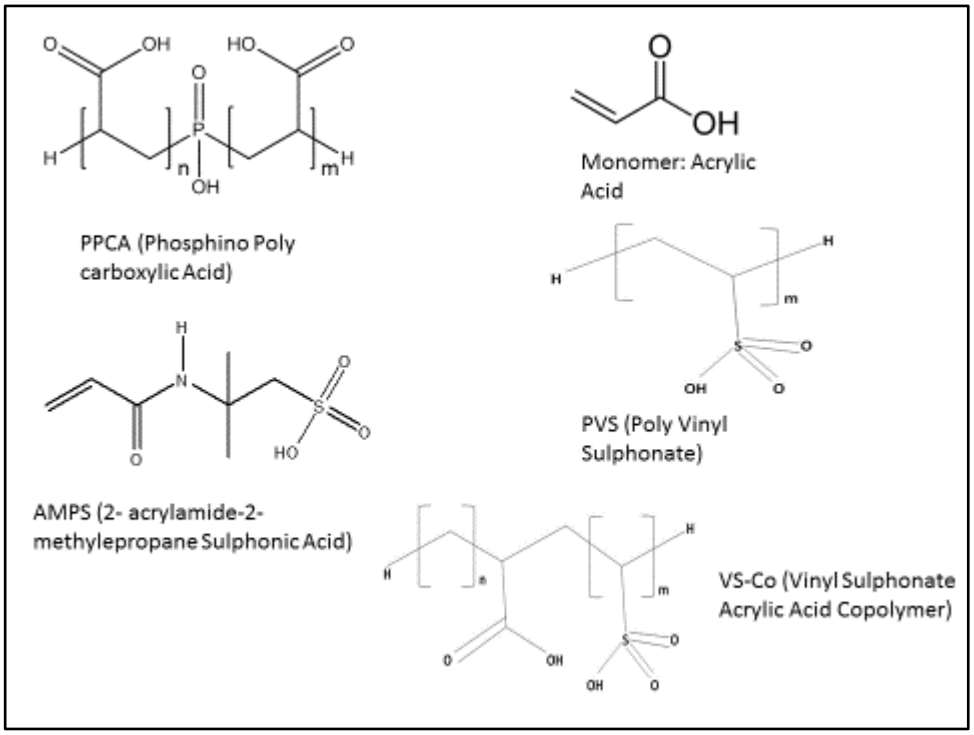

Figure 2: Chemical Structure of Polymeric Scale Inhibitors

2.3.3 "Green" Scale Inhibitors

The oil industry is moving more towards the development and deployment of polymeric SIs (particularly "green" chemistries) because of environmental concerns. Jordan et al (2010) reported the recent government legislation which prohibits the use of phosphonate SIs in Norway, including PMPA (Phosphinomethylated polyamine- a poly-phosphonate). The main problem associated with green polymers, which contain no phosphorus and no sulphur, is that their IE performance tends to be much poorer, particularly over longer periods of time.

It is for this reason that many P-tagged polymers have been synthesised, such as PPCA, SPPCA, P-functionalised polymers and co-polymers, etc. These products typically contain < 5% phosphorus, and are considered *yellow* products, rather than fully *green*. Firstly, their IE properties are generally better than the fully green products such as maleic acid ter-polymer (MAT), and they are not as environmentally hazardous as small molecular phosphonates (which contain a higher %P). Secondly, by P-tagging polymeric SIs, this enables such products to be assayed by ICP spectroscopy via measuring phosphorus in the laboratory (Boak and Sorbie, 2010).

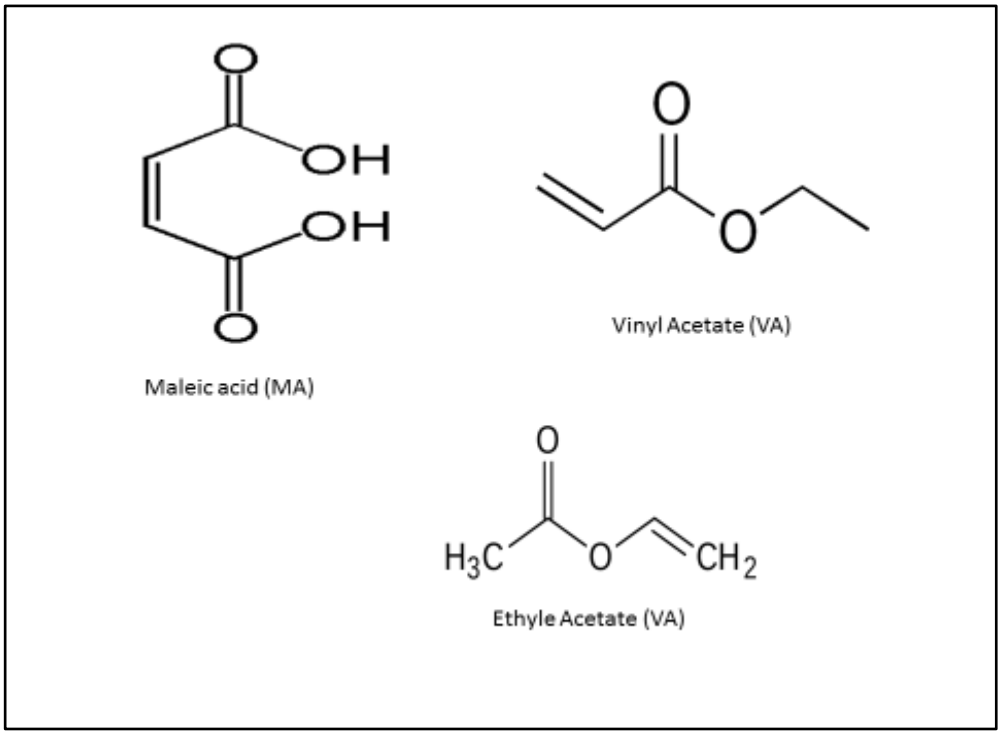

Figure 3: Chemical Molecular Structure of the monomers- Maleic Acid (MA), Vinyl Acetate (VA) / Ethyl Acrylate (EA).

2.4 Performance Testing

Scale inhibitor performance testing is carried out in order to determine which SI products work best for a given field application. A range of tests is performed designed for the following purposes:

i. to evaluate the concentration levels of selected SIs (i.e. the MIC) required to prevent scale formation;

ii. to determine which chemicals have suitable compatibility in the application and formation brines;

iii. (for downhole SI applications) to carry out a limited core flood study (using a chosen products from stages (i) and (ii)), in order to better assess issues of formation damage and expected squeeze lifetime;

iv. (for downhole SI applications) to carry out a modelling study to design the initial squeeze treatments in this formation.

From this information, it is possible to make a more informed prediction of the likely squeeze lifetimes and the required frequency of treatments (Jordan et al., 1996; Graham

et al., 2001; Graham et al., 2001). These tests are used routinely throughout the industry for scale inhibitor selection and optimisation studies for potential topside and downhole applications. Downhole application refers to the squeeze treatment whereas topside application refers to continual injection of chemical inhibitors at any point in the flow lines. The table below shows the tests involved in the performance testing along with the aims of each of the individual tests.

Table 1: Performance Test List

Performance Testing List	Aim of the Test
Static Bottle Tests	• Used to establish the MIC of the scale inhibitor for various physical/chemical conditions. • Divalent cations such as calcium and magnesium have been found to influence the IE performance of different scale inhibitor species by varying degrees. For instance, increased calcium concentration can significantly enhance IE performance whilst magnesium has been observed to 'poison' performance. • pH can be varied in static IE experiments
Tube Blocking Tests	• The dynamic "tube blocking" rig can be used to establish the "dynamic" MIC and, for practical reasons, this is the best test for purely carbonate scales
Compatibility Tests	• Compatibility of SI solutions with injection and formation brines is tested to ensure the products do not precipitate out before they can be deployed.
Thermal Ageing	• Such tests are used to establish the stability of the SI species. The IE is tested for unaged and aged solutions. Higher temperature (>150°C) fields are now being developed and many of the SI chemicals used in lower temperature reservoirs (100 - 120°C) are chemically unstable.
Coupled Adsorption / Precipitation Tests	• To confirm which rock/scale inhibitor retention mechanism i.e. pure adsorption or coupled adsorption/precipitation is occurring, a number of different mass/volume ratios should be examined
Corefloods or Sandpack floods	• Core or sandpack floods are used to determine how well the SI is retained in the rock. This is important for the modelling and design of downhole SI squeeze treatments.

The laboratory test protocols are very similar and are broadly standardised throughout the oil industry for the various types of test listed above. However, differences in detail occur in some tests depending on the precise application which is involved; e.g. the exact sequence of steps in a core flood may differ depending on the SI application. Some procedures were adopted relating back to NACE standard test, such as TM 019797 (Nace Standard TM 0197-97, 1997). These test procedures have been described in many previous papers (Yuan et al., 1998; Graham et al., 1997).

2.5 Scale Inhibitor Squeeze Treatments

The most common and efficient method for preventing the formation of sulphate and carbonate scales in producer wells is through the application of scale inhibitor squeeze treatments. The SI must perform the following tasks at very low concentrations (MIC or threshold concentration, C_t):

1. Prevent or delay sulphate scale formation which will occur when injected sea water (containing sulphate ions) mixes with formation water (containing barium, calcium and strontium) in the near wellbore.
2. Prevent or delay carbonate scale formation which will occur at various stages including the production tubulars, topside equipment and in the near wellbore formation area.
3. Interact with reservoir substrates in order to give long inhibitor return profiles at or above the MIC level.When the concentration of the inhibitor falls below the MIC, the well should be re-squeezed.

In order to be an effective scale inhibitor, the chemical needs to be stable to thermal degradation under the wells downhole condition and also compatible in the particular brine system. Brine compatibility is a major issue of concern since premature precipitation of inhibitor complexes during injection may lead to the formation of pseudo-scale with associated fines plugging. Two type of inhibitor squeeze treatment are routinely carried out where the intention is either:

1. Adsorption Squeeze treatments where the aim is to adsorb the inhibitor by physic-chemical process onto the rock matrix; or

2. Precipitation Squeeze treatments are applied in order to extend the squeeze lifetime by precipitation (or phase separation) which is commonly carried out by adjusting the solution chemistry ([Ca^{2+}], pH, temperature) of polymeric and phosphonate inhibitor solutions.

These mechanisms – adsorption and precipitation – individually or working together are responsible for giving a long return curve of SI after a near-well SI squeeze treatment. The above two interaction mechanisms of the scale inhibitor in the squeeze treatment will be discussed in detail later in this chapter.

2.6 Squeeze Procedure

The procedure for applying a squeeze treatment in the field normally involves the following six stages (Sorbie and Gdanski, 2005; Patent No. US6995120 B2; Patent No. US 2012/0032093; MacEwan, 2013; Sorbie et al., 2000).

1. ***Pre-flush Injection:*** After the producing well is shut in, then a volume of brine (usually a very dilute solution of scale inhibitor in seawater – ~10s – 100s ppm SI) is first injected into the formation. This displaces the tubing volume and production fluids back into the formation and it also serves a number of additional functions including, (a) reducing the near wellbore temperature since cooler injection brine is used (reduces SI adsorption close to the wellbore); (b) acting as a spacer between the in situ reservoir fluids and the injected main (high concentration) scale inhibitor slug, (c) changing the near well wetting state to more water wet conditions if mutual solvent (or possible some surfactant) is applied leading to higher SI adsorption in the hotter region away from the wellbore.

2. ***Main Treatment or Inhibitor Injection Slug:*** the main scale inhibitor slug is pumped into the water producing zone normally in the concentration range of 2.5% to 40%. The function of this SI is to propagate into the formation where it is retained by either chemical adsorption or by temperature/chemical activated precipitation. For some specific treatments, this inhibitor solution may contain other additives.

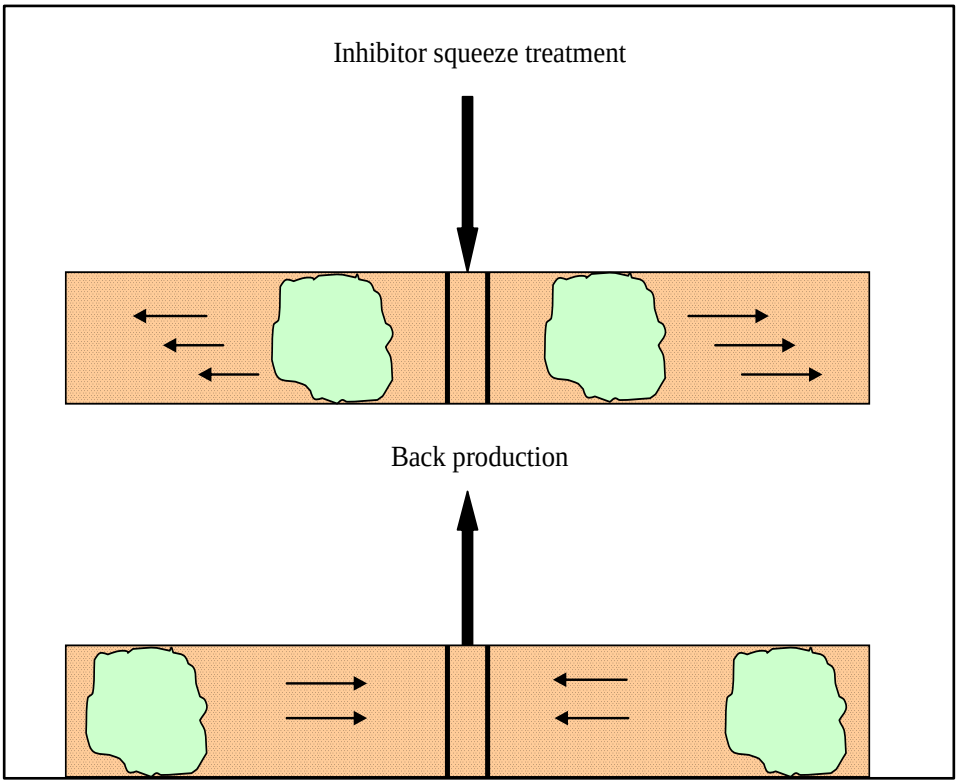

Figure 4: Inhibitor Squeeze Treatment (Source: FAST Scale Courses)

3. ***Over-flush Injection:*** an over-flush of fluid (usually brine, seawater or sometimes diesel or even gas) is injected into the well to push the main treatment further into the formation. The objective is to propagate the SI further into the formation away from the wellbore where it may absorb and/or precipitate and give a longer treatment life (in terms of time before the next treatment or, more commonly, in terms of the volume of produced water treated with SI concentration returned at [SI] > MIC).

4. ***Well Shut-in:*** the well is then shut-in (i.e. flow is stopped) for a certain period of time (usually 6-24 hours) to allow adsorption or temperature/chemically induced precipitation to occur and reach close to equilibrium.

5. ***Back Production of the Well:*** the well is then put back onto production, and the fluids in the near well formation flow back into the production well. Fluids are back produced broadly in the reverse order from their injection, i.e. first the overflush, then the main SI treatment and then the preflush followed by normal production fluids (i.e. oil, produced brine and gas) from the reservoir. Well clean-up may take some time since large quantities of injection brine and chemicals have been injected into the near well reservoir formation. However, if

the SI is successfully retained in the formation (by adsorption/precipitation mechanisms), then the SI is back produced over a long period of time (i.e. it is present at >MIC concentrations in a large volume of produced brine) and this presence of SI in the produced brine prevents mineral scale formation.

The success of the treatment is defined by the squeeze lifetime which is specified in terms of how long the SI is back produced at a concentration level greater than the 'MIC'. Often the squeeze lifetime is better described in terms of the volume of produced water that is protected by present [SI] ≥ MIC (Graham et al., 2003; Boak, 1996). The squeeze lifetime in turn depends to a large degree on which mechanism the SI is 'retained' within the porous medium, i.e. by adsorption or precipitation. Besides the interaction mechanism of the inhibitor with the formation (adsorption/precipitation), the lifetime of the squeeze depends upon a number of other physical and chemical parameters of the reservoir such as the surface chemistry of the formation (quartz or clays), the wettability of the rock surface, the pH of the aqueous media contacting the formation, the formation temperature and pressure etc. and some of these factors are discussed in detail later in this section in the light of their relevance to the research topic of this thesis.

2.7 How Scale Inhibitors Are Retained in the Reservoir?

It has been known for many years that the two major retention release mechanisms that have been found to occur in a formation are adsorption/desorption and precipitation/dissolution. These two mechanisms have already been mentioned above but they are now discussed in more detail below.

2.7.1 Mechanism of Adsorption

Since the inhibitor chemicals are generally applied in a squeeze process, a small amount of inhibitor is required to desorb from the formation rock surface over the back production period, typically for 3-12 months, in order to prevent scale deposition. The adsorption of scale inhibitor is thought to occur through electrostatic and van der Waals interactions between the inhibitor and formation minerals and this is generally described

by an adsorption isotherm, Γ(C), which describes the amount of SI adsorption (in units of mg/g for example) as a function of the scale inhibitor concentration, [SI] = C.

The surfaces of soil particles carry net negative charges, as a result, they attract cations and repel anions, both of which originate from the aqueous medium. Therefore, the surface charge governs the nature and extent of ionic and molecular bonding to the particle. Regardless of the nature of the particle, it can be modelled as a solid sphere, with a uniform charge distributed over its surface, surrounded by water containing ions in solution. Distribution of these ions on and around the particle can be quantified by 'double layer' theory (Lewis, 2009). The liquid layer surrounding the particle exists as two parts; an inner region (Stern layer) where the ions are strongly bound and an outer (diffuse) region where they are much less firmly associated. Within the diffuse layer there is a notional boundary inside which the ions and particles form a stable entity. When a particle moves (e.g. due to gravity), ions within the boundary move it. Those ions beyond the boundary stay with the bulk dispersant. The electrical potential at this boundary (surface of hydrodynamic shear) is the zeta potential. The magnitude of the zeta potential gives an indication of the potential stability of the colloidal system. If all the particles in suspension have a large negative or positive zeta potential then they will tend to repel each other and there will be no tendency for the particles to come together. However, if the particles have low zeta potential values then there will be no force to prevent the particles coming together and flocculating (Hunter, 1988).

Graham (1994) in his PhD thesis concluded that, in high salinity brines, the bonding possibilities are greatly increased. The reason for this is due to increased number of charged sites on silica surface with high salinity brines at any given pH, while on the other hand, the thickness of the electronic double layer will be greatly reduced (Hiemenze, 1986; Ile, 1979; Schramm et al., 1991). In high salinity brine, the magnitude of the coupling potential decreases. As a result, the negative coupling potential produces negative zeta potential also. Therefore, in the presence of high salinity brine, the diffuse layer thickness reduces to zero (or a very low value) in which case, the counter charge resides entirely within the stern layer. Thus, zeta potential also falls close to zero. Therefore, an ion interaction causes the reduction in the thickness of the diffuse layer at high salinity. Moreover, the counter charge required to balance the mineral surface charge is not accommodated entirely within the stern layer, so the diffuse layer does not collapse to zero (Jaafar, 2009).

However, this results in two approaches, primarily, for hydrogen bonding materials, it allows the approach of polymeric species close to the surface free from electrostatic counterion repulsions and secondly, the counterions present at the surface are drawn closer to surface charge sites which, in effect, leaves a larger area for hydrogen bonded polymers to adsorb onto.

The amount of inhibitor adsorbed and the lifetime of the adsorption squeeze are dependent greatly on the properties and surface chemistry of the reservoir system. The interaction of SI through an adsorption mechanism with the rock surface is described by an adsorption isotherm, Γ(C), which is a function of pH, temperature, mineral substrate and involves cations such as Ca^{2+}. The metal cation interaction with the silica surface above pH value 5 (Hiemenze, 1986) are illustrated below:

$$Si_sOH + Ca^{2+} \leftrightarrow Si_sOCa^{+} + H^{+} \quad (1)$$

The precise form of Γ(C) determines the squeeze lifetime, as has been described in detail in a number of previous papers (Sorbie et al., 1991, 1992; Sorbie, 1991; Yuan et al., 1991). Figure 5 shows the apparent adsorption, r_{app} (C), as a function of [SI] = C, which is the apparent amount of SI on the rock assuming it is all retained by adsorption whether it actually is or it is in fact really a combination of true adsorption and precipitation. This quantity is plotted as a function of mass to volume ratio (m/V); m = the mass of adsorbing material such as sand or crushed rock and V is the volume of the SI solution used in the adsorption test. The important observations from the theory underlying the r_{app}(C) vs. C results when plotted as a function of (m/V) in Figure 5 are as follows (Kahrwad et al., 2008; Ibrahim et al., 2012):

1. At lower concentration, a clear region of pure adsorption was observed; it is identified as such since pure adsorption is not a function of (m/V) ratio;

2. A region of coupled adsorption/precipitation was observed where the apparent adsorption is clearly a function on the (m/V) ratio with the adsorption seeming to increase as (m/V) decreases.

The theory, explanation and mathematics of the above observations are fully explained in Kahrwad et al. (2008).

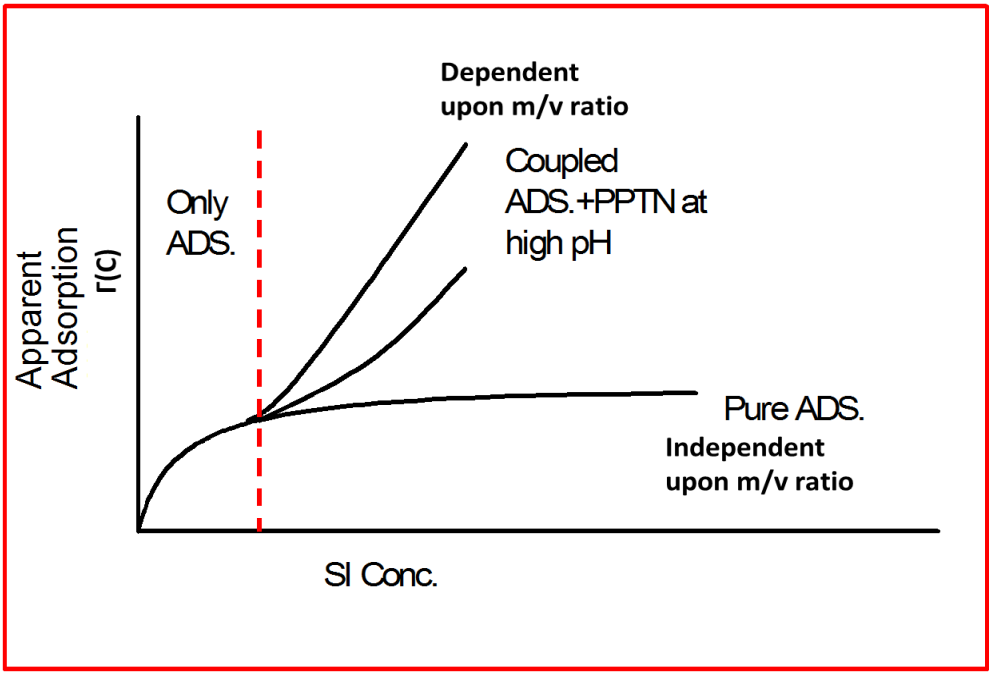

Figure 5: Schematic Diagram of Only Adsorption and Coupled Adsorption and Precipitation Behavior (Source: FAST Scale Courses)

Static Inhibitor Adsorption: In static inhibitor adsorption tests, the equilibrium is established between the scale inhibitor solution and crushed reservoir core (from the formation into which the chemical is to be squeezed), under a known set of test conditions. Such measurements are conducted over a range of pH which the SI may encounter during injection and production. From these tests, which are carried out for each SI, it is possible to rank the SIs from good to poor in terms of their probable adsorption performance in the reservoir. Typically a good adsorption level, Γ, at a moderate inhibitor concentration (say, ~2500ppm) would be in the range Γ = 0.5 – 4mg/g (mg of SI per gm of core).

Previously Wat and his team, (1991; 1992) presented clear evidence of enhanced adsorption in studies of PPCA using high calcium concentrations. It is confirmed from the research that the adsorption characteristics of these electrolyte inhibitors is also a function of pH and [Ca^{2+}]. This is partly due to the activity of the water being reduced by the formation of hydrated ions and thus the polymer molecules will be driven close to the silica surface long before phase separation (or precipitation) occurs. Also, the [Ca^{2+}] in the aqueous phase will cause an increase in the number of calcium ions adsorbed on the surface and a corresponding increase in the number of possible points

of electrostatic attachment for the inhibitor. A combination of these points leads to enhanced inhibitor adsorption at the rock surface.

2.7.2 Precipitation or Phase Separation Mechanism

Recently, more emphasis has been placed on precipitation/phase separation squeeze treatments. However, in precipitating chemicals within the rock formation the possibility of the formation damage increases and this has meant that such treatments have often been avoided (Payne, 1987; Hardy, 1992; Plummer, 1987). In a precipitation squeeze treatment, the inhibitor is retained within the formation as a solid or gel-like precipitation phase (Miles, 1970; Shuler and Jenkins, 1989; Carlberg, 1983; 1987; Olson et al., 1992; Pardue, 1991; 1992). In these precipitation treatments, a homogeneous and mildly acidic solution of the inhibitor is injected into the formation and placed several meters from the wellbore by means of a brine post flush. This process mainly depends upon the physical conditions such as the inhibitor interaction with certain divalent metal cations such as Ca^{2+} (which may either be present naturally in the reservoir or introduced with inhibitor), pH and temperature. Therefore, for a particular inhibitor concentration under mildly acidic conditions, a subsequent increases in pH, temperature and $[Ca^{2+}]$ may lead to a phase change occurring. These phase changes generally occur due to the formation of a calcium/scale inhibitor complex where the fluid system has crossed a phase separation boundary as it is driven into the hot region of the reservoir. The inhibitor-precipitate often forms a gel-like semi-solid structure within the near-wellbore formation. Such processes can bring about extended squeeze lifetimes (Pardue, 1991; 1992; Yuan et al, 1993; Olson et al 1992; Carlberg, 1987). Indeed, this description is very like the precipitation processes described later in this thesis for the PPCA/brine systems used.

When this phase separation process described above is occurring, and then simultaneous adsorption is almost certainly occurring at the same time. Both the phase separation and adsorption processes are controlled by temperature, brine composition (mainly $[Ca^{2+}]$) and also pH (Carlberg, 1983, 1987; Olson et al., 1992). Such processes can bring about extended squeeze lifetimes when compared with those achieved through a conventional adsorption/desorption approach using similar inhibitors. The level of inhibitor in the return curve is then thought to be governed by the solubility (Cs) of the inhibitor/calcium complex and the rate (r_2) of release of inhibitor into the produced

water (Carlberg, 1987; Browning and Fogler, 1993; Wat et al., 1993). A mathematical model of this process, explaining the roles of both the solubility and the dissolution rate (Cs and r_2) in precipitation squeezes has been presented recently by Sorbie (2012) and modelling work on this process dates back to the 1990s (e.g. Malandrino et al, 1995).

2.8 Review of Previous Experimental Studies

As noted above, the return curve of a precipitation squeeze processes is governed by two main factors, viz. the solubility (C_s) of the inhibitor-calcium complex and the rate of dissolution (r_4) of the precipitation complex (Malandrino et al., 1995; Sorbie, 2012). The physical-chemical mechanisms that govern the success of precipitation squeeze treatments are much less understood than those of the adsorption squeezes (Barthorpe, 1992; Boak, 1996; Cushner et al., 1988; Shaw et al., 2010a; 2010b).

Polyacrylate-based inhibitors are used in this research and these are presently preferred in the North Sea for precipitation squeeze treatments. These inhibitors are believed to reduce the potential for formation damage relative to phosphonate inhibitors on account of their tendency to separate from brine as a viscous phase or glaze rather than as a solid (Shuler and Jenkins, 1989; Olson et al., 1992).

PAA is used as a standard polymer for studying the properties of linear polyelectrolyte. Polyacrylates are well known to adsorb on sandstones. PPCA contains a phosphino polycarboxylic group in which two acrylate chains are linked by phosphino group as shown in Figure 2. As a result, PPCA is different by only one group (phosphino group) from a classical PAA. The addition of the phosphino group is useful in raising the quality, reducing the cost and also the environmental-friendliness of the polymer. Under typical boiler conditions (i.e. PPCA was being applied in the inhibition of scales in industrial boilers), Chang and Patel (1996) reported that PPCA showed advantages over PAA and phosphonates for thermal stability, dispersion and iron transport.

Rabaioli and Lockhart (1995; 1996) and Andrei et al (1999; 2003) concluded in their studies that the phase behaviour and precipitation yield of phosphine polyacrylate (PPAA) inhibitor are governed by the factors suck as SI and Ca^{2+} concentrations, pH and temperature. Varying these factors experimentally gives the most convenient and systematic way to identify the conditions under which the inhibitor solution is homogeneous or is in a phase separation (precipitation) state. It is well known from the literature that the higher calcium concentration the more precipitation of the polymer

occurs, leaving less for adsorption (Pardue, 1991). The phase envelope of the PPCA reported by Andrei et al (1999) suggested that, the phase boundary at pH>10 reflects the conditions under which insoluble Mg^{2+} and Ca^{2+} hydroxides were formed. If sufficient [Ca^{2+}] was present for precipitation, then the threshold pH for phase separation was fairly constant around pH 4. The study also showed that a minimum [Ca^{2+}] was necessary to induce precipitation; and this increased with increasing inhibitor concentration. Andrei et al (1999) also described that preferential precipitation of the high M_w of the PPAA inhibitor occurred. These workers also studied the solubility of the precipitate and suggested that it was far higher than the typical inhibitor return concentrations. They also noted that dissolution equilibrium takes some time to achieve. They concluded that the dissolution kinetics must control the concentration of the inhibitor in the produced brine and that the process was kinetically slow. To some extent, these effects were qualitatively predicted by some previous modelling work (Malandrino et al, 1995).

2.8.1 Effect of pH on Scale Inhibitor Performance

The polymeric SIs (MW $<10^4$) with a polycarboxylate base tend to be good performance scale inhibitors over a range of pH and temperature conditions. However, their effectiveness deteriorates quite markedly as the pH is lowered (Breen et al., 1990). This is directly related to the pKa values of the particular functional groups along the backbone of the polymer and the relationship to the extent of dissociation present at a particular pH.

Graham et al (2002) has shown that polymeric scale inhibitors which contained sulphonate functional groups have pKa <<2.5 (i.e. they were strongly acidic) and those which contain carboxylic functional group had pKa ~4.5 value approximately (weakly acidic). This and much other work established that effective barium sulphate inhibition required ionised acid groups. The polymeric nature of sulphonated copolymers (Vs-Co), however, means that the pKa values of the acrylic acid groups will be expected to range between 3 and 6. For this reason, the inhibitor such as polyvinyl sulphonate (PVS), which contains the strongly acidic sulphonic acid units, provides good barium sulphate inhibition, even at lower pH (<4), because these species are completely dissociated at lower pH values. The addition of a single phosphonic group in polymeric scale inhibitors acts as an active functional group and the pKa range lies between 4 and 5. At

pH 5.5, essentially all of the sulphonic acid groups in the polymer product are already ionised, therefore any further increase in the pH has minimal effect.

Xiao (2001) also found similar results in his research. He noted that over 83% of PPCA is in the deprotonated form when pH >5.76. Therefore, it is expected that the efficiency of PPCA is less pH dependent when the brine pH >6.

2.8.2 Effect of Divalent Ions on Scale Inhibitor Performance

In SI squeeze treatments, the presence of calcium ion concentration in the produced or injected brine can influence the amount of scale inhibitor retained in the formation through both adsorption and precipitation processes. This is due to the surface/inhibitor complexation mechanisms in which calcium ions strongly participate. Barthorpe (1992) showed that the physical conditions – such as higher pH, temperature and inhibitor concentrations – favour the complexation between calcium ions and the inhibitor.

2.8.3 Adsorption of Phosphonate/phosphate on Silica

The phenomenn of atoms or molecules adhering to the surface from a gas, liquid or dissolved solid is termed adsorption. The molecule that adsorbs is the adsorbate and the surface is the adsorbant. Chemisorption and physisorption are the two types of adsorption.

Chemisorption occurs when a molecule chemicall binds to a surface, through a covalent bond. The energy of this adsorption is 200KJ/mol. On the other hand, the physisorption occurs when molecules physically interact with a surface through weak van der Waal forces. The energy of adsorption is approximately 20KJ/mol insufficient to break bonds. Therefore the adsorbed molecules retain their identities (Lyo and Gomer, 1975).

The adsorption of SI molecules onto the solid surface has been cited as a mechanism which affects the mobility of phosphorus in the aqueous system (Olsen, 1958; Williams et al, 1971). The avaibility of the area of surface is directly proportional to amount of solid adsorbed. The extent to which it occurs is a function of temperature, pH, competitor ions, mineral type, oxidation reduction state and particle size (Mack and Barber, 1960; Van Olphen, 1963; Patrick and Khalid, 1974; Williams and Saunders,

1956). Based on laboratory experiments, investigators believe that the hydrated surface of aluminium and iron oxides and clays are responsible for much of the adsorption process. These studies show that, when inorganic phosphorus concentration was added in the sediment water, the phosphorus is retained by hydrous oxides of iron and aluminium and by calcium carbonate first by an adsorption mechanism and then a precipitation mechanism. The mechanism of adsorption is due to the pH-dependent charge of metal oxides found on aquatic surface (Stumm and Morgan, 1981). The P sorbing species is bound directly to the metal coordinating ion by the ligand exchange between OH^{2+} or OH groups. The adsorption of phosphate results in the increase of the negative charge on the surface of the sediment (Hingston et al, 1972)

2.8.4 Effect Particle Size present in the Formation Matrix

The particle size or the grain size of the sediment is an important aspect to be considered for adsorption mechanism. Variation in particle size can influence the chemical behaviour of sediment in fluvial system. The surface area of a constant mass of sediment increases with decreasing particle size and the adsoption rate is directly proportion to the surface area (Adamson, 1976). Stone (1987) confirmed in his adsorption studies which indicate that phosphate adsorption per unit mass increases in a non-linear fashion with decreasing grain size. The increased adsorption activity in the smaller particle sizes was apparently due to the presence of metal oxides (Al, Fe, Mn amd Ti) associated with clay minerals and organic material. Although smaller grain size (<23μm) adsorbed more phosphate than larger grain size fractions, the smaller fractions are also capable of desorbing large amounts of phosphate into solution.

2.8.5 Role of Molecular Weight Distribution in Polymeric Scale Inhibitor

Polymeric scale inhibitors are made up of repeating structural units called monomers. The process of linking the monomers by chemical reaction to form long chains is called polymerization. As a result, the polymeric species always contain some degree of polydispersity (spread of MW). This means that in practice we are never dealing with discrete single molecular species but with a range of species of identical generic type but slightly different MW. Therefore, the role of MW and the presence of functional

groups are very important to understand in order to study the IE and the adsorption/desorption or precipitation studies of the polymeric scale inhibitor.

The adsorption mechanism would be affected, if an incorporated functional group showed significant hydrogen bonding which would promote adsorption to the scale (or rock) surface. The strongest association with a surface is through electrostatic bonds, weak acids such as acrylic acids give the strongest bond. The increase in the polymer hydrophobicity (aromatic or aliphatic) will adversely affect the IE performances because bulky hydrophobic groups sterically prevent polymer approaching the scale surface.

The coupled adsorption/precipitation or phase separation during a squeeze treatment is also associated with the MW of the polymer (Pardue, 1991; 1992). Hills et al (2005) clearly reported in their study that IE performance was dependent to a larger extent on the MW of the polymer (with low level of functional group incorporations) than on the actual composition. The paper also reported that an optimum MW existed for maximum nucleation inhibition over 2 hours, an observation which was also made by Graham and Sorbie (1994). The latter authors concluded that there was an intermediate MW which would be best for nucleation inhibition but for crystal growth inhibition, the larger the MW, the better the inhibition performance.

Graham and Sorbie (1995) observed in their dynamic core flooding experiments that preferential adsorption of higher MW components occurred and that preferential desorption of lower components of polymeric scale inhibitors was also seen. The study also showed that all the MW components present in a high polydispersity of polyacrylate-based inhibitor had the capacity to adsorb. The shape and level of the adsorption isotherm and the amount of material remaining effectively irreversibly adsorbed was related to the average MW of the species. They also suggested that the polydispersity of the polymeric SI should be represented as one of the components for the polymeric inhibitor modelling purposes.

The review of the above literature provides the motivation to investigate more precisely how the parameters, such as temperature, pH, calcium concentration, MWD are interlinked and how they affect precipitation squeeze treatments. This study builds on the knowledge which has been gathered by other workers (Andrei and Malandrino (2003), Andrei et al (1999), Breen et al (1990), Graham and Sorbie (1995, 1996),

Malandrino et al (1995) and Rabaioli and Lockhart (1995, 1996)) to date and extends this further in the ways described below.

2.9 Aims of the Thesis

Several chemicals including scale inhibitors are used to protect oil production systems against scale deposition. However, in the production system these chemicals encounter a wide range of physical conditions such as temperature, pressure, salinity, hardness, different mineralogies, multivalent ions, pH variation, etc. For flow assurance purposes, it is important that these chemicals function well and are ideally employed in an optimised manner. The main aim of this thesis is to contribute to our depth of understanding on the detailed mechanisms involved when polymeric scale inhibitors are deployed in precipitation squeeze treatments. To do this we have studied and elucidated the roles played by various physical and/or chemical factors, which affect the overall performance of polymeric scale inhibitors.

Our research on precipitation squeeze treatments aims at fully developing its potential to provide reliable, safe, economic and long-lived squeeze treatments. This research provides the fundamental understanding of the two related areas of work, viz. (1) on the phase envelope of PPCA and (2) on mapping of the PPCA phase envelope to locate the maximum precipitation on the basis of MWD of PPCA. Our detailed objectives are as follows:

1. To develop the full understanding of the Phase Envelope of PPCA
2. To define the important role of MWD of PPCA in the return curve of the precipitation squeeze treatments.
3. To provide detailed experimental results which will in time enable the development of a model based on the MWD of the precipitate/supernatant/stock for designing precipitation squeeze treatments using polymeric scale inhibitors.

In this research, we have developed the Phase Envelope of PPCA for the higher calcium conditions in the reservoir and we have investigated the factors affecting the phase behaviour of PPCA. These factors affect the IE performances and the retention of the PPCA inhibitor. We further strive to do the following:

1. To develop a full understanding of the ‘Phase Envelope’ of PPCA.

2. To define the important role of MWD of PPCA in the return curve of the precipitation squeeze treatment.
3. To determine the stoichiometry of the PPCA_Ca_n complex (i.e. the value of n) in precipitated PPCA at different temperatures.
4. To investigate the kinetics of the PPCA_Ca complex precipitation/dissolution for longer residence times.
5. To determine experimentally the IE and the MIC level for the various fractions of PPCA i.e. precipitated and supernatant PPCA compared with those for the stock PPCA samples.
6. To establish the effect of temperature, pH and [Ca^{2+}] on the efficiency performances of these various fractions of PPCA (i.e. precipitate, supernatant and stock).
7. To find out the response levels of various analytical methods (wet chemical Hyamine method vs. ICP analysis) for the precipitated and supernatant polymer fractions.
8. To establish the effect on the solubility of the precipitated PPCA_Ca complex in different brines and at different temperatures.
9. To make some preliminary investigation of other polymeric inhibitors such as SPPCA and poly-functionalised copolymer (PFC) in order to understand whether the understanding we have developed for PPCA applies to other polymeric SIs.
10. To carry out some sand-pack floods in order to investigate the precipitation/dissolution characteristics of coupled adsorption precipitation squeezes at various flow rates for the PPCA system.

By addressing the above questions, this research has established that the solubility of the PPCA_Ca complex is not described by a simple "solubility product" model and a novel "stripping" model based on the MWD of the precipitate is proposed. All the above investigations carried out in this experimental research program will provide a background for the further understanding and modelling of polymeric scale inhibitors in precipitation squeeze treatments.

CHAPTER 3- **EXPERIMENTAL METHODOLOGY**

3.1 Introduction

This study is primarily concerned with identifying the phase envelope of PPCA and studying the solubility behaviour of the precipitated PPCA_Ca complex in terms of both threshold IE and squeeze lifetime. This chapter gives the detailed description of all the experimental work carried out in the course of this PhD, and all the experimental procedures are presented in the appendix. Topics are discussed under the following headings:

1. The combination of static compatibility tests and static coupled adsorption/precipitation tests with different masses of sand helps to differentiate between pure adsorption (Γ) and coupled adsorption/precipitation (Γ/Π) behaviour. This will be discussed in detail in Chapter 4.

2. Precipitation/Re-dissolution experiments are used to study the stoichiometry* of the PPCA_Ca complex and the solubility of the precipitated PPCA. (*i.e. the value of n in the complex Ca_n_PPCA). These experiments are also helpful to produce samples for MWD studies of PPCA. This is discussed in detail in Chapters 4, 5 and 6.

3. IE Tests - experimental IE results are used to establish the MIC of various fractions of the PPCA including the Stock, the Supernatant and the Precipitated PPCA. This is discussed in detail in Chapter 4.

4. Wet Chemical Analysis (by Hyamine) is used to make an accurate assay of the lower end concentrations polymeric content at in the various PPCA fractions including the supernatant, the precipitated PPCA and the stock PPCA solution. These wet chemical polymeric assays are compared with ICP values. They both produce the concentration of PPCA by two different methods. This is discussed in detail in Chapter 4.

5. Other Polymeric SIs were introduced in Chapter 8 to study the IE and MWD behaviour of other species in order to compare the results with those for PPCA.

3.2 Precipitation Test Methodology for this Research

The schematic diagram shown below represents the thesis methodology and approach. The test methodology is comprised of 4 stages as follows:

1. Compatibility Stage
2. Re-dissolution Stage
3. Analysis on the 3 fractions of SI- IE Test, Wet Chemical Analysis and MWD Study
4. Sand-pack Flood Studies

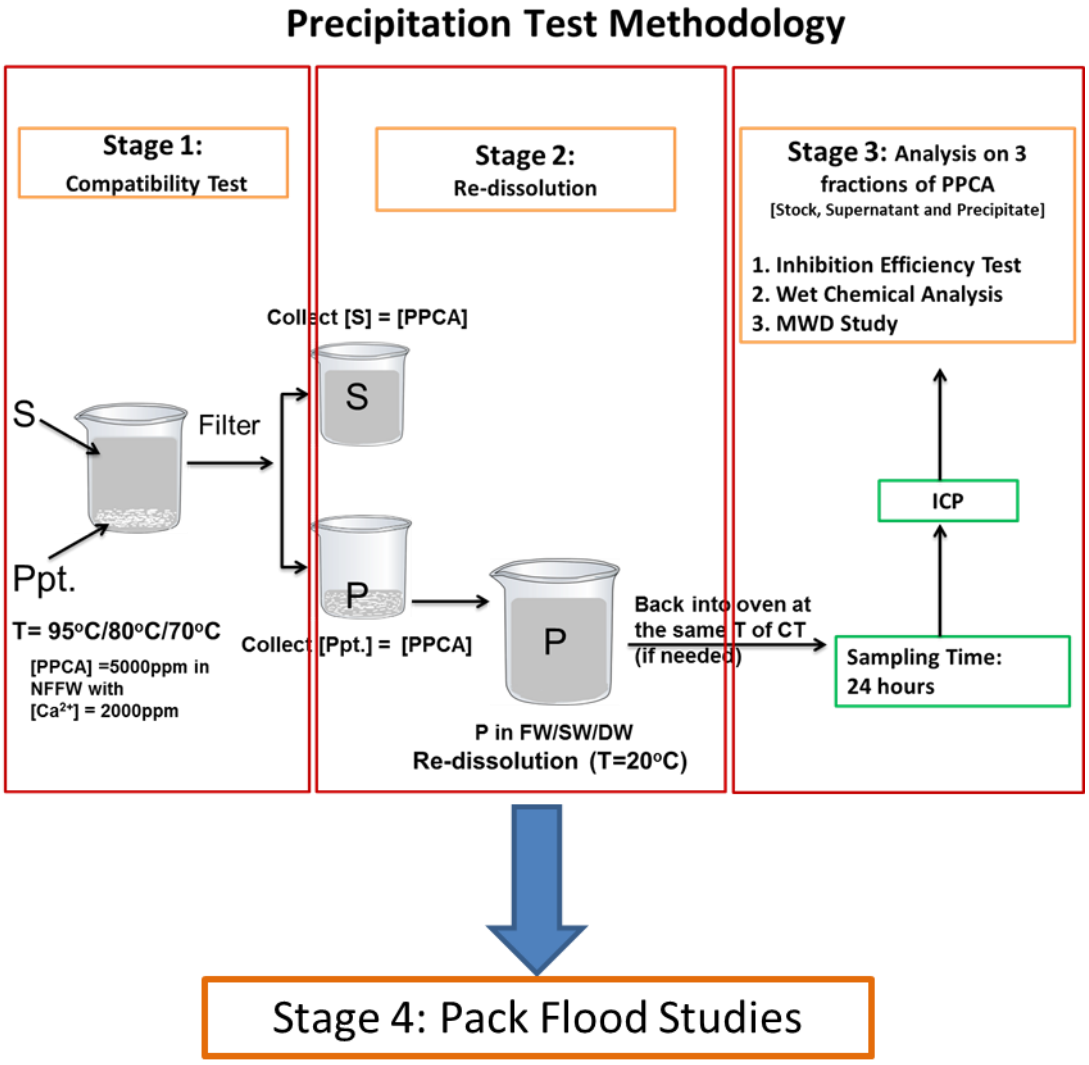

Figure 6: Schematic Diagram of the Test Methodology and general approach of this Research

In the compatibility stage, the single phase PPCA solution at elevated temperature separated into two phases; these are denoted throughout this work as precipitate and supernatant. A range of experiments were performed in this stage in order to check the effect of pH, temperature and [Ca^{2+}] on the overall phase behaviour of the PPCA/brine system. The experiments, such as the static compatibility and coupled adsorption precipitation tests, were performed to find the precipitation and/or adsorption regions for the PPCA/brine system. The details of these experiments are discussed later in this chapter, and the results are discussed in Chapter 4. The experiments from this stage of the study led to the development of the phase envelope of PPCA. The phase envelope of PPCA is used as a map to locate the regions of maximum precipitation and it allowed us to study the range of factors affecting the precipitation and the performance of PPCA.

From the compatibility stage, three fractions of PPCA were identified and obtained as separate samples; i.e. stock, supernatant and precipitated PPCA. The detailed characterizations of the various fractions of PPCA were carried out in re-dissolution stages as described in Chapter 5, which deals with the solubility of the precipitate as a function of various parameters. The re-dissolution study of the PPCA_Ca complex led to the proposal of a solubility product which will be discussed in detail in Chapter 5 and also linked to the results on MWD of the various PPCA fractions presented in Chapter 6.

Each of the three fractions of PPCA obtained in stage 1 were analysed for their IE performance and their polymer content (by Hyamine). How the IE performance and polymer content of each fraction was affected by temperature was also studied and results are discussed in Chapter 4. The MWD study for each fraction of PPCA is discussed in Chapter 6. The experimental details for each analysis method are provided later in this chapter.

Following the detailed characterization of PPCA by static bottle tests, we then study the PPCA/brine precipitating system in a series of dynamic sand pack floods carried out at multiple flow rates. The experimental details for this stage are discussed in Chapter 7.

After developing a good understanding of the PPCA/brine system as it applies in precipitation squeeze treatments, a similar study was conducted on some other related

polymeric SIs having similar chemical structure to PPCA; viz. SPPCA and PFC; the details of these experiments and the results obtained are discussed in Chapter 8.

3.3 Experimental Details

3.3.1 Materials

All the experimental work was performed on the polymeric SI - PPCA which is supplied as an active product. The industrial name of this SI is Bellasol S40. This is one of the commercial ranges of polymeric SI products, widely used in oilfield applications. This particular product was originally supplied by Biolab. Details of SI, commercial name and activity are presented in

Table 2. All inhibitor solutions were prepared in NFFW; composition is presented in Appendix A, Table 17. For all the experiments, the pH was adjusted to pH 6, unless otherwise stated.

PPCA – Phosphino poly carboxylic acid

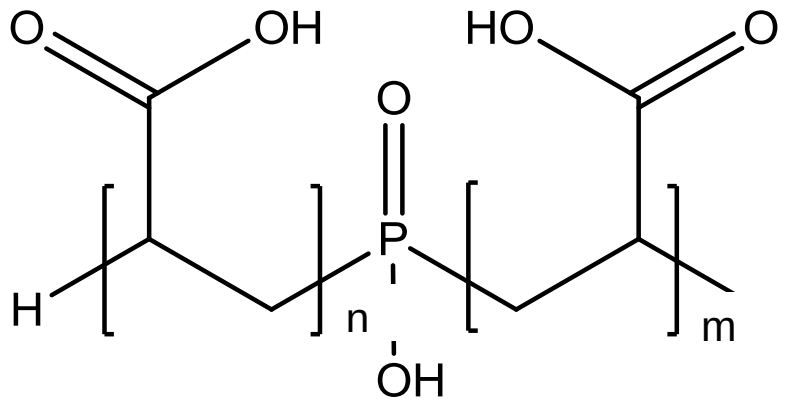

Figure 7: Chemical Structure of PPCA.

3.3.2 Solvent Preparations:

Prepare 1L of 10,000ppm active FW stock solution for scale inhibitor:

Supplier	Scale Inhibitor	Weight Required (in 1000ml FW)
Biolab	Bellasol S40 (PPCA)	23.80g

Table 2: Details of Polymeric SI, group and Activity

Supplier	SI name	Generic name	Type	Batch number	Date received
Biolab	Bellasol S40	PPCA	Polymer type	BFEJ04C2	APR 2008

3.4 Results Discussed in Each Chapter are as follows:

3.4.1 Chapter 4 will discuss the following:

I. Static Compatibility and Coupled Adsorption/Precipitation Experiments

Static adsorption tests and static compatibility tests were performed to evaluate the adsorption and coupled adsorption/precipitation behaviour of PPCA polymeric SI with synthetic NFFW. For the static adsorption tests, the experiments were performed using different masses of sand (m = 10g, 20g and 30g) at a fixed volume (V) of SI solution (typically, V = 0.08L) to evaluate the apparent adsorption or coupled adsorption/precipitation behaviour. In the corresponding static compatibility tests, the experiments were performed to evaluate the pure precipitation (only) behaviour, since no mineral was used in these tests.

Both types of experiment were performed at a range of temperatures viz., 50^{o}C, 80^{o}C and 95^{o}C at pH = 6 in all cases. Stock solutions of PPCA were prepared using synthetic NFFW. The composition of NFFW is given in Appendix A, Table 17. Experiments were conducted at the following range of concentrations, – blank (0), 50, 100, 500, 800, 1000, 2000, 4000ppm of PPCA. After 24hrs at the respective temperatures, the solutions were filtered through a 0.22μm filter paper and then analysed for phosphorus, calcium, magnesium and lithium by using ICP and the pH values were measured using a pH probe. The amount of SI retained by the mineral, Γ (adsorption in mg SI/ g rock), was calculated using the expression (Kahrwad et al, 2008):

$$\Gamma = V\left(c_o - c_f\right)/m \qquad (2)$$

Where c_o and c_f are the initial and final SI concentrations, V is the SI solution volume and m is the mass of the substrate. For static compatibility tests, the filter papers were weighed and sent for ESEM-EDAX analysis to check the presence of phosphorus, calcium and magnesium.

Objective: The objective of static adsorption experiments was to investigate the apparent adsorption (Γ_{app}) vs. [SI] isotherm behaviour. The coupled adsorption precipitation experiments indicate the level of precipitation at higher concentrations and level of adsorption at lower concentrations when SI is mixed with formation water brine in the presence of selected rock minerals. The concentration of the cations including phosphorpous and lithium can be analysed before and after heating by ICP. The difference in concentration of these elements before and after experiment will indicate the system is whether adsorption or precipitation based.

Mineral: To study the adsorption behaviour of PPCA, dry silica sand (as supplied) is used as an adsorbent as the majority of sandstone rock is quartz. X-ray diffraction analysis shows this sand has a composition of ~80-90% quartz. The shapes of the particles are either round or square. The chemical compound silicon dioxide (chemical formula SiO_2), also known as silica, is an oxide of silicon. Silica sand also represents a simple model of a sandstone formation.

Test Conditions: For all the coupled adsorption/precipitation experiments, except temperature, all the test conditions are identical, and are set to achieve consistent and comparable results.

Temperature (T) = 95oC, 80oC, 60oC
pH = 6

Volume of test solution (V) = 0.08L

Mass of Substrate (m) = 10g, 20g and 30g

Pressure (P) = N/A

Mixing Ratio = N/A

Flow Rates = N/A

Mineralogy = Sand (as supplied)

Sampling Times = 24 hours after heating. Each test was performed in duplicate

Note:

1. All samples including the blank are pH adjusted to pH 6 by using dilute HCl or NaOH prior to starting the experiment.
2. The three masses of mineral substrate (10g, 20g, and 30g) were used in all the experiments, while the fluid volume is fixed at 0.08L (80ml). The precise (m/V) ratio is important. It gives us apparent adsorption vs. [SI] results at different (m/V) ratios which allow us to differentiate between pure adsorption and coupled adsorption precipitation behaviour.

Preparation of Bottles and Labelling: The volume of brines used for each static adsorption test is 80ml (0.08L). The bottles are numbered to track each concentration used. Each experiment was carried out in duplicate to assure the consistency of the results.

Table 3: showing number of bottles and their labelling

Bottle No.	*[SI], ppm active*
1	Blank
2	Blank
3	50
4	50
5	100
6	100
7	500
8	500
9	800
10	800
11	1000
12	1000
13	2000
14	2000
15	4000
16	4000

Preparation of SI concentration and Volume: To prepare 1000ml, of 10,000ppm PPCA active solution in FW, (1000ml is prepared to cater for four experiments) use 1000ml volumetric flask.

1. Static Adsorption Test- 10g
2. Static Adsorption Test- 20g
3. Static Adsorption Test- 30g
4. Compatibility Test- No Sand

Each experiment requires 250ml solution. It is highly recommended that the stock for all above experiments should be the same for good consistency results.

II. Static Inhibition Efficiency Test

The procedure for the IE test is not straight forward for this research; therefore the two step experiment was conducted to check the efficiency performance of the various fractions of PPCA.

In the compatibility stage, the supernatant was separated from the precipitate, but without filtration. ICP analysis determines the concentration of PPCA in the supernatant. This is used in the back calculation of the precipitate which is dissolved back into the FW up to a volume where we dilute [SI] of the precipitate such that it is redissolved. After dissolving the precipitate back in to the FW, ICP determines the concentration of PPCA again in precipitated sample. This is the end of stage 1.

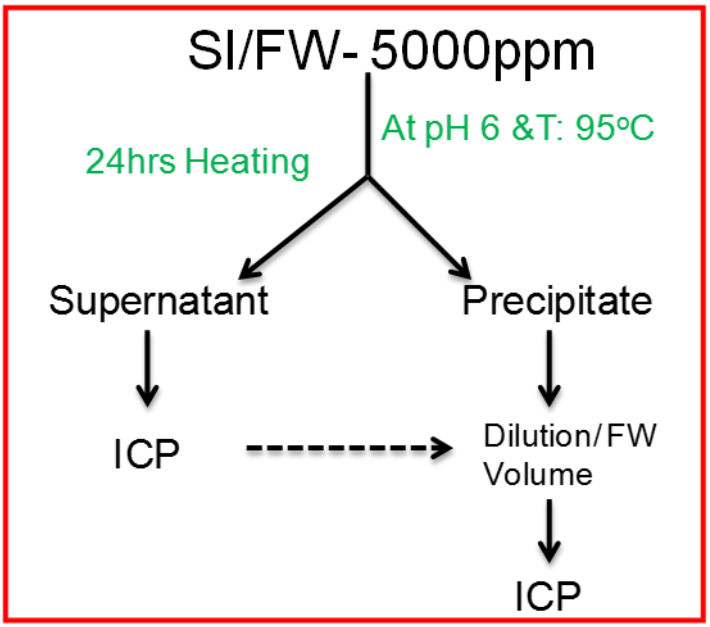

Figure 8: Schematic Diagram of Compatibility Test- Stage 1

In stage 2, we now have solutions of stock (the original PPCA sample) along with supernatant and redissolved precipitate which are further diluted down to further test PPCA concentrations e.g. 10, 20 and 40ppm. It is these diluted solutions of PPCA which then must be used in IE tests. The IE testing ratio was 50:50 for the FW/SI with SW. This test is performed only at 95°C. The buffer was added to the solution (FW/SI) to maintain the pH at 5.5. In the 50:50 mix, the concentration of PPCA was 5, 10 and 20ppm. For IE tests, we measure the concentration of barium which was left in the solution after 2 and 22 hours.

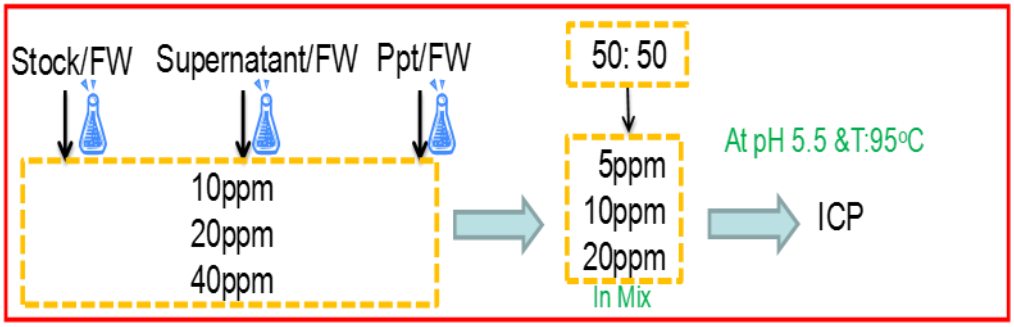

Figure 9: Schematic Diagram of Inhibition Efficiency Test- Stage 2

Objective: The objective of this two staged experiment is to develop different fractions of PPCA e.g. stock, supernatant and precipitated PPCA and compare the IE performance against barite scale. This experiment is performed at two different temperatures, viz.

95^{o}C and 70^{o}C to check the variation in the MIC level for each fraction. The SI and cation consumption for all the experiments, and the [Ba^{2+}] at various stages of a static IE test were assayed by ICP spectroscopy.

ICP Spectroscopy: ICP is recognised as a very effective tool for monitoring ion compositions in water originating from a variety of industrial and natural processes. Many laboratories routinely use this technique to determine the ionic composition of oilfield brines. The inhibitors that were analysed are phosphonates and a polymer based inhibitor containing P, in both synthetic and field produced waters. The methods employed gave accurate assay results for both inhibitors, in both the synthetic and field produced brines. Phosphonate analysis is performed on the ICP; however it has been observed that better sensitivity and repeatability is gained for PPCA, not by ICP but by wet chemical analysis (Hyamine). The technique of ICP has the advantage of robustness with respect to solution interferences which affect many wet chemical techniques. Also, ICP is cost effective, quick, and can analyse many samples in a single run. It is much less time consuming than Hyamine for the analyst and can therefore be used more commonly to determine residual levels of scale inhibitor in produced water.

ICP is an instrumental analysis technique based on atomic emission spectrometry. The quality of the results therefore depends primarily on the quality of the spectrometer used to analyse the light emitted by the atoms in the sample introduced into the torch. ICP-OES (Optical Emission Spectroscopy) uses inert, optically transparent Argon gas to create a high temperature plasma (up to 10,000K), generated by radiomagnetic fields induced by a copper coil. Samples are introduced via an autosampler and nebulised into an aerosol before entering the plasma in which the atoms of the various analyte elements are excited. The atoms in the plasma emit light (photons) with characteristic wavelengths for each element. This light is recorded by one or more optical spectrometers, which provide optimum sensitivity across the full wavelength range from 160-800nm, when calibrated against standards. For PPCA, the calibration standards use PPCA scale inhibitor so a measure of [P] is directly related to [PPCA], thus providing a quantitative analysis of the original sample.

III. C18 / Hyamine / Spectrophotometric (CHS) Analytical Technique

This is the third stage experiment discussed in Chapter 4. After compatibility stage 1 as shown in Figure 6, we now have solutions of stock (the original PPCA sample) along with supernatant and redissolved precipitate. In this work, the "reference" method of assay of the polymer is by ICP analysis (for total phosphorus, P as in PPCA). The most accurate method for the determination of PPCA (and PAA/PMA) is the Hyamine method described below. This relies strongly upon the separation (and concentration if required) of the polymer's functional group from interfering species, such as the brine salts. This is accomplished by the use of reverse phase, single-use C-18 chromatography cartridges.

The polymeric content of SIs is typically assayed by the wet chemical C18/Hyamine assay method (see Boak and Sorbie, 2010). In the C18- Hyamine method, a calibration graph is constructed for known polymer concentrations and their corresponding determined absorbance values. A rule of thumb for dilution of unknown sample concentrations is to assume maximum concentration used in the experiment and perform an appropriate dilution so that the determined absorbance value lies in the middle of the calibration range.

This method is based on turbidimetry in which light is passed through a filter creating a light of known wavelength, which is then passed through a cuvette containing the solution to be measured. A photoelectric cell collects the light which passes through the cuvette. The instrument is zeroed against a sample with all the reagents but none of the reactant (analyte) so that it fulfils the requirement for a blank that is optically equal to real samples with a zero concentration. A measurement is then given for the amount of light absorbed. A sample with lower concentration absorbs more light than the control and samples with high concentration absorb even more light than lower concentration.

The method involves making measurements of a series of standards. This establishes the connection between absorbance and reactant, i.e. a calibration curve is constructed. The data obtained from this calibration are used in a linear regression to obtain an equation relating absorbance and concentration. This can be used to calculate reactant concentration in real samples from their optical absorbance using the same chemical reaction. Therefore the results of Hyamine 1622 tests were used to compare with the

results from ICP. They both measure the concentration of PPCA by different methods described above. ICP and Hyamine methods measure different physical/chemical properties of the PPCA. ICP measures phosphorus concentration and Hyamine measures polymeric content via the functional group concentration.

Overview: This method is based on the turbidimetric determination of the precipitation obtained by the interaction of anionic polyelectrolytes, such as COO^- ions from COOH groups, with a quaternary ammonium salt such as Hyamine 1622. Baker Performance Chemicals supplied a working method to the former FAST, the OSRG, in 1994. This was examined for a range of polyacrylate based inhibitors in synthetic sea water. Since the method is susceptible to interferences from dissolved ions, in particular chloride ions, a separation stage involving adsorption onto C18 cartridges is necessary. Thus, the analytical procedure is much more solution robust than those for phosphonate based inhibitors. The process by which these cartridges perform is discussed in the appendix.

Batch List: The Hyamine experiments were performed in 3 different batches for 3 different concentrations for each fraction of PPCA. The maximum we can analyse are only 10 samples at a time.

0ppm	0ppm	0ppm
1ppm Standard	5ppm Standard	8ppm Standard
1ppm Stk	5ppm Stk	8ppm Stk
1ppm Stk	5ppm Stk	8ppm Stk
1ppm Supernatant	5ppm Supernatant	8ppm Supernatant
1ppm Supernatant	5ppm Supernatant	8ppm Supernatant
1ppm Ppt	5ppm Ppt	8ppm Ppt
1ppm Ppt	5ppm Ppt	8ppm Ppt
0ppm	0ppm	0ppm
1ppm Standard	5ppm Standard	8ppm Standard

3.4.2 Solubility Experiments (Discussed in Chapter 5)

For all the solubility experiments, the precipitated PPCA was recovered from compatibility experiments at 5000ppm of PPCA with 2000ppm of calcium in NFFW at pH 6 at 95^{o}C. The solubility and properties of the PPCA_Ca precipitate can then be measured at various temperatures and salt concentrations. The solubility of this precipitate in various brines was measured i.e. FW, SW and DW and its solubility under successive exposure of the precipitate to the fresh brine was studied.

Short descriptions of the experiments are presented along with results wherever discussed in this thesis.

3.4.3 Molecular weight Distribution of PPCA (Discussed in Chapter 6)

The average weight averaged molecular weight (M_w) of PPCA is given as 3800g/moles (3800Da) by the supplier. To describe the properties of the polymer, not only average molecular mass but the MWD is also required. This work set out to either demonstrate or refute the hypothesis that most of the experimental beaker test results on the IE, precipitation behaviour and assay of PPCA can be explained in terms of what was happening to the MW of the PPCA. More specifically, it was thought that all results would be even better explained if we could determine the MWD of the PPCA for different stages of the precipitation/dissolution process. After precipitation (or phase separation) of aqueous polymers, either by changing the temperature or adding a non-solvent (e.g. methanol), the highest molar mass species phase separate first and so polymer fractions are precipitated in order of decreasing molar mass. The experimental details with the following results will be discussed in Chapter 6.

3.4.4 Multiple Flow Rate Dynamic Pack Flood (Discussed in Chapter 7)

The above chapters discussed the various aspects of the bulk PPCA/brine system in the context of its use in precipitation of squeeze treatments. In these dynamic tests, the SI (PPCA) is flooded into a sand pack core at reservoir conditions and back produced at multiple flow rates using formation water and/or 1%NaCl solution. The experimental details will be discussed along with the results in Chapter 7.

3.4.5 Other Polymeric Scale Inhibitors (Discussed in Chapter 8)

The two more polymeric scale inhibitors, viz. SPPCA and PFC were studied in some detail. SPPCA is a sulphonated copolymer of the standard PPCA and the PFC is a copolymer including phosphonate and sulphonate groups along its backbone. In these studies, we have evaluated the compatibility of these inhibitors under different conditions (pH and temperature), in order to understand their phase behaviour in operating conditions in the oilfield. The supernatant and precipitate were obtained in a similar manner as for the PPCA samples in compatibility tests. The samples were analysed by GPC to determine Mw, Mn and MWD of these polymeric scale inhibitors. This was then used as in the PPCA case to understand the IE performances of the various fraction of the SIs. The experimental details will be discussed along with the results in Chapter 8.

CHAPTER 4- **PHASE ENVELOPE OF PPCA**

In this chapter, we will discuss the Phase Envelope of PPCA. We will examine the effects of various parameters on this phase envelope, such as concentration of calcium and scale inhibitor (SI), pH, and temperature. Later, we will also consider the molecular attributes which influence the behaviour of the SI_Ca phases. We will scan the Phase Envelope using the following experimental approaches:

1] Coupled Adsorption Precipitation Experiments;

2] Precipitation and Redissolution Experiments;

3] Experiments to establish the Stoichiometry of PPCA_Ca complex;

4] Inhibition Efficiency of the fractions of PPCA (stock, [S], [P]);

5] Wet Chemical Analysis on different fractions of PPCA (Stock, Supernatant [S] and Precipitate [P])

4.1 Introduction

In precipitation squeezes, we try to use a scale inhibitor designed to give a controlled, more uniform inhibitor concentration return level in produced water. PPCA is a polymeric SI widely applied in the oil industry in precipitation squeeze treatments. PPCA contains phosphorus on the backbone of the polymer chain which is detectable by ICP. In addition, the PPCA can also be assayed by wet chemical analysis which establishes the polymeric content of the species. In field precipitation squeeze applications, the PPCA may include a proprietary electrolyte activator that promotes phase separation (or precipitation) in order to create the desired retention/ release behaviour.

PPCA works in the field by going through a transition process as it is heated to reservoir conditions. The added electrolyte helps to increase the ionic strength of the solution. Thus the ions can be adsorbed onto the polymer chains and repulsive forces between the chains can be reduced which causes them to coil at low temperature and makes the viscosity much lower. In the application brine, the polymer dissociates into anions;

PPCA is described as poly-anionic. When the mixture is heated, the remained polymer uncoiled (rod like configuration) in the solution begins to associate with cations such as calcium (Ca^{2+}) which are present in the brine solution. At elevated temperature, the solution first gets cloudy and then, as the temperature goes up, polymer forms a complex with cations and precipitates out at the bottom. The precipitated polymer complex is rather more like a semi-solid or gel than a solid precipitate (Rabaioli and Lockhart, 1995).

In this chapter, we develop the phase precipitation diagram of PPCA – referred to as the 'PPCA phase envelope'. We investigate the behaviour of the PPCA by examining various factors which are responsible for influencing the phase separation. This will continue with our detailed characterization of the PPCA phase envelope and some gaps in our knowledge of this phase envelope will be filled.

The phase behaviour of PPCA is studied at a range of solution pH values and we note where precipitation of PPCA occurs. We also examine the effect of calcium in compatibility tests and we measure the quantitative losses of PPCA and calcium which occur in the formation of the precipitated SI_Ca complex. Such measurements allow us to determine the actual stoichiometry of the complex i.e. the value of n in SI_Ca_n. We also studied the effect of temperature by performing coupled adsorption/precipitation experiments over a range of temperatures.

MW effects have been shown to be important for PPCA in precipitation or phase separation squeeze treatments. These processes rely upon the interaction of the inhibitors with certain metal cations such as calcium and these interactions also depend on pH and temperature. It is well known from the literature that higher MW components are more efficient scale (crystal growth) inhibitors, and that these higher MW components also exhibit preferential precipitation. Therefore, MW is clearly a controlling factor in the inhibition, adsorption and precipitation behavior of polymeric scale inhibitor species, such as PPCA. We discuss the MWD in detail in Chapter 6; however, in this chapter we will see the effect of MWD in different fractions of PPCA generated from the compatibility tests. Furthermore, in the current set of precipitation experiments, we will determine the actual PPCA concentration in both the supernatant and in the precipitate by using C18- Hyamine method and the results from such wet chemical tests are then compared with the corresponding ICP results (which measure

only elemental phosphorus). In addition, we also study the IE of both the precipitated and supernatant PPCA solutions at different temperatures since this will have relevance not just in determining the concentration of the polymer (PPCA) in the return curve but also in its ability to prevent scale formation (i.e. its IE in the PPCA return curve).

4.2 Experimental Details

Material: PPCA is used as a SI in these experiments mainly deployed in NFFW brine. These experiments were performed over a range of temperatures (from 20^{o}C to 95^{o}C) at pH 6 with varied [Ca^{2+}] = 1000ppm and 2000ppm and varied [SI_{active}] = 500ppm, 2000ppm and 5000ppm. At each temperature, the solutions were studied in duplicate over a 24 hour period. For details of the experiment refer to Chapter 3.

Static precipitation/redissolution tests were performed to develop the phase envelop of PPCA. Each inhibitor concentration was adjusted to pH 6 and at 5 temperatures viz., 20^{o}C, 40^{o}C, 60^{o}C, 80^{o}C, 95˚C. This test involves heating the test bottles at each temperature over 24hrs to observe any precipitation of the SI_Ca complex before repeating the process by then subsequently gradually reducing the temperatures and again holding the solution at each temperature for 24 hours. Performing such temperature scanning cycles (i.e. stepped rise of temperature followed by a stepped decrease) allows us to monitor both the precipitation and then re-dissolution of any SI_Ca complex formed. After 24 hours at each temperature on the scanning cycle, the sample was taken from the top of the bottle without disturbing any precipitate and was diluted to 10x dilution with 1%Na as NaCl. No filtration was required for these samples since the top part of the bottles were always quite clear. After sampling, the temperature was then adjusted to the next required temperature. Since, 24 hours was given for each temperature stage to be at equilibrium (which was checked), then this experiment was carried out over about 2.5 weeks. The test was performed twice in an oven to check the consistency of the results.

The diluted samples were analyzed on ICP for [SI], [Ca^{2+}], [Mg^{2+}] and [Li^{+}]. The sample solutions down to 10x in 1%Na to find C_o values (initial concentrations), and C_f values (final concentrations after the precipitation or re-dissolution process).

4.3 Results and Discussion

4.3.1 Phase Envelope of PPCA

The phase envelope of PPCA was developed in 3 stages. The precipitation was first observed qualitatively to find its general form, the same parameter space was then measured quantitatively and finally the quantitative phase envelope of PPCA was mapped out using contours (see below).

Qualitative Check - PPCA Precipitation: The first experiments which were carried out in this work were simple visual checks where no ICP measurements were performed. This experiment was designed to check at what temperature and at what particular [SI] and [Ca^{2+}] that PPCA will starts to precipitate at pH 6. This was done to scope out the phase envelope of PPCA before more detailed quantitative measurements were performed (see below). In these purely visual tests, results were defined on a subjective scale (represented in Table 1). 0 denotes a clear solution; where 1 and 2 denote a cloudy or hazy appearance and 3, 4, 5 denote successively higher observed levels of precipitation. Such qualitative results are shown at 3 temperatures in Figure 10, Figure 11 and Figure 12.

Table 4: Subjective Scale for the Precipitation of PPCA

Subjective scale for the Precipitate of PPCA	
Clear	0
Hazy/Cloudy	1, 2
Precipitate	3, 4, 5

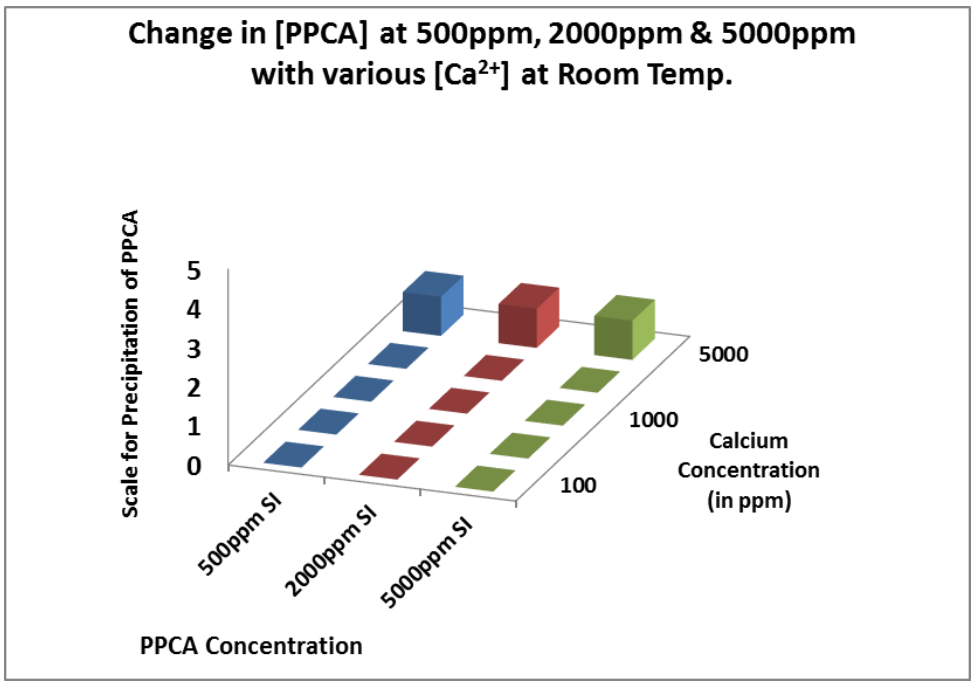

Figure 10: Change in [PPCA] at Room Temperature ($20^{O}C$)

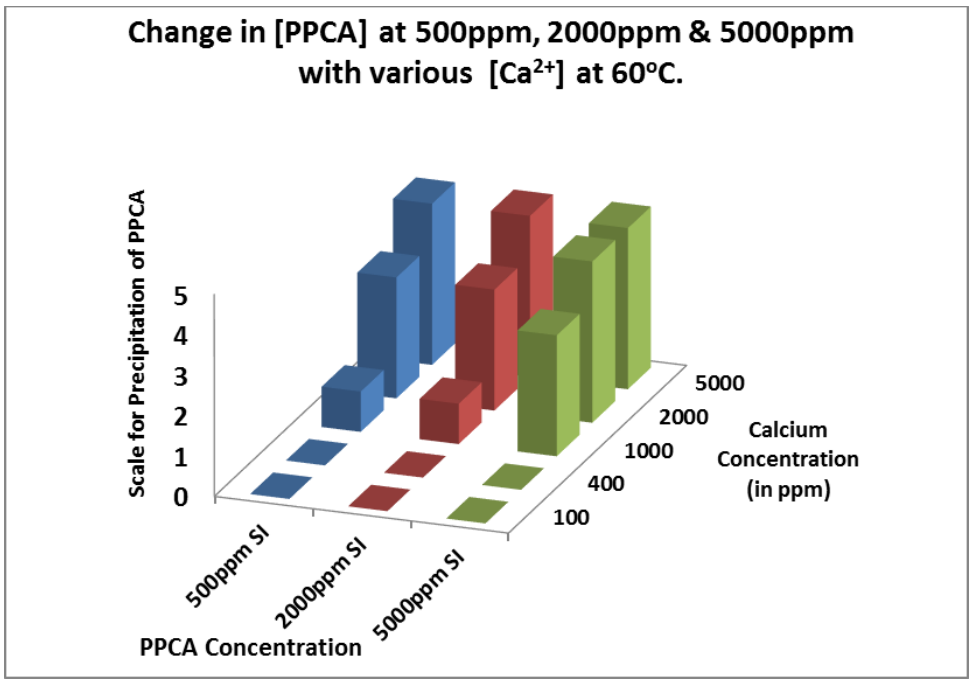

Figure 11: Change in [PPCA] at $60^{O}C$

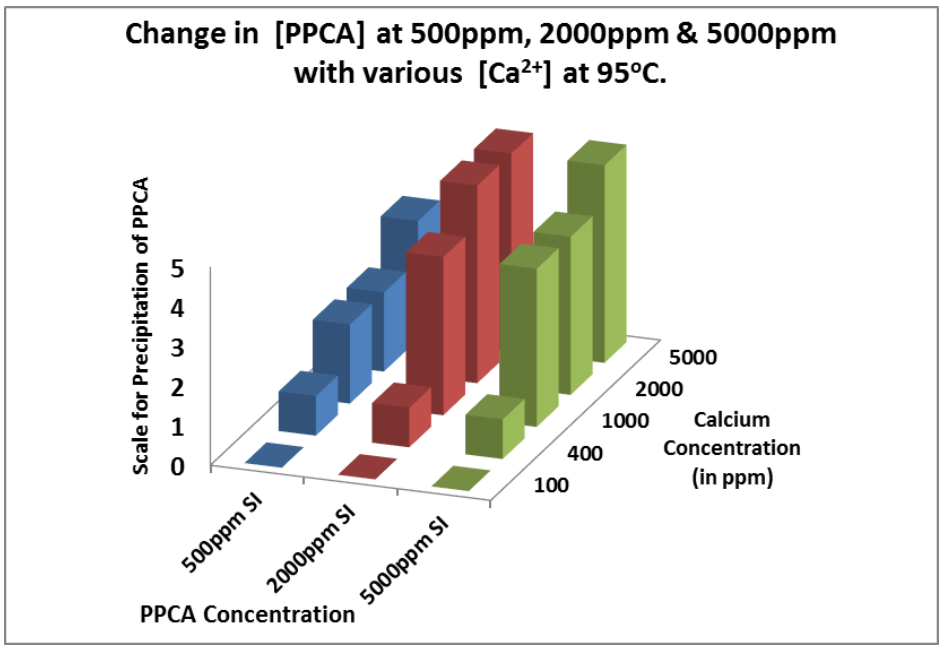

Figure 12: Change in [PPCA] at 95^{O}C

The qualitative check for the precipitation levels of PPCA performed through compatibility tests at 500ppm, 2000ppm and 5000ppm at room temperature (RT, ~20^{o}C), at 60^{o}C and at 95^{o}C, respectively. The experiment was conducted at five different calcium concentrations, [Ca^{2+}] = 100, 400, 1000, 2000 and 5000ppm at 3 temperatures (20^{o}C, 60^{o}C and 95^{o}C). Clearly, in these compatibility tests, only pure precipitation of PPCA_Ca complex is being observed.

The precipitate was generated by first preparing the homogenous solution of inhibitor in calcium rich brine. This phase envelope experiment was performed in an oven except for two [SI], i.e. 2000ppm and 500ppm, which were performed in a water-bath at 60^{o}C. It was clearly observed that water bath precipitates more than the oven and so this should be noted in future experiments.

The results presented in Figure 10, Figure 11 and Figure 12 give a clear idea of the PPCA_Ca precipitation region, which actually starts at 60^{o}C from 1000ppm of [Ca^{2+}] and 5000ppm of [SI]. However, when temperature rose from 60^{o}C to 95^{o}C, precipitation starts at 500ppm of [SI] with 5000ppm of [Ca^{2+}]. Particularly, the phase map shows that the 1000ppm [Ca^{2+}] is the threshold for the phase separation, even at lower inhibitor concentrations. This basic experiment for phase separation also shows that the extent of PPCA precipitation is quite small at room temperature. In conclusion, the observed trends in these results show that, as the temperature increases, precipitation occurs even

at lower PPCA and calcium concentrations. This is in good agreement with previous findings and is quite expected (Rabaioli and Lockhart, 1995; Browning and Fogler, 1993). The next section, however, shows the amount of precipitate formed is strongly influenced by the composition of the inhibitor/brine solution and the conditions of temperature and pH; such information will be important in the design of an optimal precipitation squeeze treatment using PPCA.

4.3.2 Precipitation and Re-dissolution Tests:

In the light of the above results, we undertook a systematic investigation of inhibitor precipitation as a function of pH, temperature and the concentrations of [Ca^{2+}] and PPCA. This experiment was designed as a quantitative evaluation of the precipitation of the PPCA_Ca complex. Initially inhibitor/calcium compositions with 1000ppm and 2000ppm [Ca^{2+}] brine were exposed to the cycle of temperatures i.e. from lower to higher temperature and then the subsequent re-dissolution from the same bottle from higher to lower temperatures at pH 6. This information will be useful to check the molar ratio of PPCA to calcium (see below). Results are shown in Figure 13 and Figure 14.

In the experiments described here, the stock samples remained at room temperature whereas samples were placed in the oven at the test temperature. The loss of concentration of species was measured at each temperature by ICP, i.e. [P], [Ca^{2+}], [Mg^{2+}] and [Li^{+}]. Any divalent ion levels above stock solution concentration are not expected or must be within its analytical error of less than 5%. The limit of analytical error is defined by the difference between the estimated value of a quantity (i.e. ICP assayed concentration) and its true value. In this thesis, it is expressed as the percentage of the true values. The decrease in the solution divalent ion levels is due to the complexation with SI, and the formation of the precipitate of SI_M complex. Any changes in [Li^{+}] were also noted in order to check the evaporation from the bottles in the oven. Lithium is used as an inert tracer ion which is usually unaffected by any reaction or physical conditions.

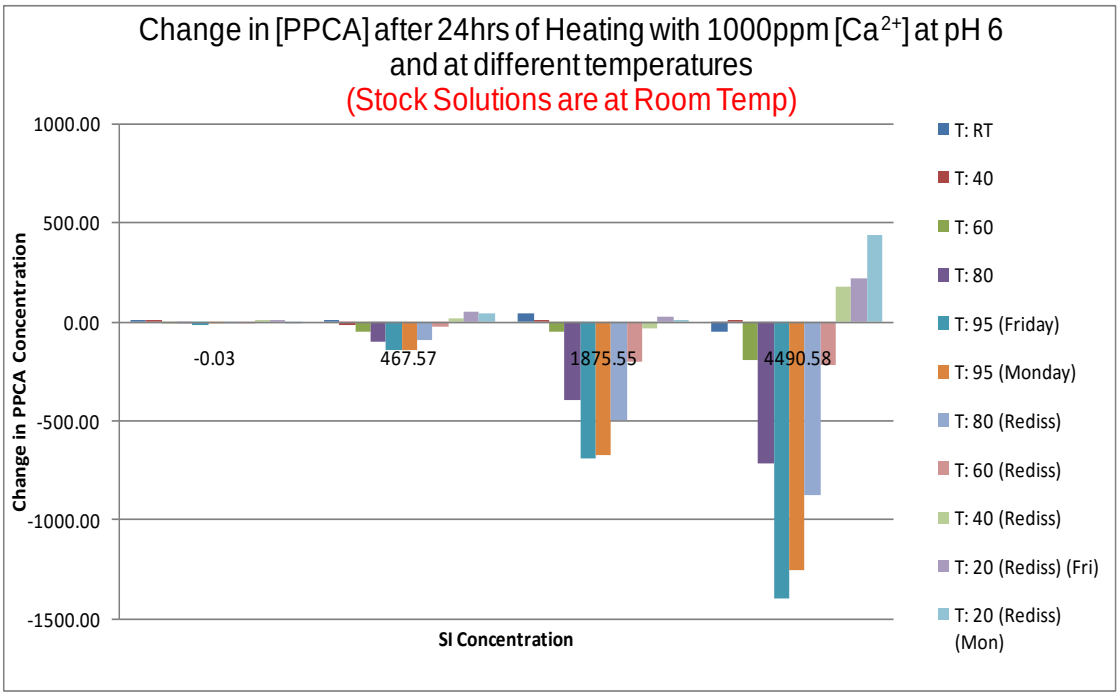

Figure 13: Change in [PPCA] at 1000ppm [Ca^{2+}]

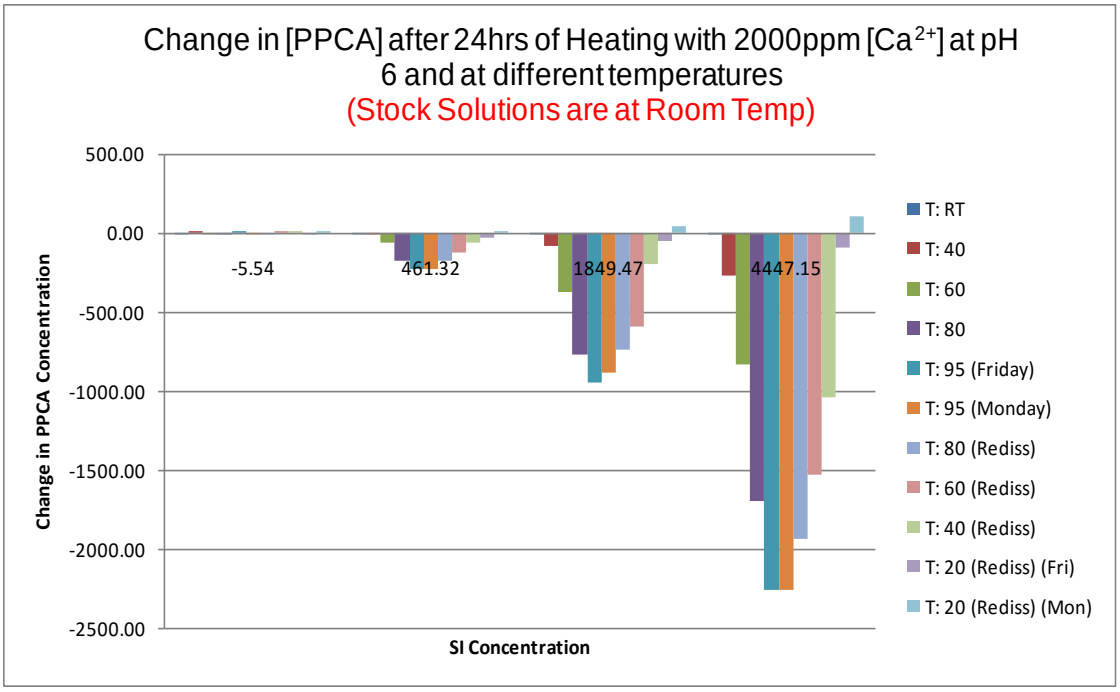

Figure 14: change in [PPCA] at 2000ppm of [Ca^{2+}]

Figure 13 and Figure 14 show the change in [PPCA] at 1000ppm and 2000ppm initial [Ca^{2+}], respectively at pH 6. The change was measured using stock samples at room temperature and the samples were carried forward from lower to higher temperatures. The graph clearly shows that as the temperature increases, more of SI drops out of the solution. Likewise, when the temperature reduces, scale inhibitor redissolved back into

the solution. It is also noted that, in some cases, there is a small increase in the [PPCA] assay on re-dissolution which is not expected, but this is below 5% i.e. within the acceptable range of analytical error. The corresponding changes in [Ca^{2+}] are shown in Figure 15 and Figure 16.

From Figure 13 and Figure 14, it is quite clear that the change in [PPCA] corresponds closely to the change in [Ca^{2+}]. Increased [Ca^{2+}] in the original solution causes more precipitation in the [PPCA] solution, i.e. more of the PPCA_Ca complex is formed. Results also indicate that, as the temperature increases, PPCA precipitates more and when the temperature reduces PPCA re-dissolves back into the solution. However, as noted above, the amount of re-dissolution of PPCA was *less* than the amount which initially precipitated.

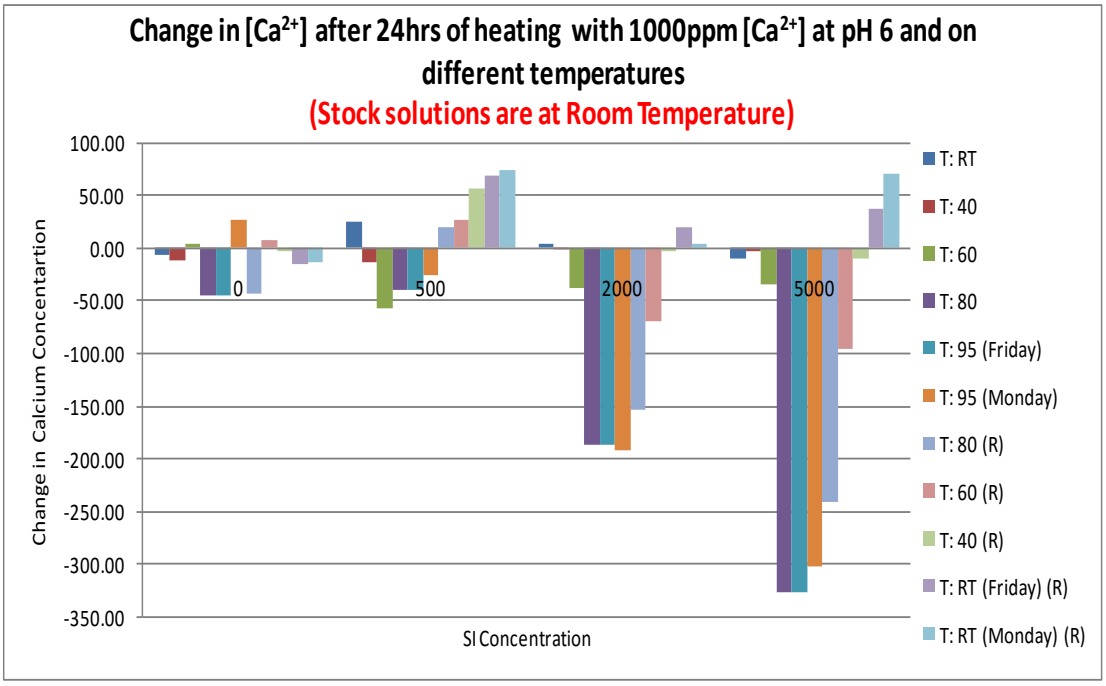

Figure 15: Change in [Ca^{2+}] when initially [Ca^{2+}] = 1000ppm

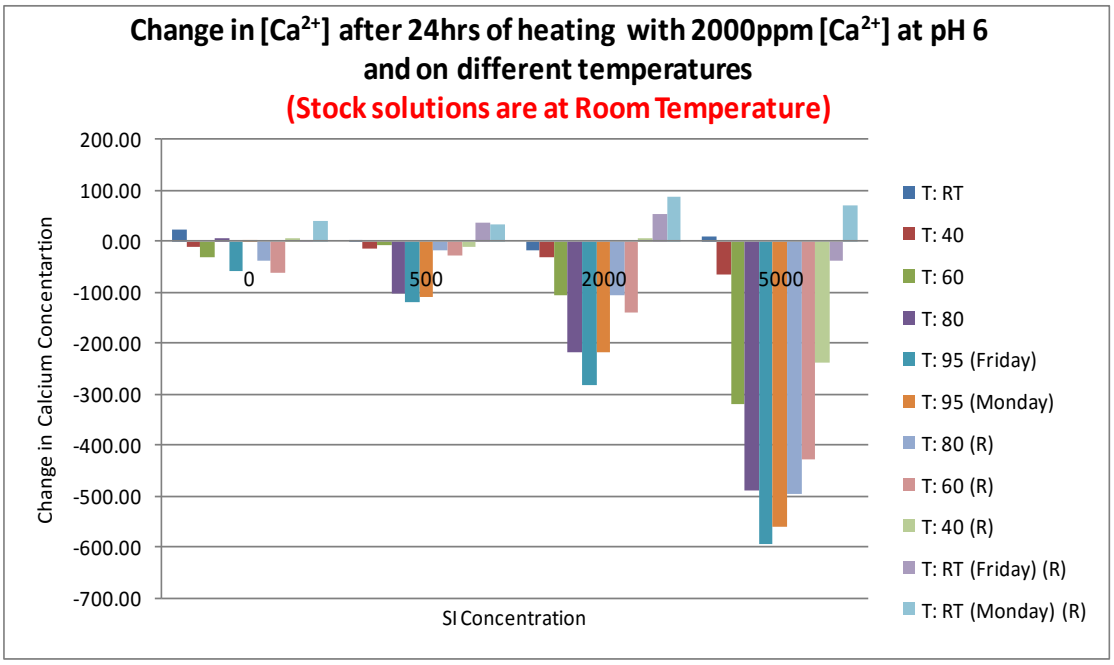

Figure 16: Change in [Ca^{2+}] when initially [Ca^{2+}] = 2000ppm

Figure 15 and Figure 16 show the change in [Ca^{2+}] from initial 1000ppm and 2000ppm [Ca^{2+}], respectively, at different temperatures. These figures show a significant reduction in calcium ion concentration at 2000ppm of [PPCA] and even more reduction at 5000ppm. That is, the reduction in [Ca^{2+}] increases as the [SI] and temperature increases. Clearly, this is due to the formation of the SI_M complex precipitate. The changes were measured using stock samples at room temperature and the sample bottles were taken through the temperature cycle from lower to higher temperature. The results indicate that [Ca^{2+}] shows a corresponding change to the [SI] in all cases; the actual drop in [Ca^{2+}] starts from ~2000ppm of [SI] and as the temperature reduces less PPCA_Ca complex forms.

ICP was also used to monitor the magnesium and lithium tracer concentrations. The results suggests that magnesium is not participating in the complexation of the PPCA since there is hardly any significant change observed in the initial and final concentration of the Mg. Lithium is used as inert tracer in the FW brine. The graph shows an increase of 1% to 3% in [Li^{+}], which indicates that acceptably low levels of sample evaporation were observed and the changes in [Li^{+}] and [Mg^{2+}] were within the acceptable range of analytical error (i.e. ~5%).

Quantitative Phase Envelope of PPCA: Using the results from the above experiments, we are now able to construct a quantitative version of the phase envelope of PPCA which was shown qualitatively in Figure 10, Figure 11 and Figure 12. Results are plotted in percentage (%) loss of PPCA against [PPCA] and temperature.

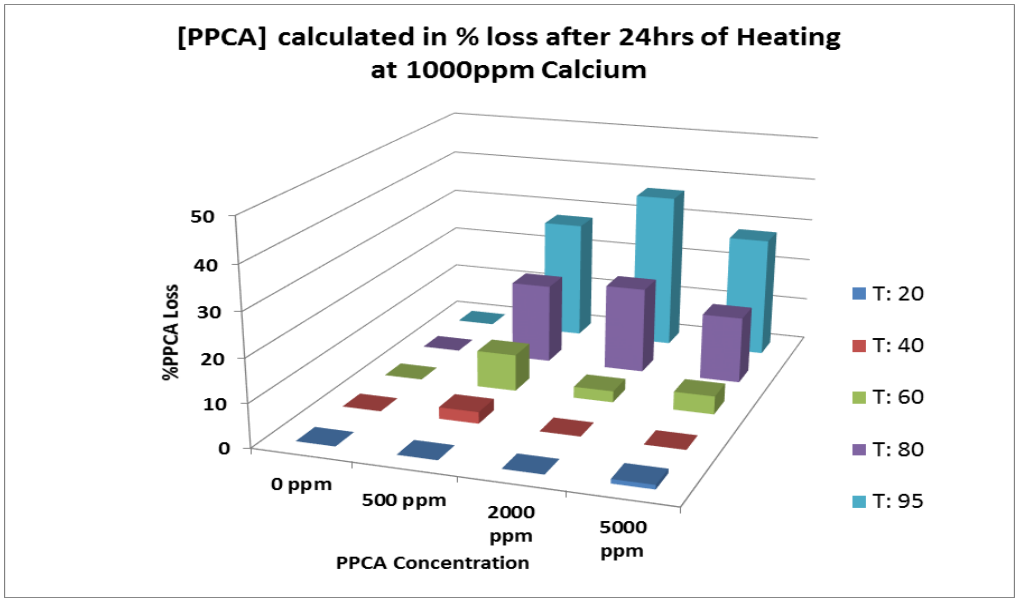

Figure 17: Quantitative % loss of PPCA; when [Ca^{2+}] = 1000ppm

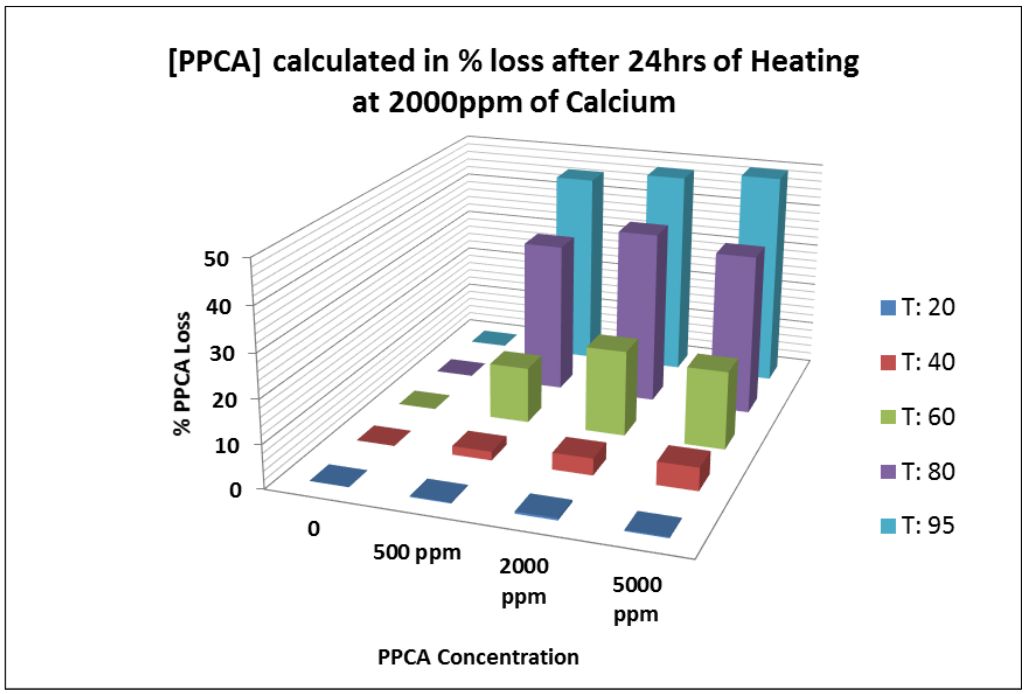

Figure 18: Quantitative % loss of PPCA; when [Ca^{2+}] = 2000ppm

Figure 17 and Figure 18 shows some interesting trends; for example, for a fixed initial [PPCA] = 5000ppm, we note that the onset of precipitation is at T ~40^{o}C, but as T

increases up to 95°C, then the amount of precipitate increases i.e. the solubility of the PPCA_Ca_n complex is lower at higher temperature. Thus, there is not a sharp phase boundary for PPCA but instead the boundary starts as a slight clouding and then deeper inside the phase envelope a much clearer "precipitate" is observed. Overall, higher temperature, higher calcium concentration and increased pH enhance the precipitation level of PPCA. Again, this is in good accord with previous experiments carried out by FAST and by several other workers (Andrei and Malandrino (2003), Andrei et al (1999), Breen et al (1990), Graham and Sorbie (1995, 1996), Malandrino et al (1995) and Rabaioli and Lockhart (1995, 1996)).

Phase Envelope of PPCA: Using the results of the precipitation and re-dissolution experiments, we are now able to construct a quantitative version of the phase envelope of PPCA which is shown in Figure 19.

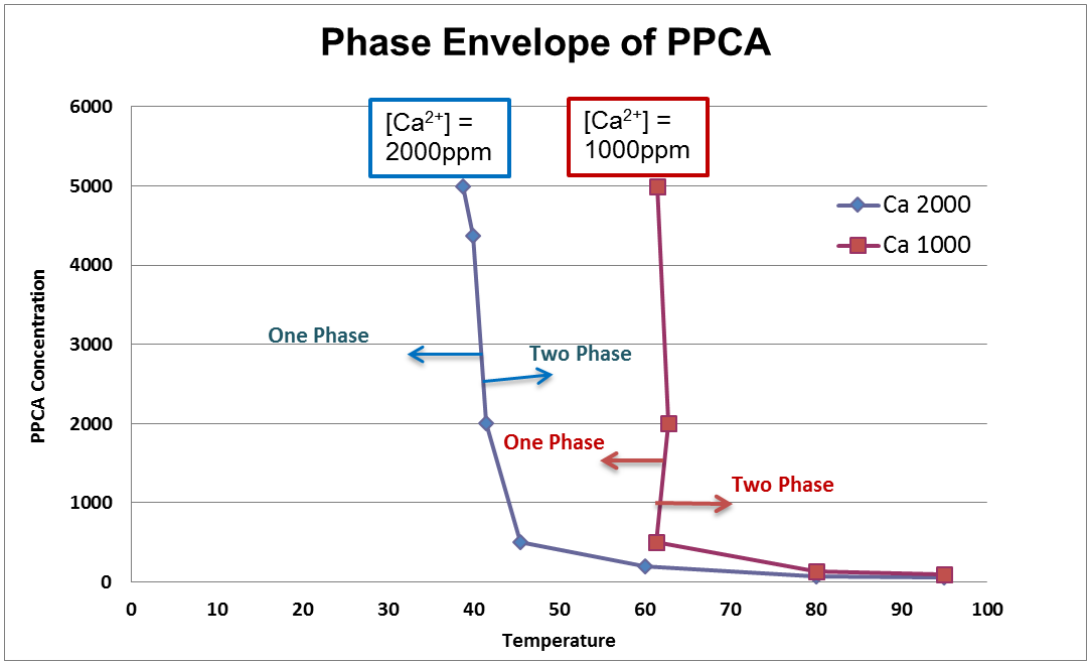

Figure 19: Phase Envelope of PPCA

Figure 19 shows the phase envelope of PPCA representing the precipitation of PPCA at a function of temperature and [Ca^{2+}]. It clearly shows that the two phase region of PPCA_Ca begins at 40°C when calcium is 2000ppm and when calcium is 1000ppm, the two phase region appears at 60°C. This result is based on taking a measured PPCA_Ca precipitation level above 5% which is about the level of analytical error. At this stage, a further set of experiments was designed in order to scan the phase envelope in a systematic manner. From the above results, and also from the literature, we know that

higher [Ca^{2+}] induces more precipitation of PPCA and therefore 2000ppm [Ca^{2+}] was chosen for these further experiments.

4.4 Characterization of the Phase Envelope

Establishing the phase envelope of PPCA was greatly assisted by also characterizing the physical and chemical mechanisms which govern the phase behaviour of the PPCA/Ca/Brine/T system. The phase behaviour of the PPCA_Ca precipitate is controlled by the following parameters- [SI], [Ca^{2+}], pH and temperature. Later we will also show that the PPCA MW also plays an important role. Here in this section we will scan the phase envelope at different points by various methods, and these results will help us to build up this understanding of the roles played by the various parameters listed above in forming the two phase region of the PPCA.

4.4.1 Coupled Adsorption and Precipitation of Scale Inhibitors

For the purposes of "scanning" the phase envelope, a series of coupled adsorption/ precipitation experiments were carried out at temperatures 50^{o}C, 80^{o}C and 95^{o}C, at pH 6 which are located on the phase envelope of PPCA in Figure 20; the schematic locations on the phase envelope shows how far we are from the phase line when performing these coupled adsorption/ precipitation experiments. The detailed description of the experiment and its methodology was reported in chapter 3. In the static adsorption tests, experiments were performed using 3 masses of sand (m = 10g, 20g and 30g) at a constant volume of SI solution (V = 0.08L). These experiments were carried out and compared directly with parallel static compatibility tests (no sand present) to evaluate the coupled adsorption/precipitation behaviour of PPCA. The brine used was the usual NFFW, composition given in Chapter 3.

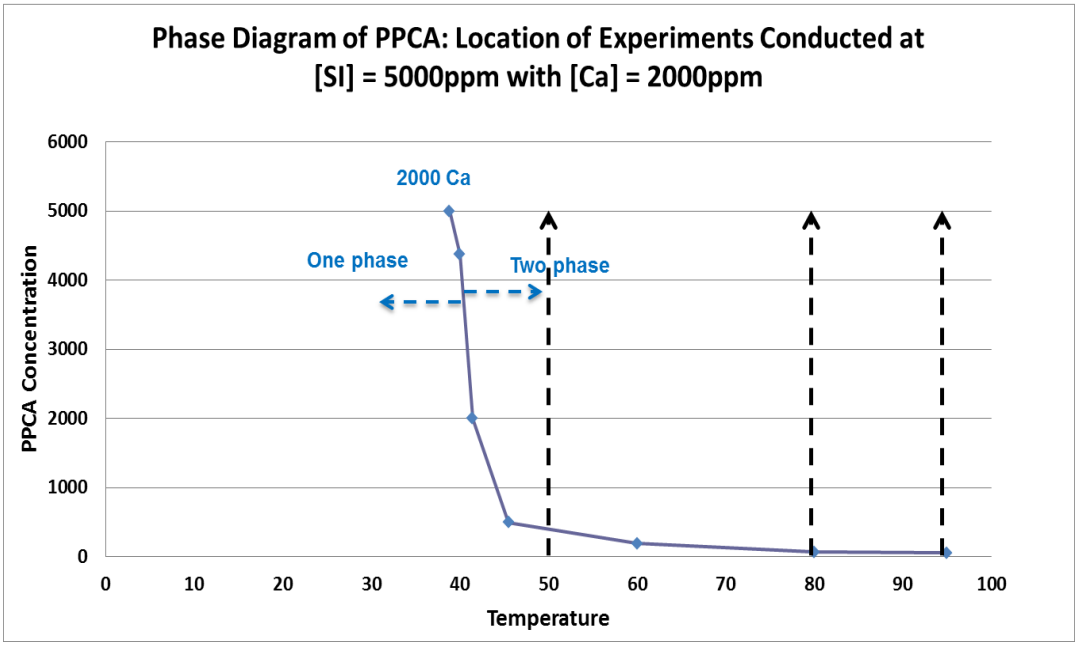

Figure 20: Schematic diagram of the phase envelope showing the scanning by the Coupled Adsorption Precipitation Experiment at 50°C, 80°C, 95°C.

Theory of Coupled Adsorption and Precipitation*:* It is very important to understand whether the SI/brine system is operating through an adsorption or precipitate mechanism. Therefore, we present a detailed description of these processes which have previously been established experimentally by the FAST team (Kahrwad et al, 2008).

Adsorption/Desorption: Adsorption/Desorption refers to the mechanism where SI is physically or chemically adsorbed onto the mineral surface of the porous medium. It is normally described by an adsorption isotherm, Γ(C), and the actual adsorption level in a given bulk SI/mineral experiment is shown schematically in Figure 21 (Kahrwad et al, 2008).

Static Adsorption: A schematic of a static adsorption experiment is shown in Figure 21 where the notation is also given. A SI of initial concentration, C_o (ppm or mg/L), in a volume, V (L), is allowed to come to equilibrium with a mass, m (g), of mineral. At equilibrium concentration of the SI, C_{eq}, then by material balance the adsorption level is as follows:

$$\Gamma = \frac{V(c_0 - c_{eq})}{m} \qquad (3)$$

where, in the units used, then Γ is in mg of SI/g of rock.

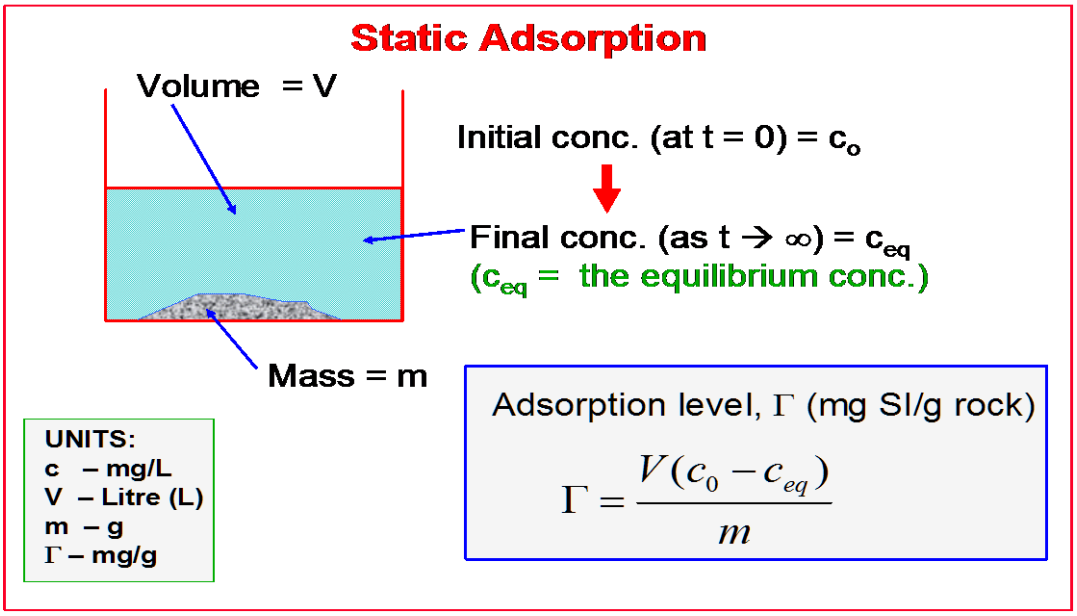

Figure 21: Shows the process of simple static adsorption on a porous medium comprising a mineral separate, of mass m e.g. sand, kaolinite, siderite etc. (Source: FAST Group, Oilfield Scale Course)

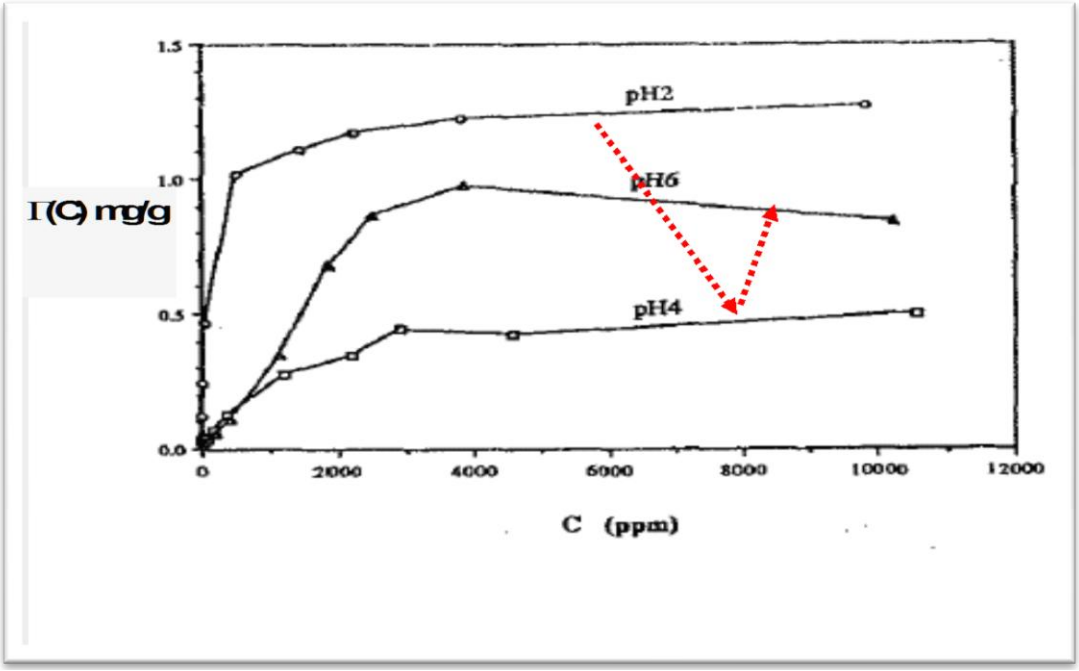

Figure 22: Experimental static adsorption isotherms, Γ(C), for DETPMP on crushed core material. At various pH values, 2, 4 and 6 at T = 25°C (Source: Yuan et al., 1994).

Yuan et al. (1994) studied the effect of pH on the adsorption of penta-phosphonate (DETPMP). The Figure 22 shows measured experimental static adsorption isotherms, Γ(C), of the penta phosphonate DETPMP on crushed core material, at pH values, 2, 4 and 6 at T = 25°C. It is quite clear from these results that the level of SI adsorption is

also strongly dependent in pH as well as on [SI] and hence we should strictly write Γ = Γ (C, pH) or Γ = Γ (C, $[H^+]$).

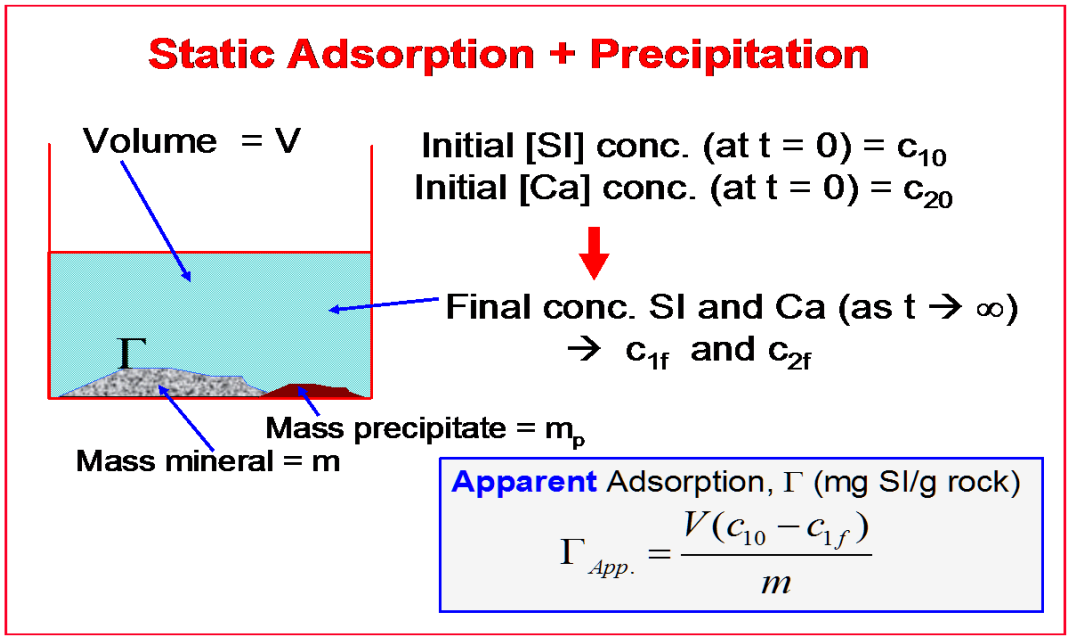

Figure 23: Schematic showing how both coupled adsorption and precipitation can occur showing how this could be interpreted as an "apparent adsorption", $\Gamma_{App.}$ (Source: FAST Group, Oilfield Scale Course)

Coupled Adsorption/Precipitation: Pure adsorption can be extended to the case where both adsorption and precipitation can occur simultaneously, which is shown schematically in Figure 23. In this process, we envisage that precipitation occurs by the formation of the calcium salt of the SI, i.e. by precipitation of *SI_Ca*. In general, the stoichiometry of this precipitation reaction is as follows:

$$SI + n.Ca \approx SI\_Ca_n \qquad (3)$$

Where n Ca ions may bind to a single SI molecule. The solubility of this sparingly soluble salt may be described by an equilibrium solubility product, K_{sp} , of the form:

$$K_{sp} = [SI].[Ca]^n \qquad (5)$$

Whereas:

c_{10} and c_{1f} - initial (t = 0) and final equilibrium (t→ ∞) SI Molar concs. (M);

c_{20} and c_{2f} - initial (t = 0) and final equilibrium (t→ ∞) Ca Molar conc. (M);

Γ – is the adsorption which depends on c_{1f}, $\Gamma = \Gamma\left(c_{1f}\right)$ (mg/g);

The precipitation process depends on both c_{1f} (SI conc.) and c_{2f} (Ca conc.) through K_{sp} as follows:

$K_{sp} = \left(c_{1f}\right).\left(c_{2f}\right)^n$ in this notation when the system is at equilibrium; units of $K_{sp} \rightarrow M^{n+1}$;

m_p is the actual mass of precipitate which forms.

From the above quantities, we note that the initial and final values of SI concentration are c_{10} and c_{1f}.

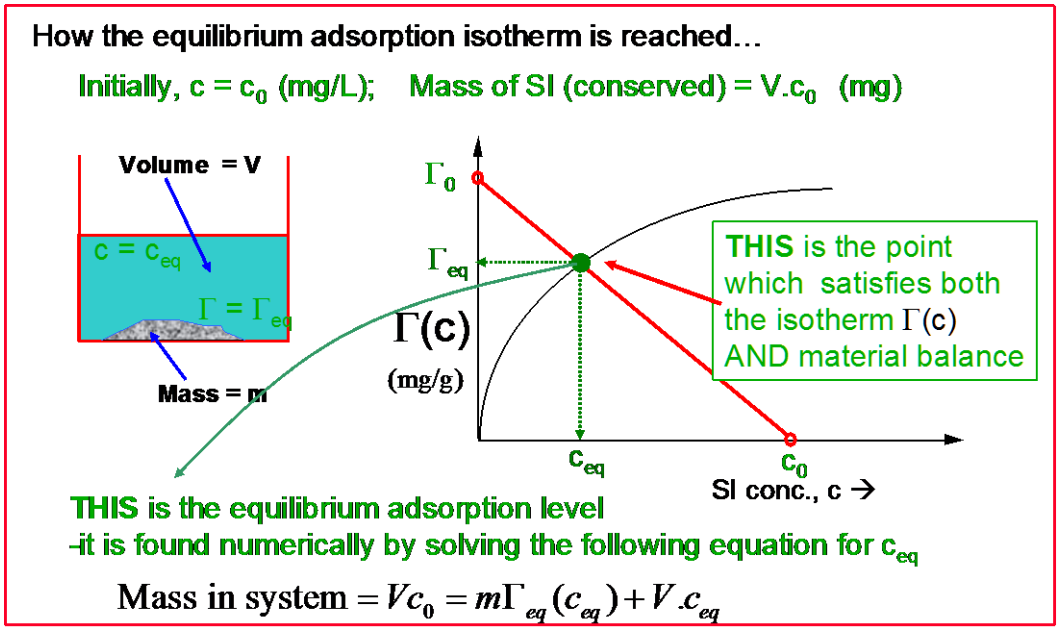

Figure 24: Schematic showing how the static adsorption isotherm is reached as $c_0 \rightarrow c_{eq}$ such that the mass conservation is consistent with the adsorption isotherm, Γ(C). (Source: FAST Group, Oilfield Scale Course)

Some of this SI which is "missing" from the bulk solution is adsorbed and the remainder of it is part of the precipitate. However, if we assumed that *all* of this "missing" SI is adsorbed, then we would calculate an "apparent adsorption", $\Gamma_{App.}$, as follows:

$$\Gamma_{App.} = \frac{V(c_{10} - c_{1f})}{m} \qquad (6)$$

This would clearly be an *over*-estimate of the actual adsorption (since some of this would be precipitate) but it is what would be seen in an actual experiment if the above formula were applied.

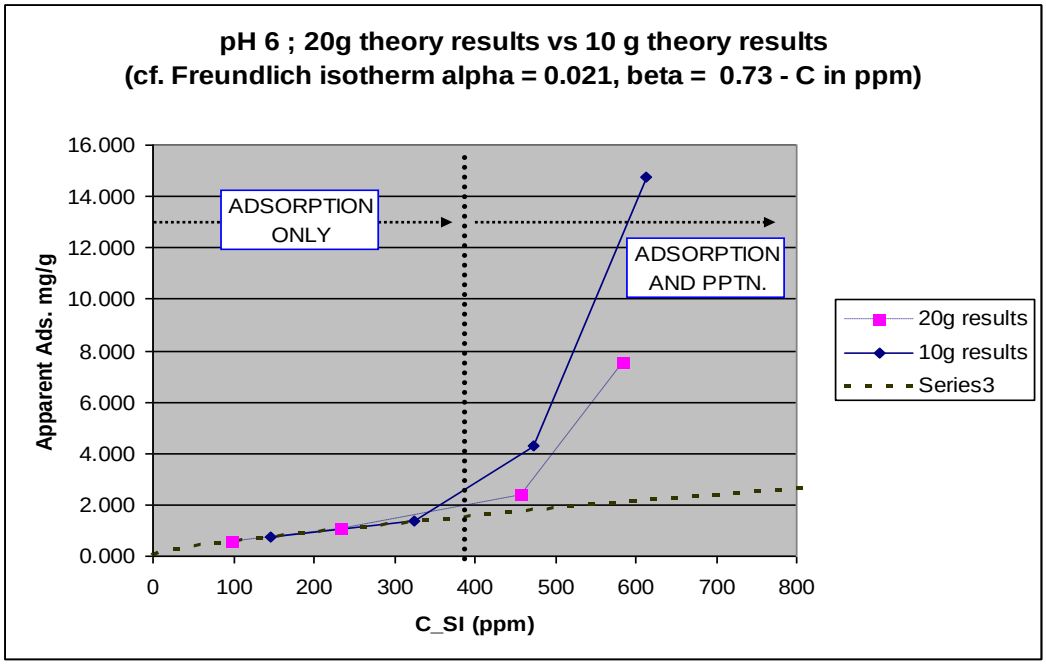

Figure 25: Calculated "apparent adsorption", $\Gamma_{App.}$ vs. concentration of SI for the model parameters (Source: Kahrwad, Heriot Watt U., 2008).

Kahrwad et al. (2008) studied these calculations and concludes the following points:

(i) there is a clear region at lower concentrations where purely adsorption is observed since the "apparent adsorption" is clearly not a function of the (m/V) ratio;

(ii) At higher concentrations, a region of coupled adsorption/precipitation is observed where the "apparent adsorption" is clearly a function on the (m/V) ratio with the adsorption seeming to increase as (m/V) decreases.

4.5 Experimental Results and Discussion

The results from the coupled adsorption/precipitation tests are presented in Figure 26 - Figure 34. It can be seen that very similar changes occur in the [PPCA] in cases both with and without sand. This means that the presence of sand for PPCA does not make a very significant difference as compare to the change in the [PPCA] in the compatibility tests. The changes are quite visible from concentrations as low as 100ppm of the [PPCA]. Plots of apparent adsorption vs. [PPCA] for various (m/V) ratios are shown in Figure 27, Figure 29 and Figure 31 and these demonstrate quite conclusively that this system is in the *precipitation* regime and that adsorption, although it is certainly occurring*, is low. *We know that there is *some* adsorption since there is a clustering of apparent adsorption measurements at low [PPCA] ~ 100ppm for all values of (m/V) ratio but this adsorption level is very low (possibly, $\Gamma \sim 0.1$mg/g).

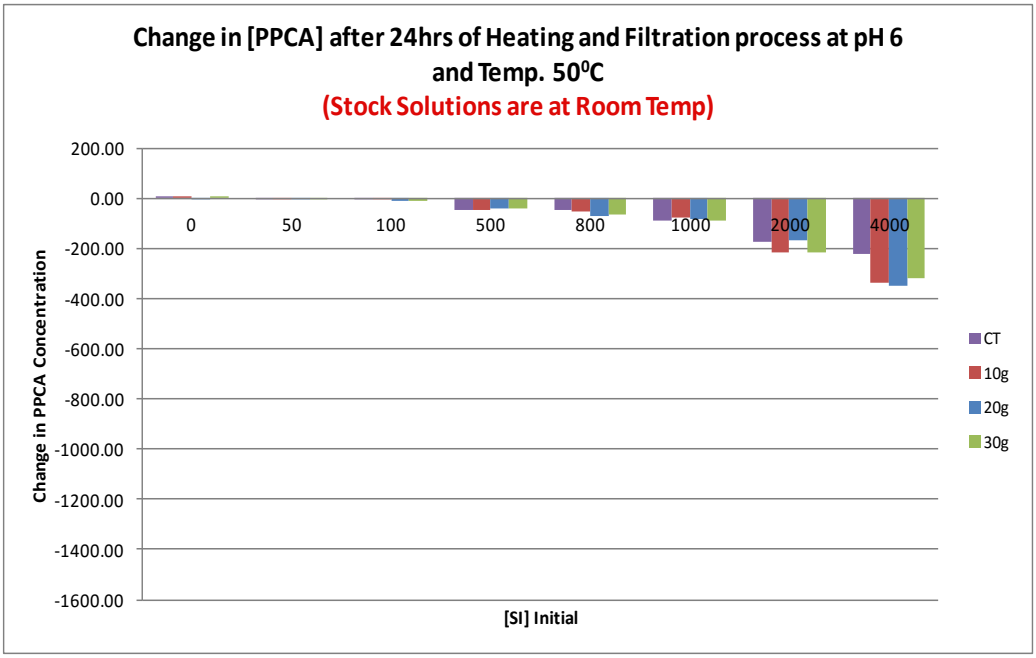

Figure 26: Coupled Adsorption Precipitation of PPCA at 50°C

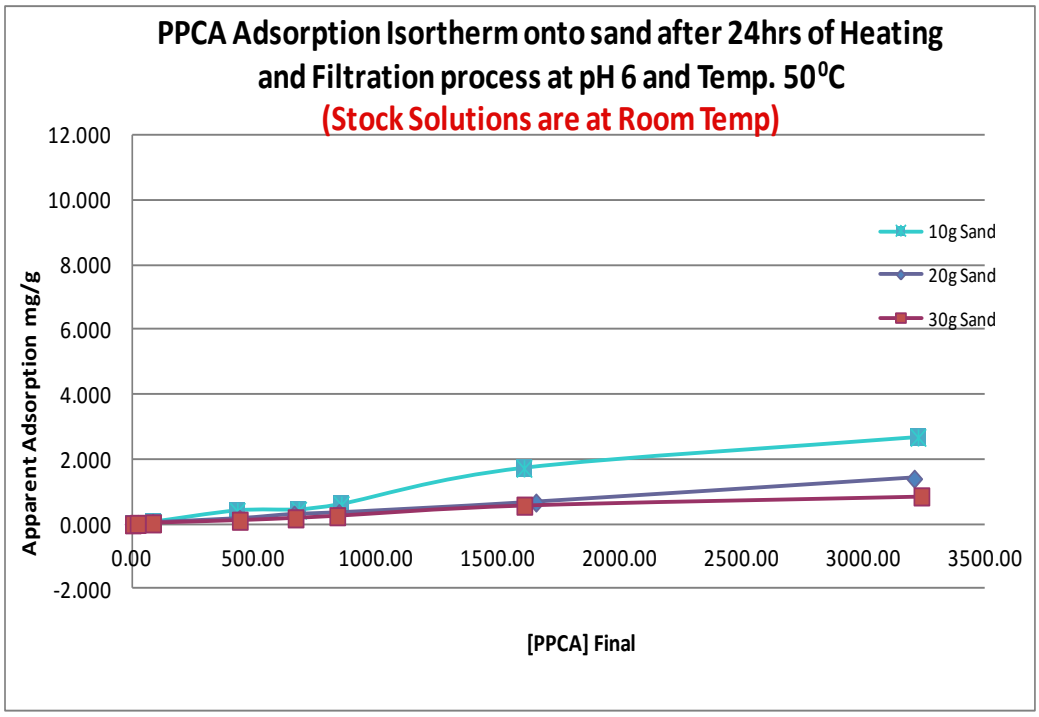

Figure 27: Apparent Adsorption of PPCA at 50°C

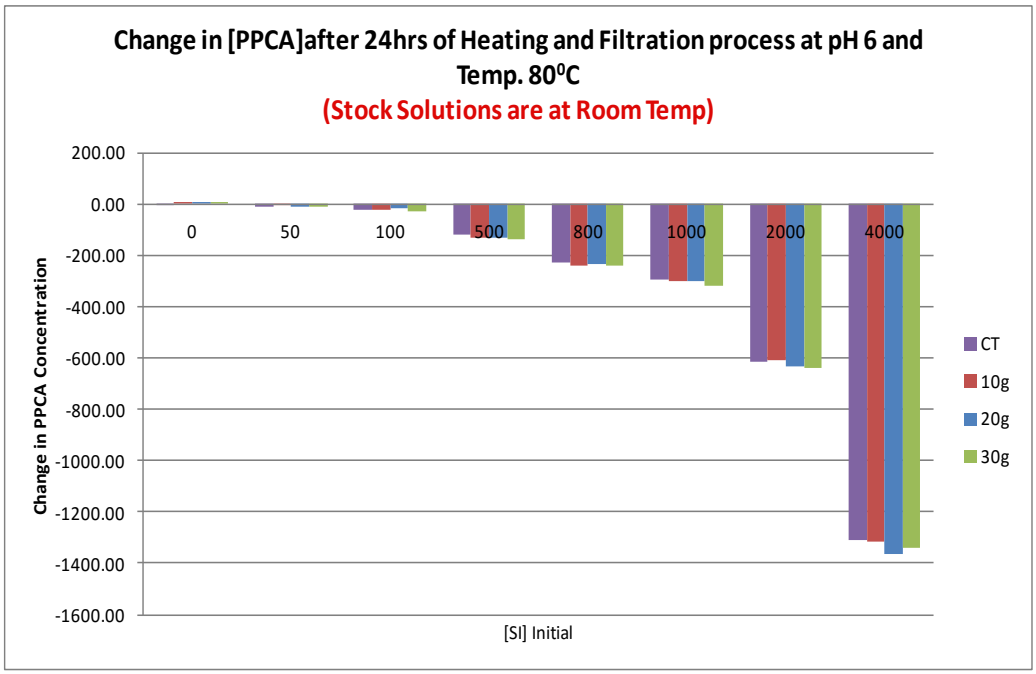

Figure 28: Coupled Adsorption Precipitation of PPCA at 80°C

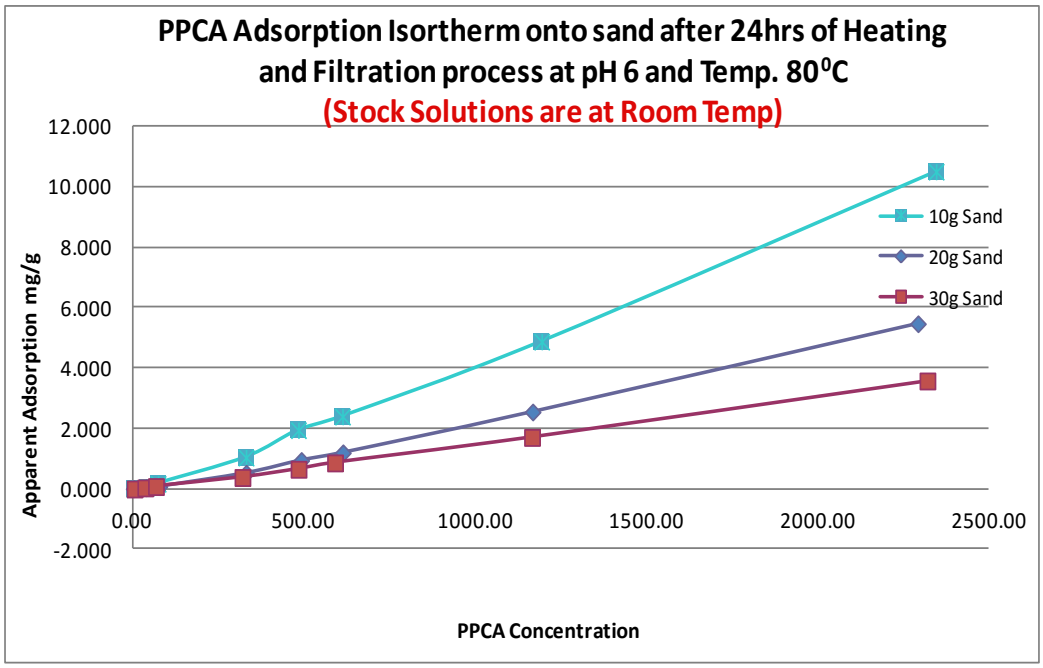

Figure 29: Apparent Adsorption of PPCA at 80°C

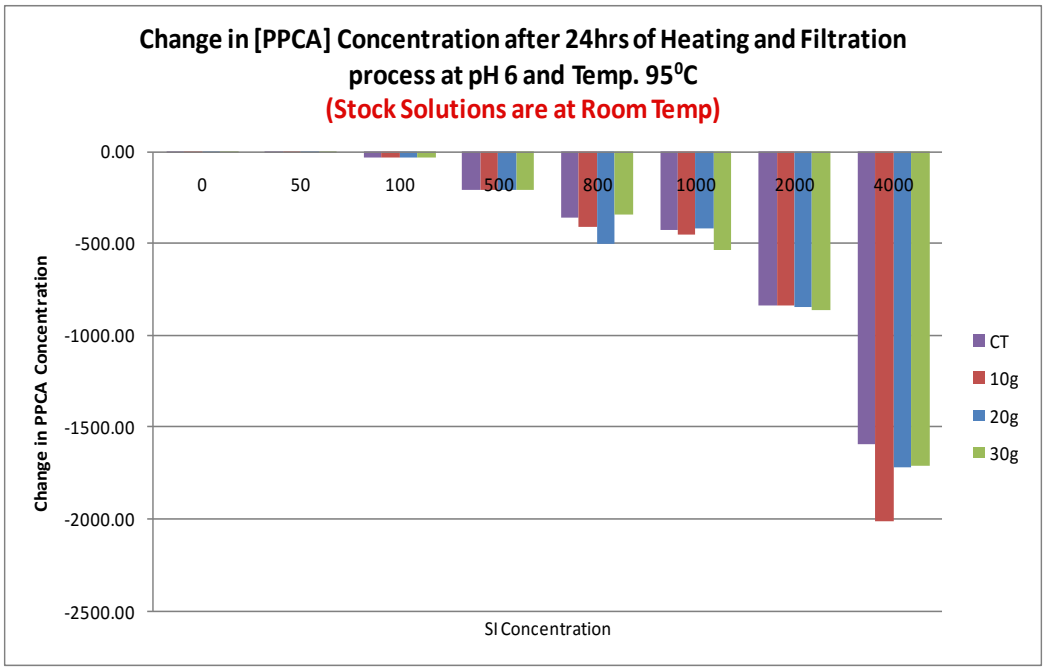

Figure 30: Compatibility Test: Precipitation of PPCA at pH 6 and temperature 95°C

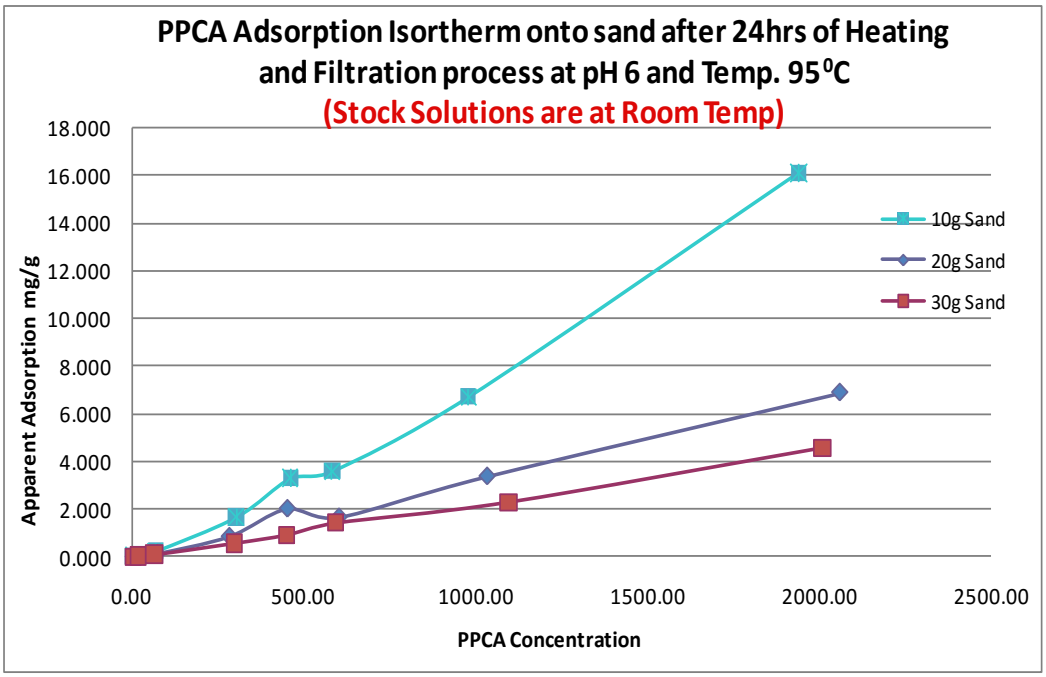

Figure 31: Apparent Adsorption Isotherm of PPCA at pH 6 and temperature 95°C.

From the measured change in [PPCA], we were able to construct the apparent adsorption isotherm of PPCA for the various (m/V) ratios at all temperatures, 50°C, 80°C and 95°C. These figures (Figure 27, Figure 29 and Figure 31) show that a clear coupled adsorption/precipitation regime of PPCA exists since the apparent adsorption curve at each (m/V) ratio is different. Depending upon the mass of the sand (i.e. the m/V ratio), the curves start to deviate due to coupled adsorption and precipitation. As expected when this behaviour is seen, the apparent adsorption seems to increase as the mass to volume (m/V) ratio decreases – this is in accord with theory (Kahrwad et al., 2008).

The change in [PPCA] for both compatibility and adsorption test are showed in Figure 26, Figure 28 and Figure 30 for 50°C, 80°C and 95°C respectively. The significant changes in [PPCA] appears from 100ppm SI concentration, and as the concentration of PPCA increases from 100ppm to 4000ppm, the remarkable increase noticed in the change of [PPCA]. Another clear observation can be seen in the effect of temperature. When we raise the temperature from 50°C to 80°C and from 80°C to 95°C successively, more precipitate is formed, and the apparent adsorption was observed to be the highest at 95°C.

Any divalent ion levels above stock solution concentration are not expected or must be within an analytical error of less than 5%. It is known that Ca^{2+} and Mg^{2+} ions do not

significantly adsorb* onto sand, so the differences are due to cation bridging between the SI and the Ca^{2+} and Mg^{2+} ions onto the sand. However, there may be some ion exchange of Ca^{2+} and Mg^{2+} ions onto the rock/mineral surface but this is not a large effect for such pure quartz sand – can be much larger in clays]. However, it is shown in the phase envelope section previously that magnesium does not take part in chemical reaction with PPCA and mainly the PPCA complexation was with calcium ions. The change in [Mg^{2+}] and [Li^{+}] were measured and their changes were under the range of analytical error. It is also noted that in almost all cases, there is a small increase in [Ca^{2+}] and [Mg^{2+}] ions, which is not expected, but they are again all within its analytical error limit.

The decrease in the solution divalent ion levels are due to either precipitation of PPCA_M complex or because of the involvement of divalent ion levels in the pure adsorption process (e.g. by cation bridging). Any changes in [Li^{+}] were also noted in order to check whether any evaporation was taking place. There should not be any changes in [Li^{+}] as it is an inert tracer ion which does not adsorb onto sand or react with PPCA.

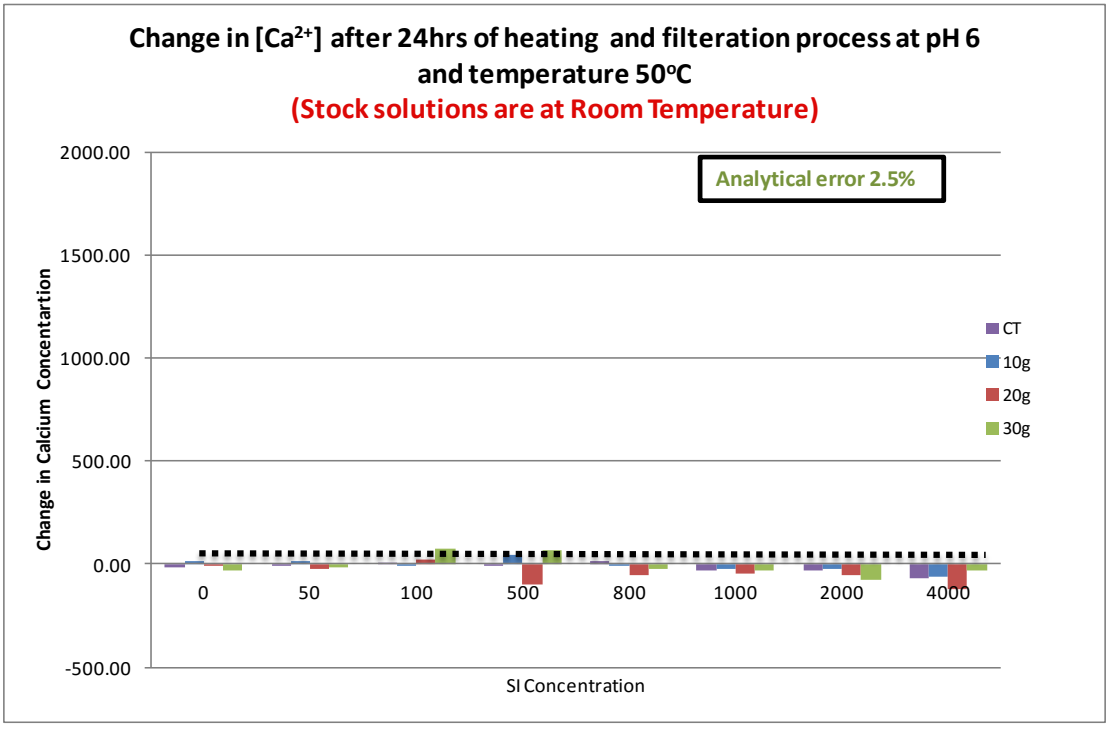

Figure 32: Change in [Ca^{2+}] at 50°C

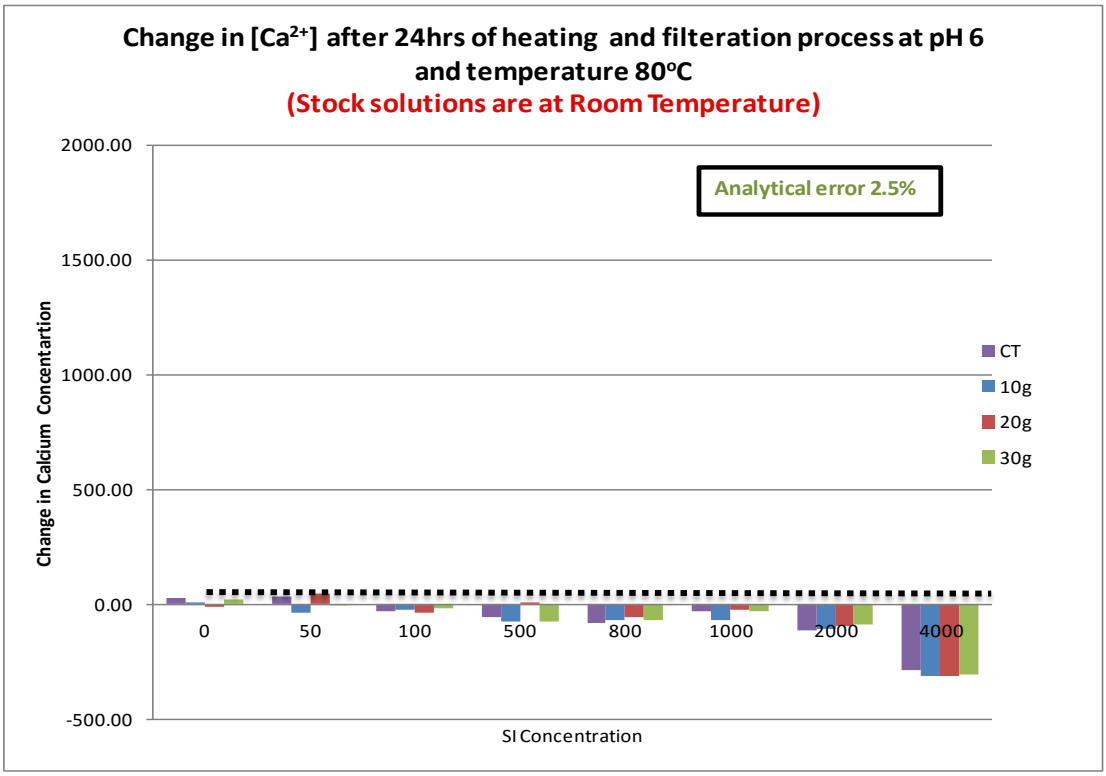

Figure 33: Change in [Ca^{2+}] at 80^{o}C

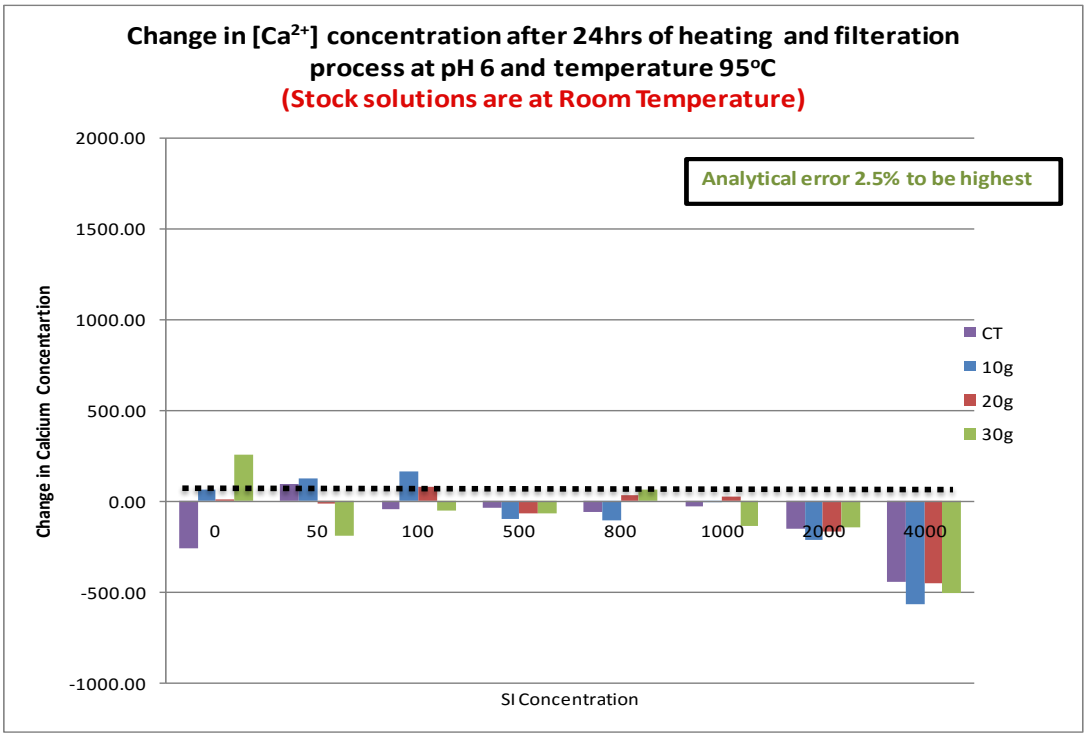

Figure 34: Change in [Ca^{2+}] at pH 6 & 95^{0}C

The above figures show the corresponding changes in [Ca^{2+}] at 50^{o}C (Figure 32), 80^{o}C (Figure 33) and 95^{o}C (Figure 34). Initially, [Ca^{2+}] in the test brine was 2000ppm. The changes in the [Ca^{2+}] were actually visible from 2000ppm of [SI]. Earlier results on

PPCA have shown that the changes in [Ca^{2+}] starts from ~1000ppm of [PPCA], but later results confirmed that the consistency for the change in [Ca^{2+}] is maintained at 2000ppm of [PPCA]. It suggests that 1000ppm of [SI] would be at the edge of the 2 phase region of the phase envelope. The calcium levels above stock solution concentrations are not expected or must be within an analytical error of 5%.

It is clear from these experimental results that, as we move further into the 2 phase region, more precipitation of PPCA is observed. This leads to the conclusion that the range of coupled adsorption precipitation and apparent adsorption increases with increasing temperature. Similarly, a corresponding change was observed on the [Ca^{2+}] to that of [PPCA] at the increasing temperature.

4.5.1 Molar Ratio of PPCA and Calcium for Precipitation and Re-dissolution

Stoichiometry of the SI_Ca complex is very important in order to get the good yield of precipitation [Browning and Fogler, 1993]. This precipitation/re-dissolution experiment was designed to scan the phase envelope of PPCA in terms of determining the stoichiometry of the SI_Ca complex.

Initially, a range of SI concentrations (e.g. 0, 500ppm, 1000ppm, 2000pppm, 3000ppm, 4000ppm and 5000ppm) was used to precipitate the polymer with 2000ppm of calcium at the following temperatures 20^{o}C, 30^{o}C, 35^{o}C, 40^{o}C, 45^{o}C, 50^{o}C, 55^{o}C, 60^{o}C, 70^{o}C, 80oC. The two temperatures used to check the re-dissolution of PPCA in FW were 70^{o}C and 60^{o}C. In this experiment, the same bottle went through a temperature cycle up to the maximum test temperature (80^{o}C in this case) and then down to two temperatures (70^{o}C and 60^{o}C). These experiments were performed at pH 6 and [Ca^{2+}] = 2000ppm in NFFW.

Figure 35 shows a schematic of the methodology which was applied in this experiment where path of the actual temperature cycle is shown. 3000ppm [SI] is used as an example to give a clear picture of this methodology for the compatibility test. The same static bottle was used for the sampling at all the temperatures, while increasing the temperature for precipitation and reducing the temperature for re-dissolution.

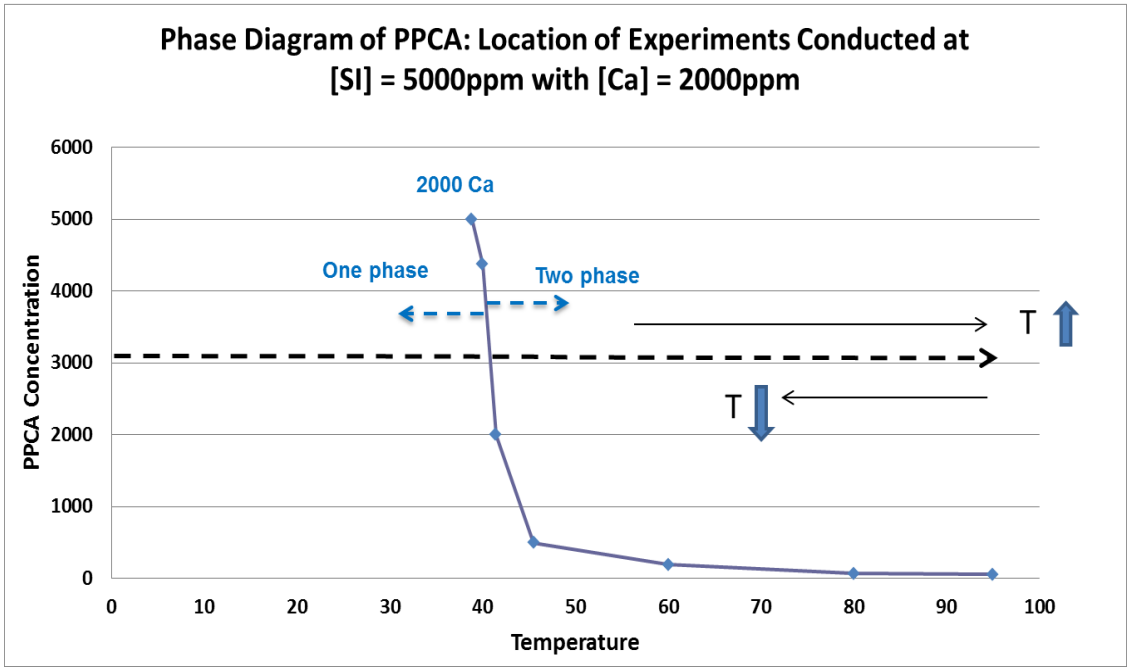

Figure 35: Schematic of how this experiment is performed by successively increasing the temperature, sampling after a time then increasing T; the same procedure is used as the T is decreased.

Experimental Results and Discussion

The molar ratio of PPCA to calcium in the precipitate (PPCA_Ca complex) has been calculated at all temperatures over both the precipitation (temperature increasing) and re-dissolution (temperature decreasing) cycles.

The static bottle results for the change in [PPCA] is shown in Figure 36 and for the change in [Ca^{2+}] shown in Figure 37. These results show that with each increasing temperature the amount of the formation of precipitate also increases. Moreover, the higher the initial PPCA concentration, the more precipitate formed. These results are very much in accordance with the previous result for the phase envelope reported above.

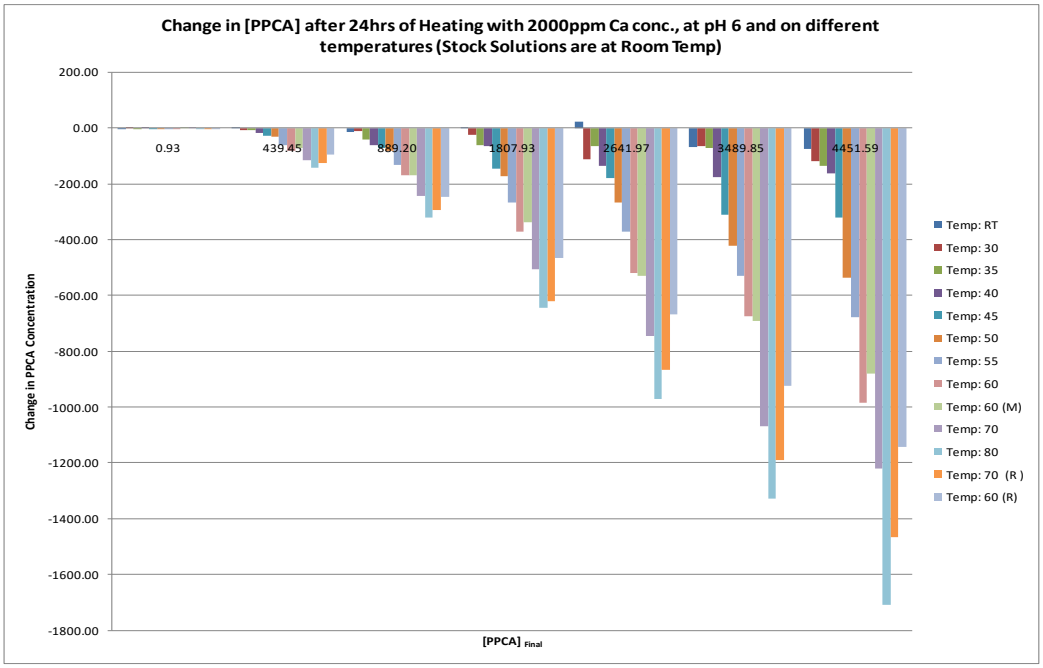

Figure 36: Precipitation/re-dissolution result showing change in [PPCA] at different temperatures

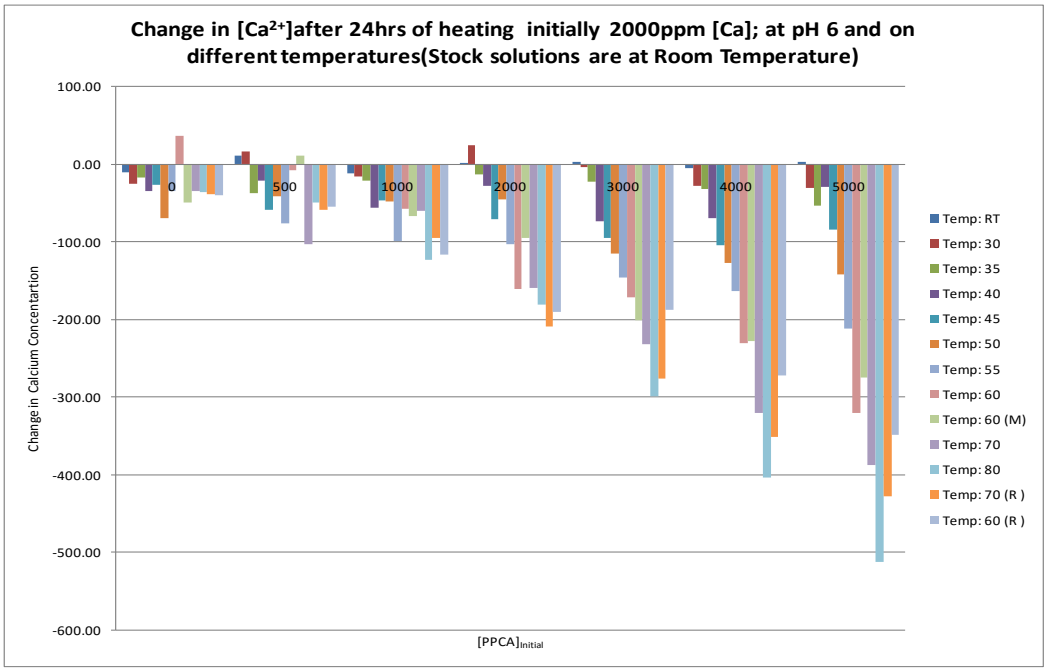

Figure 37: Precipitation/re-dissolution result showing change in [Ca^{2+}] at different temperatures

The static bottle test results shown above can be used to quantify the stoichiometry of the PPCA_Ca complex. To get the molar ratio, the following steps must be followed:

1. Change in [PPCA] and [Ca^{2+}] in ppm
2. Change the ppm to moles/L

3. Obtain the Molar Ratio of Ca/PPCA at each temperature by correlating the molar losses of ΔCa and ΔPPCA from solution (see below).

Figure 38 to Figure 40 below will follow these steps to work out on the stoichiometry of the PPCA_Ca complex at each temperature. Figure 41 shows the position of the coordinated value on phase envelope.

Molar Loss of Calcium to PPCA at Precipitation Stage:

Figure 38 shows the change in [PPCA] and [Ca^{2+}] in ppm at 95^{0}C, which are plotted against the final [PPCA] in ppm. The corresponding molarity of the PPCA and Ca involved in the precipitation process is found by conversion from ppm to moles/litre (M/L) by dividing PPCA and calcium by their respective MWs (PPCA by ~3800 (approx.) and calcium by 40.08). Figure 39 shows the final molarity *loss* from the solution of PPCA and calcium as functions of the final [PPCA] in M/L. Finally, Figure 40 shows the correlation between the molar *loss* of calcium and PPCA from solution (denoted ΔCa and ΔPPCA), which shows a very strong correlation (R^2=0.9999). That is, to find the stoichiometry, we plot ΔCa vs. ΔPPCA and the slope of this line is n in the formula PPCA-Ca_n. Figure 41 shows the locations of the molar ratio correlation points of PPCA and calcium on the phase envelope.

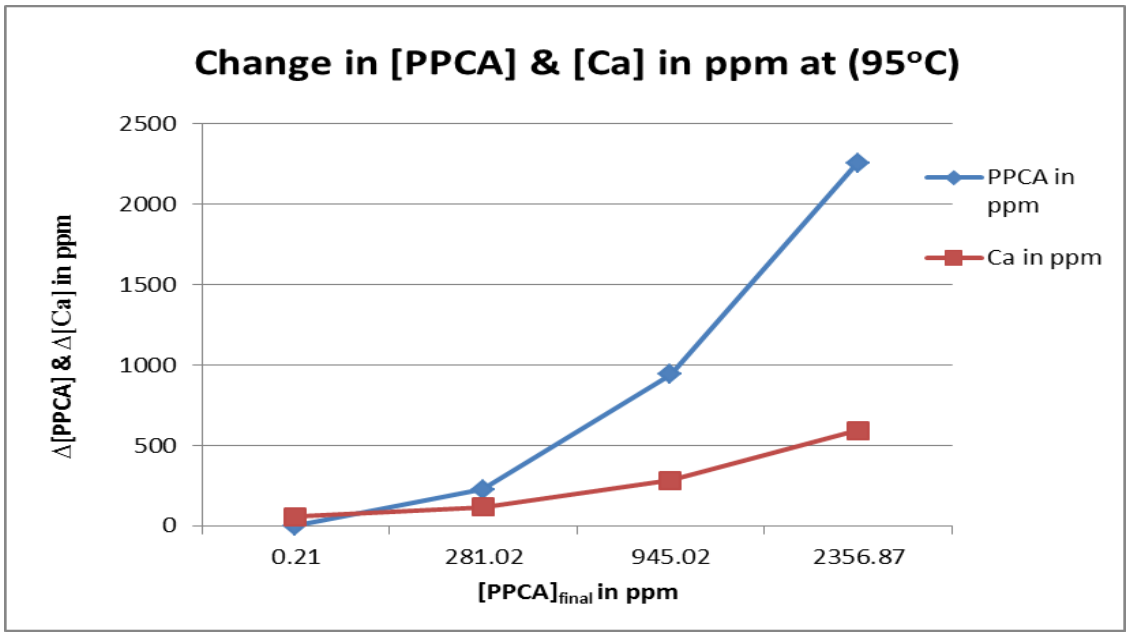

Figure 38: This graph represents the change in [PPCA] and [Ca^{2+}] in ppm against final [PPCA] in ppm at 95^{o}C

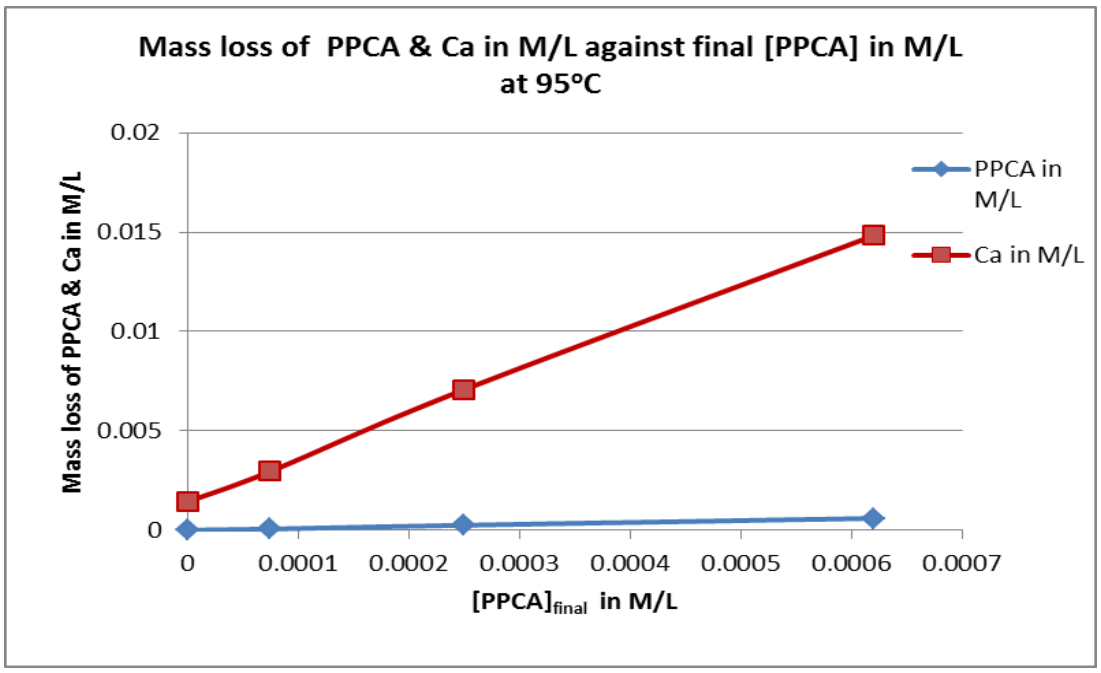

Figure 39: This graph represents the Mass loss of [PPCA] and [Ca^{2+}] in moles/Litre (M/L) against final [PPCA] in M/L at 95°C

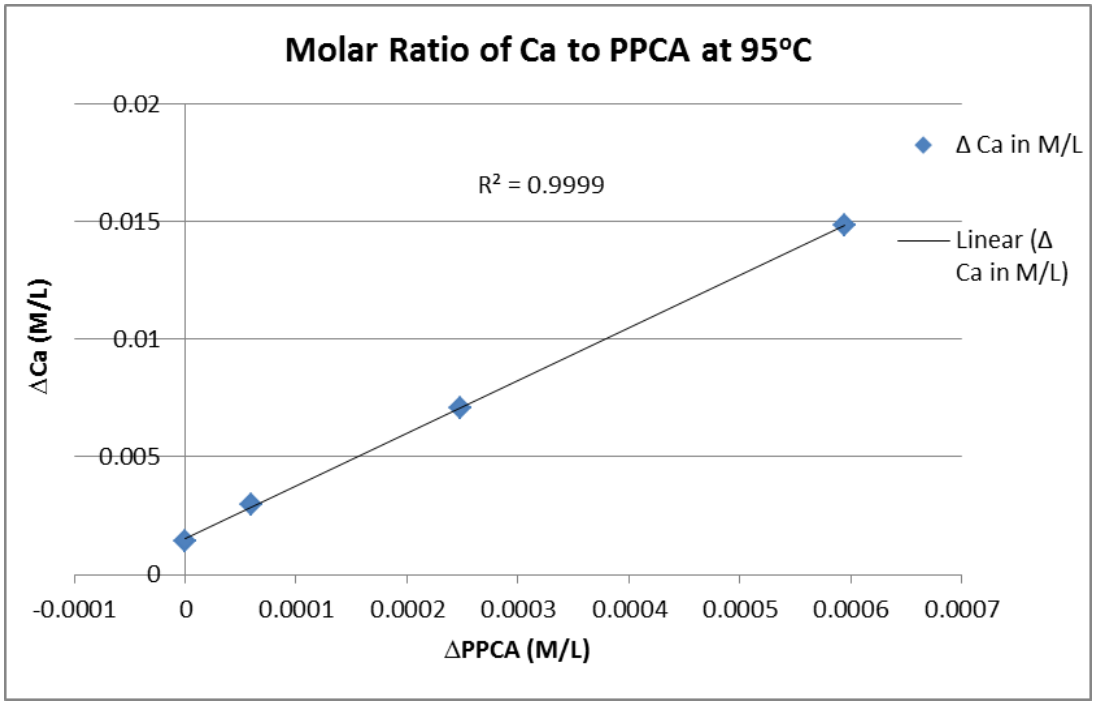

Figure 40: This graph represents the molar ratio of Ca and PPCA at 95°C

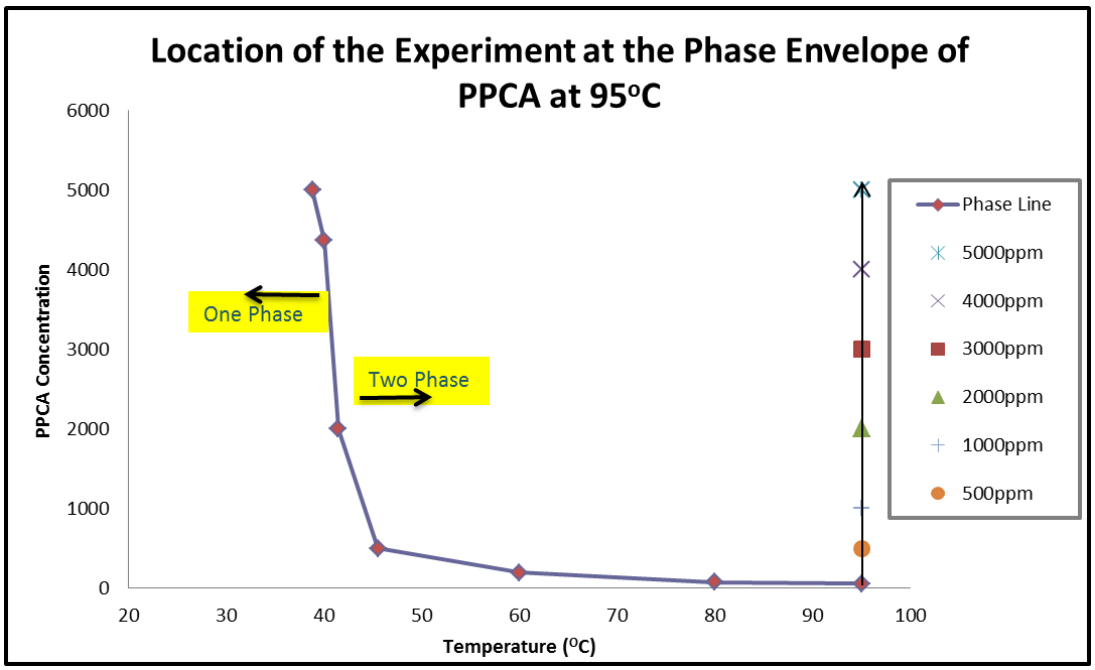

Figure 41- This graph represents the position of the test on Phase Envelope of PPCA

Similar, molar ratios of the loss of PPCA and calcium from solution (ΔCa vs. ΔPPCA) were observed at other temperatures for precipitation and also for re-dissolution. In all cases, an excellent correlation was observed as shown in the results in Figure 42 to Figure 47. From these results, we can conclude that the molar ratio of PPCA_Ca in the precipitated PPCA_Ca complex is ~ 30:1 at high temperatures like 95°C, 80°C, 70°C and 60°C.

Theoretically, the PPCA is a copolymer with MW of 3800g/mol having monomer acrylic acid (AA). The MW of AA is 72g/mol.

Therefore the amount of AA monomer in the polymer is approximately

(3800g/mol) / (72g/mol) = 53 monomer of AA/ polymeric chain;

Two monomers are required to bind one calcium (Since one acrylate has one negative charge). Therefore, 53/2 = 26 (theoretically; Experimental value ~30);

Of the 53 monomers, because two acrylic acid moieties are required to bind to one divalent calcium ion, polymer can only bind approximately 26 divalent ions. The theoretical values are quite close to experimental values (~30) only when we get maximum precipitation which is possible at high temperature. However, reducing the temperature makes the correlation weaker, hence the yield of precipitation gets poorer.

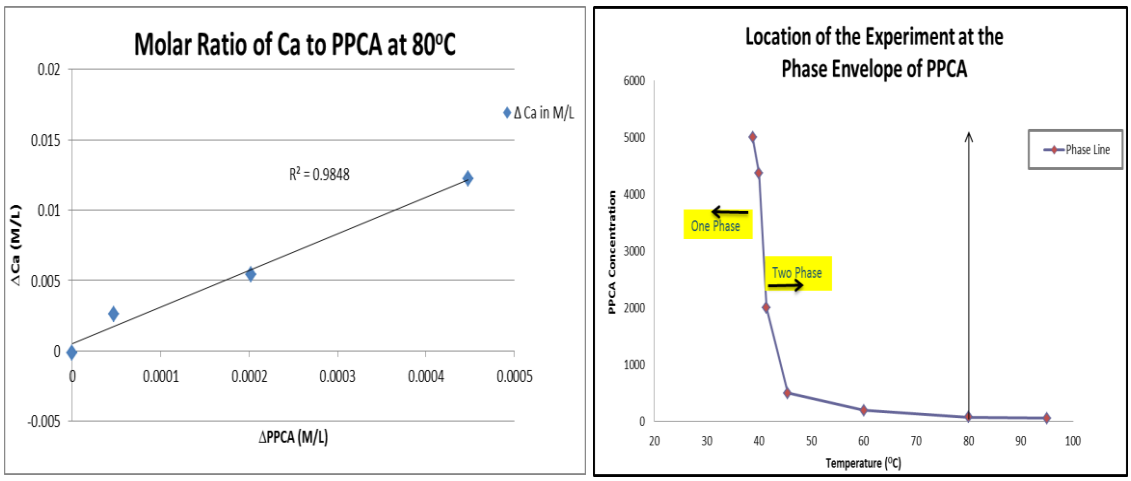

Figure 42: Ca to PPCA Molar Ratio at 80°C

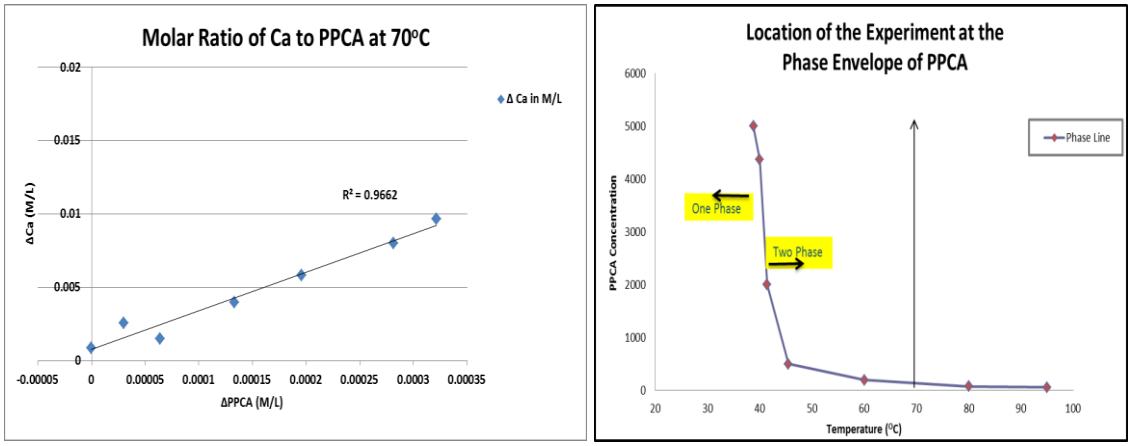

Figure 43: Ca to PPCA Molar Ratio at 70°C

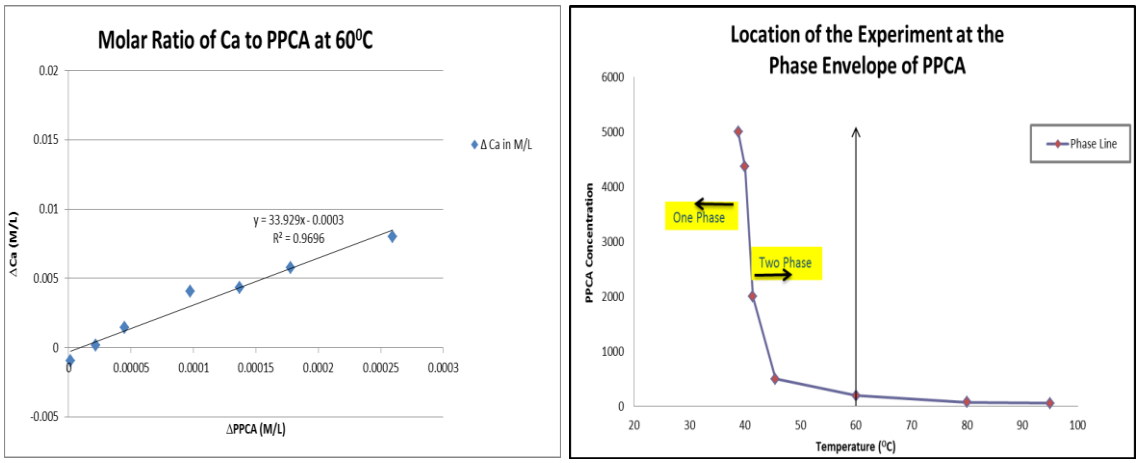

Figure 44: Ca to PPCA Molar ratio at 60°C

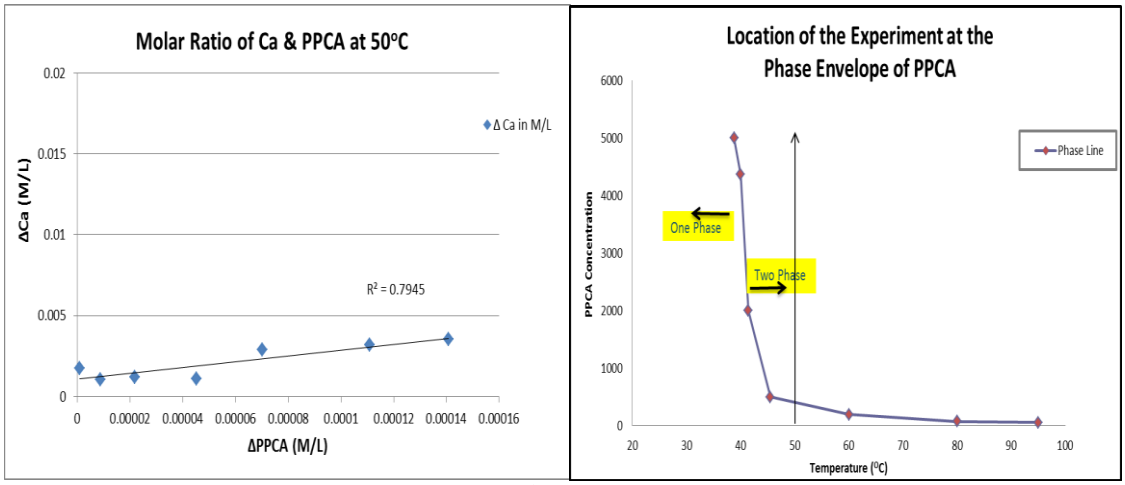

Figure 45: Ca to PPCA Molar Ratio at 50°C

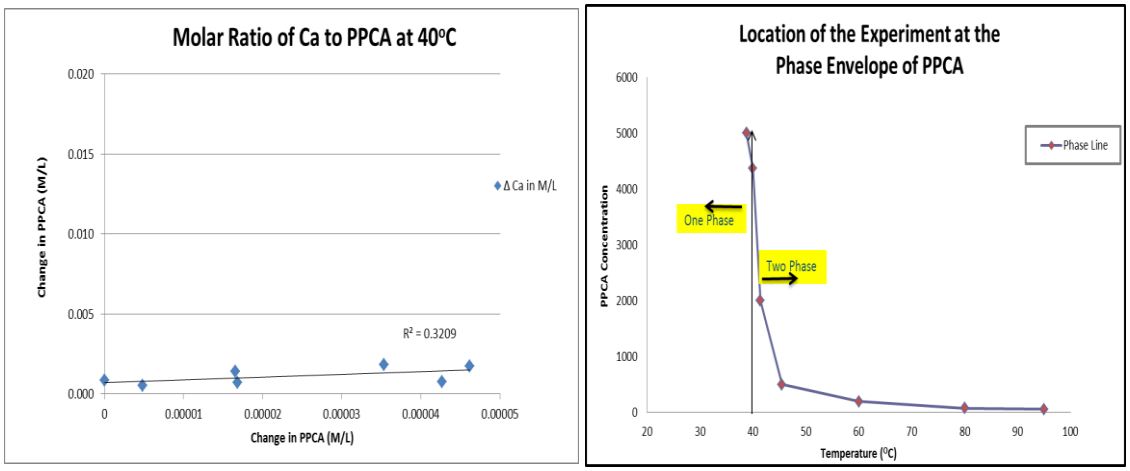

Figure 46: Ca to PPCA Molar ratio at 40°C

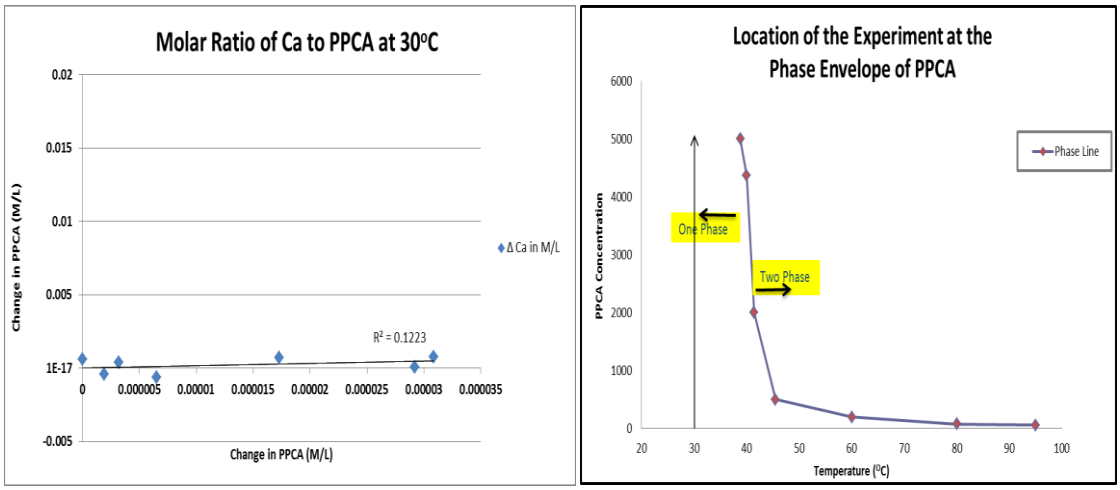

Figure 47: Ca to PPCA Molar ratio at 30°C

From the above molar ratio loss results of calcium to PPCA, we conclude that, on average above 50°C, PPCA and calcium loss shows a very strong correlation. Below 50°C, visually the solution looks cloudy and it does not actually precipitate and at 50°C the system is on the edge of the 2 phase envelope.

Molar Loss of Calcium to PPCA on the Re-Dissolution (RD) Stage:

The results below shown in Figure 48 to Figure 50, show the correlation of PPCA and calcium loss (ΔCa vs. ΔPPCA) over the re-dissolution temperature cycle (i.e. as temperature decreases). The results showed that the ΔCa and ΔPPCA molar losses from solution are also strongly correlated over the re-dissolution stage. The fact that there is a slight quantitative difference between the precipitation (temperature increasing) and the re-dissolution (temperature decreasing) stages may be due to a kinetic effect.

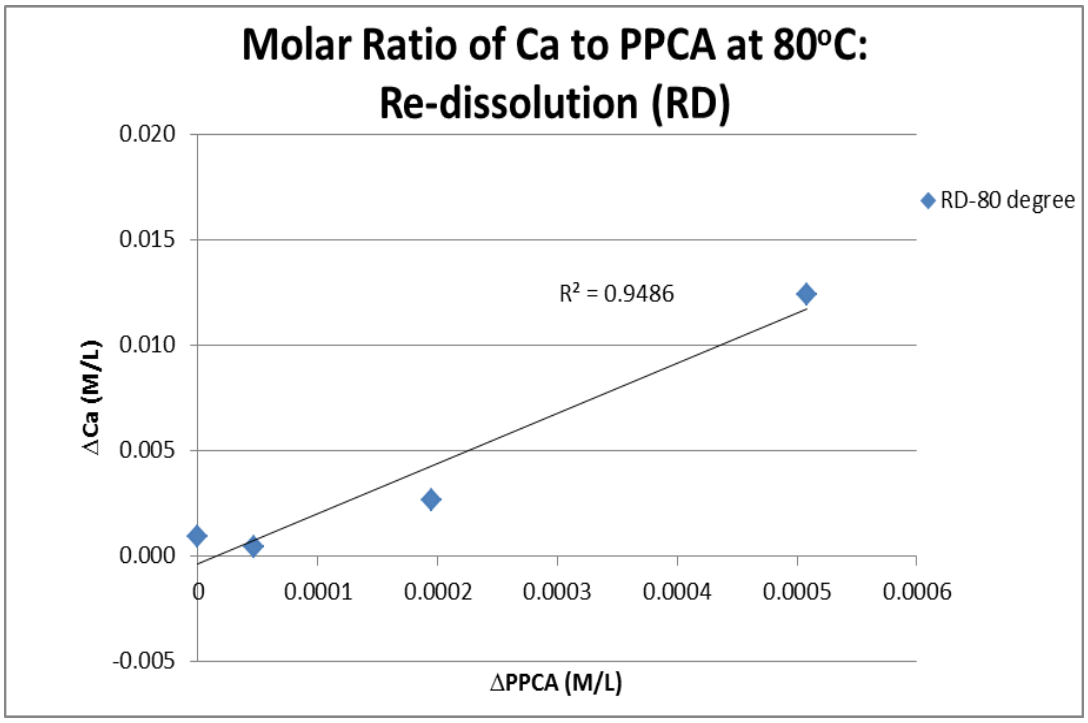

Figure 48: Ca to PPCA Molar Ratio at 80°C- Re-dissolution

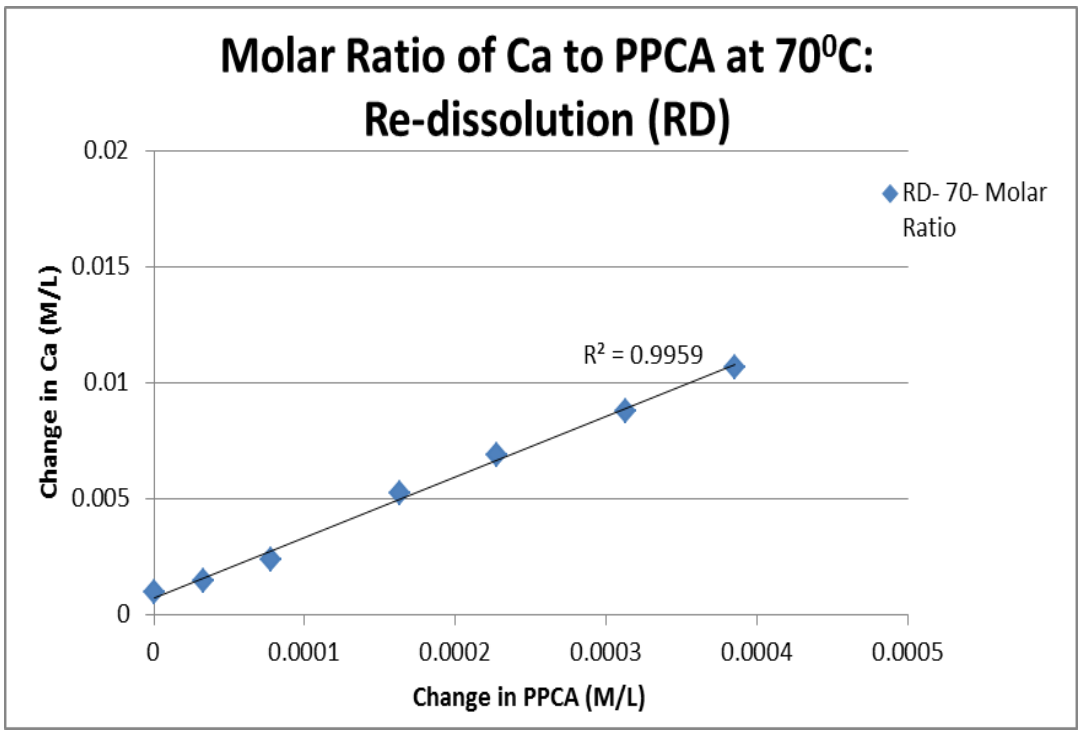

Figure 49: Ca to PPCA Molar Ratio at 70°C- Re-dissolution

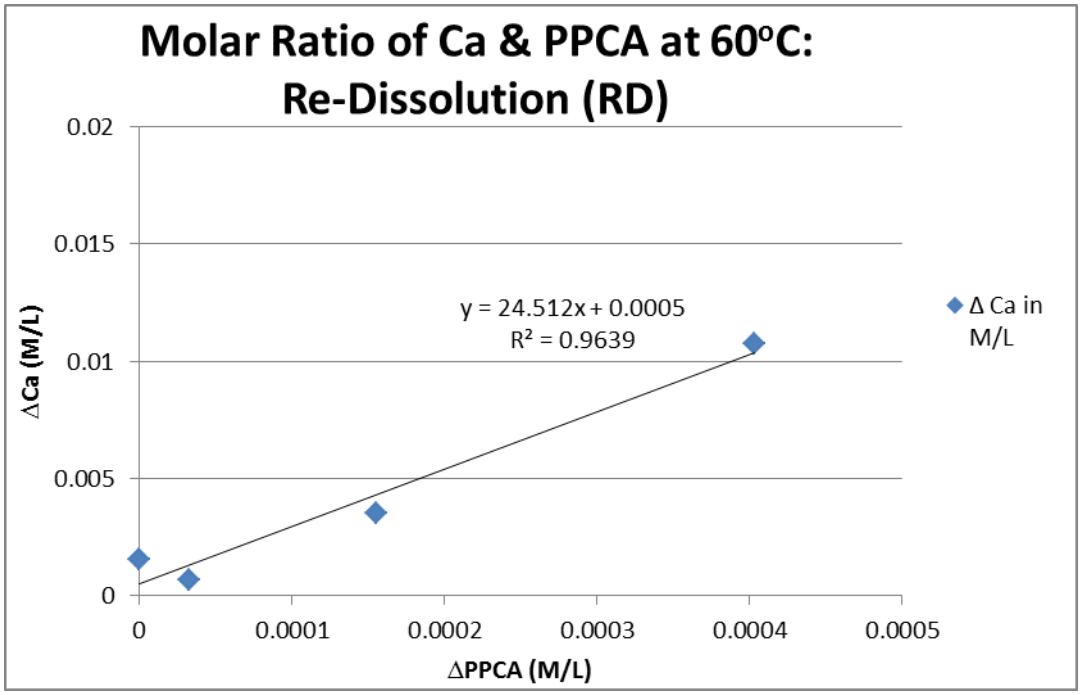

Figure 50: Ca^{2+} to PPCA Molar Ratio at 60°C- Re-dissolution

4.5.2 Inhibition Efficiency of Stock, Supernatant and Precipitated PPCA

Having established the behaviour of the overall structure of the PPCA phase envelope, we now consider the IE of the SI which is precipitated as compared to the SI which remains in the solution (the supernatant). The key issue is to establish if these fractions of PPCA – the precipitated and supernatant PPCA - in such a precipitation process show the same or different IE levels as each other and as the stock solution before precipitation. Clearly, this has important implications for the performance of the polymer in a precipitation squeeze treatment.

Experimental Detail: This was a two stage experiment. From the compatibility stage 1, we generated different fractions of PPCA, i.e. precipitate and supernatant from an original stock sample. The stage 2 part-1 of this experiment is to test the performance of the IE test against barite scale. Each fraction of PPCA was diluted down to 10, 20 and 40ppm which is in the 50-50 mix will give 5, 10 and 20ppm of active [PPCA]. All the samples produced in stage 1 were in FW. The IE performance was checked at 95^{o}C at pH 5.5. The detail description of the experiment was given in Chapter 3. The percentage of the IE is calculated by the following.

$$I.E. = 100\left(\frac{C(t) - C_b(t)}{C_o - C_b(t)}\right) \tag{7}$$

where C(t) = test sample Ba^{2+} concentration at time, t (ppm);
C_O = control sample Ba^{2+} concentration at time, t = 0 (ppm); and
$C_b(t)$ = Ba^{2+} concentration in the blank solution (containing no SI) at time, t (ppm).

Experimental Results and Discussion

Results in Figure 51, Figure 52 and Figure 53 show the IE of PPCA at 5ppm, 10ppm and 20ppm, respectively, for the 3 different sample sources – stock, supernatant and precipitate. This is a comparison of the IE of the supernatant and precipitated PPCA samples which were “recovered” from the compatibility test with the IE of the stock PPCA solution. The barium sulphate IE test itself was carried out for a brine mix ratio of 50% NSSW: 50% NFFW. These results show that in all cases (5, 10 and 20ppm) that the precipitated PPCA had a much higher IE compared with both the stock and the

supernatant. Correspondingly, the IE of the supernatant sample is very low compared with the stock. These results strongly indicate that MW effects have a dramatic influence on the IE of polymeric species.

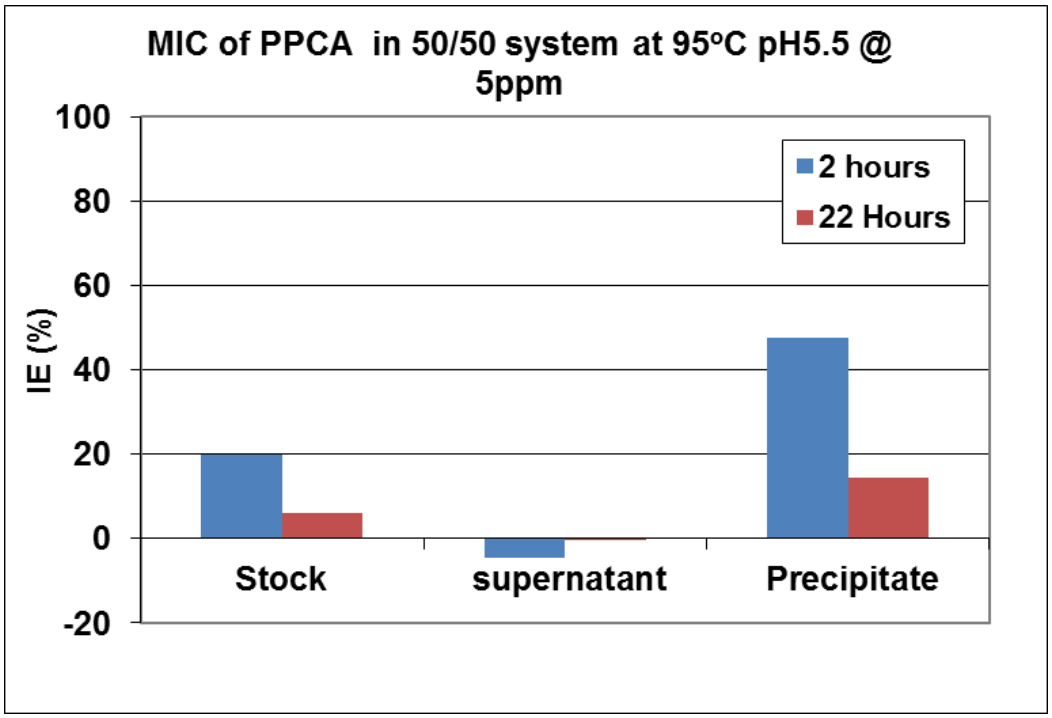

Figure 51: IE at 5ppm for stock, supernatant and precipitated PPCA from the PPCA precipitation experiments performed at 95°C.

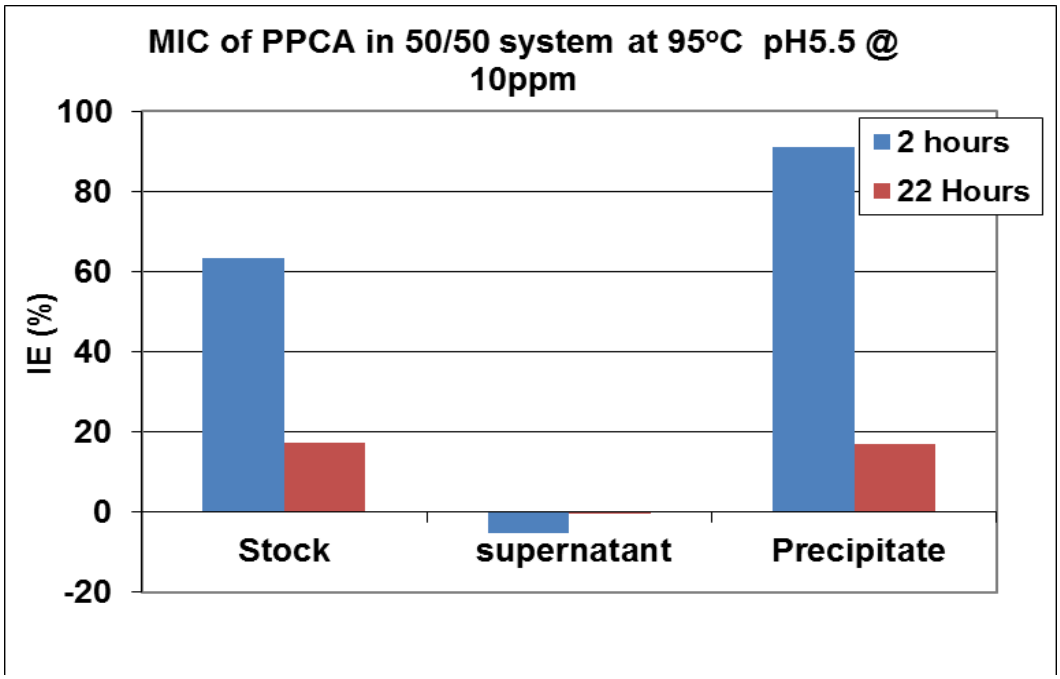

Figure 52: IE at 10ppm for stock, supernatant and precipitated PPCA from the PPCA precipitation experiments performed at 95°C.

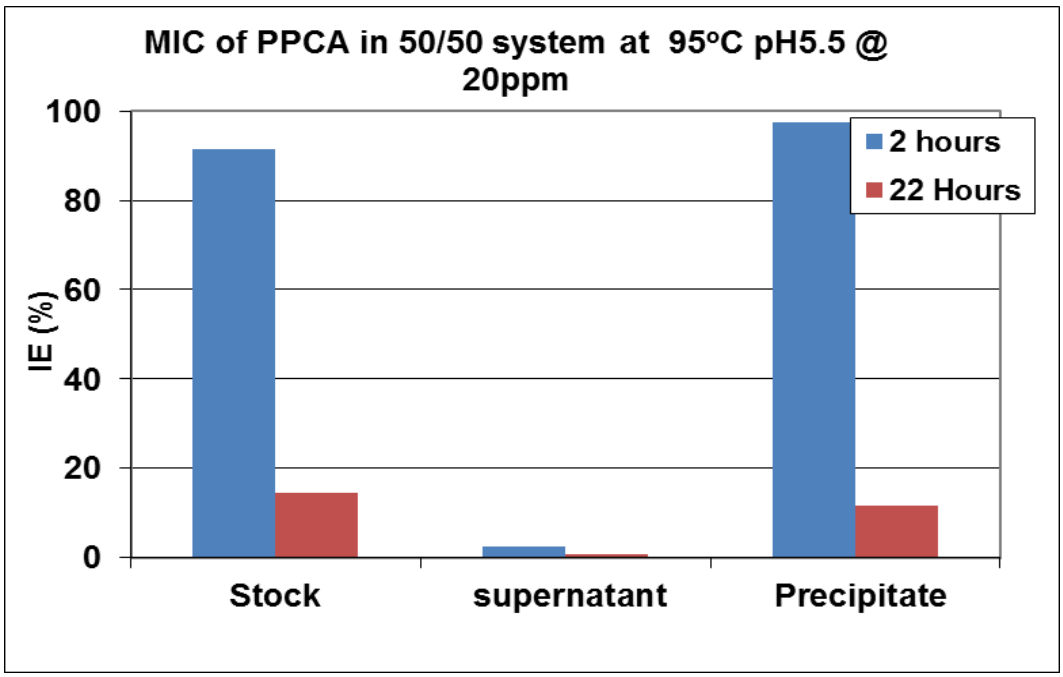

Figure 53: IE at 20ppm for stock, supernatant and precipitated PPCA from the PPCA precipitation experiments performed at 95°C.

Figure 54 shows the IE results at higher concentrations of the *precipitated* PPCA and Figure 55 shows the IE of the *stock* PPCA solution. For the *stock* solution, in the base case 60/40, 2 hour MIC is 20ppm and 22hours is 200ppm. For the base case, in the FW brine the [Ca^{2+}] is 2000ppm and [Mg^{2+}] is 739ppm and in SW the [Ca^{2+}] is 428ppm and [Mg^{2+}] is 1368ppm. Therefore in the 60/40 mix, [Ca^{2+}] = 1057ppm and [Mg^{2+}] = 1117ppm and in 50/50 system, [Ca^{2+}] = 1214ppm and [Mg^{2+}] = 1054ppm. So comparing 60/40 to 50/50 system in terms of Ca & Mg concentration, those numbers are not far apart. The MIC for the *precipitated* PPCA at 2 hours is 10ppm and for 22hours MIC is 100ppm. Therefore precipitated PPCA has much higher IE for barite scales than stock PPCA which contains both low and high MW polymer species.

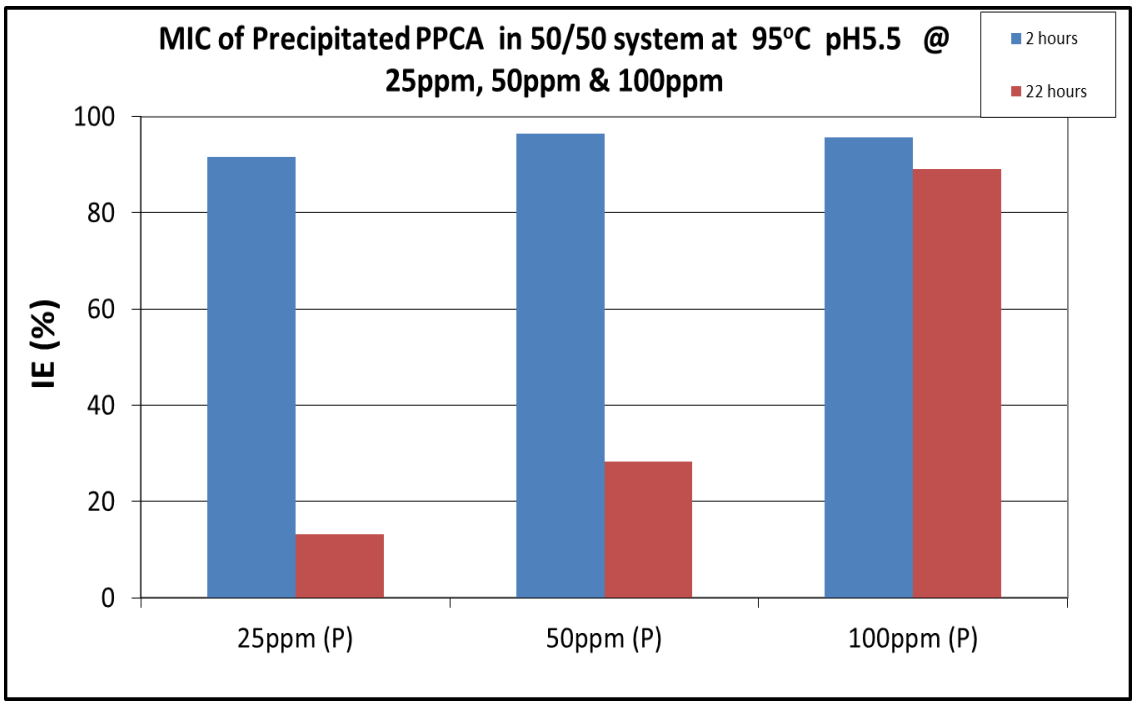

Figure 54: IE results of PPCA at 95°C for the Precipitated PPCA sample.

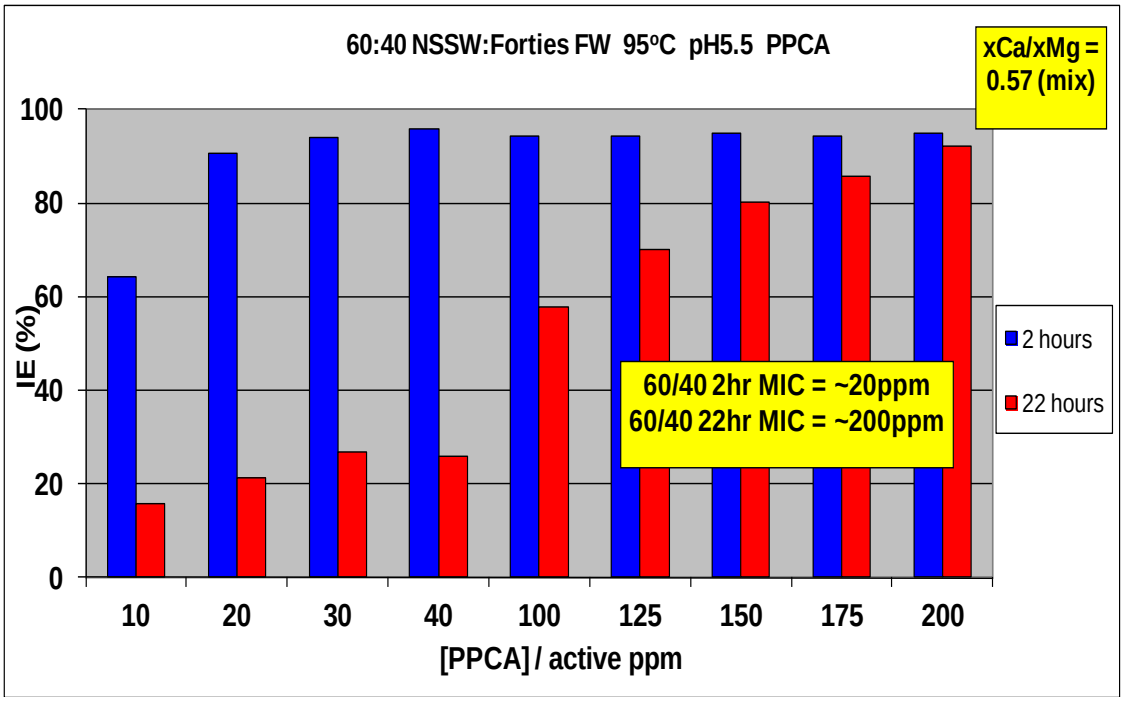

Figure 55: Stock MIC of PPCA measured in % for 2 and 22 hours (Source: S. S. Shaw, FAST, Heriot-Watt U., 2012)

Similar IE results are presented in Figure 56, Figure 57 and Figure 58 for 5, 10 and 20ppm PPCA samples, respectively, for stock, supernatant and precipitated PPCA when these latter two samples were recovered in PPCA precipitation experiments at 70°C. Clearly, at 70°C, the performance of stock and precipitate for inhibiting barite scales are quite similar to each other as compared to the 95°C results (cf. Figure 51, Figure 52 and Figure 53) where the precipitate has much higher IE than the stock. The supernatant PPCA sample in the 70°C precipitation experiment has a somewhat worse IE than the stock but this is not as low as the IE in the 95°C precipitation experiments. Furthermore, the MIC of precipitated PPCA at 70°C is 20ppm and at 95°C is 10ppm. Therefore lowering the temperature affects the IE performance of the precipitated PPCA. In other words, at the lower temperature, somewhat less precipitation occurs but this precipitate is rather more like the stock sample than is found for precipitates formed at higher temperatures.

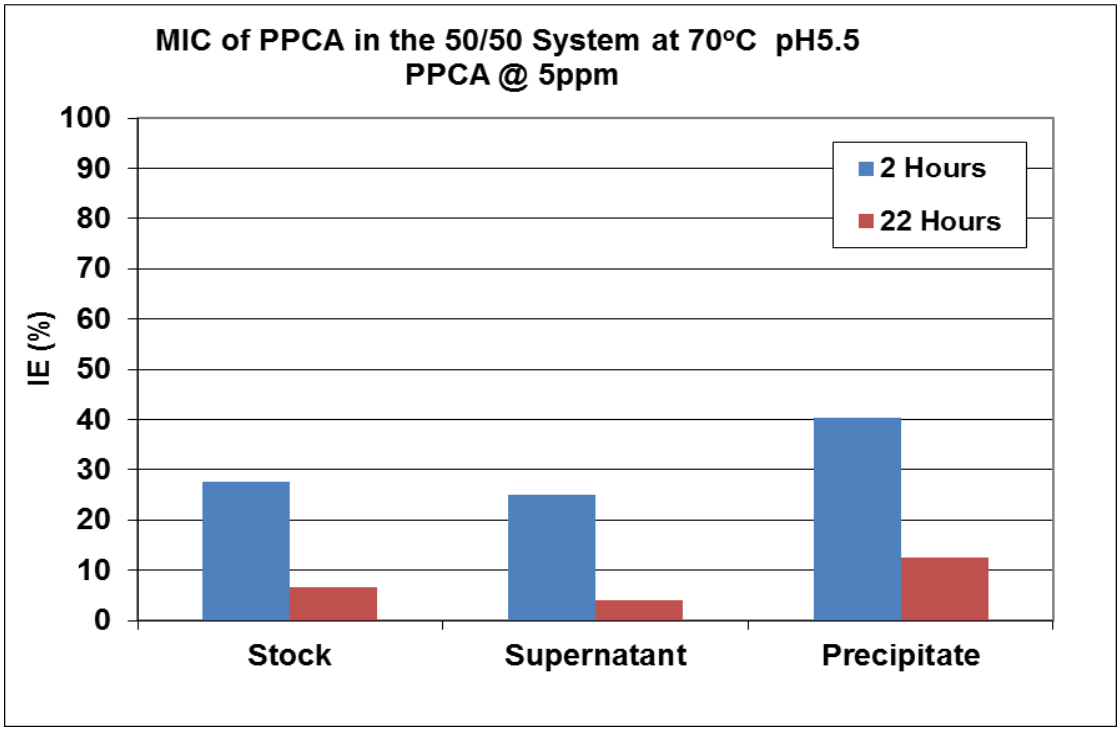

Figure 56: IE of 5ppm for stock, supernatant and precipitated PPCA from the PPCA precipitation experiments performed at 70°C.

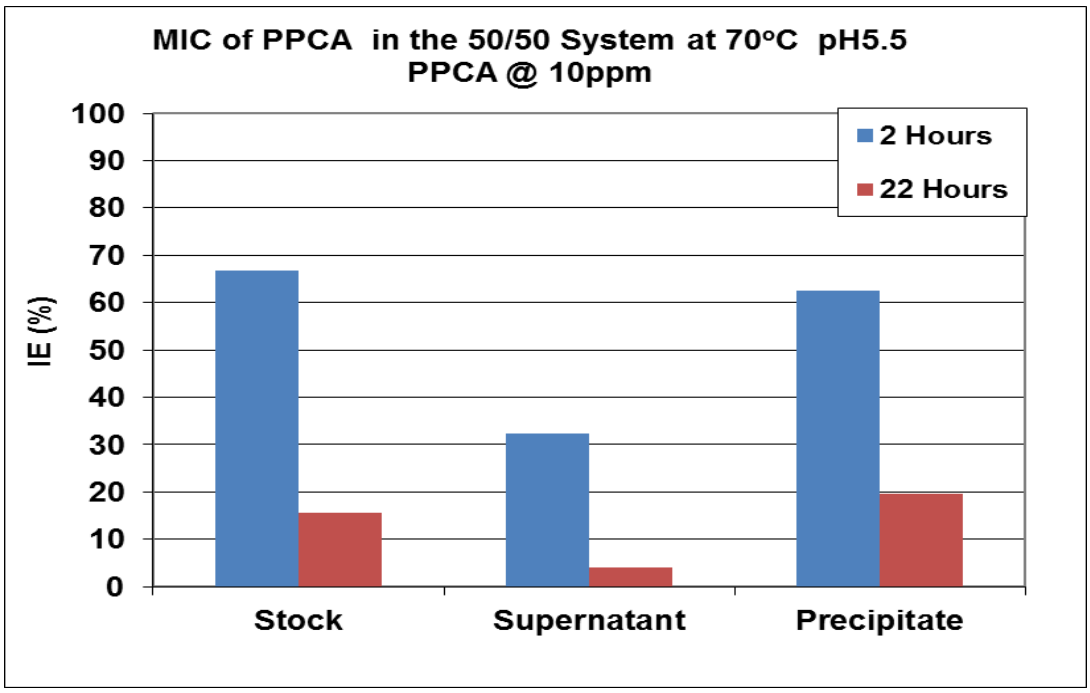

Figure 57: IE of 10ppm for stock, supernatant and precipitated PPCA from the PPCA precipitation experiments performed at 70°C.

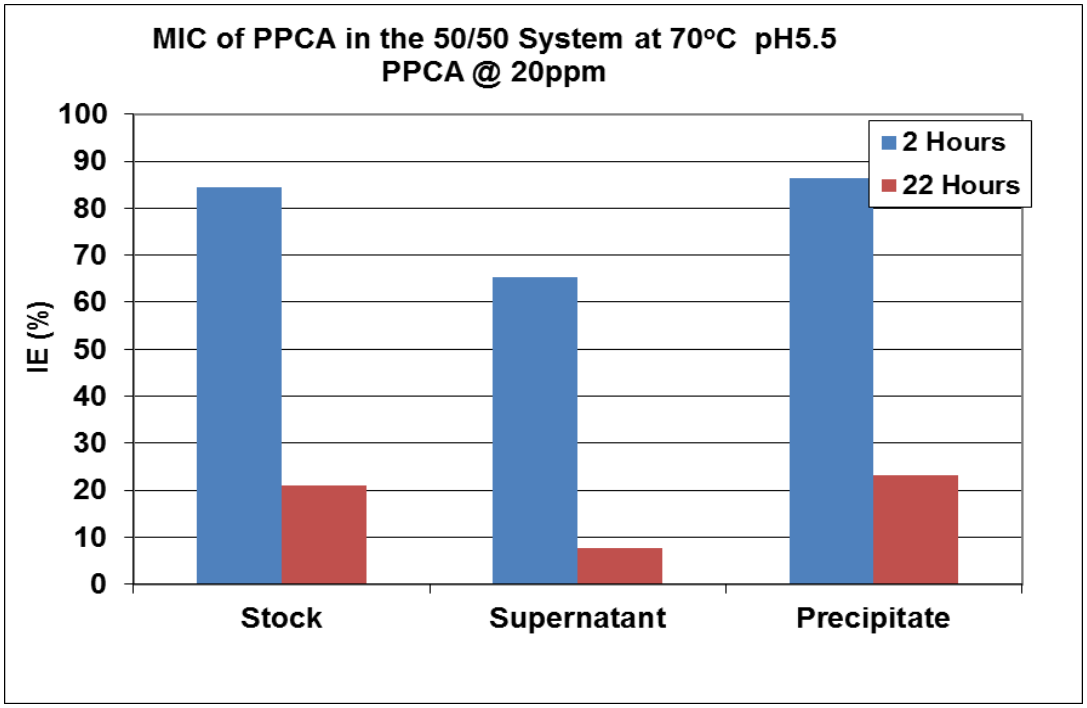

Figure 58: IE of 20ppm for stock, supernatant and precipitated PPCA from the PPCA precipitation experiments performed at 70°C.

In the 50/50 system at 95^{o}C, we attempted to establish the MIC for the supernatant from the PPCA precipitation experiment and this is shown in Figure 59. Quite clearly, the IE performance of this supernatant (S1) PPCA sample is *much* worse than the stock solution (cf. Figure 51 above). The maximum [PPCA] tested in this experiment was 400ppm but, even for this very high level, the MIC for 2 hours was not reached. This finding shows that the precipitated PPCA (at 95^{o}C) is much more efficient at inhibiting barite than either the stock or supernatant. We conjecture at this stage that this is due to the fact that the PPCA precipitate preferentially contains the larger MW species and these have an increased IE. Correspondingly, the supernatant is much depleted in the higher MW species and this leads to its very low IE performance (as in Figure 59). This MW effect is beneficial in a field squeeze PPCA precipitation treatment since the average MW of the returning PPCA is increasing as the concentration falls towards the threshold levels. MW effects will be demonstrated experimentally in Chapter 6.

The other reason for *improved* IE of precipitated PPCA is the presence of calcium ions. The overall efficiency of PPCA is somewhat enhanced by the calcium ions through decreasing the fraction of protonated PPCA and forming PPCA_Ca complexes. Calcium ions may play a bridging role connecting the crystal sites with exposed SO_4^{2-} and PPCA functional groups so that the adsorption of PPCA on the active sites of $BaSO_4$ crystal surfaces is enhanced (Xiao et al., 2000, 2001). Collins (1999) has observed a similar effect of calcium with polyaspartate as a barite inhibitor. He showed the enhanced efficiency results with the reduction of net negative charge of the poly-ion due to complexation of the polyaspartate with divalent cations but without any quantitative correlations. It is also confirmed by our study, that the correlation of loss of calcium and PPCA from solution (i.e. ΔCa vs. ΔPPCA) is a maximum at 95^{o}C i.e. 30:1 molar ratio. Thus the presence of maximum calcium ion at high temperatures may also enhance the efficiency level of precipitated PPCA.

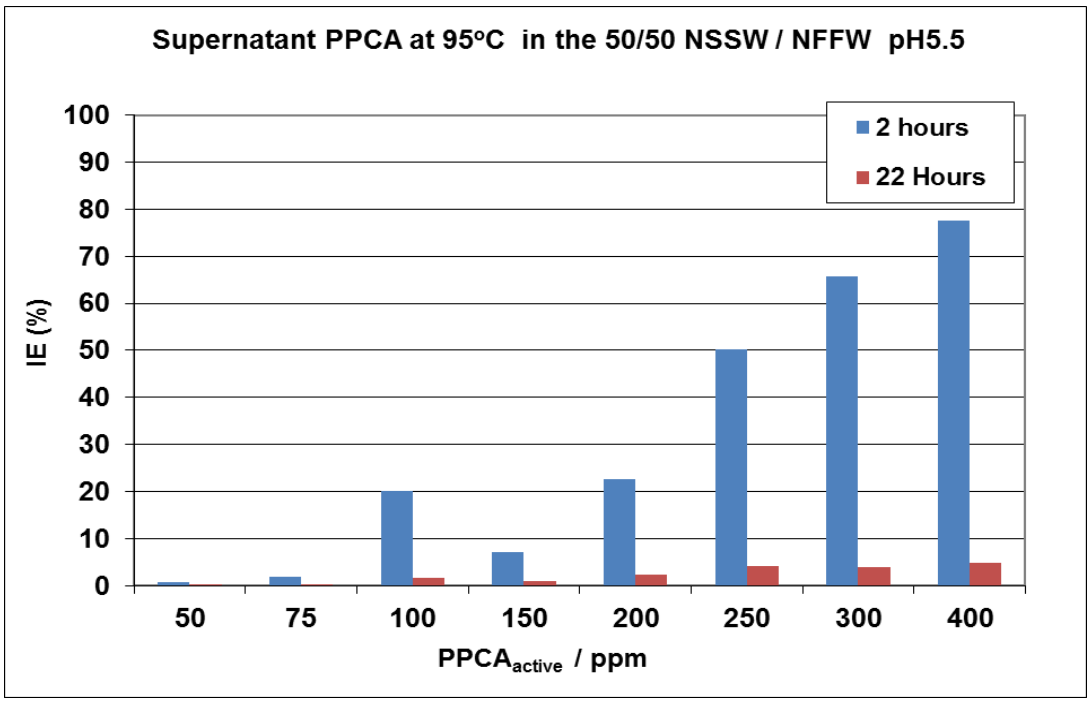

Figure 59: Barite IE performance of supernatant at 95°C showing that the MIC of this sample could not be found (cf. results for stock PPCA in Figure 55).

Relevant to the finding reported here, Graham and Sorbie (1995) noted that higher MW components return more slowly in core floods than lower MW components and have improved inhibition efficiencies for barium sulphate scale formation. However, this effect may not necessarily lead to longer squeeze lifetimes since, for these higher MW species; the adsorption isotherm may become so steep that effectively irreversible adsorption may be obtained. Therefore, some optimization of the MW may be required in order to design systems which perform both their roles (i.e. inhibition and adsorption and/or precipitation) in an efficient manner – especially in precipitation processes.

4.5.3 Analytical Results: Comparison of C18-Hyamine and ICP Results for PPCA

In previous sections, we have investigated the IE of the supernatant and precipitated PPCA recovered from the precipitation experiments. These IE results have been rationalized in terms of the polydispersity (spread of MW or MWD) of the PPCA (Sorbie, 1991). This means that in practice, we are never dealing with a discrete species but with a range of species of identical generic type but slightly different MW. The stock solution has the original MWD of the supplied PPCA, along with any additional impurities, which may be present from the manufacturing process. SIs containing a

carboxylic acid functional group like PPCA can be analysed by C18 Hyamine cartridges. The SI is applied at pH2. This ensures that the SI is fully non-dissociated allowing the SI to be retained on the C18 cartridges through H-bonding or weak interactions. This allows separation of the SI from the brine salts which flow through the cartridges and are discarded.

In all the IE experimental results in Figure 51 to Figure 59, "PPCA concentration" is quoted such as 10ppm, 20ppm etc. However, these are established by ICP which is a measure of the phosphorus (P)-content of the species. More importantly, the P factor is the practical measurement of the amount of phosphorus in a chemical. It is the measured value of the ppm phosphorus measured in a certain ppm of SI expressed as a ratio. A P factor of 1 indicates that 1 ppm of phosphorus will be measured for each 1ppm of SI (typical for phoshonates based SI) while a P factor of 400 indicates that 1ppm of phosphorus will be measured for each 400ppm of SI (typical for low phosphorus containing polymeric SIs). However, in PPCA each phosphorus is linked between the two carboxylic groups. To assay the amount of polymer by measuring the functional group at lower end of concentrations, we used a wet chemical analysis such as the C18-Hyamine method, usually (but not always) in conjunction with a solid phase extraction (SPE) using a filter cartridge such as a C18.

***Experimental Details*:** As in the IE experiments, this is also a second stage of the compatibility experiments. The 3 fractions generated from the compatibility stage, precipitate, supernatant and supernatant were analysed for polymer by C18 Hymaine cartridges. In this work, the 'base case' method of assay of the polymer is by ICP analysis (for P). In the C18- Hyamine method, a calibration graph can be constructed for known polymer concentrations and their corresponding determined absorbance values. The calibration graph may be 3^{rd} order, 2^{nd} order or linear. A successful fit of the trend line to the data should have an R^2 value very close to 1. A general rule for dilution of unknown sample concentrations would be to assume maximum concentration used in the experiment and perform an appropriate dilution so that the determined absorbance value lies in the middle of the calibration range. The experimental details of the analysis procedure were described in more detail in Chapter 3.

Experimental Results and Discussion

In this section, we show comparative analytical results using both ICP and C18/Hyamine for the PPCA stock and the various fraction of polymer recovered from the precipitation experiments – PPCA supernatant and precipitate. In later work, we will confirm these interpretations by presenting MWD results for PPCA. The precipitated PPCA species contains a MWD which is thought to be richer in the higher MW species and probably has far fewer of the "impurities" that is in the stock. The supernatant will have a MWD containing mainly lower MW species and it will also probably be higher in any impurities which may be present. It will be clear from these results that there will be strong implications for the *analysis* of the PPCA by either ICP or by wet chemical analysis.

Figure 60 shows the [PPCA] by C18/Hyamine and Figure 61 shows the [PPCA] by ICP for the three fractions of PPCA. The nominal concentrations of each sample were taken as being 1ppm, 5ppm and 8ppm *based on ICP*. However, the results in Figure 61 are very close to these values although a marginally higher value is measured for the precipitated sample.

The stock solutions are accurately assayed at 1, 5 and 8ppm which are as expected since it is the stock which is used in the calibration for the Hyamine method. However, the supernatant sample is shown to give much less polymer ~0.3, 3 and 4.5ppm in Figure 60 rather than the 1, 5 and 8ppm values prepared from ICP. Likewise, and very notably, the precipitated sample gives much enhanced levels of polymer ~2, 9.5 and 16ppm rather than the 1, 5 and 8ppm values prepared from ICP. The "8ppm" sample by ICP here is assayed at 16ppm by Hyamine i.e. it contains much more active polymer (about *double*) than indicated by its P-content.

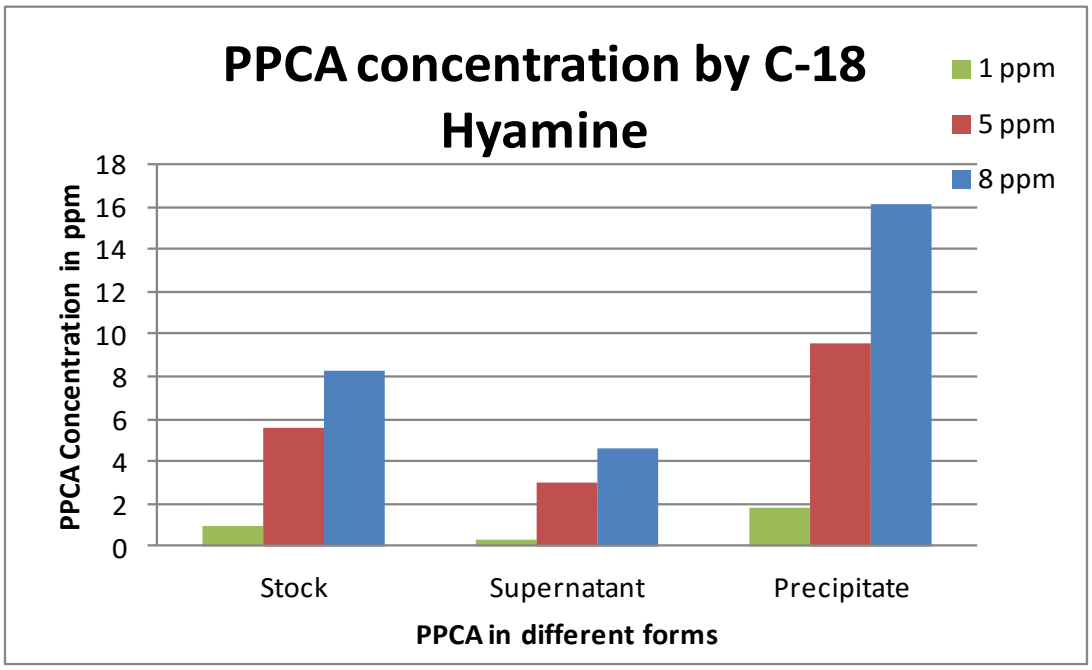

Figure 60: PPCA concentrations assayed by C18/Hyamine but prepared at 1, 5 and 8ppm by ICP assay of original samples (stock, supernatant and precipitate) recovered from PPCA precipitation experiments at 95^{o}C

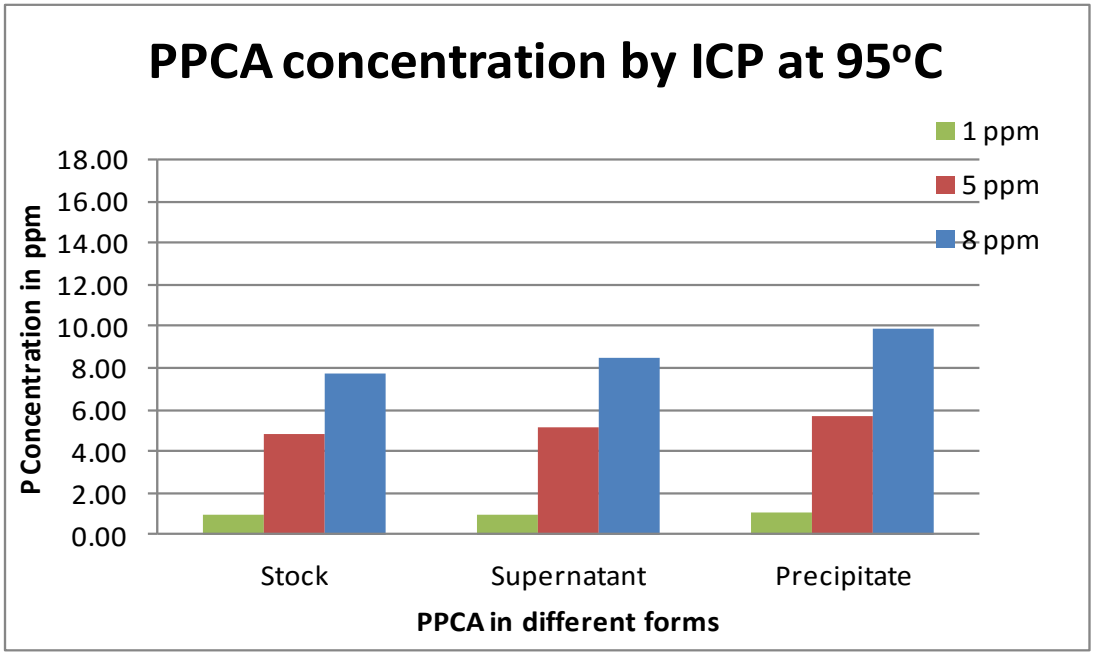

Figure 61: PPCA concentrations assayed by ICP but prepared at 1, 5 and 8ppm by ICP assay of original samples (stock, supernatant and precipitate) recovered from PPCA precipitation experiments at 95^{o}C

Similarly the compatibility precipitation experiments were carried out at 70^{o}C. The results for Hyamine and ICP analysis are presented in Figure 62 and Figure 63

respectively for PPCA. The results of these 70°C precipitation experiments are qualitatively quite similar to the results at 95°C presented immediately above. However, because the compatibility precipitation temperature is rather lower (70°C); we expect to have some high MW PPCA in the supernatant solution also. This is seen in Figure 62 where the supernatant is seen to give a higher polymer assay at all 3 concentrations than in Figure 60 (precipitation at 95°C).

All of the findings on ICP and C18/Hyamine assay presented in Figure 60 to Figure 63 are very much in line with the IE experimental results presented above and with the analysis presented in terms of MWD of the various fractions of the PPCA solution. A very complete and consistent description of what is observed within the PPCA phase envelope is clearly emerging.

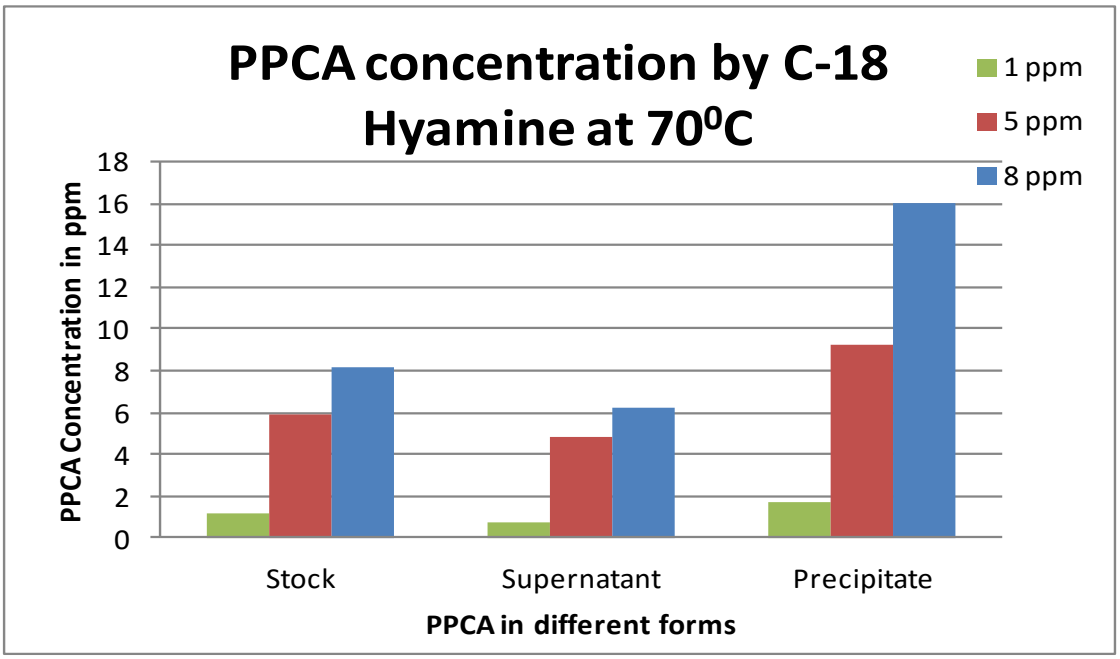

Figure 62: PPCA concentrations assayed by C18/Hyamine but prepared at 1, 5 and 8ppm by ICP assay of original samples (stock, supernatant and precipitate) recovered from PPCA precipitation experiments at 70°C

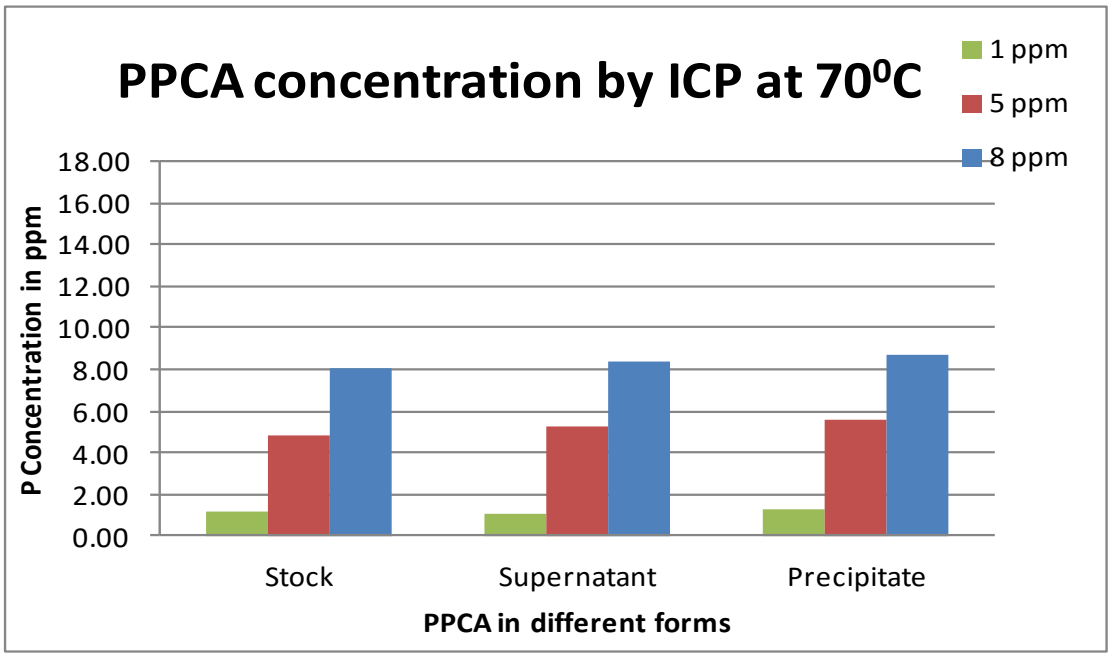

Figure 63: PPCA concentrations assayed by ICP but prepared at 1, 5 and 8ppm by ICP assay of original samples (Stock, Supernatant and Precipitate) recovered from PPCA precipitation experiments at 70^{o}C

4.5.4 Kinetics of the PPCA

At Precipitation Stage:

This experiment was performed to establish the kinetics of the precipitation process of PPCA. For example, we wished to determine how fast the precipitation approached equilibrium; the question arose – is the 24 hour period we leave the experiment enough for it to reach precipitation equilibrium? This experiment was performed in 2 ways. The 2 methods were quite similar but, in method 1, the *same* bottles were used up to the maximum test temperature. After every 24 hours, the temperature was changed. In method 2, different bottles were added in the oven at each temperature from the room temperature which is maintained at 20^{o}C. This is to check the difference of the continuing bottles with the newly added bottles. For this experiment, we have used glass bottles to visualize the difference in the precipitation at different temperatures. Results from these kinetic experiments are shown in Figure 64 and Figure 65.

***Experimental Details*:** Initially, the experiments were carried out with 5000ppm of PPCA and 2000pppm of [Ca^{2+}] in FW in a 250ml glass bottles in duplicate. The starting temperature was 55^{o}C. The samples were taken after every hour up to first 8 hours and

then after 18, 24, 42, 48, 70, 76, 96 and 128 hours; the temperature was then increased from 55 to 70^{o}C, and sampling were carried out after the same times. Again, after the 128 hours, the temperature was again increased from 70 to 95^{o}C and sampling was repeated at the same times. The same bottles were used throughout the experiment at the 3 different temperatures. The results were plotted against the amount of PPCA or Ca^{2+} in solution vs. time.

Experimental Results and Discussion

Figure 64 shows the change in [PPCA] and [Ca^{2+}] (both measured by ICP) vs. time at various temperatures (T = 55, 70 and 95^{o}C), respectively. These results clearly show that the only significant changes which occured in the [PPCA] was in the first two hours after which [PPCA] stabilises over time. Both methods of performing this experiment give very similar results which confirms the earlier finding regarding the effect of temperature i.e. increase of temperature encourages the precipitation process and that this process is effectively at equilibrium after ~2 hours. The results also reconfirmed that, at higher temperatures, more precipitation is seen to occur.

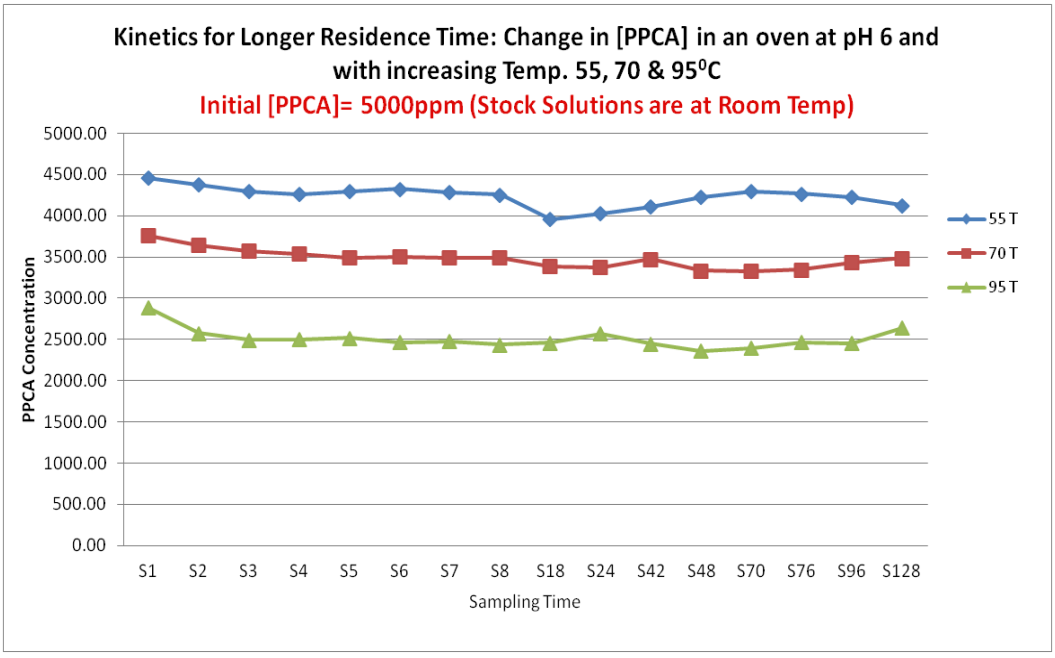

Figure 64: Kinetics of the PPCA_Ca Complex of the [PPCA] for the Longer Residence Time.

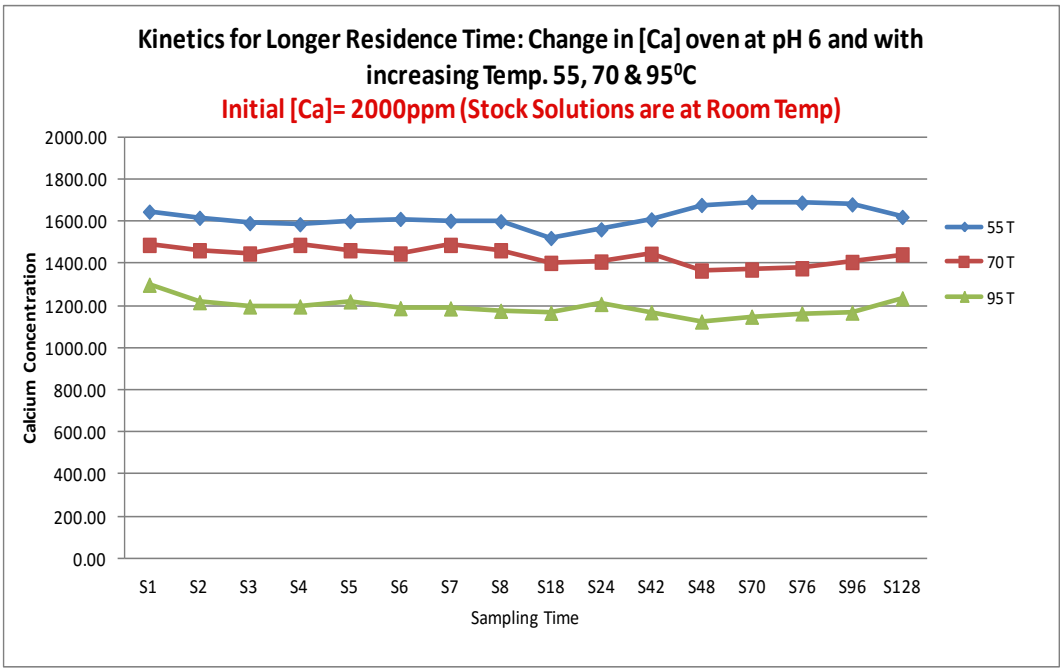

Figure 65: Kinetics of the PPCA_Ca Complex of the [Ca^{2+}] for the Longer Residence Time

At Re-dissolution Stage:

The kinetics of precipitation of the PPCA_Ca complex was also studied at lower temperatures, T = 70 ^{o}C and 95^{o}C and results for these cases are shown in Figure 66 and Figure 67 which show [PPCA] vs. time and [Ca^{2+}] vs. time, respectively. Less precipitate forms at the lower temperatures but otherwise these results were very similar to those at the higher temperature in that equilibrium was reached after 2 hours.

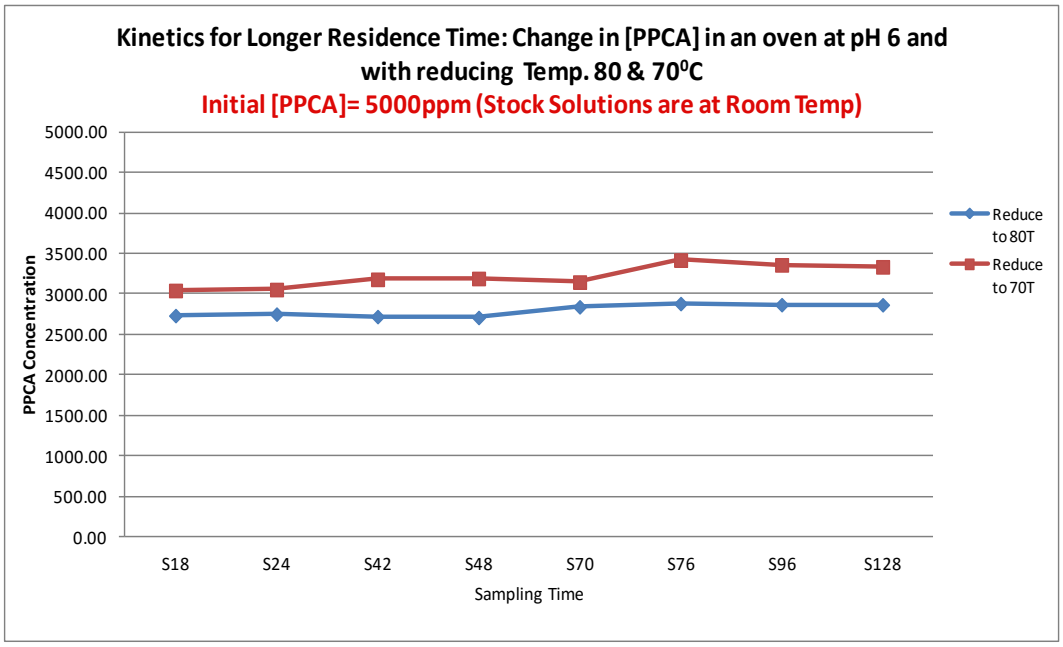

Figure 66: Kinetics of [PPCA] Precipitate Complex while reducing the Temperature at 80 & 70°C

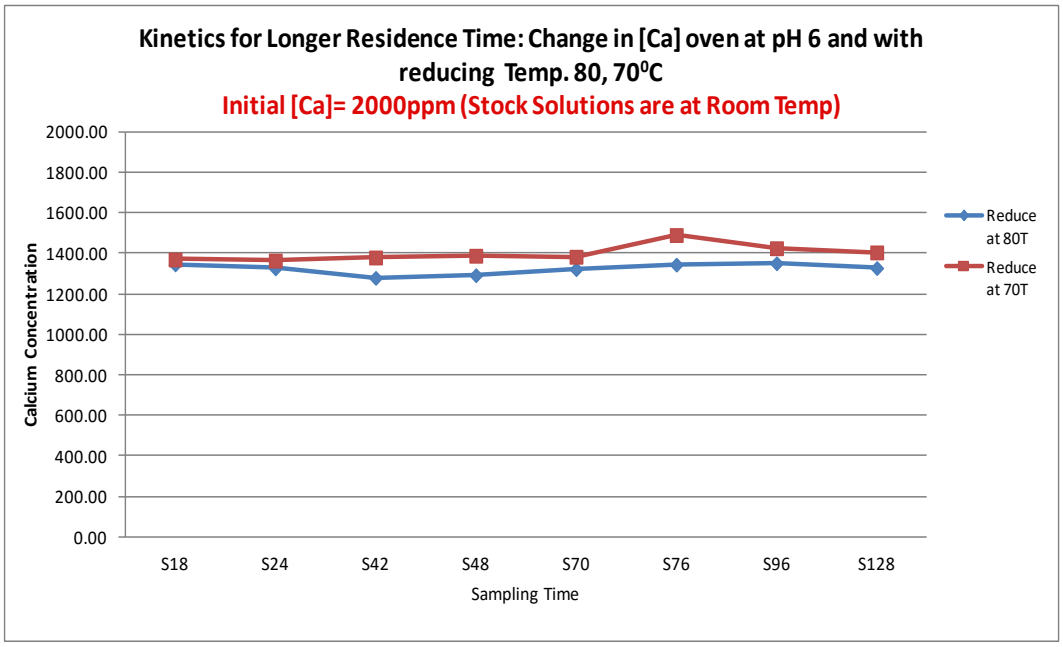

Figure 67: kinetic of [Ca^{2+}] precipitate complex while reducing the temperature at 80 & 70°C

4.5.5 Effect of pH on the Precipitation of PPCA

The other important parameter in the phase envelope of PPCA is the pH. Initially, the natural pH of the 10,000ppm active PPCA in NFFW was found to be 3.48. PPCA

maintains its single phase solution after mixing with NFFW. The simple compatibility test was conducted while keeping the [SI], [Ca^{2+}] and temperature (T) constant. The varying factor in this experiment was the range of pH. The experiment was performed at 4000ppm [SI] and 2000ppm [Ca^{2+}] in NFFW at temperature 95^{o}C with pH varying from 2 to 6. The results for 4000ppm [PPCA] were compared with the blank. The results strongly suggest that the precipitation starts from pH 5 - 6 for PPCA at 95^{o}C as shown in Figure 68.

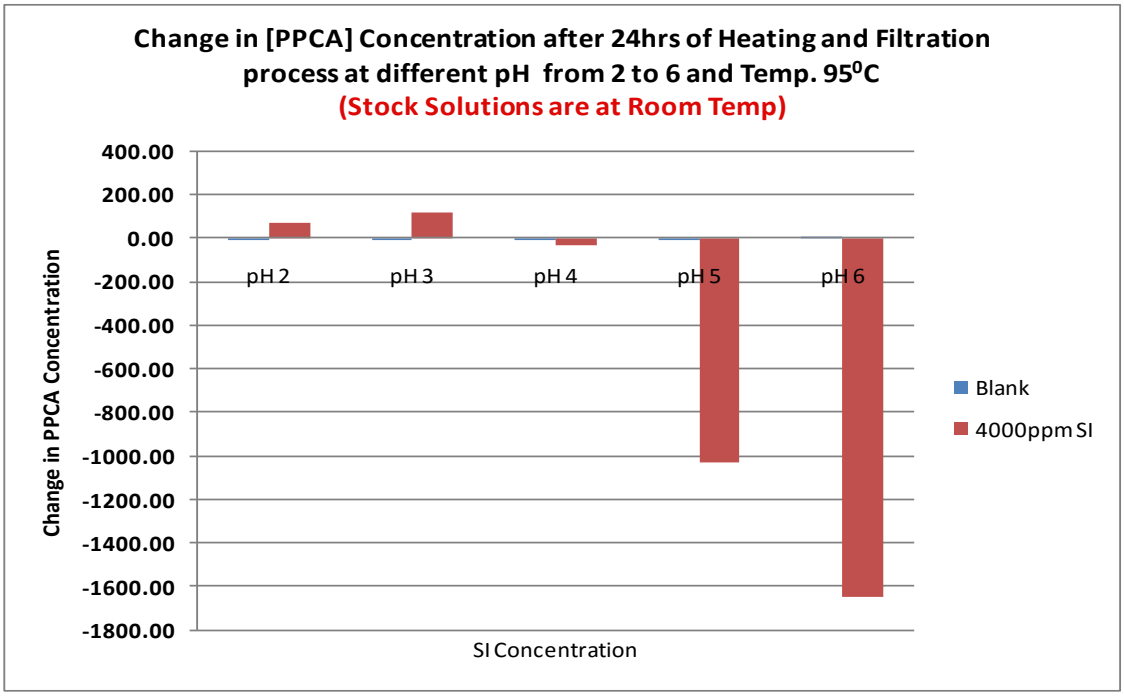

Figure 68: Change in [PPCA] at range of pH

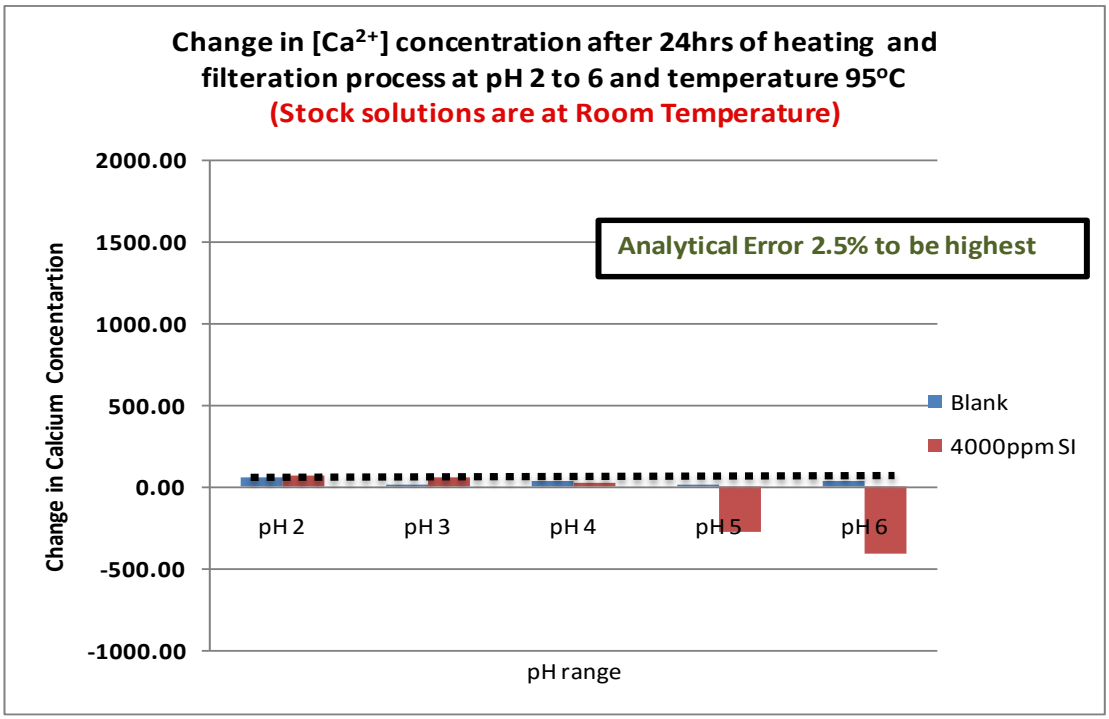

Figure 69: Change in [Ca^{2+}] at range of pH

Figure 69 shows the corresponding change in [Ca^{2+}] over the range of pH values. These changes were calculated by keeping stock samples at room temperature and experimental samples at 95°C temperature. The drop-in [Ca^{2+}] shows that a PPCA_Ca precipitates at higher pH values, i.e. pH ~5 and above.

The change has also been monitored in the final magnesium and lithium concentrations. Initially [Mg^{2+}] was 739ppm and [Li^{+}] was 50ppm and it appears that magnesium is not affected at any pH level. Therefore, it was concluded that magnesium does not play a significant role in the complexation reaction with PPCA. Lithium is used as an inert tracer ion in the NFFW brine and should not adsorb or precipitate. Lithium is analyzed to see if there was any evaporation in the system. It shows estimated reduction of 4% in the concentration which is under the analytical error limit. From previous result (Figure 68), it is clear that a drop in [PPCA] is observed from pH ~5 and pH ~6 at 95°C, although this result was confirmed for the higher concentration ~4000ppm PPCA. At this point, another compatibility experiment was conducted to check whether the change in PPCA concentration started at a lower concentration when other parameters are kept constant.

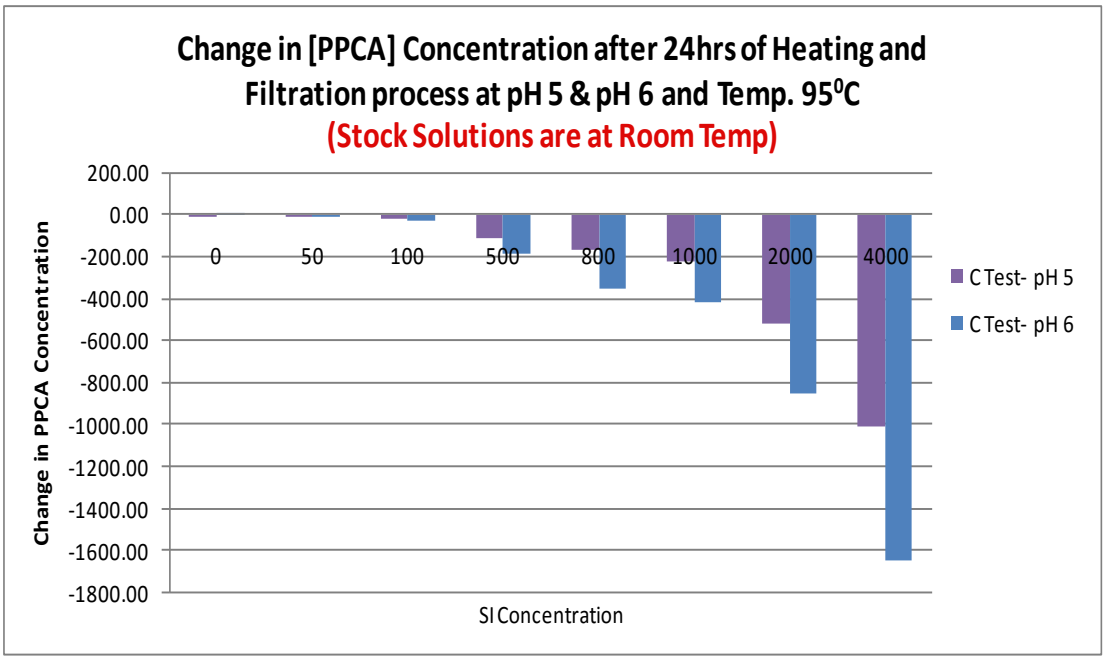

Figure 70: Compatibility Test: Change in [PPCA] from Blank to 4000ppm at different pH

Figure 70 shows the change in [PPCA] from lower to higher concentration up to 4000ppm at pH 5 and 6. These results were observed in the compatibility tests (i.e. no sand present) and thus only precipitation is involved. The results in Figure 70 confirm the observed changes which start from lower concentration of ~500ppm. These results also confirm that precipitation is related to pH value, since at pH 5 it precipitates less than at pH 6.

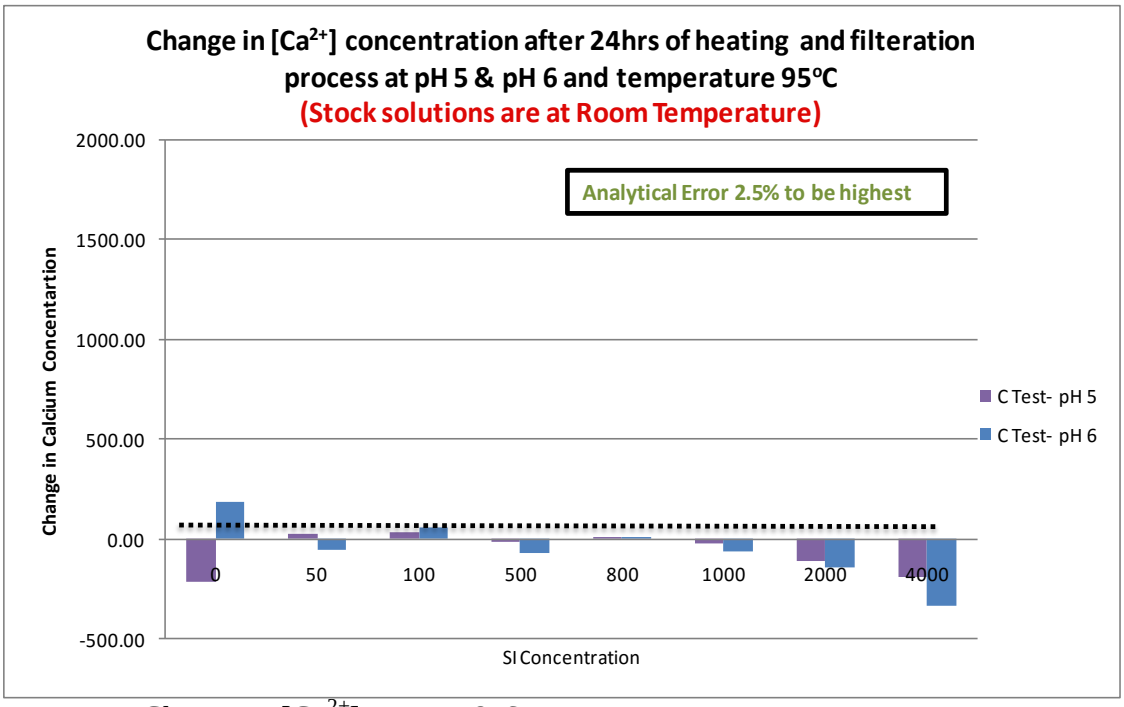

Figure 71: Change in [Ca^{2+}] at pH 5 & 6

Figure 71 shows the change in [Ca^{2+}] at pH 5 and 6. These changes (losses) in the [Ca^{2+}] were quite noticeable from 1000ppm of [SI] to 4000ppm of [SI]. This confirms that 1000ppm is just at the edge of the precipitate region. The divalent ion levels above stock solution concentration are not expected or must be within an analytical error of less than 5%. Note here that: (i) precipitation of calcium is related to pH and [SI], (ii) there is less precipitation at pH 5 than pH 6, and (iii) as the [SI] increases change in [Ca^{2+}] also increases. Thus broadly corresponding changes are observed in both the [Ca^{2+}] and the [SI] but no change was observed in [Mg^{2+}] or [Li^{+}] ion concentrations.

4.6 Summary and Conclusions

In this chapter, we have experimentally developed the phase envelope of PPCA and studied a range of factors which influence the phase behaviour such as, the calcium and inhibitor concentrations, pH and temperature. The phase envelope of PPCA was also characterized by scanning certain targeted parts of the phase envelope. The main conclusions from this chapter are summarized below:

1. ***Phase Behaviour of PPCA:*** The precipitation (phase separation) phase envelope of PPCA with formation brine is established and increased precipitation of the PPCA_Ca complex is observed with increase of T, [Ca^{2+}], [PPCA] and pH.

2. ***Coupled Adsorption/Precipitation Results:*** Within the static compatibility phase envelope, a series of "apparent adsorption" tests were carried out for a PPCA/ sand/brine system at varying (m/V) ratios to establish precisely where the system is in pure adsorption (Γ) and in coupled adsorption/precipitation (Γ/Π) regimes. It is clear that, although a small regime of pure adsorption is observed ([PPCA] ≤ ~100ppm), the precipitation regime is much larger and is the main effect for this system under these conditions.

3. ***Stoichiometry of the PPCA_Ca complex:*** In the precipitating system, the molar losses of PPCA (ΔPPCA) and Ca (ΔCa) correlate extremely well thus indicating the composition of the PPCA_Ca complex. It is found that the molar equivalents of Ca:PPCA in the precipitated complex are in the ratio ~30:1, i.e. in the formula PPCA_Ca_n, then n ≈ 30. This is true in both the precipitation (T increasing) and dissolution (T decreasing) cycles which are not quite identical possibly due to kinetic factors.

4. ***Inhibition Efficiency results:*** The barite IE of the PPCA has been determined for the original stock solution of polymer and the precipitated and supernatant polymeric species. Precipitated polymer shows much better IE than either the stock or the supernatant and, correspondingly, the IE of the supernatant polymer solution is very poor. These results are consistent with the precipitated species being rich in the higher MW components of PPCA which are known to be more efficient at inhibiting barite scale. This effect is overall beneficial since the IE increases (at a given [PPCA]) in the long return curve from a precipitation squeeze.

5. ***MIC Values of Stock, Supernatant and Precipitate:*** In order to quantify the IE results described in 4 above, we established the MIC for the supernatant and precipitated samples and compared these with MIC values for the stock PPCA. For a 50:50 Forties/SW brine at 95^{o}C the MIC values for this barite scaling system were:
   - *Stock PPCA* - 2 hours is 20ppm and 22 hours is 200ppm:
   - *Precipitated PPCA* - 2 hours is 10ppm and 22 hours is 100ppm.
   - *Supernatant PPCA* – 2 hours MIC >> 400ppm

6. ***Wet Chemical Results:*** From the analysis of the IE results on the supernatant and precipitated fractions recovered from the PPCA precipitation experiments, it is clear that MW fractionation of the polymer was occurring. This has implications for the assay of PPCA either by ICP (total P-content) or C18/Hyamine (total polymer). The observations were most marked for the 95^{o}C PPCA precipitation experimental results where:
   - the C18/Hyamine concentration for precipitated PPCA is *twice* that of the ICP concentration;
   - The C18/Hyamine supernatant PPCA concentration is half that of the ICP concentration.
   - These results are consistent with the changing MWD for the precipitated (richer in high MW species) and supernatant (less high MW species) fractions.

7. ***Kinetics of the Precipitation/Re-dissolution:*** In typical PPCA_Ca precipitation experiments, equilibration in [PPCA] and [Ca^{2+}] is largely established in the first two hours of the experiment. Test runs out to 128 hours show no changes in [PPCA] or [Ca^{2+}] after the first 2 hours and this confirms that 24 hours is a more than a sufficiently long time for precipitation equilibrium at one temperature.

8. ***Field Application and Significance of Results:*** The results from this work on polymer adsorption/precipitation processes are being used to test out recent models of coupled adsorption/precipitation (and IE). In the work presented here, we have focused on the phase behaviour of PPCA which would be useful for designing the precipitation squeeze.

CHAPTER 5- **SOLUBILITY OF PPCA_CA PRECIPITATE COMPLEX**

This study is primarily focused on the solubility of the precipitated PPCA_Ca complex produced after phase separation of PPCA. This work builds on earlier results discussed in Chapter 4 where the general form of the PPCA/Ca^{2+}/T/pH phase envelope was studied as it is relevant to precipitation squeeze processes. The work reported in this section, continues our examination of the detailed mechanism of the re-dissolution of the PPCA_Ca complex.

5.1 Introduction

In precipitation squeeze treatments, calcium is the most important divalent cation which is known to precipitate with polymeric scale inhibitors. The three main sources of the calcium ion are, 1) from the *in situ* (connate) water, 2) from the brine over flush, or 3) from the rock calcite cement by dissolution or indeed from the rock itself in carbonate reservoirs. During the shut-in stage, a sufficient amount of calcium ions and polymeric scale inhibitor must be present for complexation, otherwise precipitation will not occur. It is important to know the concentration of PPCA and calcium ion required ensuring precipitation, and this is established in experiments of the type described in detail in Chapter 4. In addition, the molar ratios of SI and Ca in the PPCA_Ca complex (i.e. n in PPCA_Ca_n) in the precipitating solution should also be established since this also affects the degree of precipitation.

The release of the inhibitor in the precipitation squeezes depends on two main factors; viz. the solubility (Cs) of the inhibitor-calcium complex and the rate of dissolution (r4) of the precipitation complex (Boak, 1996; Browning and Fogler, 1995; Barthorpe, 1992; Melandrino et al., 1995). The dissolution rate effect implies that the steady state concentration level in the returns depends on the local fluid velocity as it sweeps over the rock containing the surface precipitated complex. This local velocity depends on the depth of penetration of the precipitated slug into the radial near well formation, which

therefore affects the level of inhibitor concentration in the return curves. When the well is brought back onto production, the objective is for the return concentration level of the inhibitor in the produced brine to be at or above a certain threshold level. This threshold level is the minimum inhibitor concentration (MIC) required to prevent the formation of mineral carbonate or sulphate scales in that well.

In this chapter, we study the detailed solubility behaviour of the PPCA_Ca complex which, as noted above, plays an important role in precipitation squeeze treatments. We describe several novel findings on the solubility of (PPCA_Ca) complex system, as follows:

1. The precipitated PPCA_Ca complex was isolated and used to determine experimentally the solubility of the species involved in a field squeeze for various compositions and temperatures.

2. The solubility of the inhibitor-calcium complex and the rate of dissolution of the precipitation complex are discussed in some detail.

3. The solubility of the precipitated PPCA_Ca complex becomes lower as it is exposed to successive fresh supernatant brine and the behaviour is very unlike that expected from a "solubility product" model. A novel "stripping model" is later proposed based on the MWD (see Chapter 6).

Several novel features of the solubility of the PPCA_Ca complex have been found in this work which can only be understood by considering the changes in MWD that are occurring. The mechanism of precipitation/re-dissolution of PPCA, and indeed other polymeric scale inhibitors, is very different from similar processes for phosphonates, as explained below. Our finding on the MWD effects have relevance not just in determining the concentration of the polymer in the return curve ([PPCA]) but also in its ability to prevent scale formation (i.e. its IE in the PPCA return curve) and on how the process should be modelled correctly.

5.2 Experimental Details:

Material: All the experiments were performed using phosphino polycarboxylic acid (PPCA) as a scale inhibitor with Nelson Forties Formation Water (NFFW) Brine. Initially, 5000ppm PPCA active was prepared in NFFW brine which contains 2000ppm of Ca^{2+} ion concentrations along with other divalent metal ions. 50ppm lithium was also present in the brine as an inert tracer ion. The precipitated PPCA_Ca complex was recovered from the compatibility test at 95^{o}C at pH 6.

The set of experiments in this chapter were generally carried out in three stages to generate the PPCA_Ca complex. Stage 1 is the compatibility stage, in which the precipitated complex formed. The complex is then filtered using a 0.22μm filter and then used for further analysis. Stages 2 and 3 are somewhat different according to the analysis required for the test. These various stages are explained and discussed in detail below along with their experimental results.

5.3 Results and Discussion

5.3.1 Effect of Temperature on the Solubility of the PPCA_Ca complex

In this first set of experiments, the "true solubility" of the precipitated PPCA_Ca complex which was precipitated at T = 95^{o}C is now established. The compatibility test carried out at 95^{o}C with 5000ppm of [PPCA] and 2000ppm of calcium was followed by a re-dissolution test of the precipitate in FW. Figure 72 shows a schematic of the methodology of the true solubility experiment. This experiment is performed to check the solubility of the precipitate at a range of temperatures in the re-dissolution stage and the results are shown in Figure 73.

After the compatibility stage, the precipitated complex was separated from the supernatant by filtration. The second stage was the re-dissolution stage, in which the hot precipitate was immediately dissolved back into the hot FW brine. The temperature of the re-dissolution brine was the same as in the precipitation process, i.e. 95^{o}C, so that the precipitate will yield the solubility at 95^{o}C. The solution was assayed after 24 hours (by ICP) to determine this solubility level (denoted Cs below). After the sampling at 24 hours, the temperature was reduced to 80^{o}C and then, after a further 24 hours at 80^{o}C,

the solution was assayed again. The step was repeated until the sample was at room temperature, at which a final assay was performed. All the samples were assayed by ICP analysis.

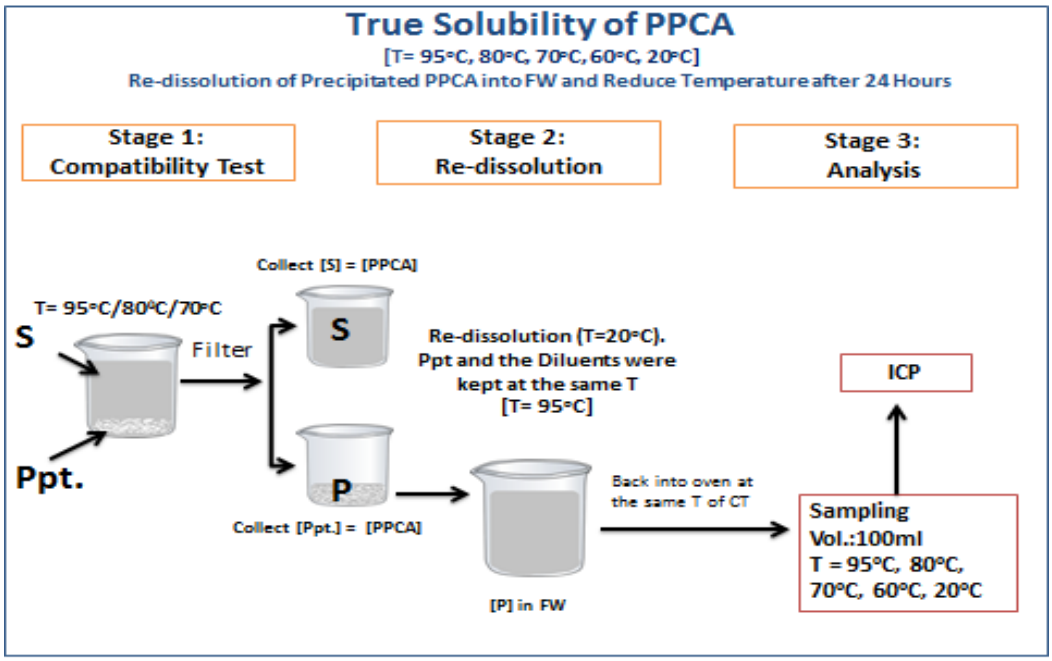

Figure 72: Methodology for the True Solubility of PPCA

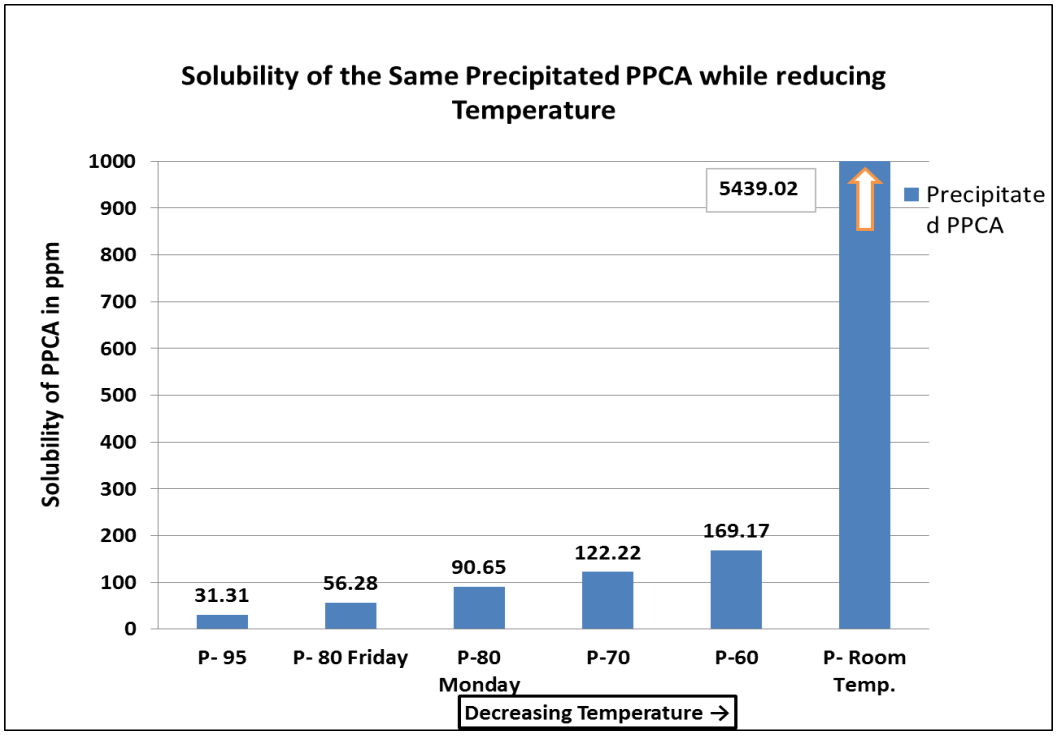

Figure 73: Solubility of PPCA-Ca precipitate at different Temperature

The results in Figure 73 show the solubility of the precipitates complex (PPCA_Ca) as a function of temperature. The results in Figure 73 clearly show that the solubility of the PPCA-Ca complex is temperature dependent. As the temperature is reduced, the solubility of the precipitate in FW gradually increases and, at room temperature, the precipitate fully dissolved back into the solution (the result in Figure 73 is not a true solubility for this reason). The solubility at 95^{o}C is ~31ppm and this gradually rises with temperature up to ~169ppm at 60^{o}C and at room temperature (20^{o}C) it solubilised up to 5439ppm. However, at 20^{o}C no precipitate was left at the bottom of the bottle whereas at higher temperatures the precipitate can easily be seen. This is why the room temperature concentration is not a true "solubility".

5.3.2 Solubility of the Precipitate in Different Brine Types

In the previous experimental results, the solubility of the precipitated PPCA_Ca complex in the FW is quite low at 95^{o}C, Cs ≈ 31ppm. Therefore, further experiments were performed to determine the solubility of the precipitate in SW and DW. The solubility of the precipitate was originally expected to be higher in DW than SW and FW, but the results turned out to be rather different from expectation, as shown in Figure 74.

The result presented in Figure 74 show the solubility of the precipitate in the three brines, viz., FW, SW and DW. The sampling was carried out at 2, 6 and 24 hours. The solubility of the PPCA_Ca complex in SW appears to be quite high (~700 – 800ppm PPCA) compared to the solubility in DW (~550ppm PPCA) and in FW (~40ppm PPCA). Thus the order of PPCA_Ca complex solubility is low in FW (~40ppm), much higher in SW (~700-800ppm), as expected, and then *lower* in DW (~500ppm). These latter results were quite unexpected. The experiment has been repeated twice and the reproducibility of the results was very good. Exactly the same order and almost the same solubilities were observed in repeat experiments, with the solubility of the PPCA_Ca complex being lower in DW than in SW.

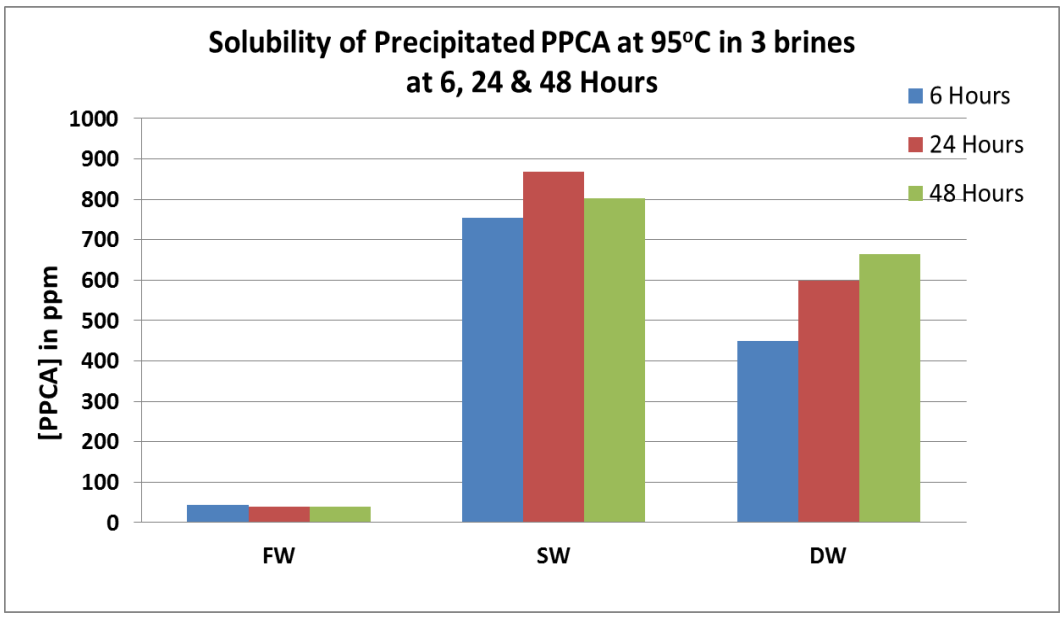

Figure 74: Solubility of Precipitated PPCA in FW/SW/DW

The most unexpected finding was the solubility of the PPCA_Ca complex is lower (~500ppm PPCA) in DW than (~700 – 800ppm) SW; SW contains ~35,000 TDS and 428ppm Ca^{2+} even though the DW has no Ca^{2+} (or any other ions) in it. This is at first glance rather puzzling, yet a very repeatable result but we will return to it later. The corresponding [Ca^{2+}] solution results for these solubility tests in FW, SW and DW are now presented in Figure 75.

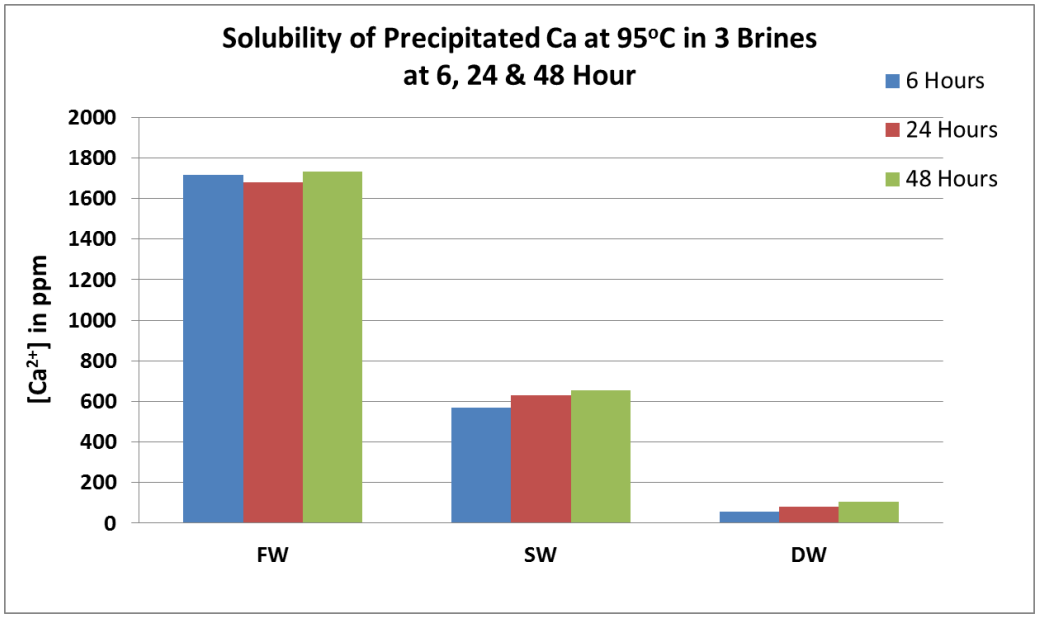

Figure 75: Solubility of the Precipitated Ca in FW/SW/DW

Figure 75 shows the [Ca^{2+}] level in the corresponding solubility experiments involving the precipitated PPCA-Ca complex and these appear to be broadly as expected. Initially the FW brine contains 2000ppm calcium, and on re-dissolution in FW the [Ca^{2+}] level is reduced a little to ~1800ppm.

Solution of FW brine has an ion in common with the soluble PPCA_Ca precipitated complex. The decrease in solubility of PPCA_Ca in FW brine is an example of the common ion effect. In general, by definition, the common ion effect is the shift in an ionic equilibrium caused by the addition of a solute that provides an ion that takes part in the equilibrium (Ebbing 1996).

In the SW case, where the original [Ca^{2+}] ~ 428ppm, the final concentration of the Ca^{2+} was found to be increased somewhat to [Ca^{2+}] ~600ppm, due to some dissolution of the PPCA_Ca complex in SW (which certainly occurs as the solubility is much higher in SW). In the DW case, which was originally calcium free, the final level is [Ca^{2+}] ~200ppm which must arise entirely from the re-dissolution of calcium from the PPCA_Ca precipitate. This shows that, a high amount of calcium suppresses the solubility of the PPCA_Ca complex in the FW case. The low calcium level and high sulphate ion concentration in SW favours the solubility of the precipitate in the SW case.

The entire PPCA_Ca complex re-dissolution experiment was repeated at 80^{o}C & 70^{o}C and very similar results to the 95^{o}C experiment were found. The 2 stages, i.e. compatibility and the re-dissolution, both occurred at 80^{o}C and at 70^{o}C and the trend of the results are highly reproducible at different temperatures. The solubility of the complex in FW is very low ~30-40ppm. The solubility of the PPCA_Ca precipitate is found to be lower in DW than in SW and is very consistent. The initial thought was that this lower solubility in DW may be a *kinetic* effect since in Figure 74 the [PPCA] in solution appeared to be still increasing even after 48 hours (i.e. the re-dissolution was very slow in DW). A further solubility experiment was performed where the PPCA_Ca complex precipitate was left to dissolve in DW (with occasional swirling) over 12 days (288hours) and the results shown in Figure 76 demonstrates that this is not a kinetic affect.

5.3.3 Solubility of the Precipitate Complex in DW for Longer Residence Time

The solubility of the precipitate complex in DW was observed to be unexpectedly lower than the solubility of the complex in SW. The higher complex solubility in SW compared to FW was expected. Previously, the results presented in Figure 74 shows that the maximum solubility in DW, after 24, was 500ppm and in SW and FW was 800ppm and 40ppm, respectively. In DW, where the calcium level is 0ppm, we had expected to observe a higher solubility of the PPCA complex than in SW. Therefore, a further experiment was designed to check the kinetics of the re-dissolution of the complex in DW for longer residence times.

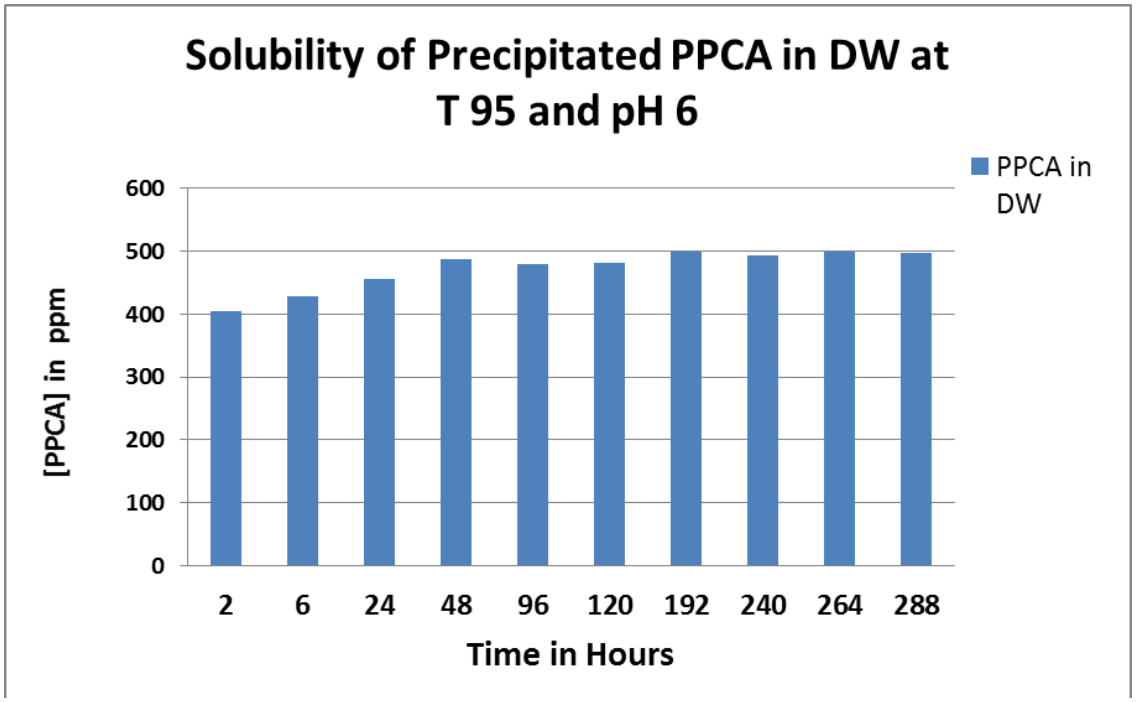

Figure 76: Solubility of precipitated PPCA in DW.

This DW solubility experiment was almost 2 weeks long and the results are presented in Figure 76 which shows [PPCA] vs. time (hours). These results show the solubility of the precipitated PPCA in Distilled Water at 95^{o}C for a starting pH 6. This long time experiment clearly shows that the maximum solubility of the PPCA_Ca complex is ~500ppm and that this solubility is reached after ~48 hours and does not subsequently change. Therefore, the lower solubility in DW is not a kinetic effect. This issue will be discussed again in terms of MWD results in Chapter 6.

5.3.4 Inhibition Efficiency of the precipitated PPCA in Different Brines

In the typical compatibility tests for PPCA described extensively above, the PPCA_Ca complex precipitate settled at the bottom of the test bottle. In Chapter 4, the IE results show that at 95^{o}C the remaining PPCA in the supernatant showed very poor IE. This was then shown that this was due to the very low polymeric content present in the supernatant as measured by the Hyamine method. On the other hand, the precipitated PPCA complex with calcium had a much higher IE and correspondingly higher polymer content. The MIC of the precipitate [P] at 95^{o}C in the 50/50 mix was determined to be 10ppm as compared with the stock PPCA which had an MIC ~20ppm. In previous sections, we determined the solubility of the precipitated PPCA_Ca complex on its re-dissolution in various brine types (FW, SW, DW and mixed brines). At this stage, we now describe an experiment designed to check the IE of the precipitated complex in some of these various brines.

Measuring the IE of the various components of the PPCA – i.e. the supernatant (S) and/or the precipitated part (P) - is the third stage of this type of experiment which follows the compatibility and re-dissolution stages. A schematic of the experimental procedure to measure the IE of the precipitated PPCA complex redissolved in different brines is shown in Figure 77.

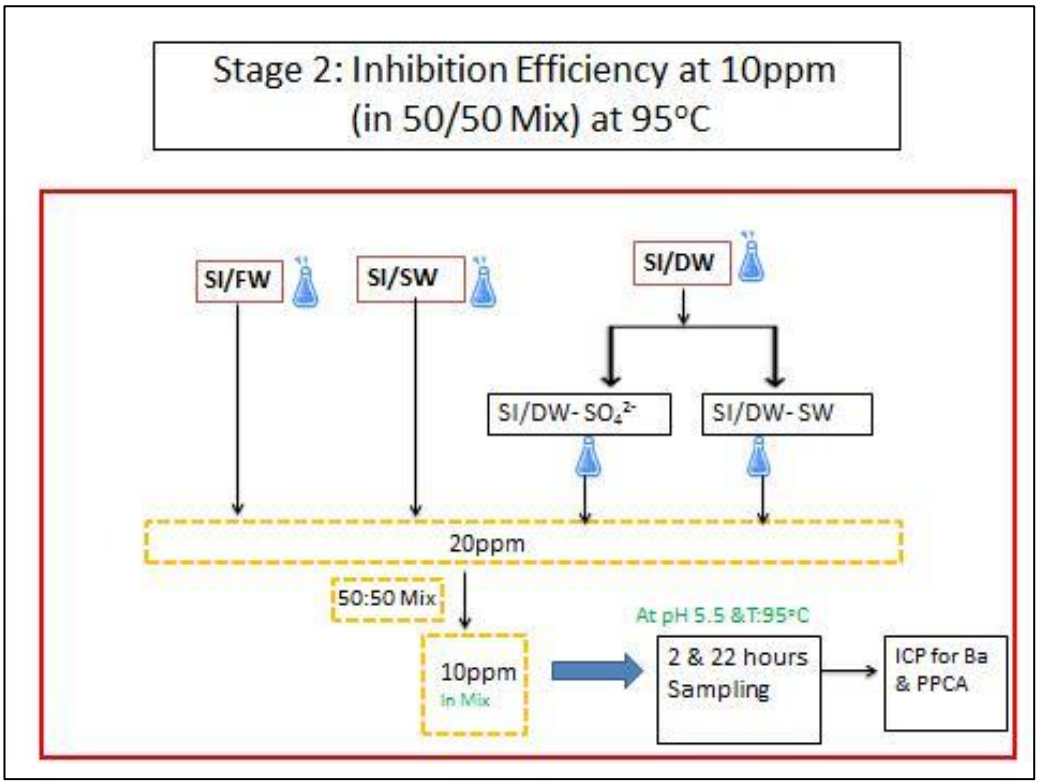

Figure 77: Schematic diagram of the IE of precipitated PPCA in different brines

The IE tests were performed at 10ppm in the mix at 95°C. The precipitated PPCA in different brines are diluted down to 20ppm, so that in the 50/50 mix, it will give a [PPCA] = 10ppm. For the barite IE test, it is necessary to have barium and sulphate ions in the separate brines such that in the mix it will form a barite precipitate. In normal IE tests, the SI is present in the FW or the SW and such tests are quite straightforward since by mixing the corresponding brines, barium sulphate is formed in the mix. However, for the case of PPCA in DW, the solution does not have either barium or sulphate ions in the brine. Two different methods were developed and applied to measure the IE of the precipitated PPCA in DW.

In method 1, a 2L solution containing 2960ppm sulphate ions in DW was prepared. A 20ppm PPCA was then prepared by diluting the DW/SI into this new DW/SO_4^{2-} solution and making up the volume to 250ml; a 50:50 mix was then prepared. In method 2, a 20ppm PPCA solution was prepared by diluting the DW/SI into SW and then making up the volume to 250ml; again a 50:50 mix was again prepared. All the four SI cases in different brine solutions were then tested in duplicate at pH 5.5 (maintained by buffer) at 95°C. The IE sampling was performed at 2 and 22 hours as usual. The IE results from these tests are shown in Figure 78 and Figure 79.

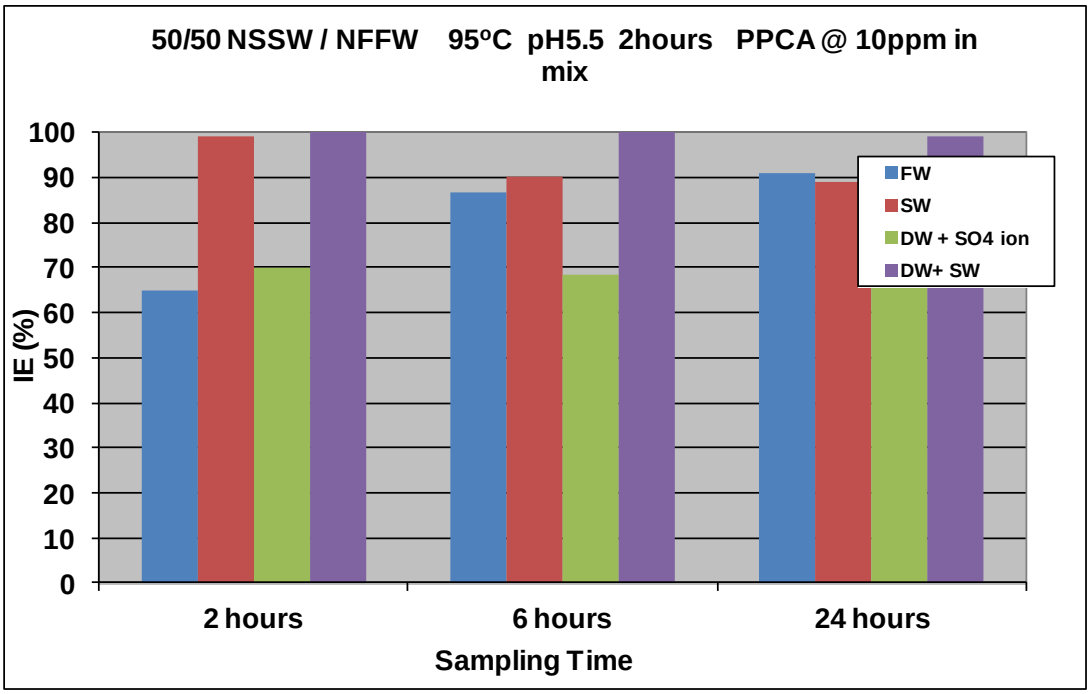

Figure 78: IE of the precipitated PPCA in different brines at 2 hours

The precipitated PPCA is believed to contain a higher MW content of polymer than the stock PPCA or supernatant solution. Previous results showed an improved IE performance of precipitated PPCA; the MIC for precipitated PPCA was 10ppm in the 50/50 barite scaling mix as compare to the stock PPCA MIC which was 20ppm. These results are very reproducible and were found again in these experiments. Results in Figure 78 shows that the IE of the precipitated PPCA is different at 2 hours in the different brines. The IE performance of the precipitated PPCA in SW seems to be much better than in FW. However, the performance of the DW/SI in SW is very similar to SW/SI. But the IE performance of DW/SI dissolved in sulphate ion brines shows 70% IE whereas the DW/SI dissolved in SW brine shows almost 100% IE. This implies that the sea water anions must have an influence on the IE performance of the precipitated PPCA.

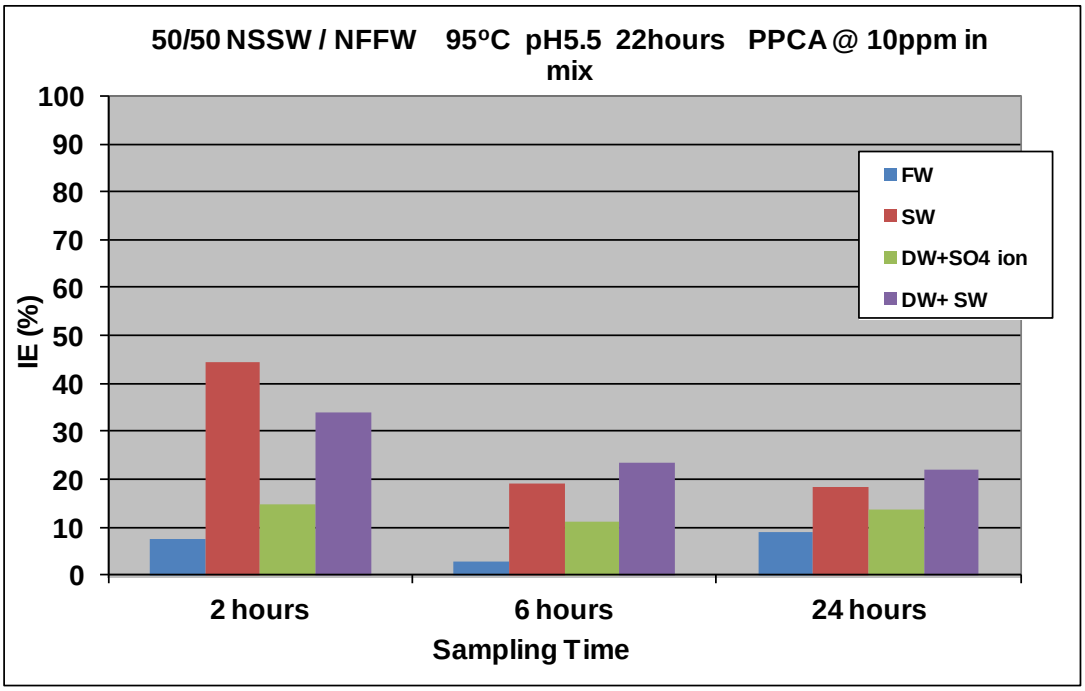

Figure 79: IE of the precipitated PPCA in different brines at 22 hours

Figure 79 shows the IE of the precipitated PPCA at 22 hours. Although these results do not reach the MIC, the performance of precipitated PPCA in SW seems to be better than the PPCA in other brines.

5.3.5 Solubility Concepts for Simple Salts and Polymer_Ca Precipitates

From all of the previous solubility results from the re-dissolution stage of precipitated PPCA_Ca complex, we now compare the behaviour of the 'polymeric_Ca' complex with the corresponding phosphonate_Ca complex. The solubility of the precipitated PPCA_Ca complex is very different to the solubility of a typical phosphonate_Ca case or of a simple sparingly soluble salt, such as barium sulphate. Consider the case of barium sulphate solubility in Figure 80. Suppose the solubility of the $BaSO_4$ salt is x ppm in 1L. By doubling the volume and make it to 2L, after reaching solubility equilibrium, the solubility will again become x ppm (as long as there is excess $BaSO_4$ solid present). Now consider what happened to the solubility of the PPCA_Ca complex? Does this behave in the same way as barium sulphate as shown in Figure 80 or is its behaviour very different?

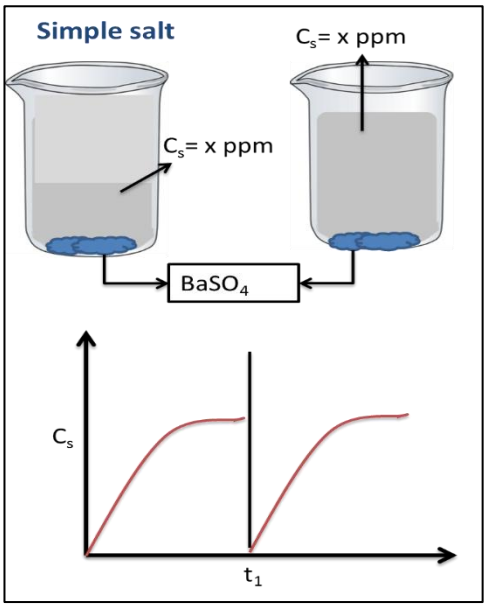

Figure 80: Solubility concept for a simple sparingly soluble material described by a Solubility Product Model (e.g. barium sulphate)

To answer the above question on the nature of the PPCA_Ca complex, another fairly complex experiment was designed. Initially, in the compatibility stage of this experiment, at 95^{o}C, 5000ppm of PPCA was precipitated with 2000ppm of calcium present in FW brine at pH 6. The experiment was performed in duplicate using a 200ml volume. The solubility of the precipitated PPCA in FW was checked using two experimental methods. After the filtration of the precipitate in the compatibility test, it was redissolved back into FW (200ml). Initially the volume used in the compatibility test was 200ml, hence in the re-dissolution stage, 200ml volume was used to get the solubility of the precipitate. In method 1, after the first re-dissolution of the precipitate, another 200ml of FW was added after 24 hours and sampling was carried out for a long period. In total, the volume in the glass test bottle was 400ml. In method 2, after the first re-dissolution, the precipitate was filtered again after 24 hours, and redissolved back into 200ml of FW. The sampling was carried out in both types of experiment up to 240hours. Both experimental methods gave very similar results as shown in Figure 81 and Figure 82.

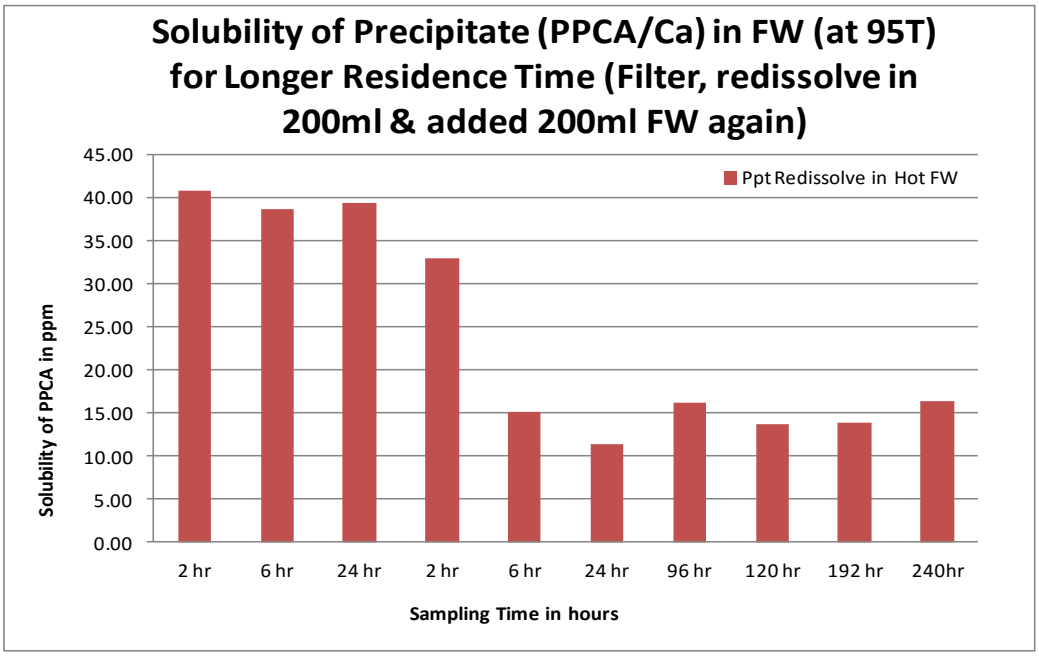

Figure 81: Solubility of the Precipitate in FW by Method 1

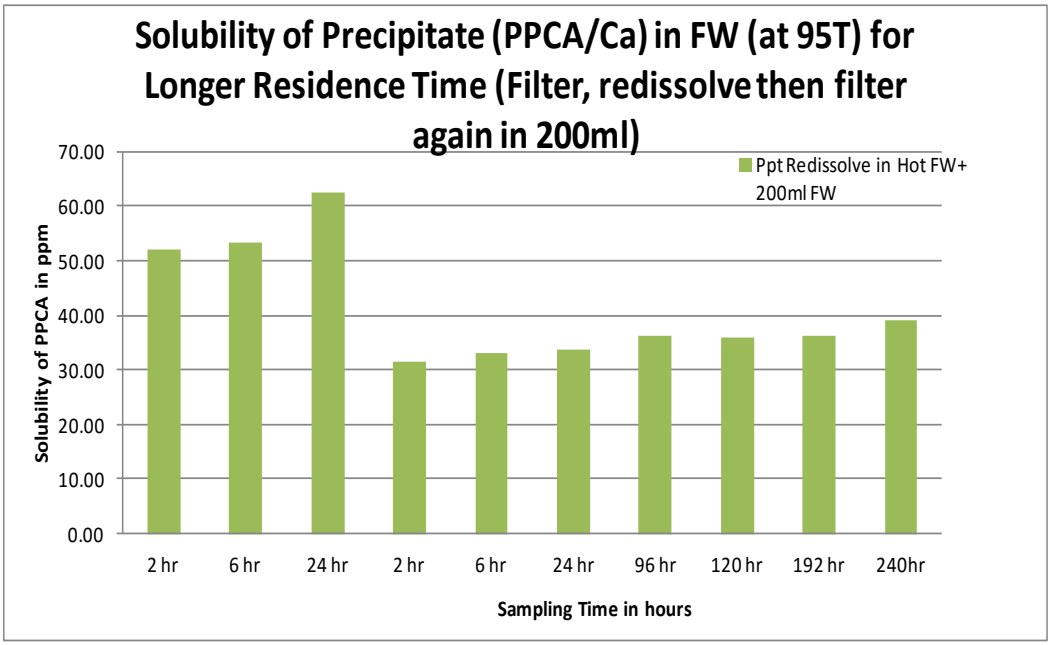

Figure 82: Solubility of the Precipitate in FW by Method 2

The results of the solubility experiment using methods 1 and 2 are presented in Figure 81 and in Figure 82, respectively. In method 1, after 24 hours of the first re-dissolution of the precipitate in the FW, another 200ml of FW was added to the solution. The results in Figure 81 clearly demonstrate that after doubling the volume, the concentration of the PPCA becomes approximately half. Very similar results were produced by the other method as shown in Figure 82.

Figure 82 shows the results from method 2 in which another filtration has been carried out after the first re-dissolution. After the second filtration, the precipitate redissolved back into 200ml of FW. As in the method 1 result, the results from method 2 shows half the concentration of PPCA after second filtration.

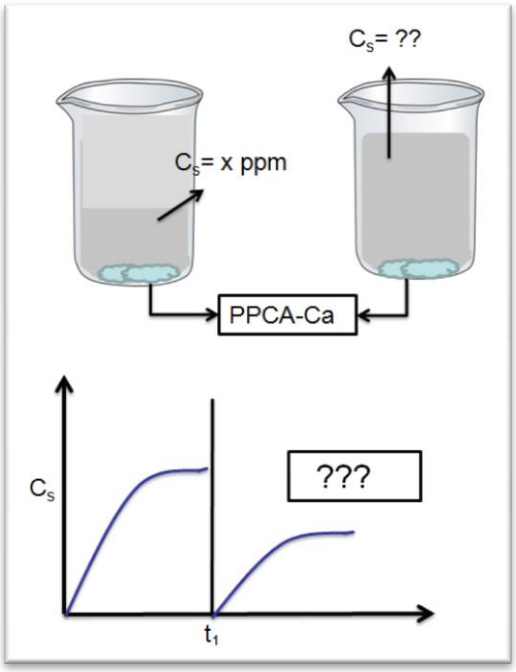

Figure 83: Solubility Concept of the PPCA_Ca precipitate in FW

Therefore, the solubility concept for the PPCA_Ca complex is definitely not the same as for a simple insoluble salt such as barium sulphate. Both of the results presented above confirmed that the "second" solubility of the precipitated PPCA_Ca complex appears to be half that of the original material. This is a very unexpected result and it has important implications on how the solubility of precipitated polymer_Ca complex should be modelled in a precipitation squeeze treatment. Clearly, it cannot be modelled by a simple solubility product model which would predict the type of result seen for barium sulphate, as shown schematically in Figure 80.

5.3.6 Solubility of Successive Supernatants of PPCA_Ca Complex

To examine the solubility of the PPCA_Ca complex in more detail, a further experiment was designed and performed to check the consistency of the above results for several *successive* solubilisations of the PPCA_Ca complex in the *same* fresh brine. In this

case, the simple solubility product model would predict that the same solubility would be observed in each case as long as excess precipitate was present. Our previous results imply that this will not be the case, but it was unclear what to expect in such a series of successive solubility experiments.

This experiment essentially applies a repetition of the compatibility stage followed by alternating filtration and re-dissolution stages as described above. As in many previous experiments, the precipitated complex was produced from 5000ppm PPCA in FW brine at 95°C at pH 6. After the initial 24 hour compatibility stage, the PPCA_Ca precipitate was filtered and the supernatant was collected. The alternating filtration and re-dissolution stages were then repeated for the same precipitate up to four times at 95°C and the solubility, i.e. the [PPCA] dissolved in the brine, was assayed by ICP for each supernatant. Successive solubility results in FW (Nelson-Forties FW with 2000ppm Ca^{2+}) are shown in Figure 84.

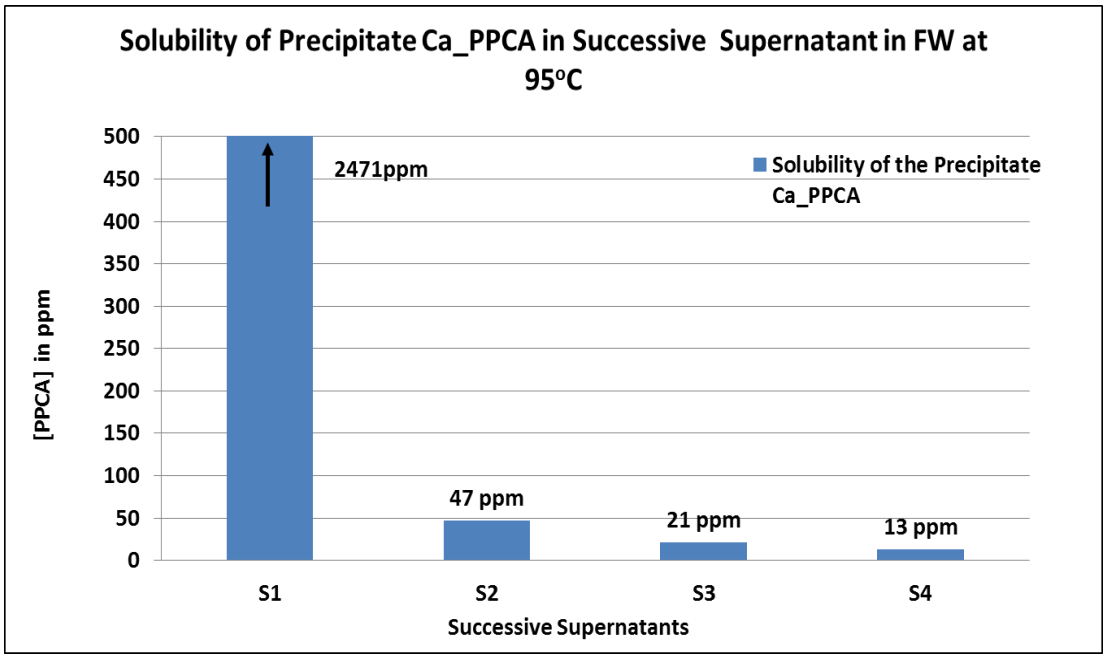

Figure 84: Solubility of the Precipitate at each Successive supernatant at 95°C

In this experiment the first supernatant (denoted S1 in Figure 84) had an ICP measured concentration of [PPCA] = 2471ppm. This is completely consistent with previous findings and these results are very reproducible; note that this is not a true "solubility" since the supernatant being assayed contains all of the lower MW PPCA material. The solubility of the PPCA in the second supernatant (denoted S2) appears to be very low as compare to S1; [PPCA] = 46.68ppm. But, from previous work, we know that S2 has

good IE with 10ppm MIC. The next 2 solubilisations give successively lower solubilities with [PPCA] = 20.75ppm for S3 and [PPCA] = 12.80ppm for S4. Thus, the solubility of the "same" precipitate in the successive supernatants appears to be approximately half that of the previous concentration as shown schematically in Figure 85. Again, this is totally unlike a normal solubility product 'phosphonate_Ca' model or a simple solubility product model and an understanding of these observations – which to our knowledge have never been reported previously – must be found.

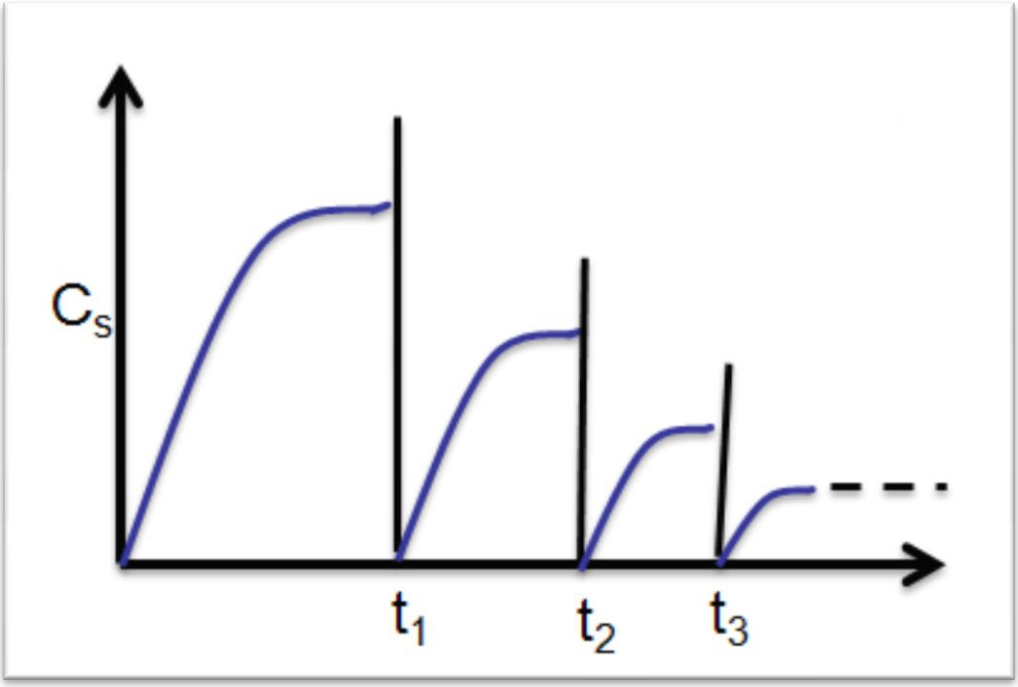

Figure 85: Solubility of the PPCA in Successive Supernatants at 95^{o}C

The graph above for the solubility of polymeric scale inhibitor would be better understood in terms of MWD; we will return to this explanation in Chapter 6 on the MWD study of PPCA.

5.4 Summary and Conclusions

In this chapter, a very detailed study has been presented on the solubility behaviour of the PPCA_Ca complex which forms in precipitation squeeze process using this polymer. The main observations are as follows:

1. ***Effect of Temperature on the PPCA_Ca complex:*** At higher temperatures, the solubility of the precipitate in FW appears to be lower i.e. ~31ppm but the solubility gradually increases as the temperature reduces and at room temperature the precipitate fully re-dissolved back into the FW brine solution.

2. ***Inhibition Efficiency of the precipitated PPCA in different brines:*** The precipitated PPCA is believed to be a "purer" form of PPCA in terms of its higher MW content, so in general, precipitated PPCA shows maximum 90% efficiency for 2 hours against barite scales in all the cases regardless of the brine TDS.

3. ***Solubility of the PPCA_Ca Precipitate:*** The solubility of the PPCA_Ca complex, originally precipitated from NFFW at 95^{o}C, has been measured (in the separate experiments – all in duplicate) in FW, SW and DW. The solubility of the precipitate at 95^{o}C is lowest in FW ([PPCA] ~ 40ppm), is significantly higher in SW ([PPCA] ~800ppm) and is then *lower* again in DW ([PPCA] ~500ppm). An explanation of these results must wait until Chapter 6 where MWD results are presented.

4. ***Solubility of the Precipitated PPCA in DW:*** The two week long experiments demonstrated that the maximum solubility of PPCA_Ca complex in DW is 500ppm and it does not change subsequently. The lower solubility of the complex in DW than SW is therefore *not* a kinetic effect.

5. ***PPCA_Ca Precipitate Solubility in Successive Supernatants:*** In a series of experiments, we have shown that the solubility of the precipitated PPCA/Ca complex becomes *lower* as it is exposed to successive fresh supernatant brine. This PPCA/Ca solubility behaviour is very unlike that expected from a "solubility product" model. The reason for this is again related to the MW of the various components of the PPCA, as discussed in Chapter 6.

CHAPTER 6- MOLECULAR WEIGHT DISTRIBUTION STUDY OF PPCA

In this chapter, we will present results on the MWD of PPCA. We will examine the effect of various parameters such as pH, temperature, concentration of calcium and scale inhibitor (SI) on MWD of the precipitated PPCA_Ca complex and on the remaining supernatant. We will also revisit a number of issues from the experimental results presented previously in Chapters 4 and 5 in terms of MWD. Many of the these results can now be fully explained in a more fundamental way in terms of the MWD of PPCA and how this changes in the precipitation process.

6.1 Introduction

Polymeric scale inhibitors are commonly employed by the industry in oilfield squeeze treatments. However, polymeric inhibitor species always display some degree of polydispersity (spread of MW). This means in practice we are not dealing with a single component but with a range of identical generic species types of slightly different MW.

Graham and Sorbie (1995) suggested that after the squeeze treatment, the MW of the inhibitor effluent may be different from that which was injected. For various commercially available polymeric inhibitors, it was demonstrated using core floods that preferential retention of higher MW components occurred and that preferential desorption of lower MW components was observed. This effect led to a gradation in MW components returning as the inhibitor concentration approaches lower threshold levels, with the higher MW species returning later. However, this is not a problem because higher MW species are more efficient scale (crystal growth) inhibitors, which is again related to the strength of the inhibitor adsorption at the scale crystal surface (Graham and Sorbie, 1995). A number of other researchers have made similar

observations related to the effect of the MW of polymeric scale inhibitors (Rabaioli and Lockhart, 1995; Browning and Fogler, 1993; Breen and Downs, 1990).

However, as noted above, the PPCA is polydisperse and the precipitated species tends to be richer in higher MW components, which we would expect to have higher IE levels. In Chapter 4, we have reported on measurements of IE (against barium sulphate scale) of both the precipitated PPCA species and the remaining supernatant solution of PPCA arising in the compatibility tests. We also assayed the SI concentration by both ICP and the wet chemical methods for the supernatant and the precipitate at both 95^{o}C and 70^{o}C and these concentration levels are compared to their stock values by means of ICP.

In Chapter 5, we discussed the two factors that govern the return curve in a precipitation squeeze treatment, viz. the *solubility* (C_s) of the inhibitor-calcium complex and the *rate of dissolution* (r_4) of the precipitation complex. Thus, we are widening our view of adsorption/precipitation (r/p) squeeze treatments by accounting for both the retention mechanisms and also the specific IE of the return effluent profile from the squeeze. This chapter mainly focuses on the MWD of the PPCA and how this is related to the other factors that governs the phase behaviour of PPCA. We have also established in Chapter 5 that the solubility of the PPCA_Ca complex is not described by a simple "solubility product" model and a novel model based on the MWD of the precipitate is proposed here.

6.2 Study of PPCA molecular weight and molecular weight distribution

It was our belief that most of the experimental results presented in previous chapters of this thesis could may be explained if we could examine what was happening to the MW of the PPCA. Indeed, it would be even better, if we were able to determine the MWD of the PPCA at different stages of the precipitation/re-dissolution process. After precipitation (or phase separation) of the polymers, by either changing the temperature or adding a non-solvent, the highest molar mass species phase were known to separate first and so the fractions are obtained in order of decreasing molar mass. Working in collaboration with the University of Warwick polymer experts, we embarked on a study to follow this line of study which is described below. Our collaborators in this work were Mr A Grice, Kay Leigh and Professor Dave Haddleton in the Department of Chemistry at the University of Warwick.

6.2.1 Background to Polymer Molecular Weight Distributions

As background, we remind the reader that any polymeric scale inhibitor such as PPCA, is characterised by an average Mw since the polymer is not a single length chain of monomers, but is a distribution of chains from short ones to much longer ones. The average MW of PPCA was ~3800g/mole as quoted by the supplier. To fully describe the properties of the polymer, not only average molecular mass but the MWD is also required. Therefore, the PPCA polymer is characterised by a MWD as shown schematically in Figure 86, where both the number averaged (M_n) and weight averaged (M_w) are shown and the polydispersity index (PDI = M_w/M_n) is also defined. Although we describe the MWD as a "frequency" vs. M (MW of a specific size), the "frequency" is essentially the derivative of the cumulative distribution function of the weight (w) of polymer below a given size, M; in results below this "frequency" is denoted as (dw/d logM). In fact, the schematic MWD in this figure is actually generated by an analytical function and the values on this figure (M_w, M_n and PDI) are the correct numbers for this function. Note that the M_w is always higher than the M_n since a higher weighting is given to the bigger molecules (i.e. the longer chain polymers which are made up of more monomer units joined together).

It is the MWD of the PPCA at various stages in the precipitation/dissolution process that we wish to measure in these experiments. The experiments below describe how the various samples are obtained for MWD determination using an HPLC method described below. The concentration of the PPCA sample must also be sufficiently high for detection in the HPLC effluent.

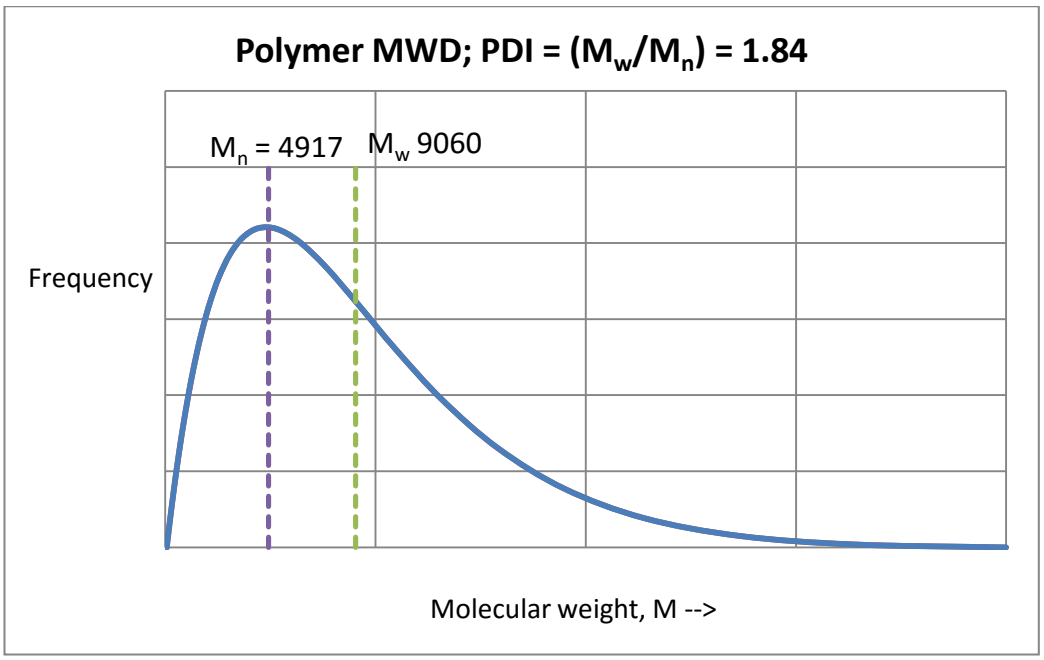

Figure 86: Schematic of a polymer MWD (in linear scale) showing both the number averaged (Mn) and weight averaged (Mw) molecular weights and the Polydispersity Index (PDI = Mw/Mn).

6.2.2 Gel Permeation Chromatography (GPC) Experimental Details

Theory of GPC: The basic principle of GPC is the separation of organic substances, carried by a mobile phase over a stationary phase (chromatographic column). The sample to be analysed is dissolved in the mobile phase. The operating mechanism of the GPC technique for polymers is related to the separation of macromolecules by size (hydrodynamic volume). The stationary phase (chromatographic column) is filled with gel forming particles inside the column that have different pore sizes. Figure 87 provides a simple view of a liquid–solid column chromatography experiment. The sample is introduced at the top of the column. As the sample moves down the column the solutes begin to separate. If the strength of each solute's interaction with the stationary phase is sufficiently different, then the solutes separate into individual bands. As shown schematically in, the smaller molecules (blue) are retained in the pores and take longer to be eluted. The larger molecules (red) do not enter the pores and thus are eluted faster as shown in Figure 87.

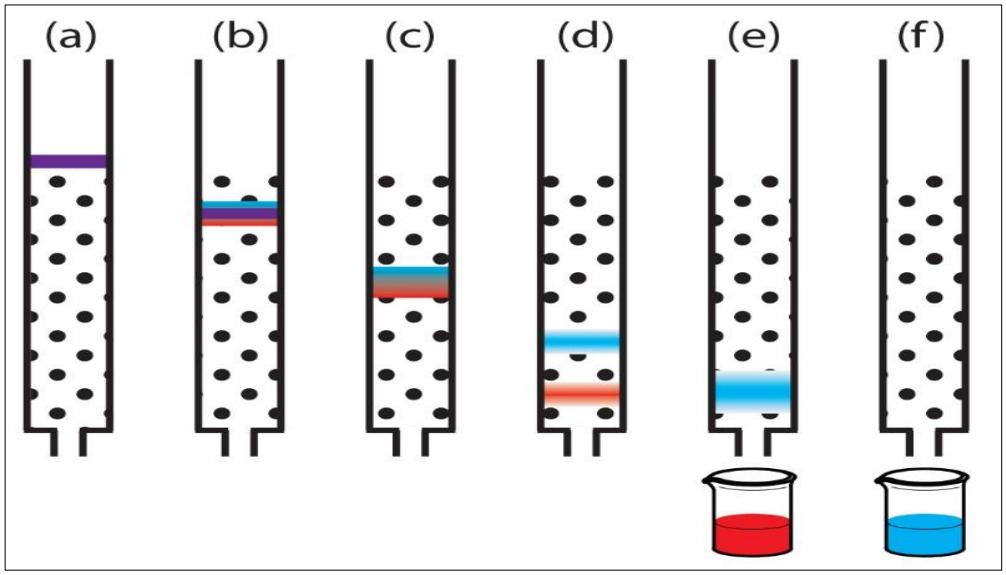

Figure 87. Progress of a column chromatographic separation of a two-component mixture. In (a) the sample is layered on top of the stationary phase. As mobile phase passes through the column, the sample separates into two solute bands (b–d). In (e) and (f), we collect each solute as it elutes from the column. (Source: Internet- Chemwiki)

Gel permeation chromatography can determine the number-averaged molecular weight (Mn) and the weight averaged molecular weight (Mw) of the polymers. The ratio (Mw/Mn) is called the polydispersity (PDI), and is a measure of the spread of the MWD. The values of Mw and MWD are very important when studying polymers regardless of the application, since these properties are directly related to the molar masses of the various species.

Gel Permeation Chromatography: All GPC data was recorded on an Agilent 390MDS instrument equipped with a differential refractive index (DRI) detector and a viscometer detector. PL Cirrus software (v3.3) was used for data interpretation. The system was equipped with 2 x PLaquagel-OH Mixed M columns (300 x 7.5 mm) and a PLaquagel-OH 8 µm guard column.

Samples were mixed in a 50:50 ratio in aqueous buffer (sodium dihydrogen phosphate dihydrate and sodium nitrate, pH adjusted to 8.2 with NaOH solution) and allowed to solubilise at room temperature for 1 hour prior to queuing in an autosampler followed by injection into the GPC column. This system does not give an absolute measure of MW; instead, it is calibrated by retention time against similar standard polymers of compatible MWs. All PPCA samples were analysed compared to a narrow poly

methacrylic acid (PMAA) standard. All M_n and M_w values over 1 kDa are reported to 2 significant figures, all values under 1 kDa are reported to 1 significant figure only. PDI values are reported to 2 decimal places. The upper limit of this system is for an Mw ~ 326,000 g mol^{-1} and the lower limit is Mw ~1,220 g mol^{-1}.

Sample Lists

Two sets of samples were sent to Warwick University for MW determination at different times over a one year period. The first samples were sent in August 2012 and the second set was sent in December 2012. In both the sets, 5000ppm of stock PPCA was sent as the common sample in duplicates and this was used to check for consistency. The graph was plotted with the 2 samples of 5000ppm of PPCA from the two sets is given below:

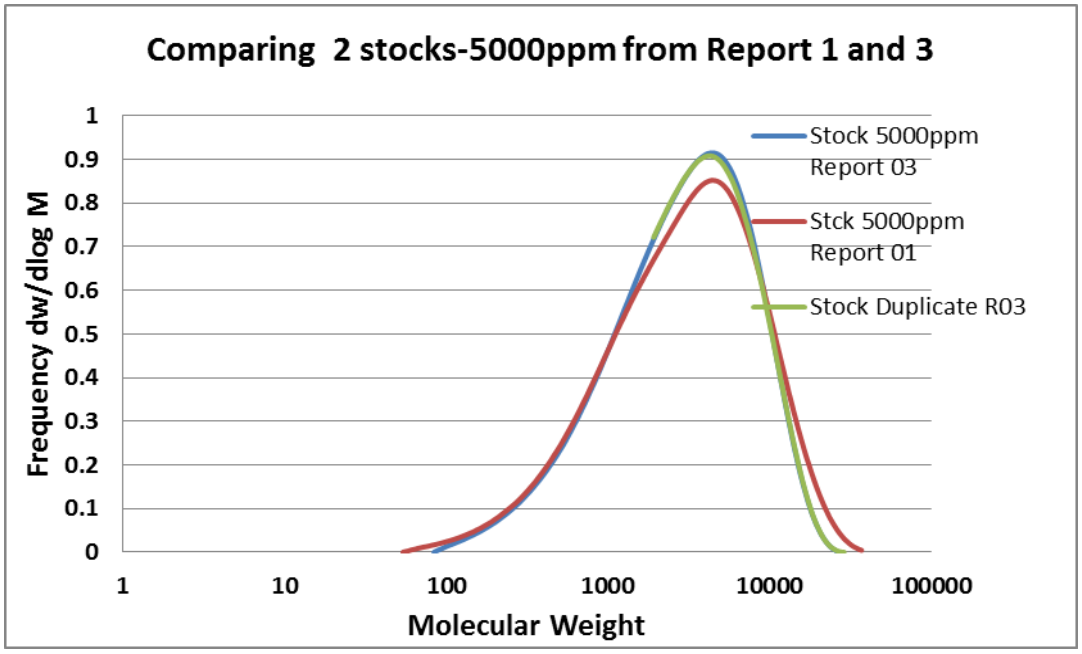

Figure 88: Graph plotted for 5000ppm of PPCA from two Different sets.

In Figure 88, the two plots of the same stock PPCA sample show some quantitative differences, but qualitatively the results are quite similar. Keeping in mind the differences in the different sets of samples, we discuss and compare the MW results for the various PPCA samples.

The list of PPCA samples which were sent for MWD analysis is given in

Table 5 and Table 7; the notation should be self-explanatory e.g. P1-95-SW 6 hours denotes that it is a precipitate (P) which was formed at 95^{o}C in SW after 6 hours, the P2 is simply a duplicate sample, S1-95 is the supernatant PPCA solution from a 95^{o}C precipitation experiment etc. The MWs, including both the number averaged (Mn) and the weight averaged (Mw) values, as determined by GPC for all the samples in Table 6 and Table 8 are presented above; the polydispersity index (PDI) is also calculated, where PDI = Mw/Mn.

Table 5: Set 1- Report 01 showing list of samples with their corresponding ICP concentrations. All samples were injected in duplicate; initial injections labelled with odd numbers and second (duplicate) injections labelled with even numbers (as supplied). This notation is reproduced throughout the report.

Sample Type	Sample Name	Duplicate Name	Diluents	Initial Conc. (mg/mL)	Conc. Post Dil. (mg/mL)
PPCA	Sample 1	Sample 2	10000ppm	9.56	4.78
PPCA	Sample 3	Sample 4	5000ppm	4.58	2.29
PPCA	Sample 5	Sample 6	S1/2-95	2.58	1.29
PPCA	Sample 7	Sample 8	P1/2-95-FW-6hrs	0.04	0.02
PPCA	Sample 9	Sample 10	P1/2-95-SW-6hrs	0.75	0.38
PPCA	Sample 11	Sample 12	P1/2-95-DW-6hrs	0.45	0.23
PPCA	Sample 13	Sample 14	S1/2-80	3.07	1.54
PPCA	Sample 15	Sample 16	P1/2-80-FW-6hrs	0.03	0.02
PPCA	Sample 17	Sample 18	P1/2-80-SW-6hrs	0.68	0.34
PPCA	Sample 19	Sample 20	P1/2-80-DW-6hrs	0.25	0.13

The above list of samples was sent to the Warwick University to study the MWD of the PPCA. The PPCA_Ca precipitate was solubilised in different brines such as FW, SW and DW at 95 and 80^{o}C. The samples were taken after 6 hours of the re-dissolution stage. The list also includes the PPCA stock solution at 10,000ppm (duplicate Samples 1 and 2) and 5000ppm (duplicate Samples 3 and 4) active and first supernatants (S1) at 95^{o}C and 80^{o}C. All samples were measured in duplicate for MWD using an aqueous GPC system and excellent reproducibility of results was found (see below). Initial injections were labelled with odd numbers and second (duplicate) injections were labelled with even numbers as in Table 6.

Table 6: Set 1- Report 01 showing Molecular Weight Averages and PDI values for PPCA samples and their duplicates

Sample Name	Molecular Weight Averages / g mol^{-1}					
	Sample (Odd No.)			Duplicate (Even No.)		
	M_n	M_w	PDI	M_n	M_w	PDI
Sample 1/2	1,800	5,600	3.08	1,600	5,300	3.33
Sample 3/4	1,900	5,500	2.84	1,800	5,400	2.95
Sample 5/6	700	1,300	1.88	600	1,200	1.92
Sample 7/8	-	-	-	-	-	-
Sample 9/10	2,300	3,600	1.55	2,400	3,700	1.49
Sample 11/12	2,800	4,100	1.47	2,700	4,000	1.49
Sample 13/14	900	1,800	2.02	1,000	1,900	1.92
Sample 15/16	-	-	-	-	-	-
Sample 17/18	3,200	4,900	1.51	3,500	5,00	1.41
Sample 19/20	3,500	5,300	1.49	3,600	4,900	1.36

The set 2, report 03 list of samples includes samples which were re-solubilised from precipitates formed under different conditions e.g. differences in the pH, at different concentrations, etc.; the re-dissolution of PPCA_Ca complex is placed in HSB-SW. But the main difference in the set 1- Report 01 samples of precipitate in different brines at 95^{o}C and 80^{o}C generated at test pH-6, where as in set 2- report 03, the samples of the precipitate at 95^{o}C and 70^{o}C were generated at test pH-6 which was then reduced to pH 2 using some drops of HCl, to dissolve all the precipitate back into the solution.

Table 7: Set 2- Report 03 showing list of samples with their corresponding ICP concentrations. All samples were injected in duplicate; initial injections labelled with odd numbers and second (duplicate) injections labelled with even numbers (as supplied). This notation is reproduced throughout the report

Sample Type	Sample Name	Duplicate Name	Diluents	Initial Conc. ** (mg/mL)	Conc. Post Dil. (mg/mL)
PPCA	Sample 1	Sample 2	Stock 5000	4.65	2.33
PPCA	Sample 3	Sample 4	[P]-FW-95	2.14	1.07
PPCA	Sample 5*	Sample 6*	[P]-SW-95	2.24	1.12
PPCA	Sample 7	Sample 8	[P]-DW-95	2.13	1.07
PPCA	Sample 9	Sample 10	[P]-FW-95	1.15	0.58
PPCA	Sample 11*	Sample 12*	[P]-SW-70	1.19	0.6
PPCA	Sample 13	Sample 14	[P]-DW-70	1.2	0.6
PPCA	Sample 15	Sample 16	[S]-70	3.47	1.74
PPCA	Sample 17	Sample 18	[P]-HSB-SW-pH6	1.92	0.96
PPCA	Sample 19	Sample 20	[S from P]-SW-No Mg	0.54	0.27
PPCA	Sample 21*	Sample 22*	[P]-SW-No Mg=HSB-SW	0.34	0.17
PPCA	Sample 23	Sample 24	[P]-HSB-SW-pH8	2.13	1.07
PPCA	Sample 25	Sample 26	[P]-HSB-SW-pH10	2.2	1.1
PPCA	Sample 27	Sample 28	[P]-HSB-SW-10,000ppm	3.43	1.72
PPCA	Sample 29	Sample 30	[P]-HSB-SW-3,000ppm	1.18	0.59
PPCA	Sample 31	Sample 32	[S]-pH8	2.12	1.06
PPCA	Sample 33	Sample 34	[S]-pH10	2.2	1.1

Again, the initial injected samples were labelled with odd numbers and second (duplicate) injections were labelled with even numbers as in Table 8 the Mw results and PDI values for the set 2- report 03 of samples with their duplicates are listed below:

Table 8: Set 2- Report 03 showing Molecular Weight Averages and PDI values for PPCA samples and their duplicates

Sample Name	Molecular Weight Averages / g mol^{-1}					
	Sample (Odd No.)			Duplicate (Even No.)		
	M_n	M_w	PDI	M_n	M_w	PDI
Sample 1/2	1,900	5,000	2.58	1,900	5,000	2.60
Sample 3/4	2,400	4,900	2.02	2,500	4,900	1.98
Sample 5/6	2,700	4,800	1.77	2,700	4,700	1.77
Sample 7/8	3,000	5,800	1.91	3,100	5,900	1.92
Sample 9/10	3,600	6,500	1.79	3,400	6,300	1.83
Sample 11/12	3,600	6,100	1.72	3,600	6,300	1.73
Sample 13/14	4,000	7,400	1.83	4,000	7,400	1.84
Sample 15/16	1,300	2,800	2.09	1,300	2,700	2.14
Sample 17/18	3,500	6,700	1.92	3,500	6,900	1.96
Sample 19/20	3,500	6,600	1.87	3,500	6,500	1.85
Sample 21/22	2,900	5,700	2.00	3,000	5,800	1.95
Sample 23/24	3,200	6,700	2.11	3,200	6,500	2.03
Sample 25/26	3,100	6,300	2.05	3,000	6,300	2.08
Sample 27/28	3,500	7,100	2.04	3,400	7,000	2.08
Sample 29/30	3,300	6,700	2.03	3,200	6,600	2.09
Sample 31/32	700	1,300	1.90	600	1,200	1.92
Sample 33/34	600	1,100	1.80	600	1,100	1.90

6.3 Static Precipitation Experimental Details

Solubility experiments have been conducted to study and analyse the effect of different factors affecting the MWD of PPCA.

These experiments were designed to generate the precipitated sample of PPCA_Ca complex at temperatures, T = 95, 80 and 70^{o}C and in various brines, i.e. FW, SW and DW. Initially, PPCA concentration was 5000ppm active and the pH of the solution was adjusted to pH 6. Like previously, in the compatibility stage, the precipitate is separated from the supernatant by filtration followed by its re-dissolution in FW, SW and DW separately. The third stage of the experiment is then to study the MWD of the precipitate using the GPC methods described below.

The ICP analysis in the third stage shows how much PPCA has dissolved at 6, 24 and 48 hours of re-dissolution. The precipitate was still present at the bottom of the test bottle in all 3 cases. The solubility of the precipitate is very low in FW [PPCA] ~40ppm which turned out to be too low for MWD determination although the higher solubility levels found in both DW and SW were suitable; in DW [PPCA] ~ 500ppm and in SW [PPCA] ~800ppm. However, the precipitate could be re-dissolved into

solution by lowering the pH to 2 using some drops of HCl. After ICP analysis of the solution, the solubility of the FW [PPCA] ~2139ppm, is quite similar to SW [PPCA] ~2237ppm and DW [PPCA] ~2131ppm. These are sufficiently high concentrations of PPCA to determine the MW using GPC.

The PPCA_Ca complex dissolution results for [PPCA] and [Ca^{2+}] at 95^{o}C are shown in Figure 132 and Figure 133 and the corresponding 80^{o}C results are shown in Figure 134 and Figure 135. The results in these 4 figures are very reproducible and they give solubility's very close to those found previously (above). Again, as found previously and reported above, the solubility of the precipitate in SW appears higher than in DW and the solubility of the precipitate in FW is very low, [PPCA] ~ 40ppm. In this specific experiment, the samples were collected for MWD.

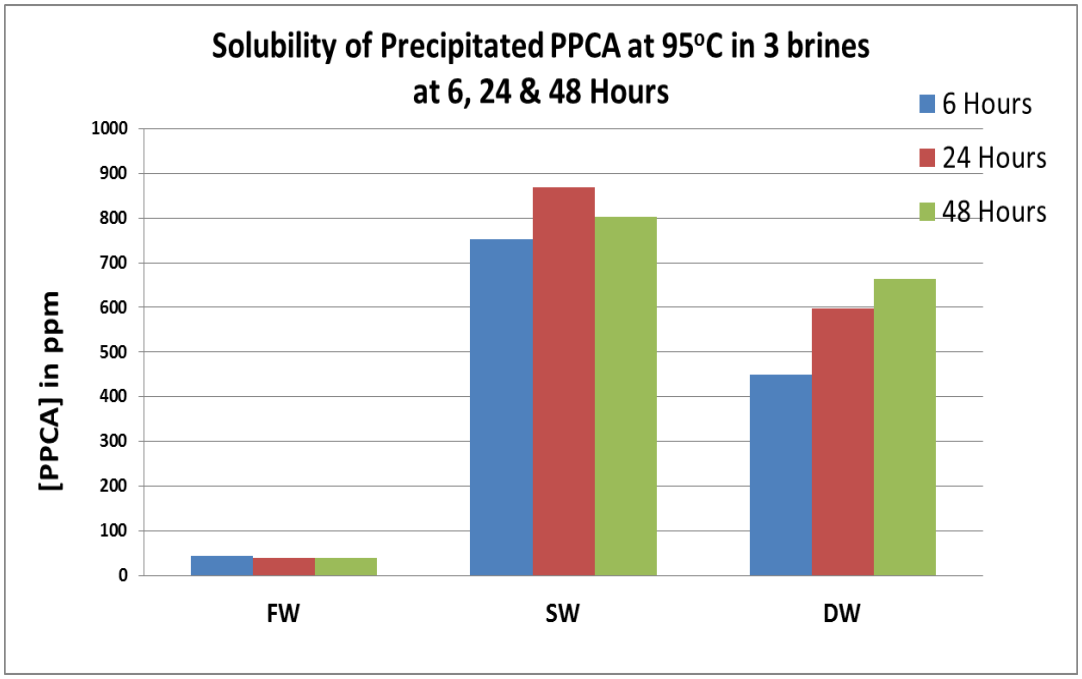

Figure 89: Solubility of PPCA from complex precipitate in different brines at 95^{o}C – these samples was collected for MWD

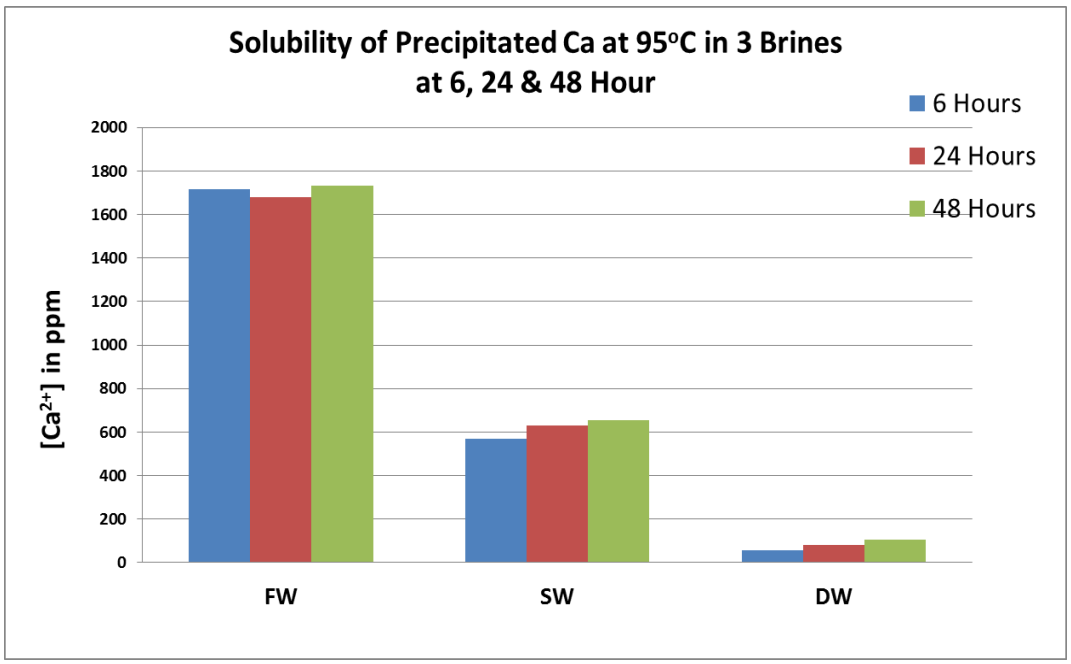

Figure 90: Solubility of calcium from precipitate complex in different Brines at 95°C

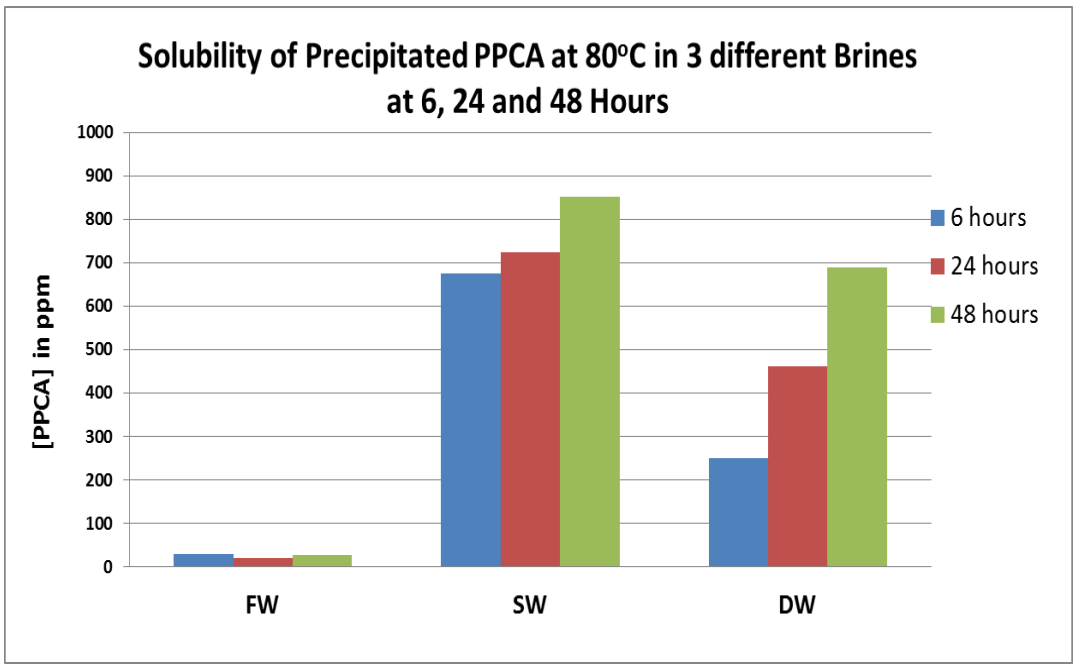

Figure 91: Solubility of PPCA in different Brines at 80°C – these samples was collected for MWD

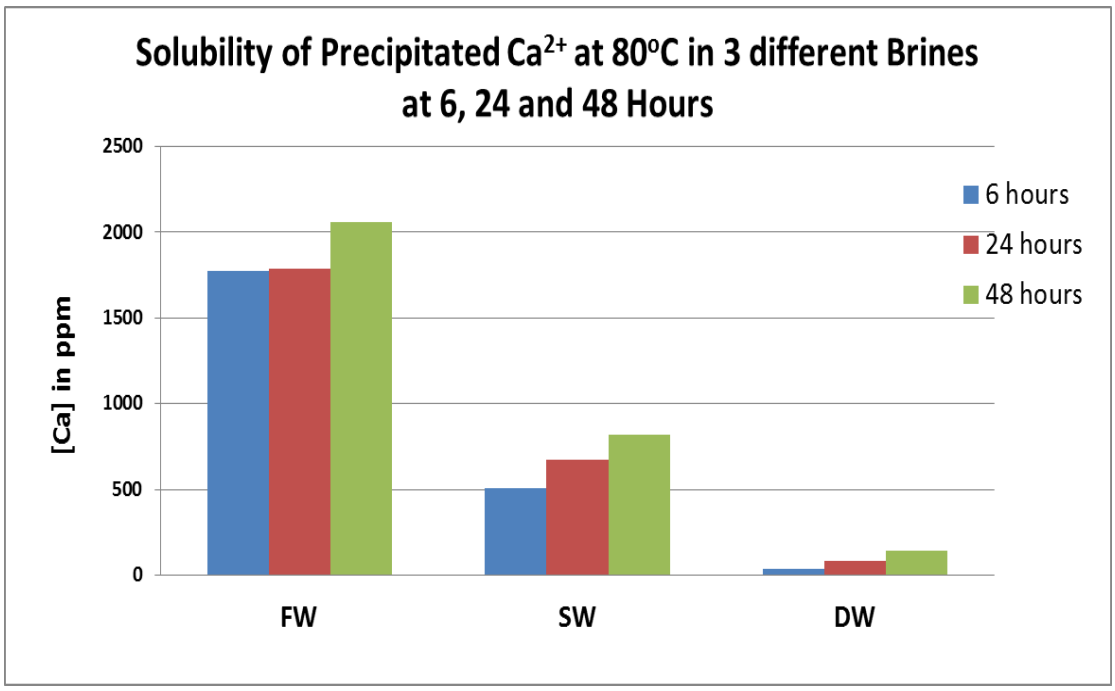

Figure 92: Solubility of Calcium in different Brines at 80°C

Similarly, precipitated PPCA samples were produced at higher pH. The pH was adjusted in the compatibility stage to pH 8 and 10. The precipitate was separated in the compatibility stage through filtration. In stage 2, the HSB-SW brine was used for re-dissolution. The HSB-SW brine contains 35000ppm of NaCl only, which is equal to the TDS of NSSW. The HSB-SW brine helps precipitated PPCA to re-dissolve completely back into solution. After ICP analysis, the solubility of the HSB-SW [PPCA] at pH 8 is ~2131ppm, which is somewhat lower than at pH 10, i.e. ~2204ppm. The supernatant at pH 8 is 2118ppm and at pH 10 is 2195ppm. Quantitatively, the amount of the precipitate formed at higher pH was not very different than at pH 6. That is, higher pH than pH 6 does not make a very significant difference to the amount of precipitation obtained.

A few other experiments have been performed on lower and higher PPCA active concentrations to check the consistency of the trend at different points on the phase envelope. In the compatibility test, 3000 and 5000ppm PPCA active concentrations were used at pH 6. Likewise, in the above experiment, HSB-SW brine was used in stage 2, to re-dissolve precipitate back into solution. The ICP results show that the solubility of the precipitate received from 10,000ppm (initially) is 3428ppm and from 3000ppm (initially) is 1184ppm.

Another experiment which was carried out was to check the solubility of the precipitated PPCA in SW brine containing no Mg. The compatibility test was performed initially at pH 6 and 5000ppm PPCA. After re-dissolution stage 2, the precipitate remains at the bottom of the test container. To recover the precipitate, the supernatant (S2) was separated out using a syringe, and the remaining precipitate was re-dissolved back into HSB-SW brine.

6.4 Results and Discussion

Stock PPCA MWD: The stock PPCA is the sample that is supplied commercially and the MWD for this is shown in Figure 93 for Sample 1 (10000ppm stock PPCA). To illustrate the reproducibility of the MWD results, Figure 94 shows a comparison of Sample 1 (the stock 10000ppm PPCA sample) and Sample 3 (the stock 5000ppm PPCA sample), which both should be identical. The estimated Mn and Mw for these 2 stock samples and duplicates are given Table 6; the average values for the stock (as supplied) PPCA from samples 1 - 4 are Mw = 5450, Mn = 1775, PDI = 3.05.

We emphasise at this point that these MW figures are *not* accurate absolute numerical values; they are based on polymeric PMAA standard. The Mw value quoted here could be out by ~30% and the values quoted here are quite consistent with values of Mw ~ 3800- 4000 often quoted for this specific PPCA. In fact, this would be ~30% difference which is quite reasonable. Having said this, the *trends* in relative sizes and the relative spreads of MWD are correct and can be relied upon to give accurate semi-quantitative results that can be interpreted, as we show below.

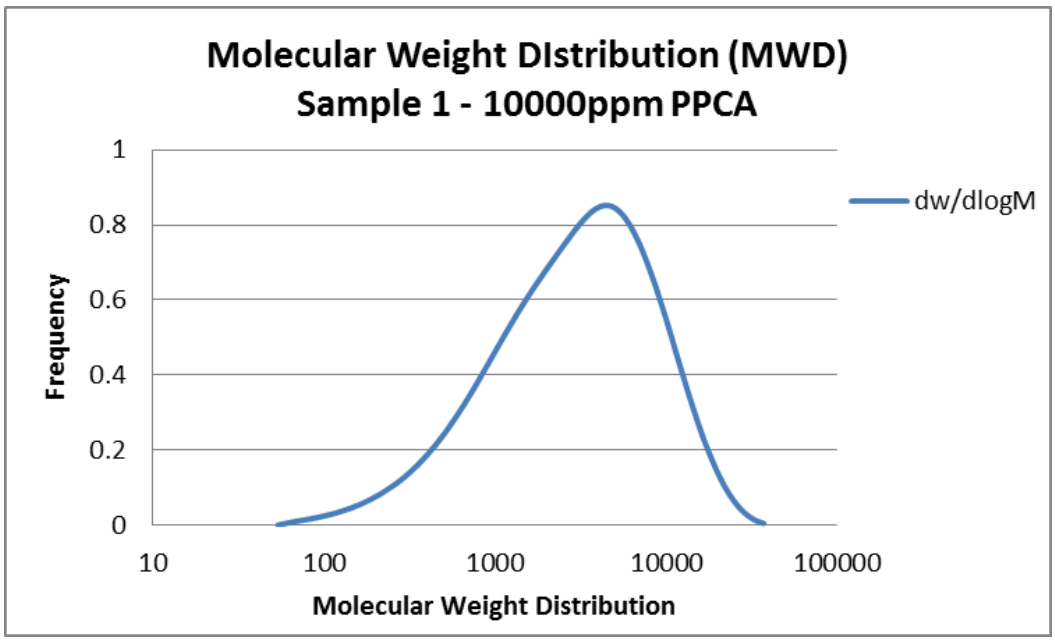

Figure 93: MWD of Sample 1 - the 10000ppm stock PPCA sample

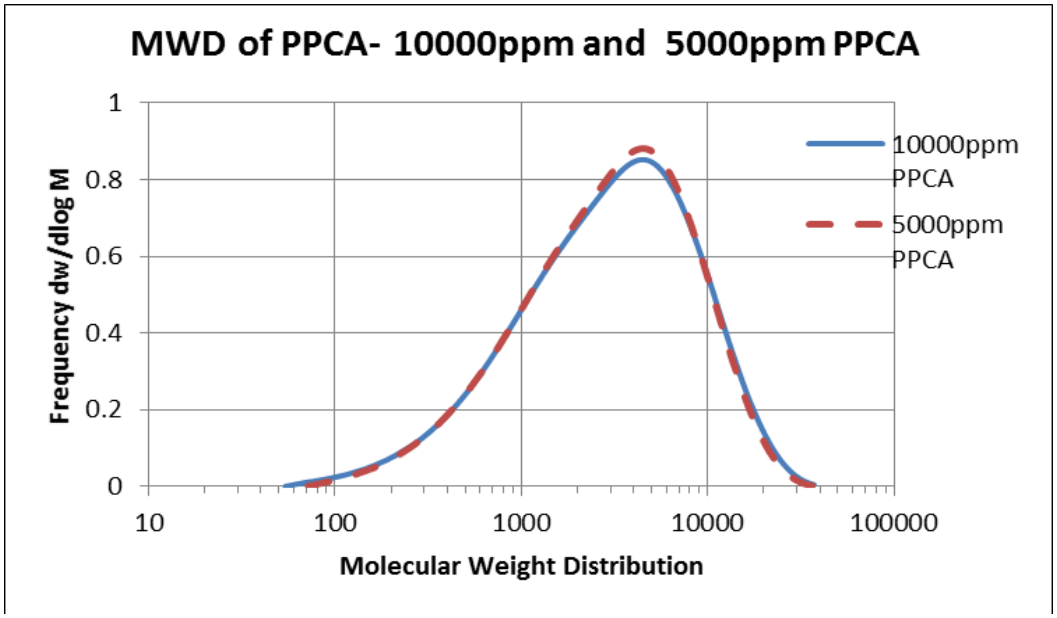

Figure 94: Comparison of MWDs for Samples 1 and 3, the 10000ppm and 5000ppm stock PPCA samples, respectively.

6.4.1 Comparing the MWD of Stock, Precipitate and Supernatant PPCA

In the original precipitation, experiments and in those presented here, it is known that the first supernatant (S1 in Figure 95) when the PPCA_Ca complex is precipitated from the stock PPCA solution shows very poor IE and is also low in polymer (by Hyamine). It was supposed that this was due to the higher MW species preferentially precipitating leaving the supernatant depleted in high MW components; hence, the low IE and the

low polymer content (by Hyamine) would be expected. However, this was not previously demonstrated experimentally.

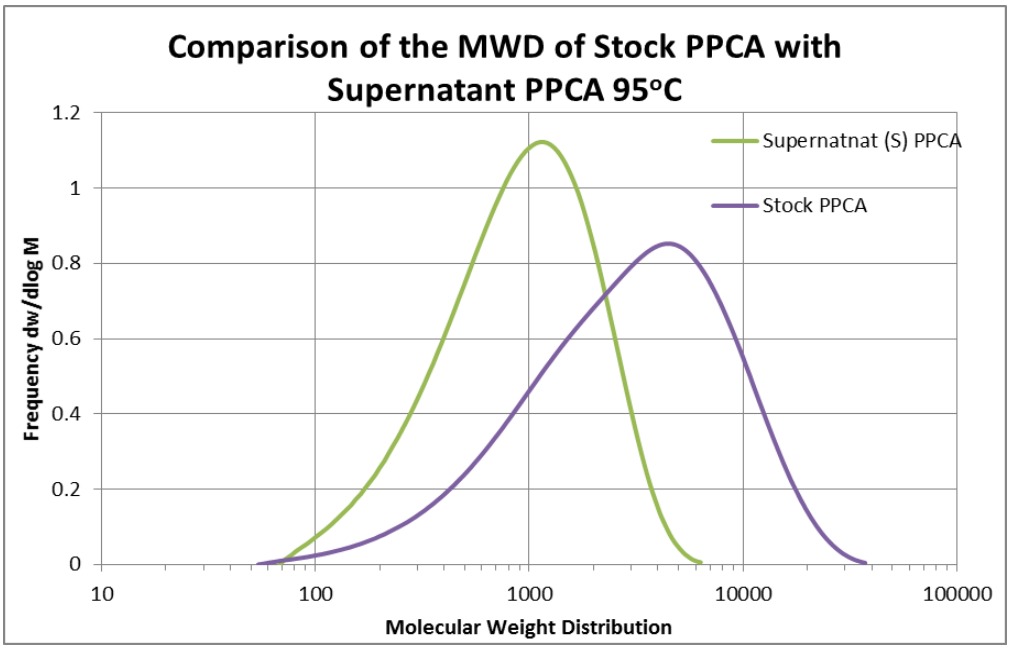

Figure 95: Comparison of the MWDs of the supernatant compared with the stock PPCA; supernatant has Mw = 1300, Mn = 700, PDI = 1.88, compared with the stock values - Mw = 5450, Mn = 1775, PDI = 3.05.

Figure 95 shows the determined MWD of the supernatant (S1) which was precipitated at 95°C, compared with the stock PPCA. The supernatant in this figure has M_w = 1300, M_n = 700, PDI = 1.88, compared with the stock PPCA values - M_w = 5450, M_n = 1775, PDI = 3.05. It is very clear from these results that the reason for the lower IE of the supernatant and its low polymer content (Hyamine compared with ICP concentration) is due to it being greatly depleted in higher MW components, as we had originally conjectured. The further implication of this result is that the precipitate must be greatly depleted in *lower* MW polymeric material and greatly enhanced in *higher* MW material, as shown in Figure 96. As noted above, the precipitate was re-solubilised by lowering the pH by adding drops of HCl. By doing this, the solubility of the precipitate in FW was increased to [PPCA] ~2139ppm. Figure 96 shows the comparison study of the stock, precipitate in FW and supernatant at 95°C. Initially, in the compatibility stage, the PPCA concentration was 5000ppm at pH 6. This result confirms that the precipitate does contain mostly the higher MW species as shown in Figure 96. This explains why the precipitated PPCA gives high IE (shown in Chapter 4, Figure 52) and possesses very

high polymeric content (shown in Chapter 4, Figure 60). For the precipitate, the average molecular weight (Mw) for precipitate is Mw ≈ 4900 and for supernatant is Mw ≈ 1300 as compare to stock, Mw ≈ 5450.

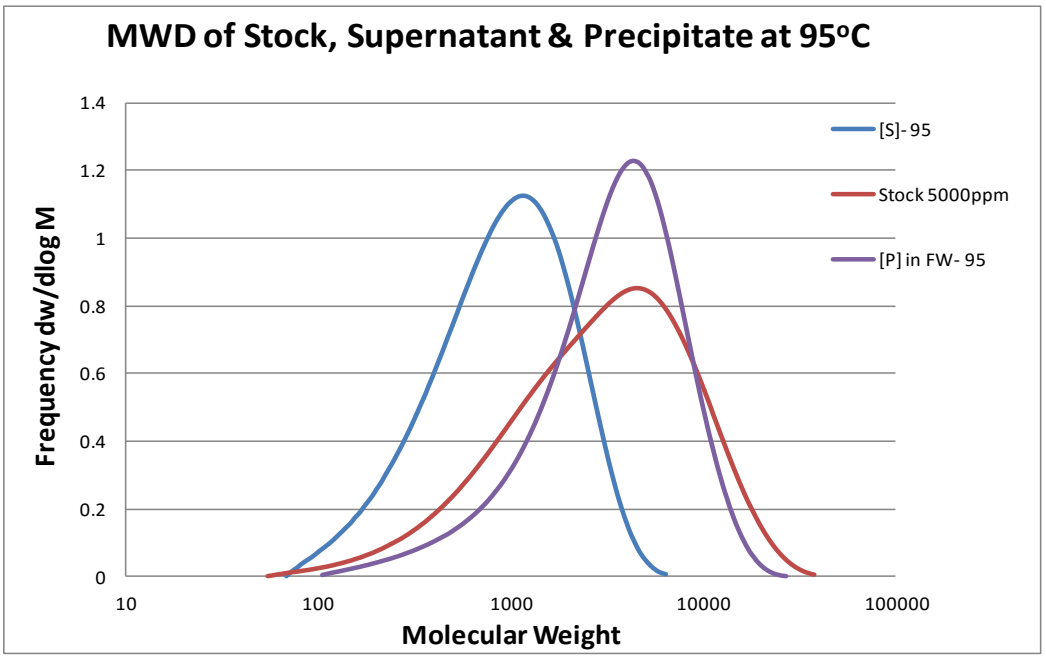

Figure 96: Comparison of the MWDs of the supernatant compared with the stock PPCA and precipitate in FW; supernatant has Mw = 1300, Mn = 700, PDI = 1.88, compared with the stock values - Mw = 5450, Mn = 1775, PDI = 3.05 and Precipitate values Mw = 4900, Mn = 2400, PDI = 2.02.

6.4.2 Solubility of the Precipitate in Different Brines

MWD determination was carried out on the precipitate produced at 95°C in the compatibility stage followed by re-dissolution in three different brines. The three brines which were used for the re-dissolution of the precipitate in separate experiments were FW, SW and DW. For more specific experimental details, refer to chapter 3. At the end of the compatibility test the pH was found to be ~6.5 (approx). After 24 hours of re-dissolution in stage 2, part of the precipitate dissolves back but some precipitate is still evident at the bottom of the container. In order to measure the MWD of the precipitate, its solubility was greatly increased by lowering the pH. The pH was reduced to pH 2 by using few drops of HCl. See the Table 9 below for ICP results.

Table 9: Comparing the solubility of the precipitate in different brines at pH 6 and pH 2

Test Solution	pH 6	pH 2
At 95^{o}C		
[P]- FW	40ppm	2139ppm
[P]- SW	800ppm	2236ppm
[P]- DW	500ppm	2130ppm
At 70^{o}C		
[P]- FW	18ppm	1152ppm
[P]- SW	709ppm	1187ppm
[P]- DW	461ppm	1201ppm

In Figure 97, the MWD results for the precipitated PPCA in three different brines are compared with the supernatant and the stock. It is clear from the results shown; that the supernatant is greatly depleted in higher MW material, as we had originally conjectured and the precipitate is enriched with the high MW material. However, the brines used in stage 2 makes a difference to the distribution of the MW. The SW and FW show very similar MWD results; Mw for precipitate in FW is Mw ≈ 4900 and in SW is Mw ≈ 4800, whereas in DW, it is Mw ≈ 5800. That is, these results show that DW tends to pick up higher MW species than SW and FW. Previously we discussed the results in Chapter 5 that show the solubility of PPCA in DW for longer residence time. Theoretically, the solubility of the high MW material is lower than the lower MW material. The long-time experiment clearly showed that the maximum solubility of the PPCA_Ca complex is ~500ppm and that this solubility is reached after ~48 hours and does not change subsequently. However, the solubility of precipitated PPCA in SW is ~800ppm and in FW it is ~40ppm. The reason for lower solubility in DW than in SW could be that it tends to re-dissolve the high MW material of PPCA which is much poorer in solubility.

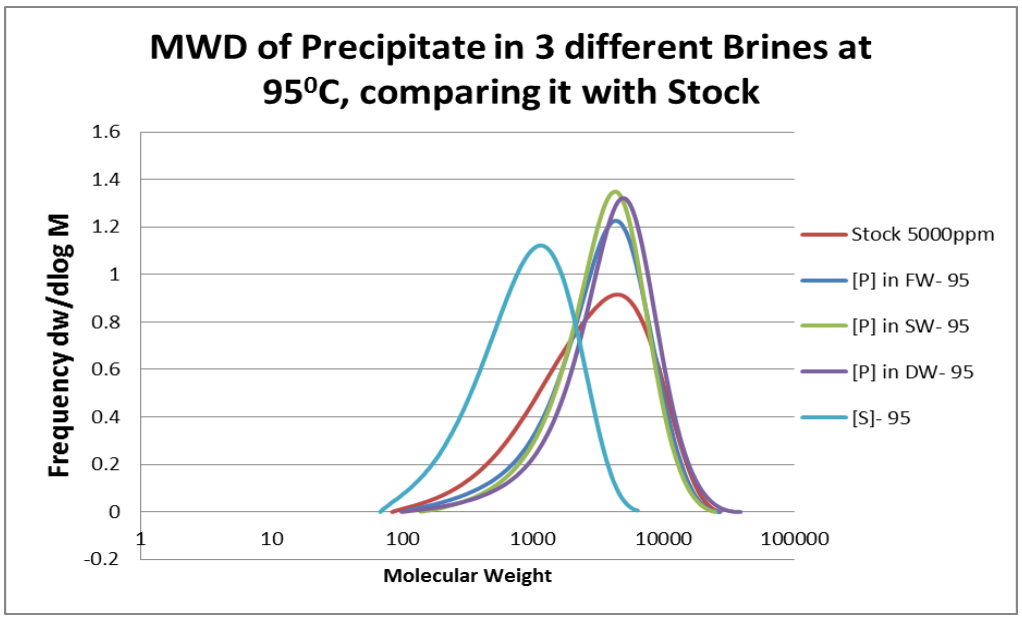

Figure 97: Comparison of the MWDs at 95°C of the Supernatant compared with the stock PPCA, Precipitate in FW, SW and DW; Supernatant has Mw = 1300, Mn = 700, PDI = 1.88, compared with the stock values - Mw = 5450, Mn = 1775, PDI = 3.05 and Precipitate in FW values- Mw = 4900, Mn = 2400, PDI = 2.02, Precipitate in SW values- Mw = 4800, Mn = 2700, PDI =1.77, Precipitate in DW values- Mw = 3000, Mn = 5800, PDI = 1.91.

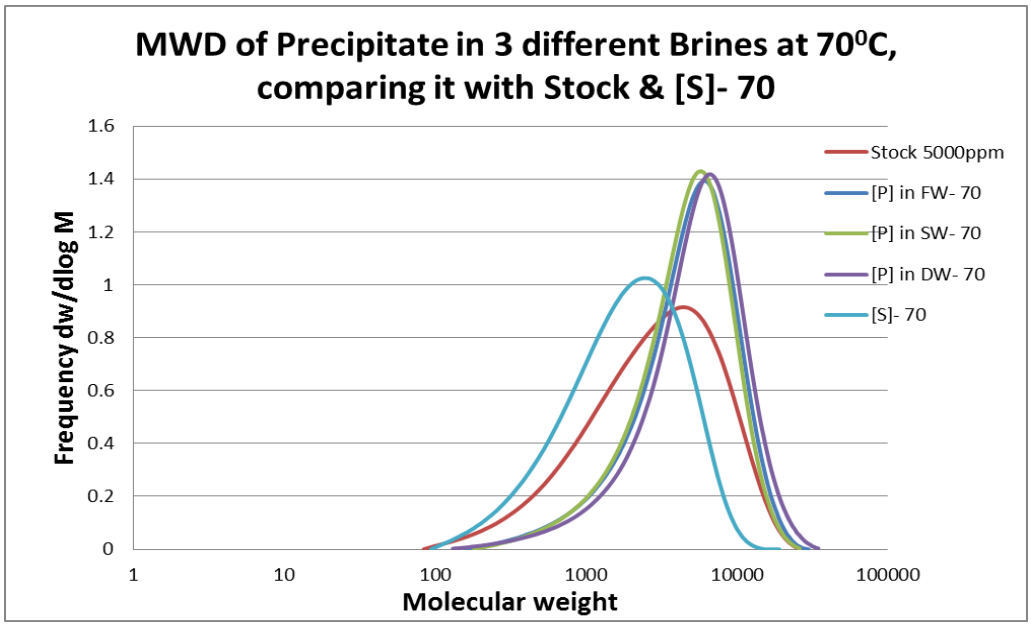

Figure 98: Comparison of the MWDs at 70°C of the Supernatant compared with the stock PPCA, Precipitate in FW, SW and DW; Supernatant has Mw = 2800, Mn = 1300, PDI = 2.09, compared with the stock values - Mw = 5000, Mn = 1900, PDI = 2.58 and Precipitate in FW values- Mw = 6500, Mn = 3600, PDI = 1.79, Precipitate in SW

values- Mw = 6100, Mn = 3600, PDI =1.72, Precipitate in DW values Mw = 7400, Mn = 4000, PDI = 1.83.

Likewise, Figure 97 shows the MWDs for the re-dissolution of the precipitate in 3 different brines at 70^{o}C. Again, the results are clear and they confirm that re-dissolution in DW does pick up more high MW material as compared to the precipitate in SW and FW. At 70^{o}C, the precipitate in DW has Mw ≈ 7400, Mn ≈ 4000, PDI = 1.83, compared to the precipitate in SW which has Mw ≈ 6100, Mn ≈ 3600, PDI = 1.72 and with the precipitate in FW => Mw ≈ 6500, Mn ≈ 3600, PDI = 1.79.

6.4.3 Effect of Temperature on the Molecular Weight Distribution of PPCA

Figure 89 and Figure 91 above show the solubility of the precipitate in three different brines viz., FW, SW and DW, and their supernatants. These experiments were performed at 2 temperatures – 95^{o}C and 70^{o}C - and qualitatively the results show similar trends although quantitatively the results are rather different to each other. The precipitate of PPCA does contain high MW material. In particular, precipitate in DW at 95^{o}C contains MW species of PPCA up to ~40000 as compared to the DW at 70^{o}C which contains up to ~35000 only; and supernatant at 95^{o}C contains mainly low MW material i.e. up to 8000 whereas at 70^{o}C it contains some high MW material i.e. up to 20000. These MWD results are completely consistent with our experimental observations on IE and on polymer assay.

The effect of temperature is made much clearer from the weight distribution of supernatant at three temperatures as shown in Figure 99. At 95^{0}C, the supernatant is enriched with lowest MW material with Mw ~1300 and Mn ~700. Lowering the temperature from 95 to 80^{o}C, the MWD of the supernatant moves towards higher MW material and at 80^{o}C the recorded Mw is 1800 and Mn is 900. At 70^{o}C, the Mw is 2800 and Mn is 1300 which shows that the supernatant contains more high MW material than at 80 or 95^{o}C. The three supernatants are compared with stock which contains both, high and low MW material and has Mw = 5000, Mn = 1900. Therefore the MW effect is quite clear where the average MW of the supernatant is increasing at the lower precipitation temperature i.e. more of the higher MW components are soluble in the brine at the lower temperature.

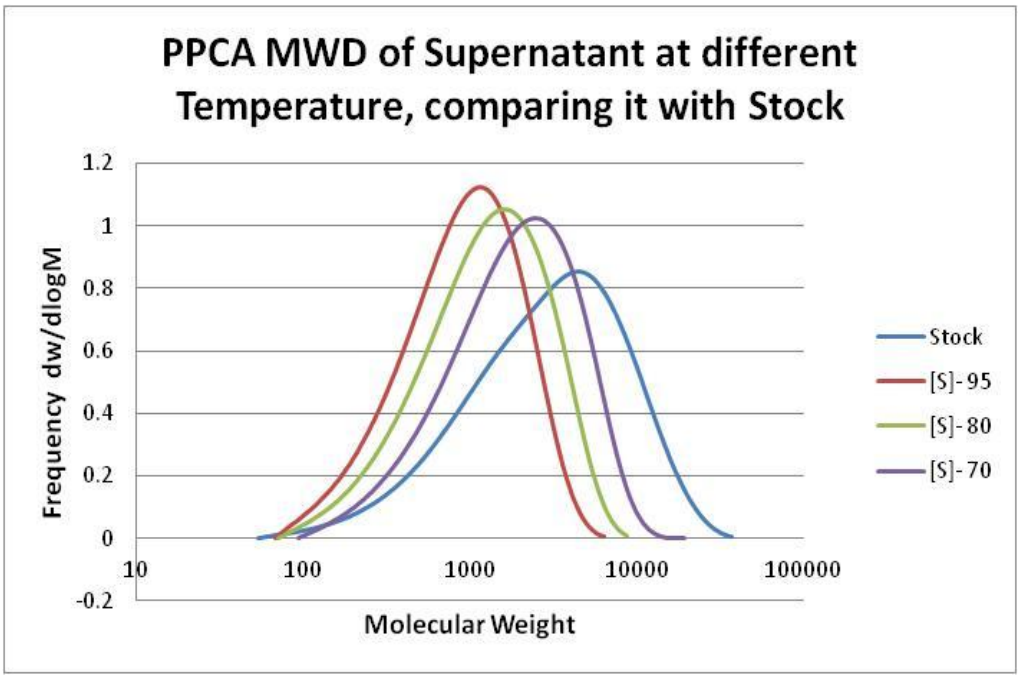

Figure 99: Comparison of the MWDs of the Supernatant at three different Temperatures Supernatant at 95^0C has Mw = 1300, Mn = 700, PDI = 1.88; Supernatant at 80^0C has Mw = 1800, Mn = 900, PDI = 2.02 and Supernatant at 700C has Mw = 2800, Mn = 1300, PDI = 2.09 compared with the stock values - Mw = 5000, Mn = 1900, PDI = 2.58.

6.4.4 Effect of pH on the Molecular Weight Distribution of PPCA

In the initial experiments, the pH was maintained at 6 in the compatibility stage for precipitation. In stage 2, after re-dissolution, the precipitate contains the higher MW material which is relatively less soluble. The lower MW material of the precipitate dissolves first because of its higher solubility but the amount of the solubility of the precipitate is different in different brine type and the pH of each solution was approximately pH ~6.5. To measure the MWD of the precipitate fully, we must get the most high MW material sitting at the bottom of the container back into solution. To achieve this, the pH of the solution is lowered. This protonates the –COOH groups on the polymer and they do not then bind very strongly with calcium and the complex dissolves.

Results in Figure 100 compare the MWDs of the precipitates dissolved in SW at 95^oC at pH 6 and pH 2. At pH 6, the Mw is 3600 and Mn is 2300. When the pH was reduced to pH 2, the most (relatively insoluble) high MW material dissolved back into solution and

the Mw became 4800 and Mn became 2700. After reducing the pH, the solution becomes crystal clear with no precipitate left behind. Comparatively in Figure 101, similar qualitative trends were observed on the MWD of the precipitate in DW at 95^{o}C. At pH 6, the Mw in DW is 4100 whereas at pH 2, Mw is 5800.

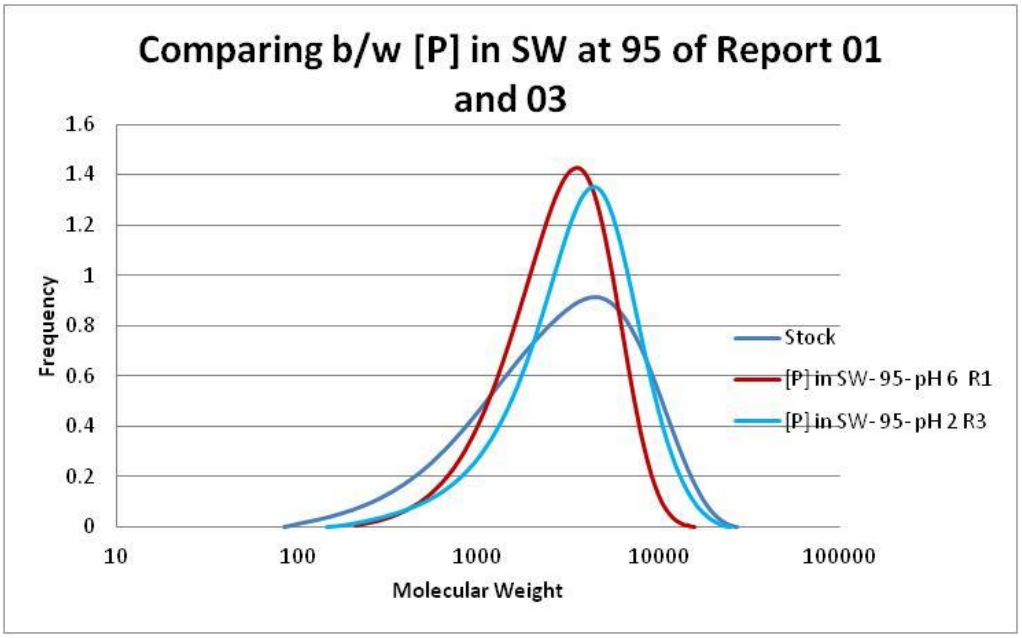

Figure 100: Comparing the MWD of PPCA in SW at pH 6 with pH 2 at 95^{0}C; PPCA- in SW-pH 6- Mw = 3600, Mn = 2300, PDI = 1.55 and PPCA- in SW-pH 2- Mw = 4800, Mn = 2700, PDI = 1.77

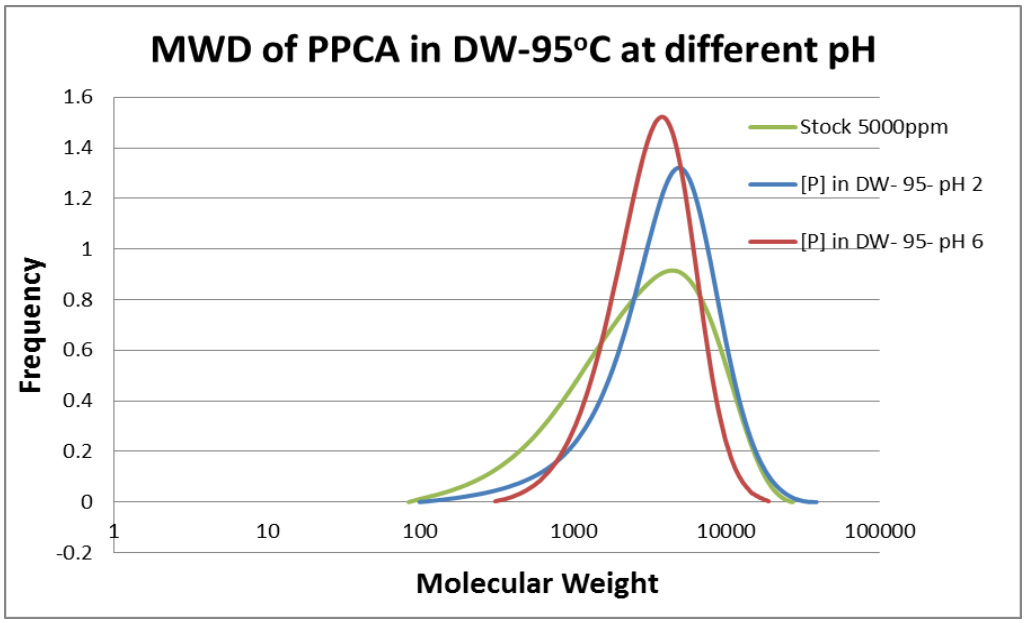

Figure 101: Comparing the MWD of PPCA in DW at pH 6 with pH 2 at 95^{o}C; PPCA- in DW-pH 6- Mw = 4100, Mn = 2800, PDI = 1.47 and PPCA- in DW-pH 2- Mw = 5800, Mn = 3000, PDI = 1.91

As discussed above, the solubility of the PPCA_Ca precipitate is higher in SW than in DW probably because DW takes up the highest MW material which is lower in solubility. This can be seen most clearly in the combined graph of the above two results.

Figure 102 shows the differences in the solubility of the MWD in SW and in DW, and the effect of lowering the pH in each case.

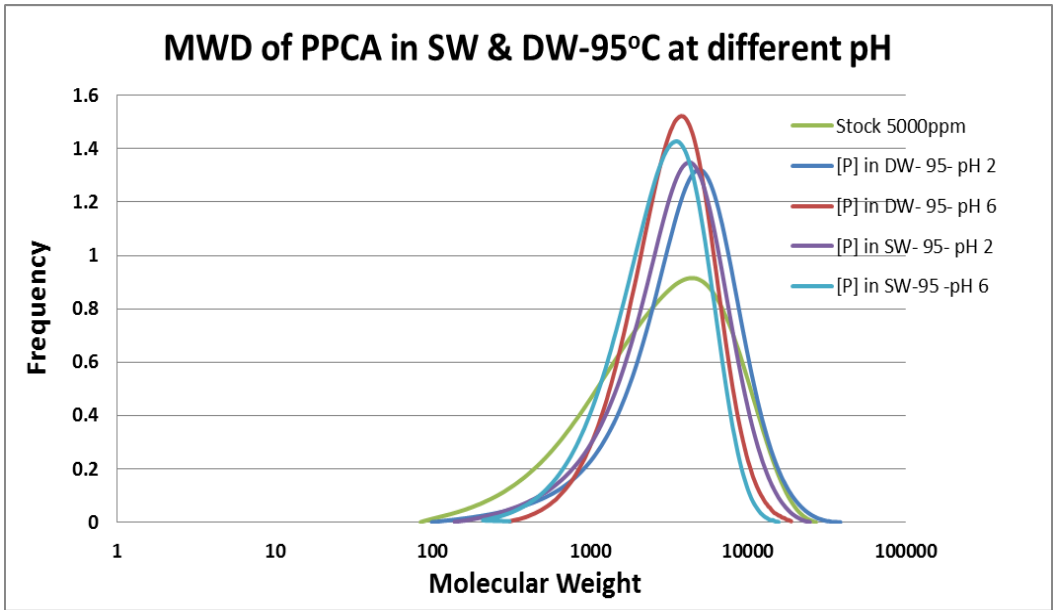

Figure 102: Comparison of the MWDs of the Precipitate both in SW and DW at 95^0C at pH 2 and 6. [P]-SW at pH 6 has Mw = 3600, Mn = 2300, PDI = 1.55; at pH 2 Mw = 4800, Mn = 2700, PDI = 1.77. [P]-DW at pH 6 has Mw = 4100, Mn = 2800, PDI = 1.47; at pH 2 Mw = 5800, Mn = 3000, PDI = 1.91. Compared with the stock values - Mw = 5000, Mn = 1900, PDI = 2.58.

6.4.5 Effect of higher pH on MWD of PPCA

pH is an important parameter which affects the phase envelop of PPCA. Therefore, we wished to establish the effect of having a higher pH on the MWD of PPCA. To study the effect of pH, experiments were performed at pH 8 and pH 10 and results were compared with the previous findings at pH 6. For the re-dissolution stage of the precipitate, HSB-SW is used which contains 35000ppm of NaCl (it is equal to the TDS of SW). This brine re-dissolves all the precipitate in 24 hours at room temperature.

Figure 103 shows the MWD of the supernatant at pH 8 (Mw = 1300) and pH 10 (Mw = 1100); and precipitate at pH 8 (Mw = 6700) and pH 10 (Mw = 6300). Again it is clear

from these MWD results that the higher MW species preferentially precipitating leaves the supernatant again enriched in low MW components. On the other hand, precipitates which formed at higher pH do not show any significant difference in the MWD of PPCA. The higher pH results are compared with pH 6 results in Figure 104 and these show no difference at all in the MWD of PPCA. In other words, higher pH will not make much difference after precipitation on the MWD of the complex; a lower pH 4 affects the precipitation of the PPCA. It appears that pH 4 seems to be close to the edge of the precipitation region of PPCA phase envelope under the conditions tested here.

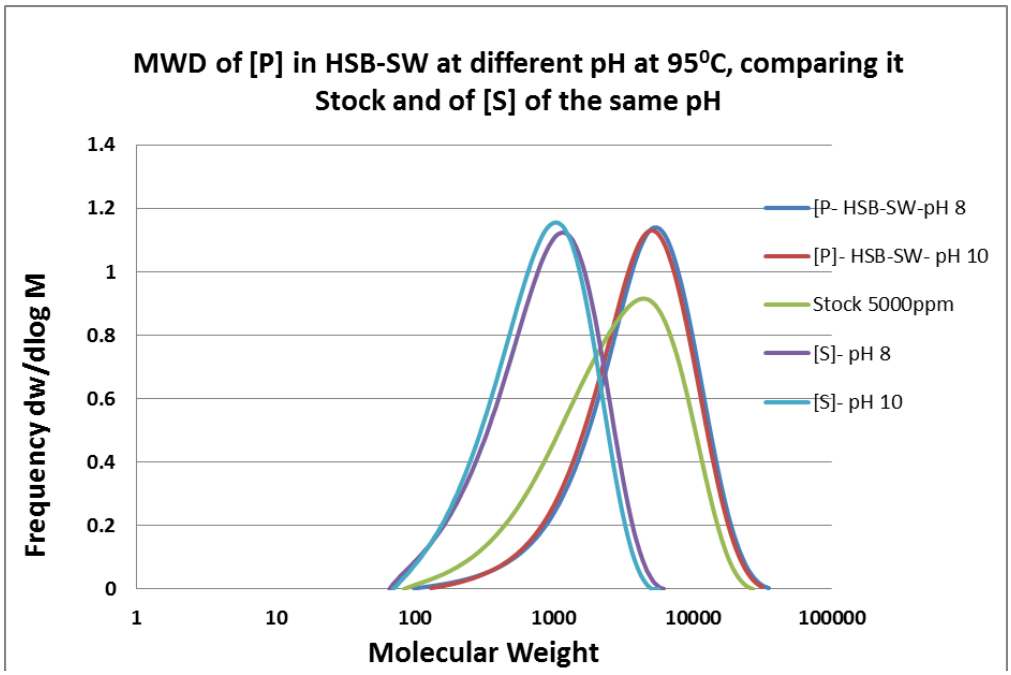

Figure 103: Comparison of the MWDs of the Precipitate both in HSB-SW at 95^0C at different pHs [P]- at pH 8 Mw = 6700, Mn = 3200, PDI = 2.11; [P]- at pH 10 has Mw = 6300, Mn = 6100, PDI = 2.05; [S]- at pH 8 Mw = 1300, Mn = 700, PDI = 1.90; [S]- at pH 10 Mw = 1100, Mn = 600, PDI = 1.80 compared with the stock values - Mw = 5000, Mn = 1900, PDI = 2.58.

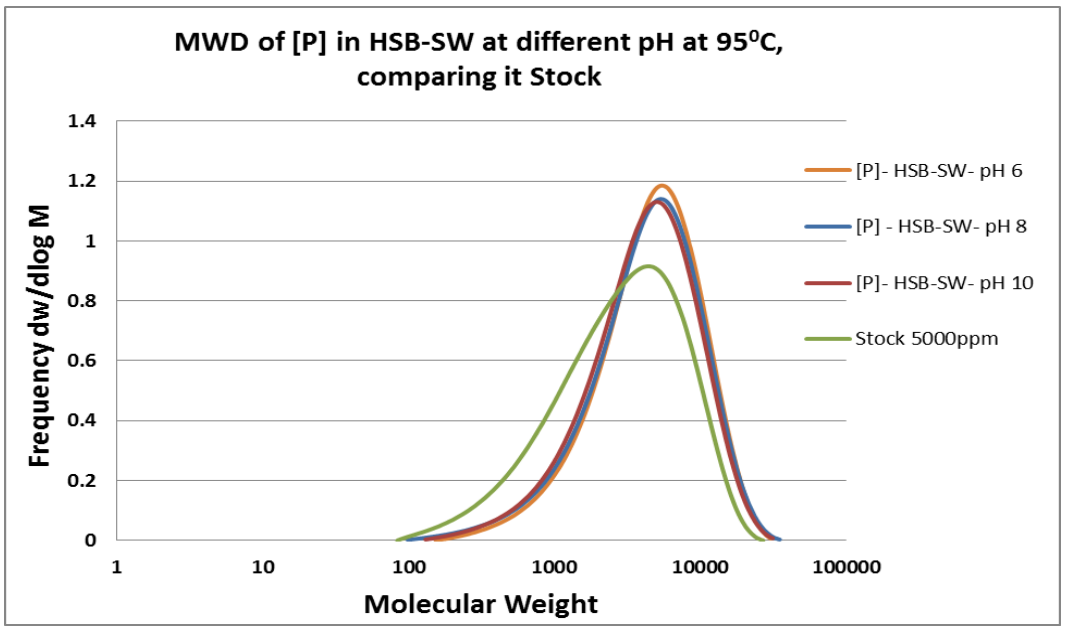

Figure 104: Comparison of the MWDs of the Precipitate both in HSB-SW at 95^0C at different pHs [P]- at pH 6 has M_w = 6700, M_n = 3500, PDI = 1.87; [P]- at pH 8 Mw = 6700, Mn = 3200, PDI = 2.11; [P]- at pH 10 has M_w = 6300, M_n = 6100, PDI = 2.05; compared with the stock values - M_w = 5000, M_n = 1900, PDI = 2.58.

6.4.6 Solubility of the Precipitate at different concentrations in High Salinity Brine (HSB) – SW

Three further experiments were performed to check on the re-dissolution of the precipitate at three concentrations. Initially, the three concentrations used in the compatibility stage were 10000ppm, 5000ppm and 3000ppm of PPCA at pH 6. The brine used in stage 2 is the HSB-SW (contained 35000ppm of NaCl only) which was used to re-dissolve the precipitate fully back into solution. ICP analysis in Table 10 shows a large difference in the results of re-dissolution of the precipitate depending upon the initial concentration. However, in Figure 105, the MWD determination of the same results does not show any significant difference.

Table 10: Showing ICP results of the precipitate with different concentrations dissolved back in HSB-SW

Brine used for Re-dissolution	Initial Concentration	ICP Value after Re-dissolution
HSB-SW	10,000ppm	3428ppm
HSB-SW	5000ppm	1916ppm
HSB-SW	3000ppm	1184ppm

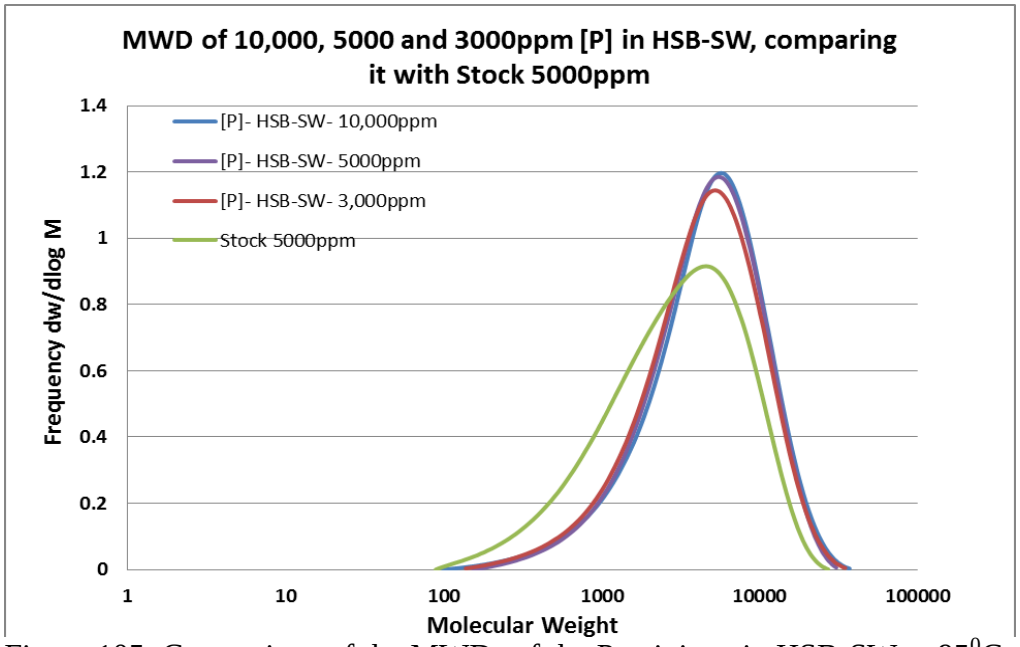

Figure 105: Comparison of the MWDs of the Precipitate in HSB-SW at 95^0C at pH 6 at three different PPCA concentration [P]- at 5000ppm has Mw = 6700, Mn = 3500, PDI = 1.92; [P]- 10000ppm Mw = 7100, Mn = 3500, PDI = 2.04; [P]- at pH 10 has Mw = 6700, Mn = 3300, PDI = 2.03; compared with the stock values - Mw = 5000, Mn = 1900, PDI = 2.58.

6.5 Proposed New Model for PPCA_Ca Solubility

The MWD results presented in the previous section point to an explanation of the PPCA_Ca solubility experiments above. The concept of a "solubility product model" (appropriate for a simple sparingly soluble salt) does not appear to be applicable for

describing the solubility of PPCA_Ca complex (see results in Chapter 5). In particular, we recall the results of 2 sets of experiments reported above, as follows: **

I. The effect of adding additional brine volume at equilibrium solubility as shown in Chapter 5- Figure 81 and Figure 82 where the concentration in the supernatant was reduced by a factor of ~2.

II. The concentration of the precipitate obtained from the successive solubility experiments were discussed in Chapter 5- Figure 84 and schematic graph shows how the successive solubility of polymer looks like in Figure 85. These results showed that the successive solubility of an original PPCA_Ca precipitate decreased when repeatedly exposed to fresh brine. In Figure 84 of Chapter 5, we found that [PPCA] = 46.68ppm in FW in the first solubility experiment in S2, the next solubilizations gave [PPCA] = 20.75ppm in S3 and [PPCA] = 12.80ppm in S4.

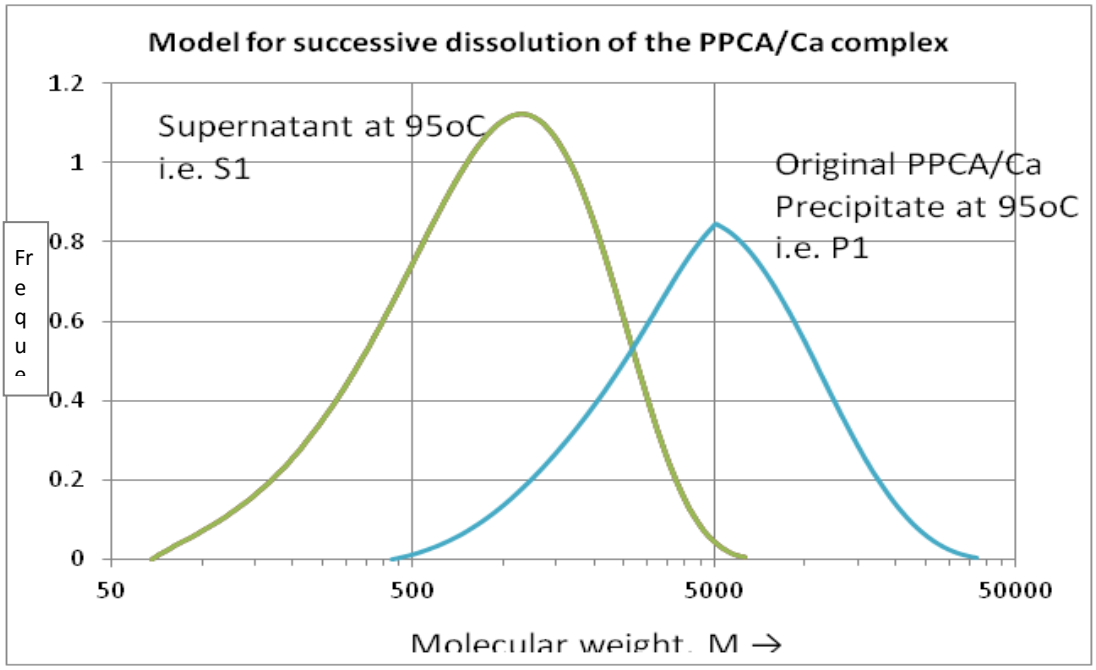

Figure 106: The MWDs of the original Supernatant (S1) in the first precipitation of the stock PPCA and the "inferred MWD" of the corresponding first precipitate (P1)

The schematic graph shown in Chapter 5 based on the successive solubility of the precipitate suggests that the original MWD of the precipitated PPCA, when exposed to fresh brine subsequently "stripped" in S2, S3, S4 etc. This was called the "inferred MWD" from the above experiments, rather than being a direct measurement.

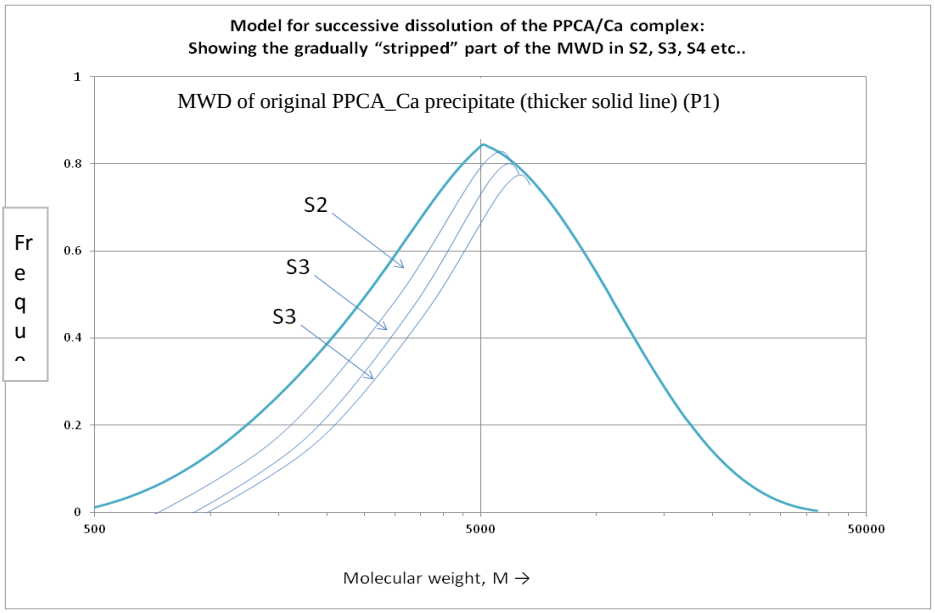

Figure 107: The "input" MWD (inferred MWD) of the original precipitate from the stock PPCA (P1); this is the original MWD that is subsequently "stripped" as shown schematically in the successive extractions S2, S3, S4 etc.

Both of the above experiments may be explained by considering what happens to the MWD in each type of experiment. Firstly, in the original precipitation of the stock PPCA, the first supernatant (S1) is mainly lower MW material as shown in Figure 106 and discussed in detail above; the corresponding "inferred MWD" of the PPCA_Ca precipitate is also shown in Figure 107. We now consider the successive dissolution experiments as in Chapter 5, Figure 84 and we summarise this in terms of MWD. A proposed mechanism for these observations is that in the successive stages (S2, S3, S4 etc.), and then gradually higher MW PPCA species are dissolved out. However, these higher MW species are less and less soluble. In terms of MWD, we envisage the successive dissolution into S1 as the original supernatant, as shown in Figure 106, the "inferred MWD" in this figure is the "input" for the subsequent dissolution experiments shown in Figure 107. To understand the subsequent dissolution of the polymer into S2, S3, S4, we must consider only the MWD of the precipitate (P1). This original MWD is then "stripped" as shown schematically in Figure 107 in the successive extractions S2, S3, S4 etc., where each subsequent extraction is stripping higher and higher MW species which are therefore less soluble. Hence, the amount extracted is less and less which explains why [PPCA] = 46.68ppm in S2, [PPCA] = 20.75ppm in S3 and [PPCA] = 12.80ppm in S4 in our experiments. This is clearly a different dissolution mechanism from a simple sparingly soluble salt and it will play an important role in polymeric precipitation squeeze processes.

6.6 Summary and Conclusions

In this chapter, the previous study of the PPCA phase envelope described in Chapters 4 and 5 has been extended to include determination of the MWD of the PPCA for various stages of the precipitation and re-dissolution processes. The main conclusions from this work are summarised as follows:

1. ***MWD of PPCA:*** Working with colleagues at the U. of Warwick, we have been able to determine for the first time the molecular weights (M_n and M_w) and the MWD for the various samples (supernatants, redissolved precipitates etc.) in our PPCA_Ca precipitation experiments. This has given us some very significant insights into the precipitation/dissolution mechanisms which are occurring in polymer precipitation squeeze processes. We have used these MWD results to confirm experimentally a number of conjectured explanations which we had previously put forward for various observations in previous chapters (see below).

2. ***Solubility of the PPCA_Ca Precipitate:*** The solubility of the PPCA_CA complex, originally precipitated from NFFW at 95^{o}C, has been measured (in 3 separate experiments – all in duplicate) in FW, SW and DW. The solubility of the precipitate at 95^{o}C is lowest in FW ([PPCA] ~ 40ppm), it is significantly higher in SW ([PPCA] ~800ppm) and is then *lower* again in DW ([PPCA] ~500ppm). Results from MWD measurements clearly show that DW picks up the comparatively higher MW material than SW and FW and the solubility of high MW material is lower than the low MW material.

3. ***MWD of PPCA : Stock, Supernatant and Precipitate:*** The MWD results for the Stock PPCA polymer show a wide range of MW species in this product, with M_w = 5000, M_n = 1900, PDI = 2.58. We emphasize that these MW figures are *not* accurate absolute numerical values but are based on polymeric PMAA standards through a calibration curve (possible error ~25%). However, they give us qualitatively correct changes in Mw and MWD which allows us to interpret the various processes – e.g. IE, dissolution, analytical results, precipitation etc. – in the experiments reported in this thesis.

4. ***Comparing Stock with Supernatant and Precipitate:*** The MWD results clearly indicate that the precipitated PPCA_Ca complex preferentially contains higher MW species, leaving the supernatant depleted in these high MW components. The supernatant shows very low IE and the precipitated material has a higher IE than the original stock PPCA hence, the low IE and the low polymer content (by Hyamine) is as expected. For example, it shows that the supernatant in the original precipitation experiment from stock PPCA at 95^{o}C is made up of *lower* MW PPCA material (M_w = 1300) and that the precipitate contains mainly *higher* MW PPCA (Mw = 4900) species.

5. ***Effect of Precipitation Temperature (70^{o}C vs. 95^{o}C) on MWD:*** Broadly similar *qualitative* behavior is observed in the PPCA precipitation experiments in terms of IE of the supernatant and precipitated PPCA_Ca complex, at whatever temperature the precipitation is carried out. However, the detailed MWD of the precipitate is affected by changing the precipitation temperature. At higher temperature, more *higher* MW material is entrained in the precipitated PPCA_Ca complex. The corollary is that, at lower precipitation temperatures, more higher MW material can partition into the supernatant. Thus, poorer IE of supernatant and better IE of the precipitate is seen for all experiments; but, these IE results become closer when the actual precipitation temperature is lower. That is, the IE results for the supernatant improve and the precipitate decrease at lower precipitation temperatures.

6. ***PPCA_Ca Precipitate Solubility in Successive Supernatants:*** In a series of experiments, we have shown that the solubility of the precipitated PPCA_Ca complex becomes *lower* as it is exposed to successive fresh supernatant brine. This PPCA_Ca solubility behavior is very unlike that expected from a "solubility product" model. The reason for this is again related to the MW of the various components of the PPCA, as discussed below.

7. ***MWD of PPCA: Re-dissolution of the* PPCA_Ca *Precipitate in FW, SW and DW:*** MWD results were obtainable for the redissolved PPCA species in FW, SW and DW at both 70^{o}C and 95^{o}C. It was clearly shown that the MWD of the redissolved PPCA species (M_w = 3600) was much higher than that of the initial supernatant (M_w = 1300) but that it was still highly depleted in the very highest

MW components of the PPCA. These MWD observations also demonstrate that the dissolution of the precipitated PPCA_Ca complex operates through a "stripping" mechanism, where the lower MW species from the precipitated complex are gradually "stripped" when it is exposed to fresh brine.

8. ***MWD of PPCA: Proposed Model for Polymer/Ca Dissolution for Squeeze Processes:*** The MWD results from this research for the PPCA_Ca complex can probably be generalized to *any* polymeric scale inhibitor which is applied in a precipitation squeeze. These results clearly point to a "stripping" model of polymer/Ca complex dissolution where the lower MW species are preferentially dissolved into supernatant brine until some equilibrium is reached. This, in turn, results in the original precipitate being enriched in (less soluble) higher MW species. This was illustrated schematically in Figure 107 where it is shown that as the "depleted" precipitate is successively exposed to new brine, then only higher and higher MW components are available for dissolution and it is known that these are less soluble than the lower MW species (and the results here amply demonstrate this). This explains the observations in experiments such as those shown in Chapter 5 Figure 85 for example. This model of dissolution is very different from a "solubility product" model as would apply to a sparingly soluble salt. This should now be taken into account in the modeling of polymeric SI precipitation squeeze processes.

9. ***Field Application and Significance of Results:*** The results from this work on polymer adsorption/precipitation processes are being used to test out recent models of coupled adsorption/precipitation (and IE) developed within the FAST project. In the work presented here, we have focused on the solubility of the PPCA_Ca complex which would appear in a precipitation squeeze. The initial observations on the solubility of this species appeared to be quite counter intuitive and were not anticipated. However, by being able to carry out MWD experiments on the various PPCA species which appeared in the process, a fairly complete understanding is being generated. This has led to the proposal of the "stripping" model of dissolution described above. Once a mathematical description of this model has been developed, it will be incorporated into future field squeeze design models for adsorption/precipitation (r/p) processes for polymers.

CHAPTER 7- NON-EQUILIBRIUM SAND-PACK STUDY OF PPCA: DYNAMIC PRECIPITATION FLOOD – MULTIPLE FLOW RATE AND SOLUBILITY EFFECTS

In this chapter, the previous static test findings from the PPCA precipitation studies will be taken forward into dynamic sand-pack studies. We will investigate the behaviour of polymeric scale inhibitor in dynamic flowing systems, at higher temperatures. We have also studied the effect of multiple flow rates on the precipitated SI effluent concentrations and the solubility of the precipitate in various post flush brine fluids.

7.1 Introduction

In this earlier work, we studied the phase behavior of PPCA in great detail. We have reviewed how all of the parameters governing the phase behavior relate to the MWD of PPCA in "precipitation" or phase separation squeeze treatments. These processes rely upon the interaction of the inhibitors with metal cations such as Ca^{2+}, pH and temperature. It is well known from the literature that higher MW components are more efficient scale (crystal growth) inhibitors, and that these higher MW components also exhibit preferential precipitation. Therefore, MW is clearly a controlling factor in the inhibition, adsorption *and* precipitation behavior of polymeric scale inhibitor species. It turns out that all of the observed results on the PPCA phase envelope concerning the precipitation behavior, IE, polymer/ICP assay, precipitate solubility etc., can be understood from these previous Mw and MWD results. This analysis explains why a simple "solubility product" model does not apply to polymeric precipitate solubility; instead, we proposed a "stripping model" based on the MWD which much better describes our observations. A full picture of these processes has now been developed and we believe that this will apply to virtually all polymeric scale inhibitors.

Now in this chapter the bulk PPCA precipitation studies will be taken forward into dynamic sand-pack experiments. This has been done in order to improve our modelling

of polymeric precipitation squeeze treatments and to understand the dynamic system of PPCA in more detail. Non-equilibrium experiments were conducted to analyze the effect of multiple flow rates on the precipitated SI effluent concentrations. Theoretically the effluent concentration changes as the flow rate changes if the system is not fully at equilibrium.

Therefore the experimental conditions for the dynamic PPCA sand-pack floods was conducted mainly with 5000ppm PPCA at 95^{o}C and pH 6 to ensure maximum precipitation with 2000ppm of calcium. In these tests, PPCA is flooded into a sand pack core at reservoir conditions and back produced at multiple flow rates using formation water and/or 1%Na as in NaCl solution. Since we know the phase envelope of PPCA very well, then these sand-pack floods have been designed to be *precipitation* flooding experiments at multiple flow rates. The multi-rate experiments allow us to establish the joint effects of both the solubility of the Ca_PPCA complex and also its kinetic dissolution rate (described in modelling by a rate parameter, κ). Very comprehensive dynamic flood data was measured in order to extend our understanding of the PPCA_Ca precipitation/re-dissolution system.

The objective of these floods was to examine the precipitation /dissolution characteristics of coupled adsorption/precipitation squeezes at various flow rates for the PPCA system. This will provide a background to understand the bigger picture of polymeric scale inhibitor for the precipitation squeeze treatments. However, the result shows very clear behavior which can be interpreted in terms of dynamic precipitation with some adsorption and is in very good qualitative agreement with our recently developed flow models.

The Dynamic Adsorption Isotherm

The basic idea of the sand pack or core flow test leads to the dynamic adsorption isotherm. Figure 108 shows a schematic of a SI being post flushed from a core and the effluent profile (the effluent [SI] vs. the PV of fluid injected) which would result for a species showing good adsorption or precipitation behaviour. Note that a log scale is used for [SI] and that there is a peak in [SI] at very early time (at ~ 1- 2 PV) followed by a low [SI] “tail” for many 100s to 1000s PV of post flush. It is this very remarkable “return curve” that makes scale inhibitors so suitable for use in a “squeeze” treatment. If

they return in this manner at a low [SI] which is greater than MIC (MIC = minimum inhibitor concentration required to prevent or retard scale to an acceptable level), then the "squeeze" is deemed to be successful.

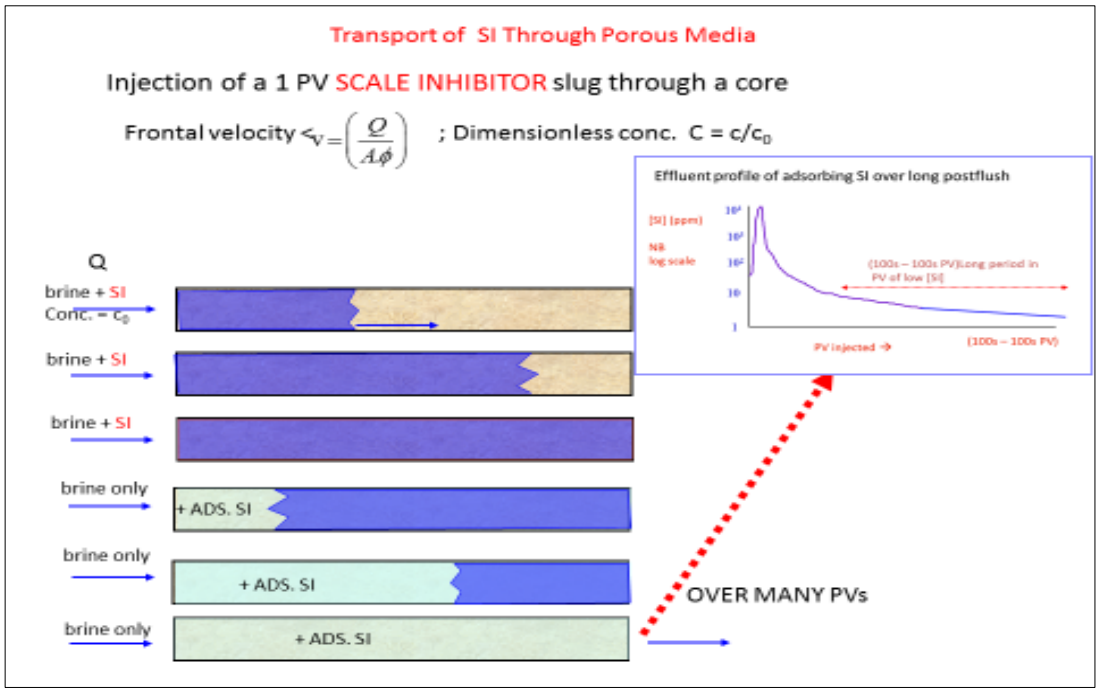

Figure 108*:* Schematic of a core (pack) flood where the postflushed scale inhibitor returns at a low [SI] over very many PVs (100s – 1000s). (Source: FAST Group, Oilfield Scale Course)

7.2 Experimental Details

As mentioned above, the unique feature of these PPCA flood experiments is that, we have fully characterised the PPCA precipitation system through our bulk studies with static tests. We know from our previous experimental work that PPCA at higher concentration of calcium and SI with pH 6 and at 95^{o}C, the system is in precipitation regime (there is some low levels of adsorption but it is a smaller effect). This earlier work is now extended to study the retention of the inhibitor in sand packs at multiple flow rates.

Materials

1. Absorbent

Silica sand was chosen as the mineral adsorbent since it replicates a simple model of a sandstone formation and the results are also reproducible. The sand used in these experiments is commercially available (BDH GPR, 150-300mesh). A Malvern Master Particle Size Analyser was used to analyse the sand. The particle size is less than 300μm (analysed previously by other students).

2. Adsorbate

The adsorbate or SI used in this study is PPCA, polymeric scale inhibitor. This is the commonly known commercial product, Bellasol S40, used in oilfield squeeze applications. The chemical structure of PPCA is shown in Chapter 2. The 5000ppm of SI concentration was prepared in standard synthetic NFFW brine and pH adjusted to pH6. For the analysis of all the cations including PPCA, ICP analytical method (Water Analysis Handbook, 1989) was used in this study and we are able to assay down to 1ppm (±0.2ppm).

3. Brine

The pack floods have used standard NFFW, for the main treatments and the first post flush. The composition of NFFW is given in chapter 3. For this study it is important not to have other form of precipitation occurring except those related to the SI itself. The brine solution was filtered through 0.45μm filter paper and degassed overnight prior to use. 0.45μm filter paper is commonly used by the industry to filter water samples to give adequate filtration of suspended solid content in the water (Patton, 1977). For the rest of the post flushes or back production stage, 1% Na is used at various flow rates. The Lithium and Iodine tracers have been used alternatively in the system to monitor the other source of precipitation in the core.

Comment on Experimental Conditions

Before interpreting the results obtained, the following comments are presented on some of the experimental conditions:

1. A relatively high inhibitor concentration 5000ppm of PPCA, with 2000ppm of calcium in NFFW was injected in order to ensure the maximum precipitation at 95^{o}C.

2. Dissolution shut-ins for 24 hours were necessary in order to allow a static equilibrium to be set up within the core, thus giving increased dissolution of inhibitor. This had the effect of increasing the concentration in the subsequent fractions collected.
3. The two different brines were used i.e. NFFW and 1%Na for post flushes solution. The NFFW has more total dissolved solids (TDS = 91,000ppm; and 2000ppm Ca^{2+}) compared to 1%Na (TDS = 10,000ppm). It is expected that Na^{+} post flush will dissolve more precipitated SI since it contains no calcium ions.

Characterization:

After Sand packing and having assembled the column in the system, the following measurements have been taken:

Table 11: Physical characteristics of Sand Pack 2

Length of the Column	23cm
Length of packed column	19.1cm
Dead Volume at RT	5.5ml
Pore Volume at RT	14.6ml
Pore Volume at 95^{o}C	13.51ml
Diameter	1.5
Porosity	43%
Mass of Sand	55.2gm

Table 12: Characteristics of Sand Pack 3

Length of the Column	23cm
Length of packed column	19.1cm
Dead Volume at RT	5.5ml
Pore Volume at RT	12.58ml
Pore Volume at 95^{o}C	12.01
Diameter	1.5
Porosity	43%
Mass of Sand	41.79gm

Table 13: Details of each stage of the sand pack experiment

A. Sandpack 1

Stage	Flow Rate	Brine	Sample Dilution	Pore Volume (PV)
Main Treatment (MT)	20ml/hr	NFFW + 50ppm Li	10* 1%Na	~5
Ist Post Flush (PF)	20ml/hr	NFFW + 50ppm I	10* 1%Na	~ +35
IInd PF	20ml/hr	1%Na + 20ppm Li	10* 1%Na for Ist 3 PV then Neat	~ +10
IIIrd PF	10ml/hr	1%Na + 20ppm I	Neat	~ +10
IVth PF	5ml/hr	1%Na + 20ppm Li	Neat	~ +10
Vth PF	2ml/hr	1% Na +20ppm I	Neat	~ +10

B. Sandpack 2

Stage	Flow Rate	Brine	Sample Dilution	Pore Volume (PV)
Main Treatment (MT)	20ml/hr	NFFW + 50ppm Li	10* 1%Na	~5
Ist Post Flush (PF)	20ml/hr	NFFW + 50ppm I	10* 1%Na	~ +55
IInd PF	20ml/hr	1%Na + 20ppm Li	10* 1%Na for Ist 3 PV then Neat	~ +10
IIIrd PF	10ml/hr	1%Na + 20ppm I	Neat	~ +10
IVth PF	5ml/hr	1%Na + 20ppm Li	Neat	~ +10
Vth PF	2ml/hr	1% Na +20ppm I	Neat	~ +10

C. Sandpack 3

Stage	Flow Rate	Brine	Sample Dilution	Pore Volume (PV)

Main Treatment (MT)	20ml/hr	NFFW + 50ppm Li	10* 1%Na	~5
Ist Post Flush (PF)	20ml/hr	NFFW	10* 1%Na	~ +40
IInd PF	20ml/hr	1%Na + 20ppm Li	Neat	~ +10
IIIrd PF	10ml/hr	1%Na + 20ppm I	Neat	~ +10
IVth PF	5ml/hr	1%Na + 20ppm Li	Neat	~ +10
Vth PF	2ml/hr	1% Na +20ppm I	Neat	~ +10

7.3 Results and Discussion

In order to study the non-equilibrium behaviour of the PPCA system, three dynamic sand pack experiments were designed using well characterised silica sand, in which the post flush was carried out at different flow rates. This chapter will summarise the results obtained from these precipitation/kinetic sand pack flooding experiments.

The three identical sand-pack floods reported on in this section were conducted using a 5000ppm active SI concentration. The SI was dissolved in NFFW brine. The first postflush solution was NFFW but, for the rest of the postflush stages, 1%Na as in NaCl was used. The experimental flooding sequence is summarised in Table 13. All brines injected, in the sandpack, were adjusted to pH 6. At the end of each stage of the flood, from main treatment through each post flush stage, the flow was stopped for at least 24 hours at 95^{o}C.

These experiments were performed on the new sand pack rig made by FAST. The purpose of this sand pack experiment is to understand the dynamic behaviour of PPCA on its return profile, along with the behaviour of the cations and also to observe the solubility of the PPCA_Ca at multiple flow rates. The following observations were recorded in these experiments:

7.3.1 Returned Profile of PPCA

The three identical dynamic precipitation floods were conducted to study the inhibitor retention in the bulk. We will discuss the result of each sand pack in turn.

Sand Pack 1: In sand pack 1, the main treatment continued up to 5 PV at room temperature, followed by 24 hours of shut-in. The water-bath temperature was then increased to 95^{o}C during shut-in and the outlet valve was left open to avoid pressure build-up in the core. This first stage of main treatment, shut-in and postflush to ~35PV is shown in Figure 109. The immediate drop in the PPCA concentration shown in the Figure 109 confirms that precipitation has occurred during the shut-in period at 95^{o}C. As the post flush 1 continues, the concentration drops continuously over ~13 PVs, apart from a spike in the concentration between 10-12 PVs, which is still unresolved. We also had a problem with leakages of valves with the new sand-pack rig. However, after the continuous drop in PPCA concentration, it follows the typical flat return curve as shown in Figure 110, at fixed flow rate 20ml/hr. This is classic effluent return curve behaviour according to the theory as shown in Figure 108. For sand-pack 1, the returned profile of cations [Ca^{2+} and Mg^{2+}] was not obtained due to analytical problems.

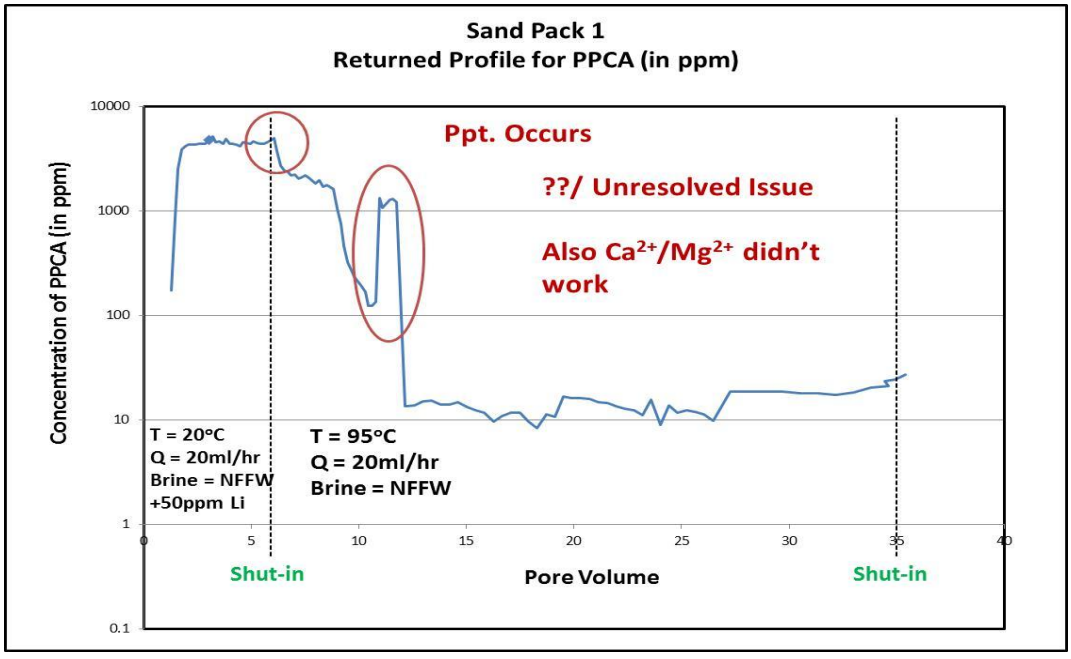

Figure 109: Returned Profile of PPCA in PF1

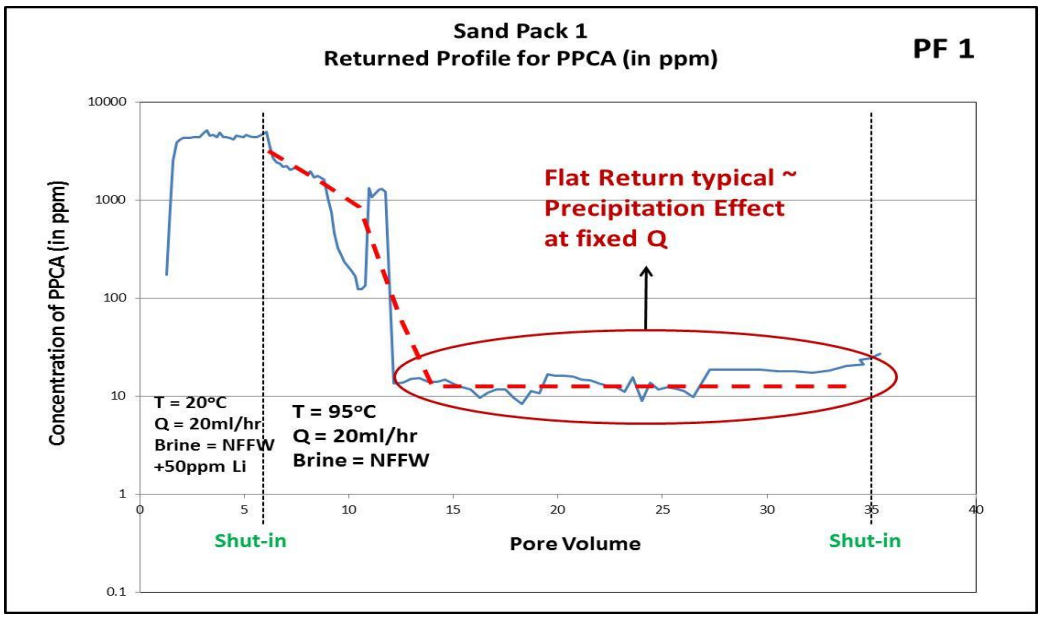

Figure 110: Returned Profile of PPCA in PF 1

Figure 111 shows the return profile of PPCA in post-flush 2 (PF2). The concentration appears to be ~10ppm by the end of post flush 1, which then rose to ~300ppm within a few pore volumes as the post flush 2 starts with 1%NaCl and with the same flow rate 20ml/hr. The post flush 2 continues for +10 pore volumes. The immediate rise in concentration shows the solubility of the precipitate increases as 1%NaCl brine re-dissolves the PPCA_Ca precipitate; but after a few pore volumes, the return effluent shows normal behaviour, i.e. [SI] reduction vs. PV throughput.

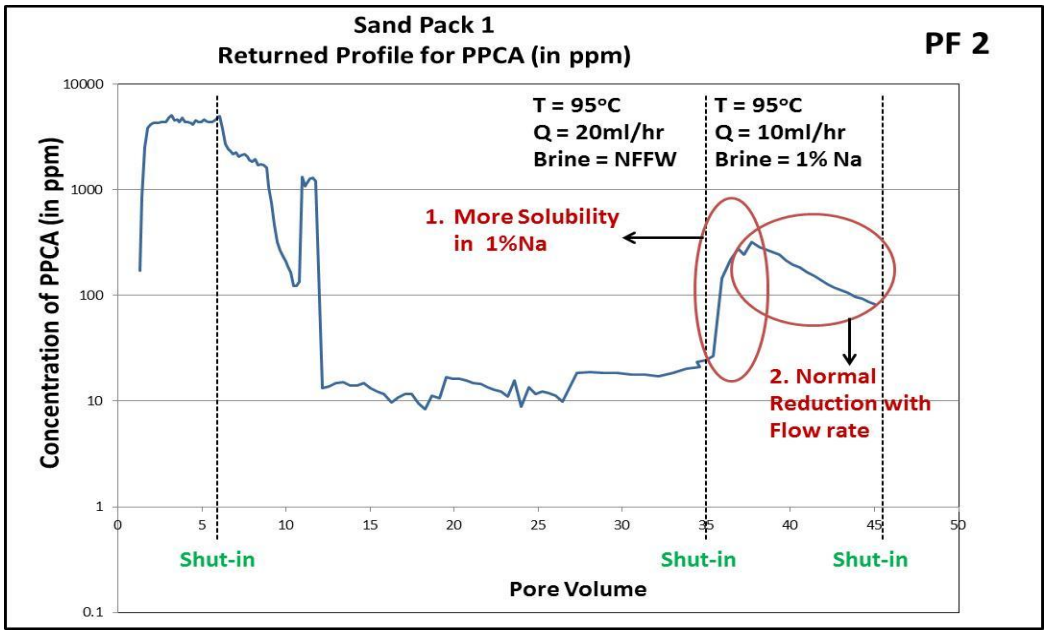

Figure 111: Returned Profile of PPCA in PF 2

Figure 112 shows the SI return profile of PPCA over post flush 3 (PF3) where 1%NaCl brine is injected but the flow rate is reduced to Q = 10 ml/hr. The small rise at the beginning of the post flush 3 shows the increase in solubility during shut-in, but the [SI] immediately drops which confirms that the system has not reached equilibrium. The reduction in PPCA concentration shows a normal with declining in [SI] vs. PV at this flow rate (Q = 10ml/hr).

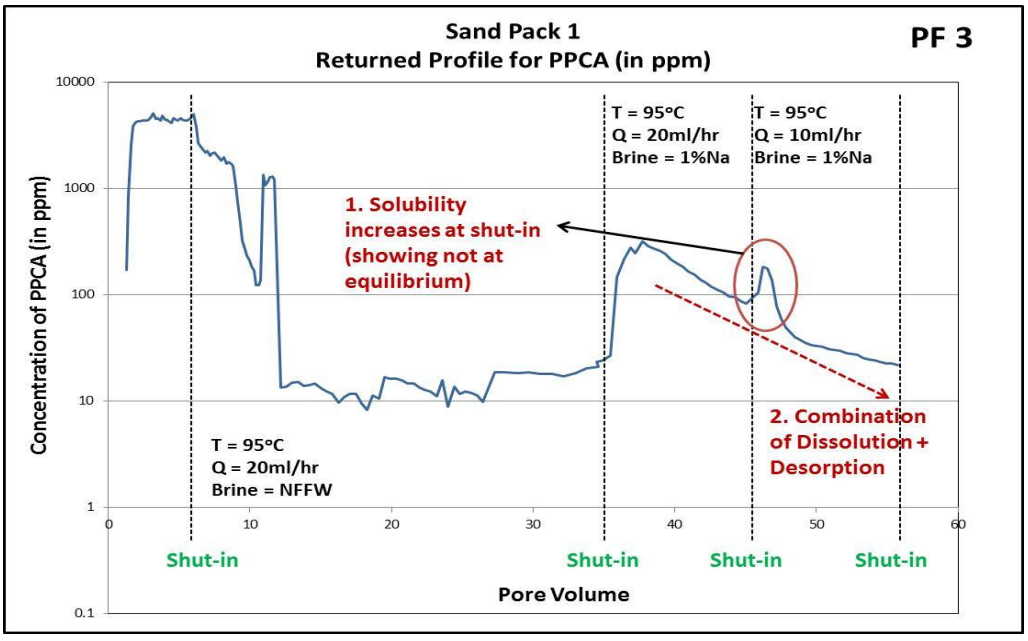

Figure 112: Returned Profile PPCA in PF 3

Figure 113 shows the PPCA return profile for post flush 4 (PF 4) where 1%NaCl brine is injected but the flow rate is reduced to Q = 5 ml/hr. This stage shows very similar trend to the effluent in post flush 3. In PF 4, the drop in the SI concentration over the next few pore volumes shows that the system has not yet achieved equilibrium. The maximum solubility observed in PF 4 was up to ~100ppm at 5ml/hr and this reduced to ~10ppm.

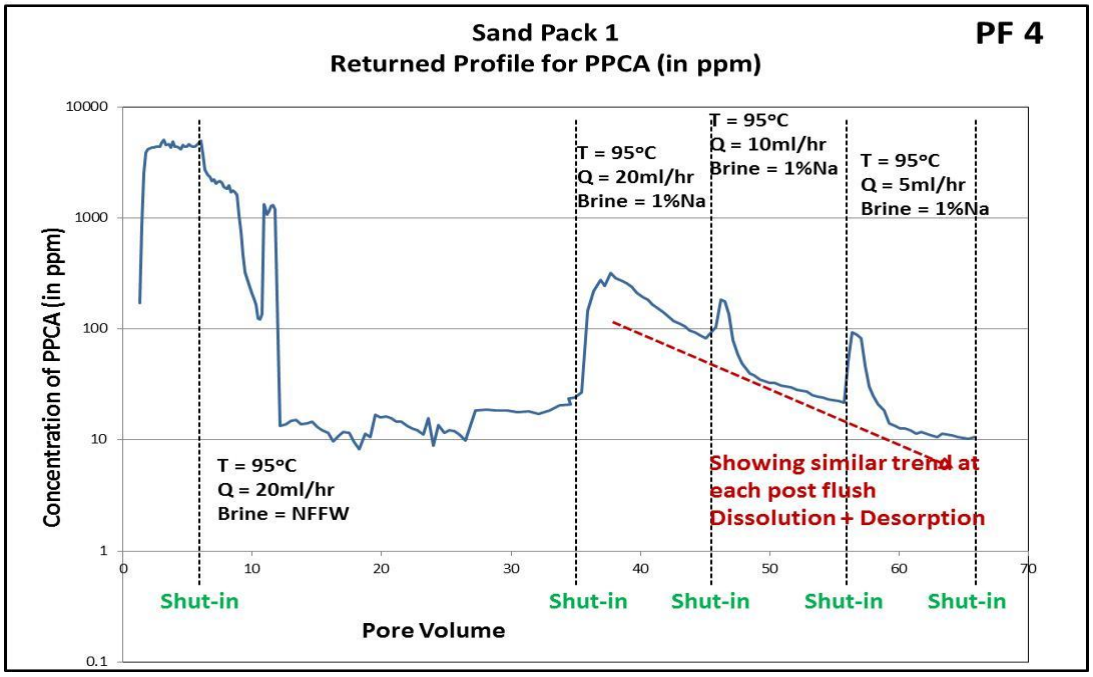

Figure 113: Returned Profile of PPCA in PF 4

Figure 114 shows the complete return profile of PPCA, now including PF 5 in which 1% NaCl brine is injected but the flow rate is reduced to Q = 2 ml/hr. At this slower flow rate there is more time to kinetically solubilise the precipitate and the effluent [SI] increases to ~50 – 80ppm. However, the subsequent decline in [SI] vs. PV in PF 5 again shows that the system is not yet at equilibrium.

PF5 was performed at the lowest rate (Q = 2 ml/hr) in this sand-pack flood and the system had not quite reached equilibrium. However, from our bulk precipitation results, it was believed that the system was “not far” from equilibrium.

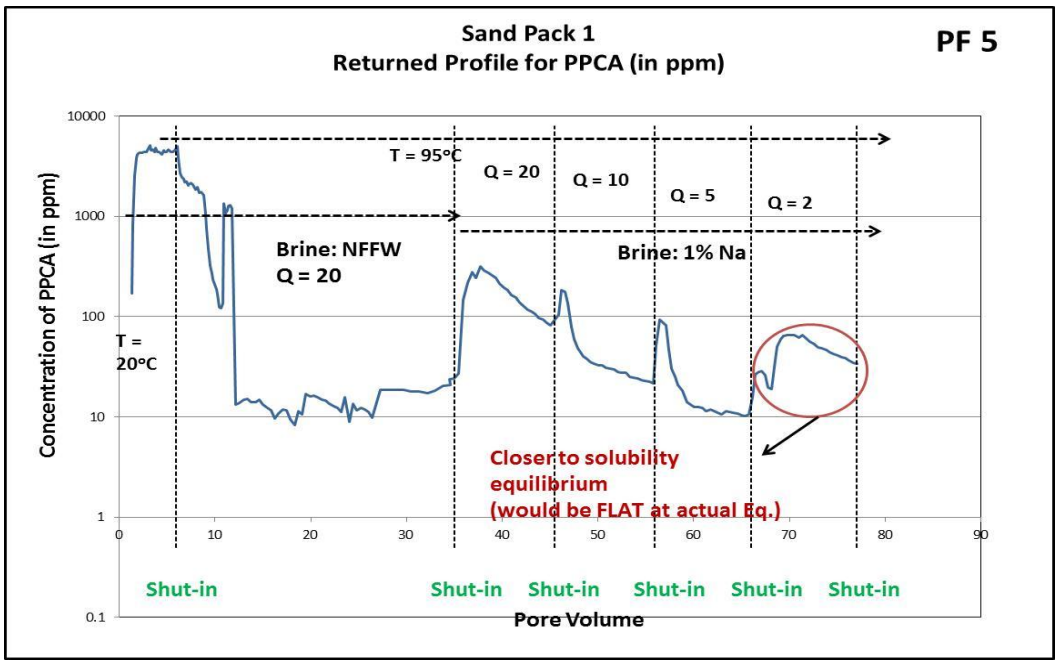

Figure 114: Returned Profile of PPCA in PF 5

Sand-pack 2: During the sand-pack 1 flooding sequence, a number of problems were encountered, such as leakages from valves and difficulties in assaying the cations-calcium and magnesium etc. but the returned profile of PPCA is in good agreement with the general theory of coupled adsorption/precipitation (Γ/Π) developed in the FAST group. It was therefore decided to repeat the same sand-pack flood under identical conditions with fresh brines.

Figure 115 shows the return profile of PPCA in sand-pack 2 for the main treatment and first post flush (PF 1) which was all carried out at Q = 20 ml/hr with formation water brine. On injection of the main treatment, the flow was completely stopped for a shut-in period. After the shut-in following the main treatment, the immediate drop in the SI concentration profile again signifies that precipitation has occurred. The steep curve at the beginning of the post flush 1 is behaving normally as before or in good accord with the theory. However, the rise in the SI effluent after ~37PV in the middle of the first post flush (PF 1) was unexpected. In fact, this was caused by loss of heating in the water-bath for a few hours, which caused the temperature to drop to close to room temperature. At this lower temperature, the PPCA_Ca precipitate is known to be much more soluble and this explains the rise in [SI] effluent over the ~38 – 58PV period of PF1 (Figure 116). A second shut-in took place at ~58PV and the temperature was again increased to 95^{o}C and it remained at this level for the rest of the post flush stages.

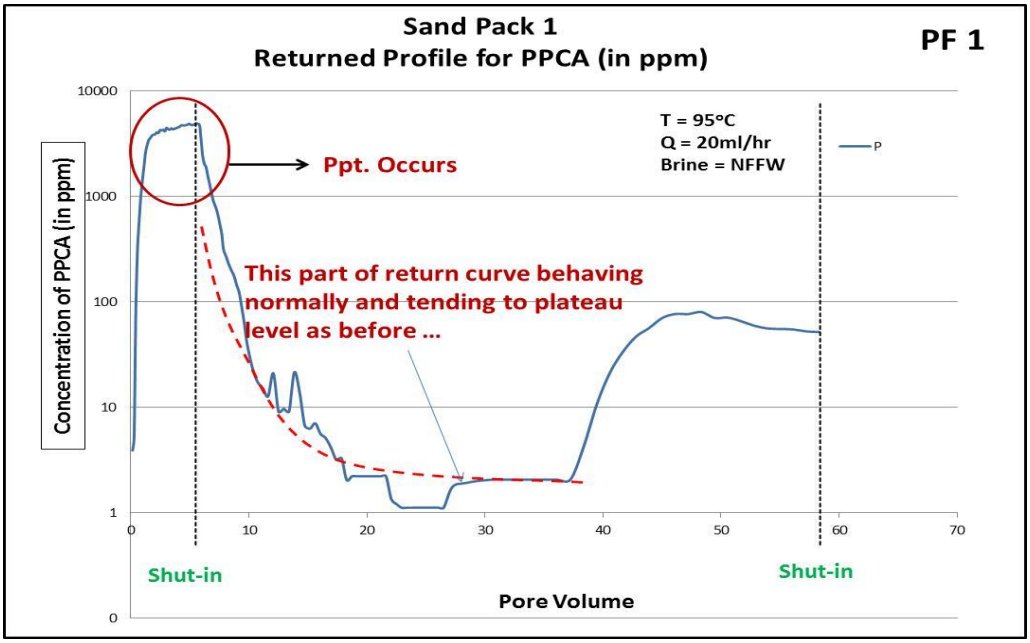

Figure 115: Returned Profile of PPCA in PF 1 of sand-pack (SP) 2

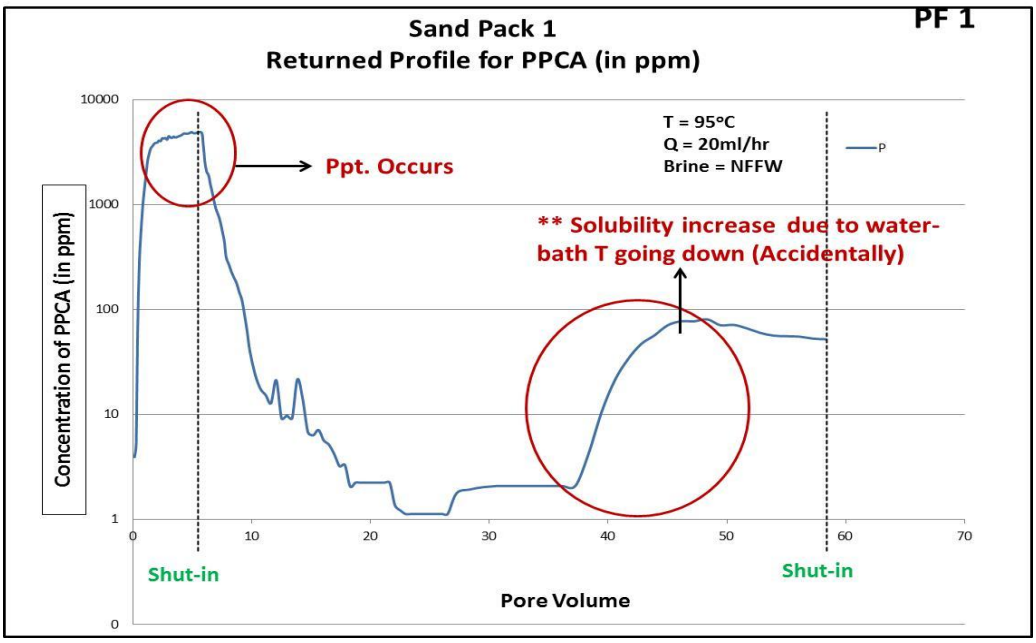

Figure 116: Returned Profile of PPCA in PF 1 of SP 2

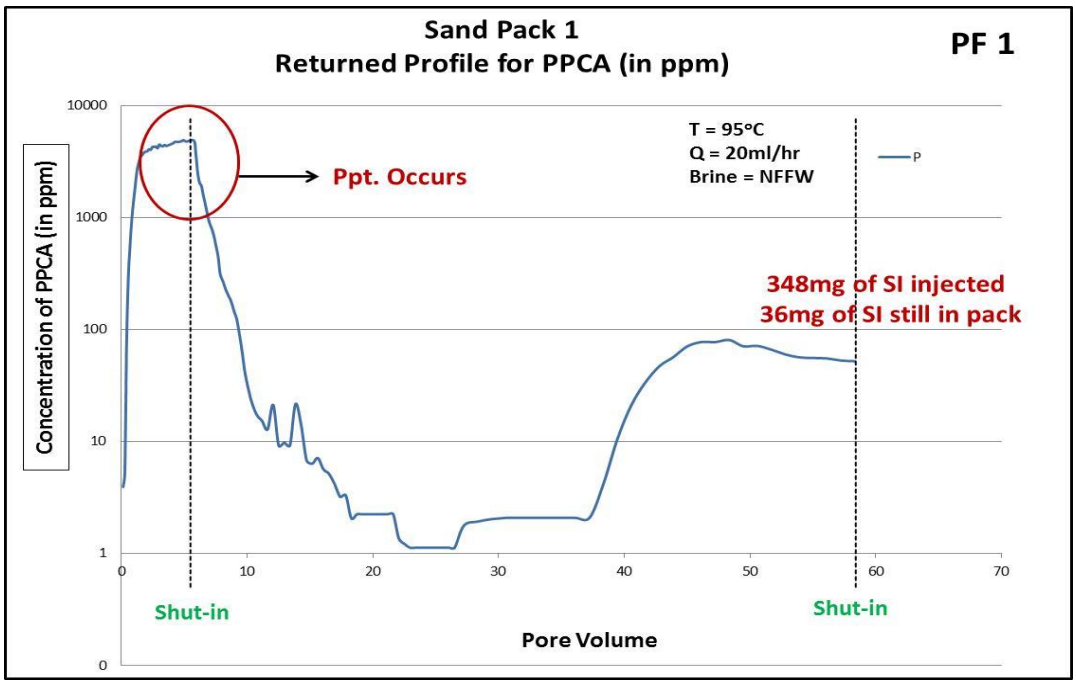

Figure 117: Returned Profile of PPCA in PF 1 of SP 2 showing Mass Balance Calculation after Post Flush 1.

During the shut-in after post flush 1, the temperature was restored to 95^{o}C. By the end of main treatment, the mass balance calculation showed that 36mg of PPCA was left in the core. The second post flush (PF 2) was then carried out at Q = 20 ml/hr using 1%NaCl brine and the [SI] vs. PV for the PF 2 stage is shown in Figure 118. The small drop in [SI] immediately after shut-in in PF 2 (Figure 117) signifies that, the PPCA in the solution was re-precipitated as the temperature increased. The subsequent rise in [SI] during PF 2 after few pore volumes shows the increased solubility of the PPCA_Ca precipitate since 1%NaCl brine is being used.

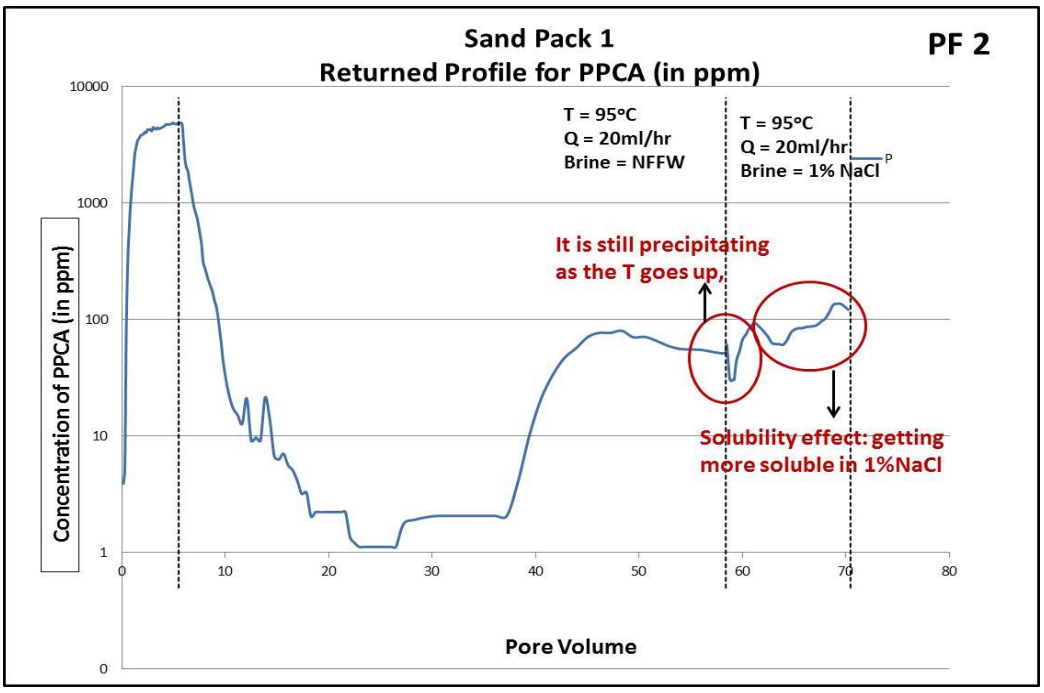

Figure 118: Returned Profile of PPCA in PF 2 of SP 2

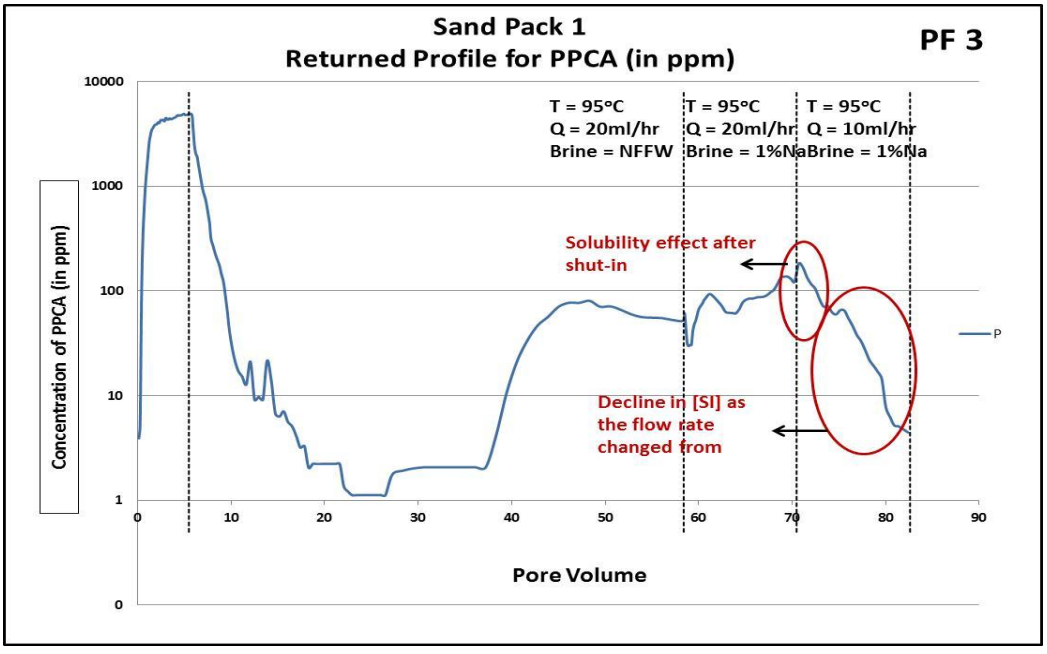

Figure 119: Returned Profile of PPCA in PF3 of SP2

Figure 119 shows the return profile [SI] vs. PV for post flush 3 where 1%NaCl was injected at Q = 10 ml/hr. The [SI] effluent shows a very similar trend to that in post flush 2. Likewise, the rise in concentration after shut-in shows the dissolution effect followed by a later decline. Later we will show that the mass balance indicates that there is still considerable precipitated material retained in the sand pack.

Figure 120 shows the complete return profile of PPCA for Post flush 4 (PF4) in sand pack 2, which injected 1%NaCl at a reduced flow rate of Q = 5 ml/hr. Again, at the slower flow rate an increased effluent concentration of SI is observed. However, the subsequent decline of [SI] vs. PV shows that the system is not yet in equilibrium.

Figure 121 shows the final stage of the return profile of PPCA for Post flush 5 (PF4) in sand pack 2, which injected 1%NaCl at a reduced flow rate of Q = 2 ml/hr. At this slowest flow rate, an increased effluent concentration of SI is observed which levels out at ~10ppm indicating that the system is very close to equilibrium.

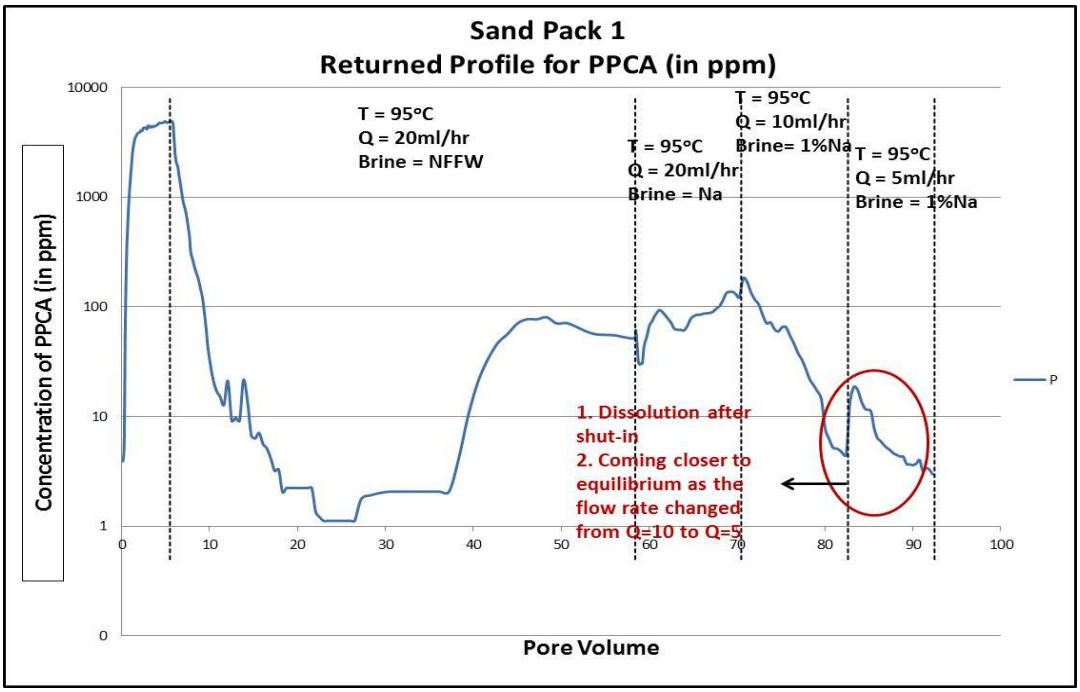

Figure 120: Returned Profile of PPCA in PF 4 of SP 2

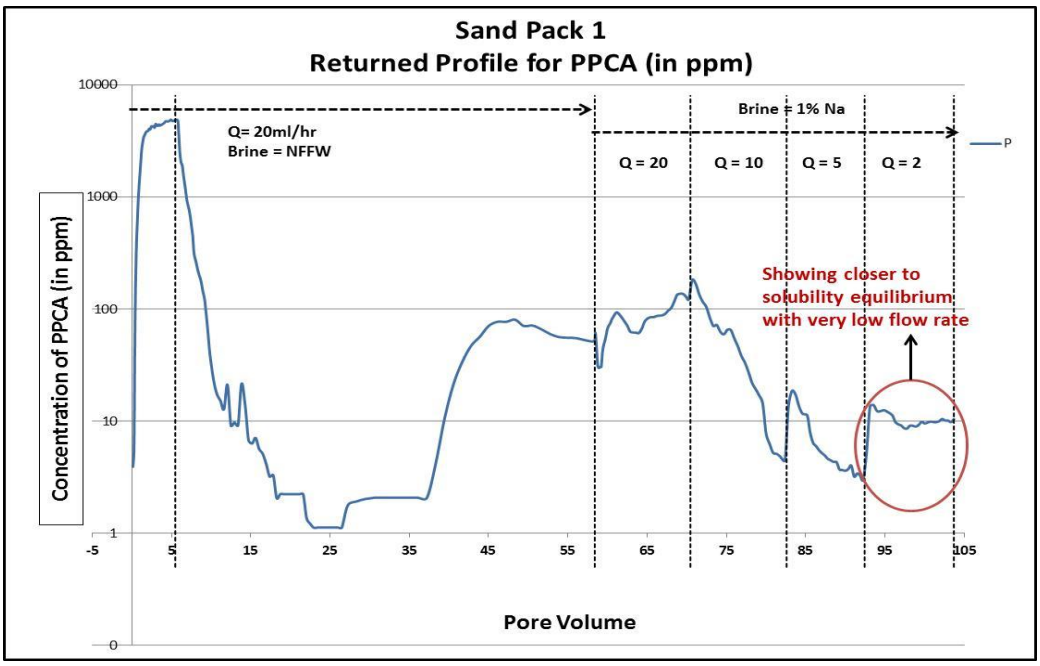

Figure 121: Returned Profile of PPCA in PF 5 of SP 2

7.3.2 Returned Profile of Cations: [Ca^{2+} and Mg^{2+}]

In the sand pack 2 floods, the Ca^{2+} and Mg^{2+} effluents were determined correctly and these are shown over all the stages of the flood in Figure 122. Our earlier static studies of the phase envelope of PPCA concluded that magnesium did not appear to participate significantly in the precipitation reaction of PPCA. However, the effluents in Figure 122 appear to indicate quite similar behaviour for divalent cations, calcium and magnesium. However, the levels of Ca^{2+} are much higher (by x10 mostly) than those of Mg^{2+} over the effluent and it is not clear if this is a complexation mechanism or possibly an "entrainment" mechanism where the Mg^{2+} becomes incorporated hydro dynamically in the precipitate. Figure 122 shows that there is a drop in both Ca^{2+} and Mg^{2+} after the initial shut-in when temperature is increased from 20^{o}C to 95^{o}C but this drop appears to be much bigger for Ca^{2+}.

The constant levels of Ca^{2+} and Mg^{2+} over the first post flush (PF1) (Figure 122) occur due to the fact that PF 1 was carried out using NFFW at 20ml/hr. After post flush 1, in PF 2 the brine was changed to 1%NaCl which contained no Ca^{2+} or Mg^{2+}. The immediate drop in Ca^{2+} and Mg^{2+} in PF 2 and subsequent posh flush stages occurs because no divalent ions are being injected and the only source of these is the

precipitated PPCA/Ca (and Mg?) complex. The levels of both divalent, track the [SI] very closely which further illustrates the previous statement.

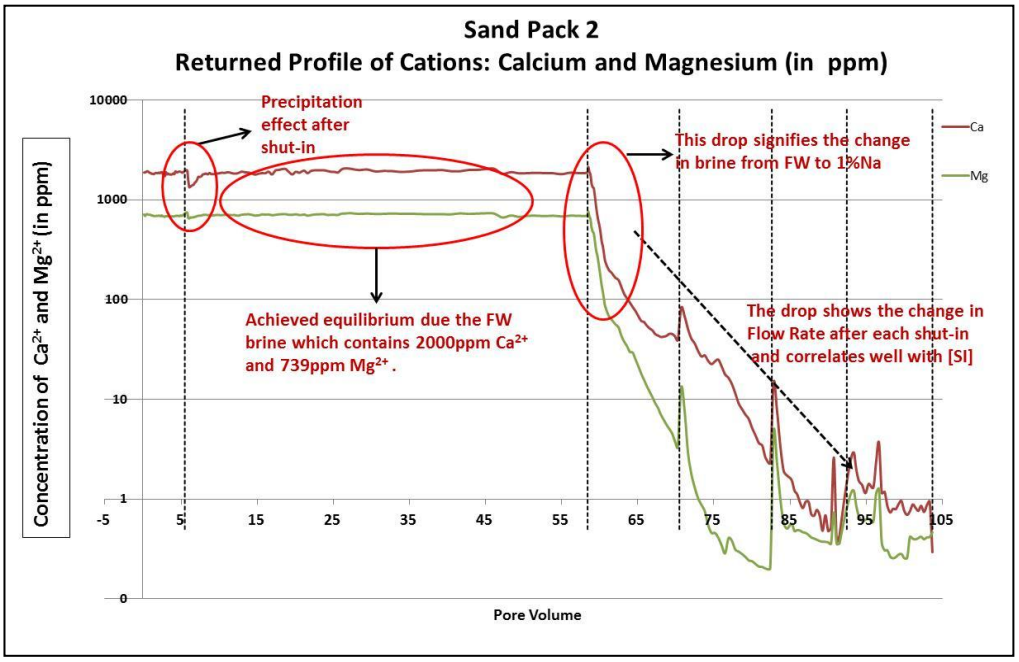

Figure 122: Returned Profile of Cation- Ca^{2+} and Mg^{2+} (in ppm) in all the 5 Post Flushes

7.3.3 Returned Profile of Lithium (in ppm)

Lithium (Li^{+}) was used as an inert tracer ion in the alternate brines in the post flush stages in sand pack 2; i.e. Li^{+} tracer was include in the main treatment, in PF 2 and in PF 4. The Li^{+} vs. PV effluent over the whole flood is shown in Figure 123. Lithium does not participate in the complexation reaction, but it is useful to monitor the system throughout the experiment. We also used Iodide tracer in alternative brines, but we did not get enough data to construct the full plots. In fact, the Li^{+} tracer results are very informative. They show a constant [Li^{+}] over the entire PF1 and then a declining [Li^{+}] over the subsequent PF3 and PF5 which tracks the divalent. This would be consistent with the "entrainment" mechanism for the Mg^{2+} rather than an actual complexation since Li^{+} definitely does not complex with PPCA.

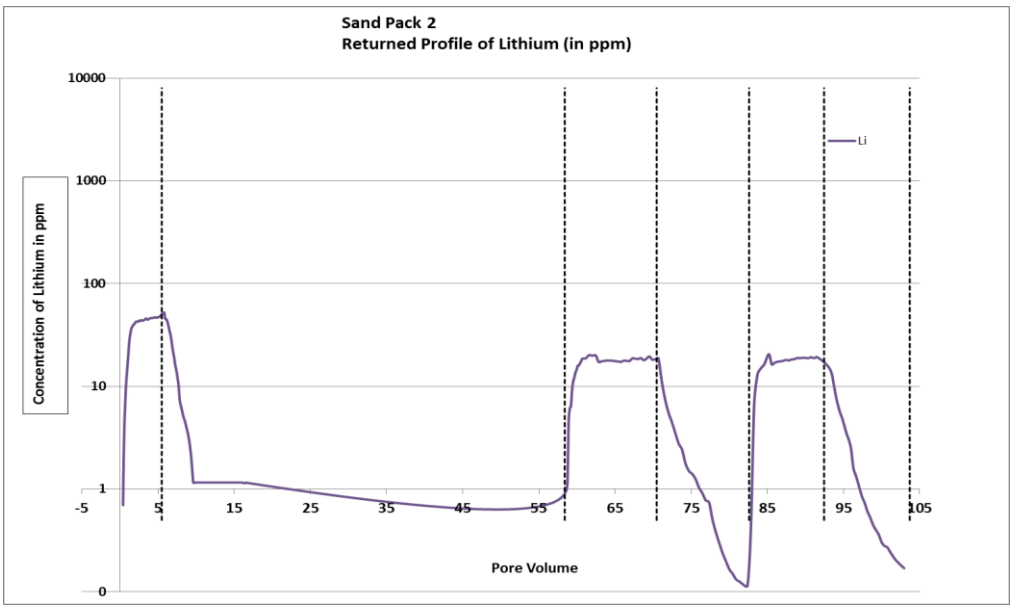

Figure 123: Return Profile of Lithium ion (in ppm)

Figure 124 shows the return profile of all the elements, PPCA, Ca^{2+}, Mg^{2+} and Li^{+}. This plot is rather messy, but it does support the various points made above.

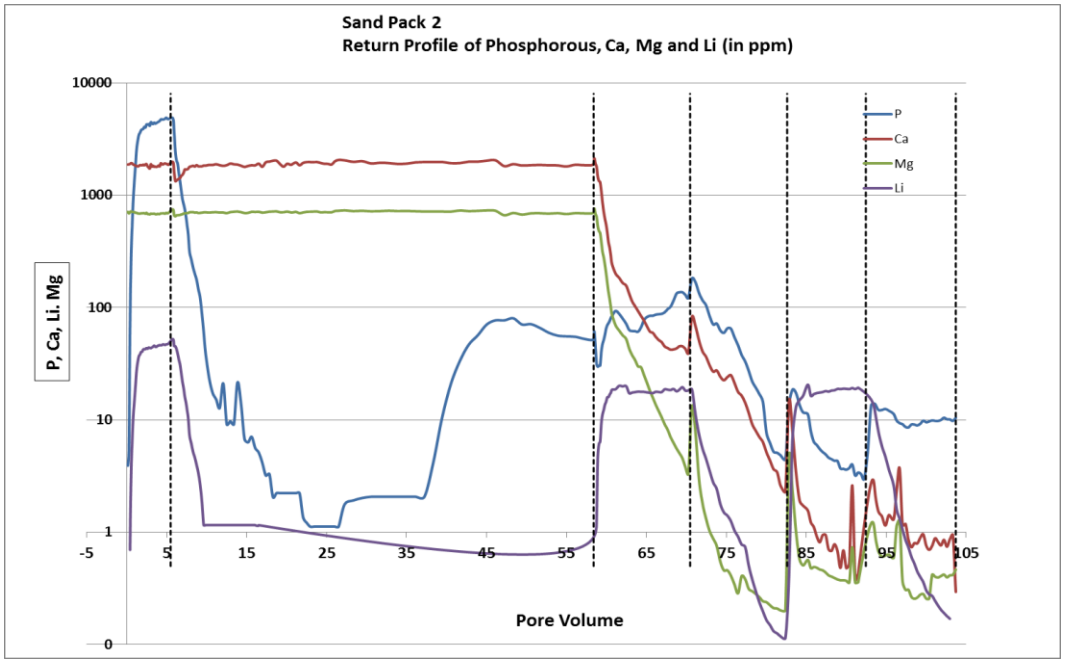

Figure 124: Return Profile of all the elements including SI PPCA

7.3.4 Mass Balance of Sand-Pack 2:

The mass balance of SI was calculated at each stage as the mass of SI remaining in the sand-pack after each post flush. All the mass calculations were made based on the total mass (input) during the main treatment. We have also considered the calculated mass based on the mass left in the sand pack after the main treatment +3PV of initial post flush to remove any of the mobile phase SI. The analysis is conducted to study how much of the original SI mass is returned after the final post flush; the amounts are shown in Table 14. The mass balance in this table shows the amount of precipitate at the end of each stage. We input ~348mg of PPCA in the main treatment and produced ~265mg back and therefore ~83mg of precipitate remains in the pack at the end of main treatment. After post flush 1, ~36mg mass left followed by ~23mg left after post flush 2 then ~15.7mg, ~14.9mg and ~13mg left after post flush 3, 4 and 5 respectively as shown in Figure 125. Therefore, by the end of all the post flushes there is still ~15% of PPCA mass left in the core. This shows that there is still SI in the sand pack after the final post flushes. Thus any mass left in the sand pack is the actual amount of mass that is being adsorbed or precipitated.

Table 14: Mass balance Calculation of PPCA for each stage of Sandpack.

	P Out	P IN	Mass Left in Sandpack mg	Retention		Mass Left in Sandpack %
MT	264.875	348.001	83.126	1.506	mg/g	23.887
PF1	46.882		36.245	0.657	mg/g	10.415
PF2	13.320		22.924	0.415	mg/g	6.587
PF3	7.188		15.736	0.130	mg/g	4.522
PF4	0.809		14.928	0.015	mg/g	4.290
PF5	1.590		13.338	0.029	mg/g	3.833
Total Out	334.663					
Mass of Sand	55.2	g				
Retention	0.24	mg/g	3.832749731	%		
Production	96.16725027	%				

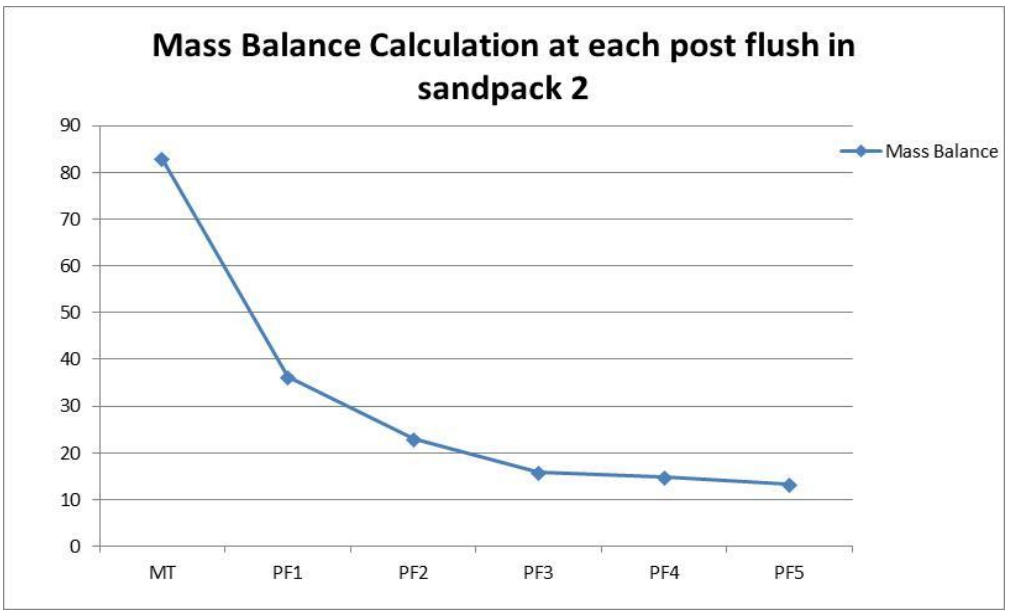

Figure 125: Mass Balance Calculation at each post flush in sand-pack 2.

7.3.5 Sand-pack 3

Results of sand-pack 1 and 2 were discussed above and we referred to various associated problems with the rig and the polymer flooding sequences. However, in spite of these experimental problems, we obtained general trends and results which were quite interpretable. The repeat experiment in Sand-pack 3 which was carried out more recently on the same rig with very similar experimental conditions was performed without any problem. We assayed the SI concentration, cations and tracers which correlate very well together. The return profile of PPCA concentration shows good agreement with the general theory of coupled adsorption/precipitation (г/п) developed in the FAST group.

A. Return Profile of PPCA

The main treatment was carried out at 20ml/hour up to 5 pore volumes at room temperature, with the bulk solution of 5000ppm SI prepared in FW with 50ppm Lithium as tracer. The flow was stopped after 5PV and during shut-in the temperature of the water bath was raised to 95^{o}C. After 24 hours, post flush 1 continued with FW with no tracer at 20ml/hr up to 40PV. Figure 126 shows the return profile of PPCA in post flush 1. The immediate drop with a little shoulder at the start of PF1 shows that the precipitation of SI occurred as the temperature rose from 20 to 95^{o}C. The SI concentration declines immediately over the next 10PV followed by a longer tail up to

40PV. By the end of PF 1, the concentration of PPCA dropped to ~10ppm (see Figure 126).

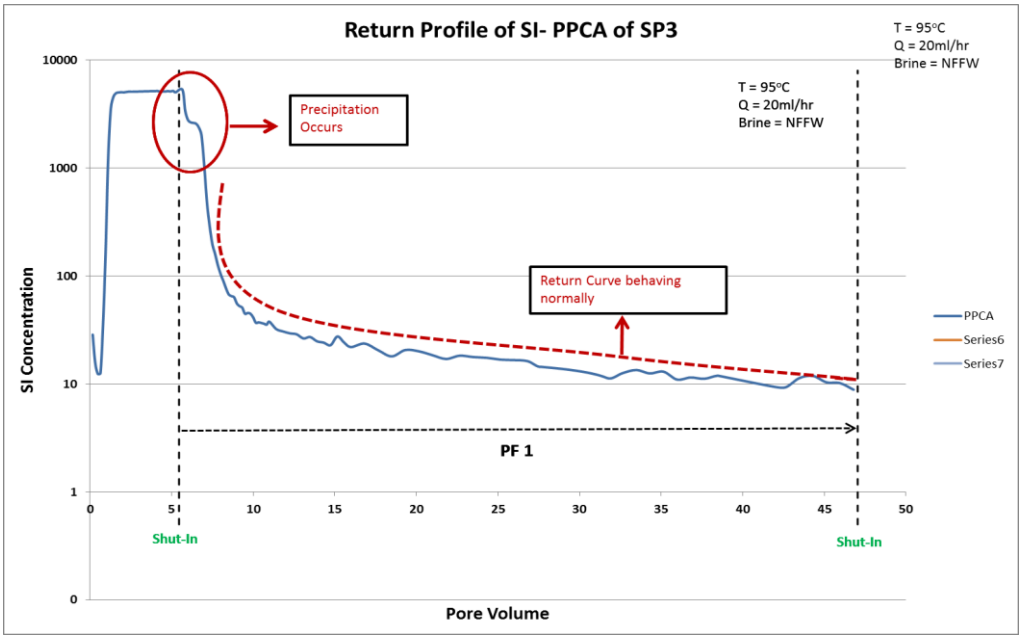

Figure 126: Retuned Profile of PPCA in PF 1 of SP 3

A shut-in was carried out after PF 1 for 24 hours. Post Flush 2 (PF 2) started with the same flow rate 20ml/hr but with 1% NaCl brine and this was carried out for a further +10PV. The change in brine composition was used to observe the solubility effect on the precipitated PPCA_Ca complex. The complex becomes more soluble in 1% NaCl as shown in Figure 127 where the PPCA concentration in the effluent rises immediately at the start of PF2. This rise in PPCA concentration at the start of PF2 rose up to ~ 900ppm and then declined gradually. This gradual decline in the concentration represents the combination of precipitation and desorption and the system does not reach equilibrium in the PF2 period.

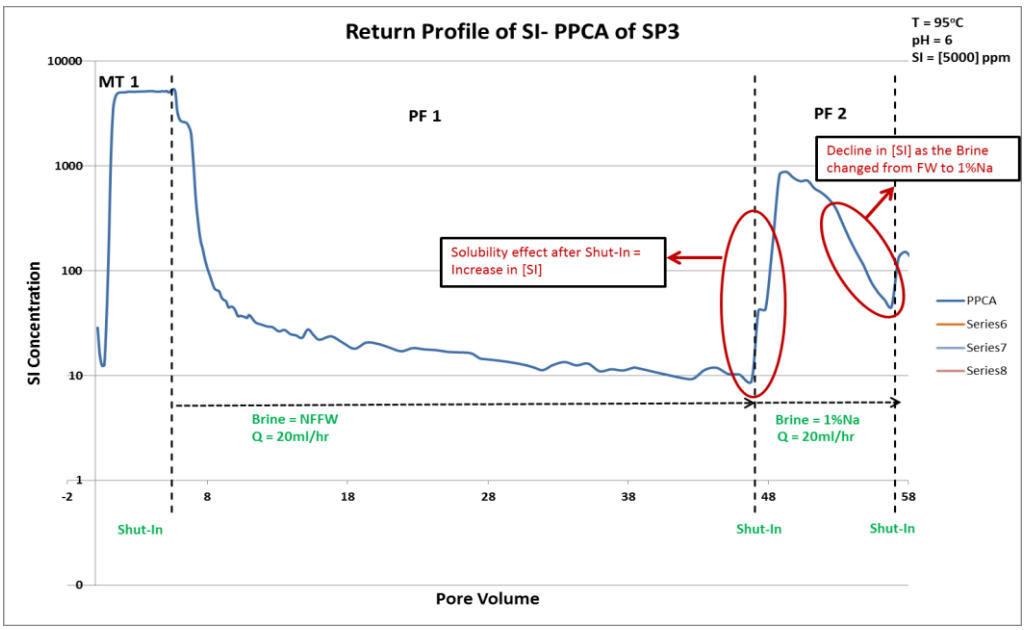

Figure 127: Retuned Profile of PPCA in PF 2 of SP 3

During the shut-in after PF1, the solubility of the complex achieves its equilibrium value (for FW), but as soon as the flow starts in PF2 (now NaCl brine) at the same flow rate, the concentration rises up again since the precipitate is more soluble but subsequently declines as equilibrium combination of precipitation and adsorption; it does not reach equilibrium by the end of PF2. A similar trend is shown in the later post flushes with serial flow rates.

The decreases in the flow rate in the subsequent post flush periods PF3, PF4 and PF5 will successively give the system more time to dissolve the complex precipitate; i.e. as low rate declines the system comes closer to equilibrium. The complete return profile of PPCA over all of these post flushes (PF3 – PF5) is shown in Figure 128. As the flow restarts in each of the post flush periods, an immediate increase in PPCA concentration is observed due to the equilibrium the dissolution of the Ca_PPCA complex precipitate during the shut-in period. Then the later decline in SI concentration vs. PV shows that the system has not yet achieved its equilibrium state. The last post flush (PF5) was carried out at the lowest flow rate Q = 2ml/hr, and this shows that the system has not quite attained its equilibrium, although it is close to equilibrium as shown by the slight flattening of the return cure at ~20ppm around 90PV. Hence, observed previously in our bulk static tests, we know that system is very close to equilibrium.

The behaviour described above for the PPCA return profile in Sand-pack 3 is exactly as expected from our adsorption/precipitation (Γ/Π) theory. Also, these results agree very well with those found in Sand-packs 1 and 2 but, in this case, the results are free from the experimental problems encountered in those earlier floods.

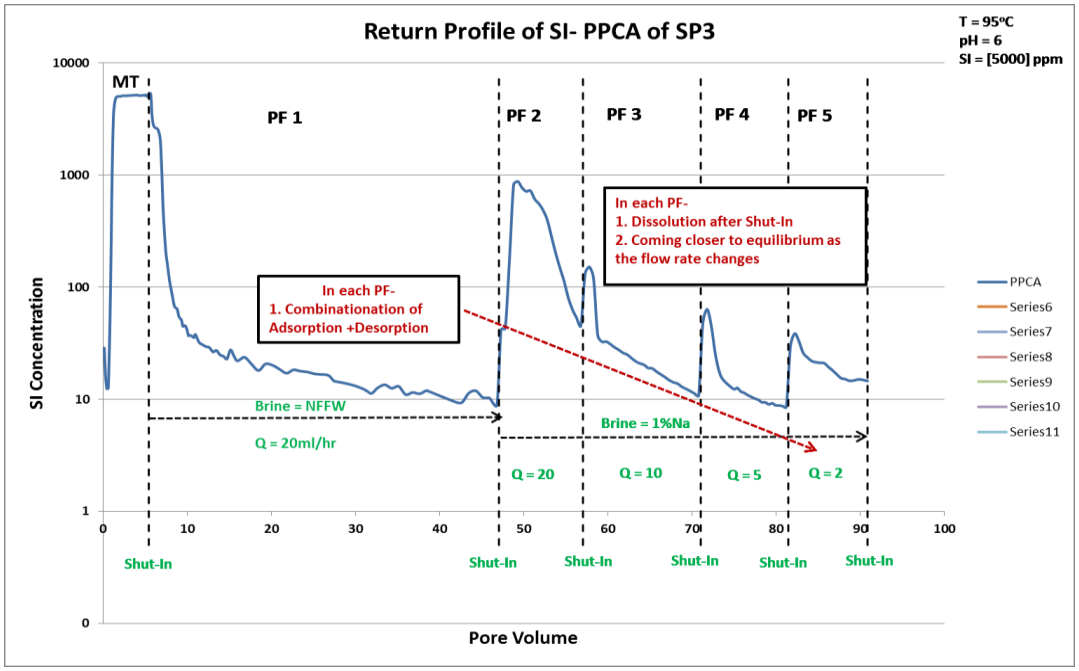

Figure 128: Returned Profile PPCA for all the Post-Flushes

B. Returned Profile of Cations

As in the Sand-pack 2 floods, the Ca^{2+} and Mg^{2+} return profiles for sand-pack 3 correlate very well with the PPCA return profile, as shown in Figure 129. The sudden dip in the calcium profile immediately after the resumption of flow shows that precipitation occurred during the first shut-in as the temperature was raised from 20 to 95°C. After a few pore volumes the profiles gains its equilibrium due to the fact that the brine used in post flush 1 contains 2000ppm Ca^{2+} and 739ppm Mg^{2+}. The brine is changed in post flush 2 (PF2 is with NaCl brine only), which does not contain any divalent cations and the return profile shows an immediate decline in PF 2 onwards.

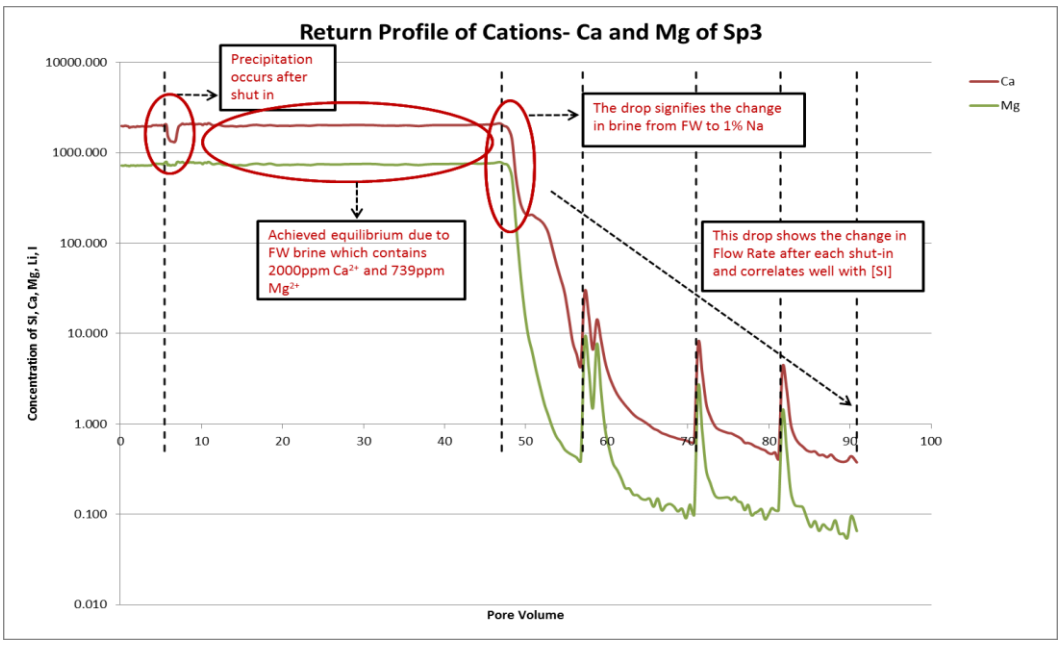

Figure 129: Returned Profile of cations for all the Post Flushes

Throughout the postflush period in the divalent results in Figure 129, the [Ca^{2+}] remains rather higher than the [Mg^{2+}]. This is only partly due to the fact that the original [Ca^{2+}] = 2000ppm and the [Mg^{2+}] = 739ppm. Actually, from the bulk PPCA_Ca stoichiometry results, we expected very little (possibly no) involvement of the Mg in the precipitated polymer complex; we expected Ca^{2+} only. However, the return profile of Mg^{2+}, closely follows the return profile of Ca^{2+} but at a much lower level. Although this *suggests* that Mg is involved in the precipitated complex, we believe that is just "entrained" as the PPCA_Ca complex precipitates in the porous medium. Very similar trends for cation return profiles were obtained in sand-pack 2 as shown earlier in Figure 122. This is not a very important result but it should be investigated in more detail to check our interpretation of these observations.

C. Return Profile of Tracers

Figure 130 shows the return profile of the tracers, Lithium and Iodine, which were used alternatively in the post flushes. Tracers were used to monitor the system throughout the experiment. In the main treatment, 50ppm Li^+ is used in FW along with 5000ppm of SI concentration. Post flush 1 flush without any tracer followed with 20ppm Li^+ in 1% NaCl again in PF 2; then alternate flushes of 20ppm iodine and lithium in 1% Na is used in the later post flushes. The return profiles of the tracers showed clearly, that the system behaved correctly and was not affected by any adverse flow conditions.

However, we also note that in the tracer change overs in Figure 130, the previous tracer showed a long tail which followed the PPCA profile; this is further evidence of tracer entrainment (rather like the Mg^{2+}) in the PPCA complex as it precipitates in the porous medium.

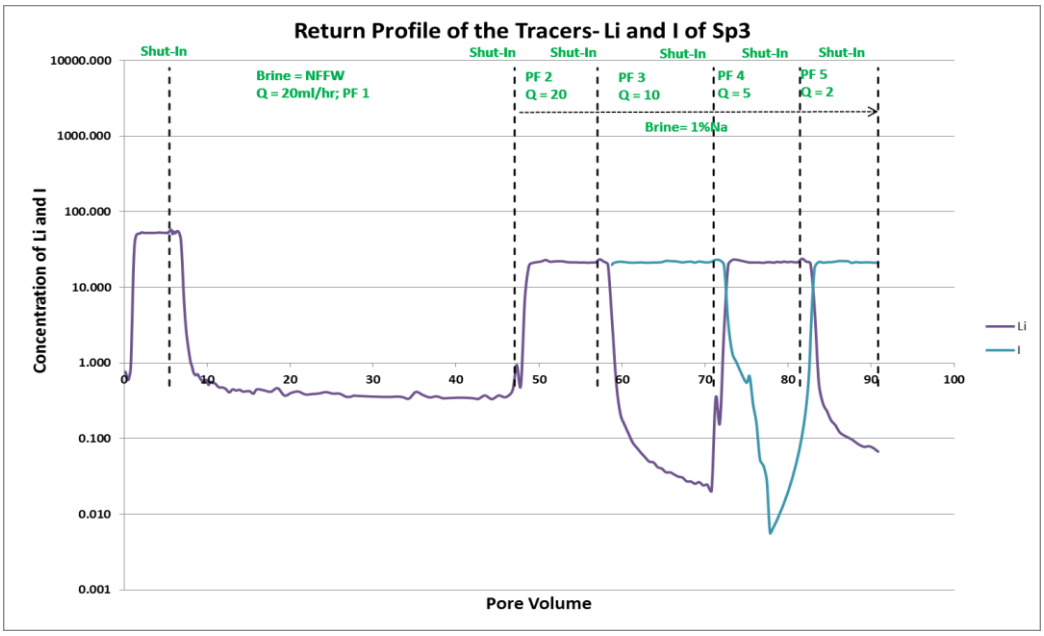

Figure 130: Returned Profile of Tracers: Lithium and Iodine

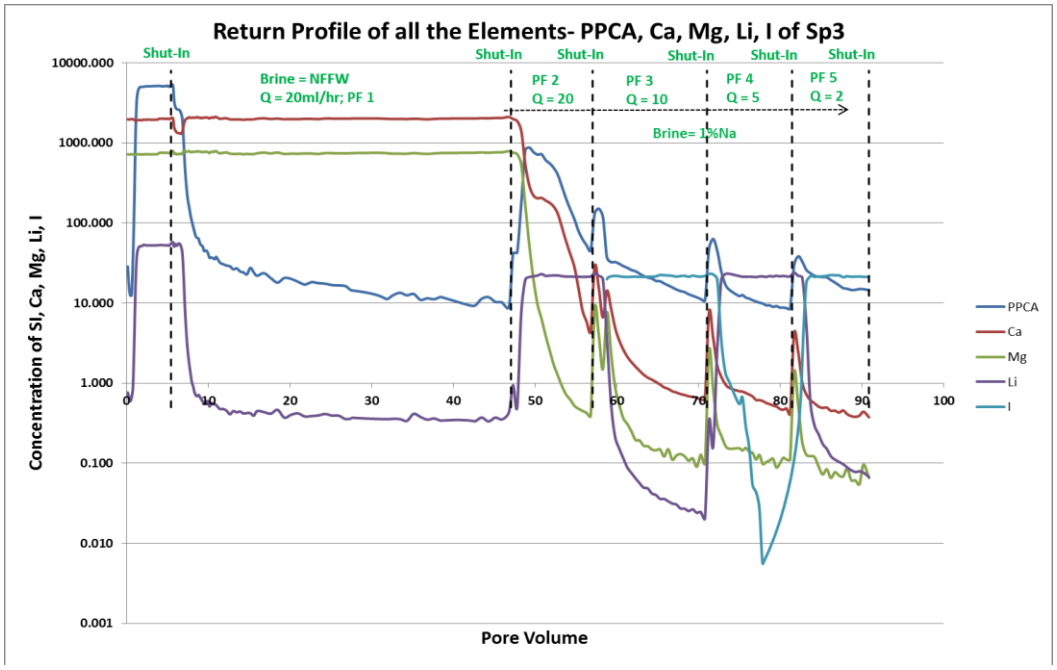

Figure 131: Returned Profile of all the elements together in all the Post Flushes

7.4 Summary and Conclusions

The sand pack floods reported in this section are the first set of systematic multi-rate floods to be carried out using precipitated PPCA with the specific purpose of verifying if our understanding of the kinetic precipitation model is correct (at least qualitatively). The results of the 3rd sand pack show the same general trends and observations as before but here they appear without any experimental problems. The results here are even more clearly interpretable, and correlate well with the static coupled adsorption precipitation theory which we investigated earlier. To date, only qualitative modelling work has been carried out in order to understand these scale inhibitor dynamic floods. To develop the complete understanding of all the phenomena which are occurring, we required more additional work. These floods will continue to investigate the behaviour of polymeric SIs in dynamic systems, with higher temperatures and also with new SI polymeric chemistries.

Our main conclusions from these sandpack results are as follows:

(i) The precipitation regions observed in these dynamic sand pack flooding experiments with PPCA agrees well with the static study of the phase behaviour of PPCA, reported extensively in previous FAST reports. In addition, the core flood [SI] vs. PV effluent results show good qualitative agreement with the inhibitor retention theory.

(ii) In the dynamic sand pack precipitation floods, the behaviour of the [SI] vs. PV effluents showed a range of characteristic behaviours after the shut-in periods when the temperature was raised from 20^{o}C to 95^{o}C. On the initial shut-in after the main PPCA treatment, there was increased precipitation; i.e. [PPCA] loss from the effluent was observed. This “dip” was evident in both the PPCA scale inhibitor and cationic concentrations immediately after the main treatment. It is a clear diagnostic that it is precipitation which is occurring in the core during shut-in at elevated temperatures.

(iii) In contrast, for the subsequent shut-ins, the effluent concentration rises quite sharply and then subsequently falls off again in the following post flush period. The initial rise in [SI] is due to the system coming closer to

precipitation equilibrium when the flow stops. Why the effluent then declines is due to (a) the dissolved (higher [SI]) being eluted from the core and then approaching a new equilibrium, and (b) the coupled effects of adsorption which is probably closer to equilibrium and causes the declining tail. (See retention theory explanation presented in the FAST Steering Meeting, 5 - 6 November 2014).

(iv) In these dynamic precipitation flood pack experiments, after the first post flush (PF1 in each flood) using formation water (NFFW), then in PF 2, 1%NaCl was used as the effluent brine at the same flow rate Q = 20ml/hr. The 1%NaCl brine increases the dissolution of the precipitate from the pack. Thus, after the shut in at the start of PF2, the [SI] rises well above that seen on the PF1 shut –in (where the polymer was less soluble due to the high salinity and 2000ppm Ca.

(v) In subsequent post flush stages (PF 3, 4 and 5), we continued to inject 1%NaCl brine at successively lower flow rates, Q = 10, 5 and 2ml/hr. In these floods, the behaviour in the return profile shows that at slower rate the effluent inhibitor concentration is ***higher*** since we are closer to dissolution equilibrium and this non-equilibrium behaviour is as expected. At the lowest flow rate in sand pack 2 (PF5, Q = 2 ml/hr, Figure 121) the effluent profile of [SI] vs. PV almost "flattened" at a level of ~10ppm which is the hallmark of reaching equilibrium dissolution. At dissolution equilibrium, then the solubility of the remaining precipitate has reached its full solubility (Cs) level. For this case (sand pack 2; PF 5; Figure 121), we find that Cs ≈ 10 ppm which is in reasonable agreement with the Ca_PPCA solubility experiments reported previously. All of these observations are consistent with the theory as presented by Sorbie (2010) and Vazquez et al (2010).

(vi) Mass balance calculations were made (for sand pack flood 2) on total mass in (input) during the main treatment. Here, mass balance is calculated based on mass left in the sand pack after the main treatment + 3PV of initial post flush to take into the account of the mobile SI phase in the sand pack. The left over mass in sand pack is either adsorbed or precipitated. It is found that mass left in the sand pack is 83mg, which is then taken as the "total mass",

for the calculation of “remaining mass” after each post flush stage. At the end of the main treatment, ~83mg of polymer remains in the pack (of ~ 348mg injected). However, at the end of PF1, ~36mg remains in the pack. Although another ~50PV of 1% NaCl brine is postflushed through the pack, there is still ~13.3mg of polymer left in the system (~17% of the total at the end of PF1). This gradual return from the precipitated material is a characteristic of the precipitation retention mechanism.

CHAPTER 8- **OTHER POLYMERIC SCALE INHIBITORS**

Previous chapters studied in detail issues concerning the solubility of the PPCA_Ca precipitate and the IE of different fractions of PPCA. The various findings were clearly related to the MWD of the PPCA as demonstrated in Chapter 6. Our hypothesis was that these findings are generally applicable to all polymeric scale inhibitors. In order to investigate this hypothesis, then two further polymers were studied, viz. SPPCA (a sulphonated version of the PPCA used in this work) and PFC, a phosphonate functionalised copolymer which also contains acrylate and sulphonate groups.

8.1 Introduction

The common types of polymeric scale inhibitors used in the oil industry are as follows:

- Polyacrylates (poly carboxylates) and related ("C/H/O") polymers and copolymer
- Sulphonated /acrylate (and poly carboxylate) copolymers
- Polyphosphonates
- Phosphino polymers and polyphosphinates
- Copolymers of all of the above sometimes including more exotic monomers (such as cationic species)

Some scale inhibitors may overlap between the above classes, for example, polymers containing both carboxylic and phosphonic or sulphonic acid groups. In such cases, priority has been given to phosphonic acid groups over sulphonic acid groups over carboxylic acid groups. PPCA is the most common phosphino polymer used in the oil industry, which contains a single phosphino group attached to two polyacrylic or polymaleic chains. The phosphino group is a joining bridge for the two acrylic acid polymers. The presence of phosphorus atoms makes PPCA polymers easier to analyse by ICP than polycarboxylic acids. Polycarboxylic acids are classified into three classes based on polyacrylic acid, polymethacrylic acid and polymaleic acid. All these linear

polymers have carbon backbones. Polymaleates are fairly biodegradable compared with polyacrylates which are poorly biodegradable. In fact, polycarboxylic acid scale inhibitors have been recently approved for use in the North Sea with >60% biodegradation by OECD 306 (Kelland, 2009; Frenier and Ziauddin, 1997).

For optimum scale inhibition, at least 15-20 active repeating units should be available in the chain to interact sufficiently with the scale crystal surface. For polyacrylates, the presence of 15-20 active groups means a MW of at least 1000 - 1500. For polymeric scale inhibitor, the range of the MW lies mainly between Mw ~ 1000 - 4000; otherwise, the performance may drop off at much higher MWs (Graham, 1994; Kelland, 2009). In previous chapters, we have studied PPCA in detail examining its phase behaviour, IE and MWD.

In this chapter, two more polymeric scale inhibitors were studied in some detail, viz. SPPCA and PFC. The reason to pick these two scale inhibitors because they have similar chemical composition like PPCA in their structures (carboxylic acid and sulphonic acid groups) and the PFC also has some phosphonate species along its backbone and are easily detected by ICP. SPPCA is a sulphonated copolymer of the standard PPCA and PFC is a copolymer including phosphonate and sulphonate groups along its backbone. In these studies, we have evaluated the compatibility of these inhibitors under different conditions (pH and temperature), in order to understand their phase behaviour in conditions broadly similar to those in the oilfield. We also studied the influence of the MWD on their IE. In addition, as for PPCA, separate measurements of the barite IE of the precipitated polymer and its remaining supernatant solution have been compared with the stock polymer.

The supernatant and precipitate were obtained in the similar way as for PPCA in compatibility tests. These samples were also analysed by GPC to determine Mw, Mn and MWD of these polymeric scale inhibitors. The results of the MWD help greatly in understanding the IE performance of stock solution, supernatant and precipitate of the scale inhibitors, SPPCA and PFC.

Our aim is to compare the results for SPPCA and PFC with previous findings of PPCA and in due course with other polymeric scale inhibitors having similar structure. We want to test if the theory which we have proposed for PPCA precipitation and inhibition

is generally applicable to all polymeric scale inhibitors. Thus, this work will help us to develop a model for polymer precipitation (and adsorption) which can be used for designing squeeze precipitation treatments for polymeric scale inhibitors.

8.2 Experimental Details

Compatibility Tests: The compatibility of both the scale inhibitors SPPCA and PFC were studied over a range of pH values. For PFC, the pH range varies from 4 to 9 and for SPPCA the tests were performed at pH values from 6 to 9. A precipitate, which is known to be a SI_Ca complex, is formed in many of the experiments under various test conditions. This precipitate can then be isolated (by filtration) and its solubility can be measured in various brines like PPCA. The three fractions of each SI, viz., stock, supernatant and precipitated SI are analyzed for IE and MWD determination. The test details of IE are kept the same as earlier for PPCA.

8.3 Results and Discussion

The studies on PPCA gave us a number of insights into how polymeric SIs precipitate and how the supernatant (S) and precipitated (P) species differed from the stock (St) PPCA solution. Many factors such as the IE of the various solutions (Sp, P and St) and their assay by ICP and wet chemical methods have been understood in terms of the MWD of these components. This resulted in the development of a mechanistic "stripping" solubility model (discussed in Chapter 5 and 6) of how polymers redissolve in precipitation squeeze processes. This model conveniently explains the wide range of behaviour which we have observed. We have conjectured that this model describes how *all* polymeric SIs actually operate in precipitation squeeze processes. The important question here to answer: "Is this behaviour specific to PPCA or is it indeed general?". Hence, our study of 2 more polymeric SI species (SPPCA and PFC) present in this chapter.

8.3.1 Compatibility Tests at Various pH Values – SPPCA and PFC

One of the many important variable as discussed before is pH which strongly influence the SI_Ca complex of the SI which in turn can affect the retention in a precipitation squeeze, and thus the squeeze lifetime. The two scale inhibitors studied have some

similar chemical grouping in their structures (carboxylic acid and sulphonic acid groups) and the PFC also has some phosphonate species along its backbone; all of these groups are susceptible to changes in pH. The results obtained for the solubility of SPPCA are shown in Figure 132 which shows that the concentration of SPPCA at higher pH values does not change very significantly.

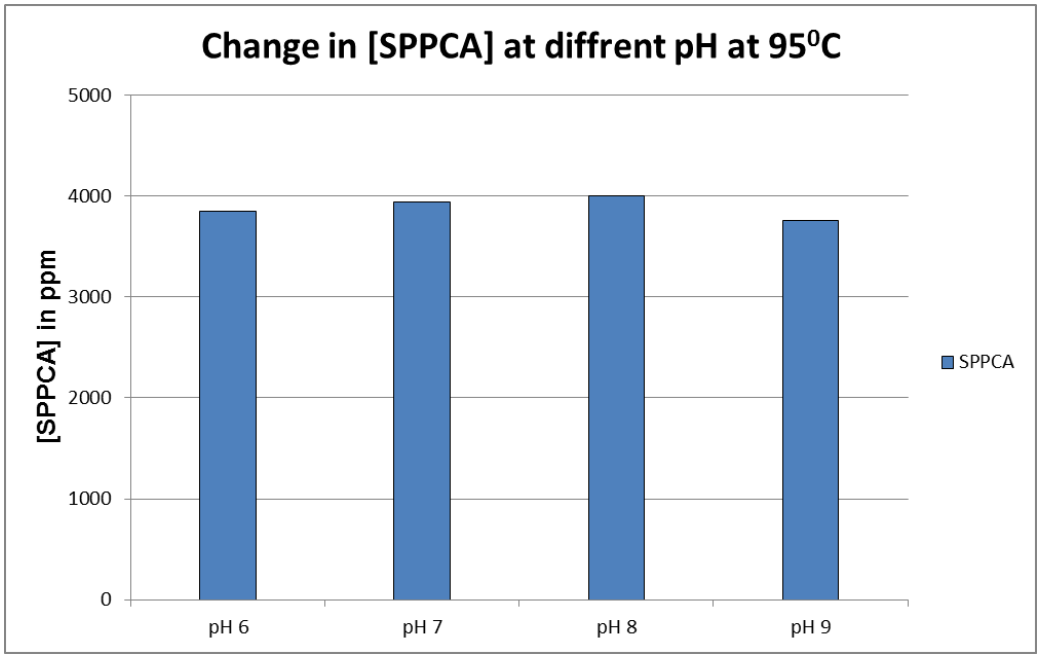

Figure 132: Concentration of SPPCA at various pH range

Figure 133 shows the effect of pH on the solubility of the PFC. This result clearly shows that the concentration of PFC decreases (i.e. more SI_Ca precipitates) as the pH increases from 4 to 9. Visual observation during the test also suggests that at pH 4 there was little precipitate formation, but at higher pH values, the precipitate was clearly evident. Like SPPCA, the results for the PFC in Figure 133 indicate that very little additional precipitation occurs above pH 6 -7.

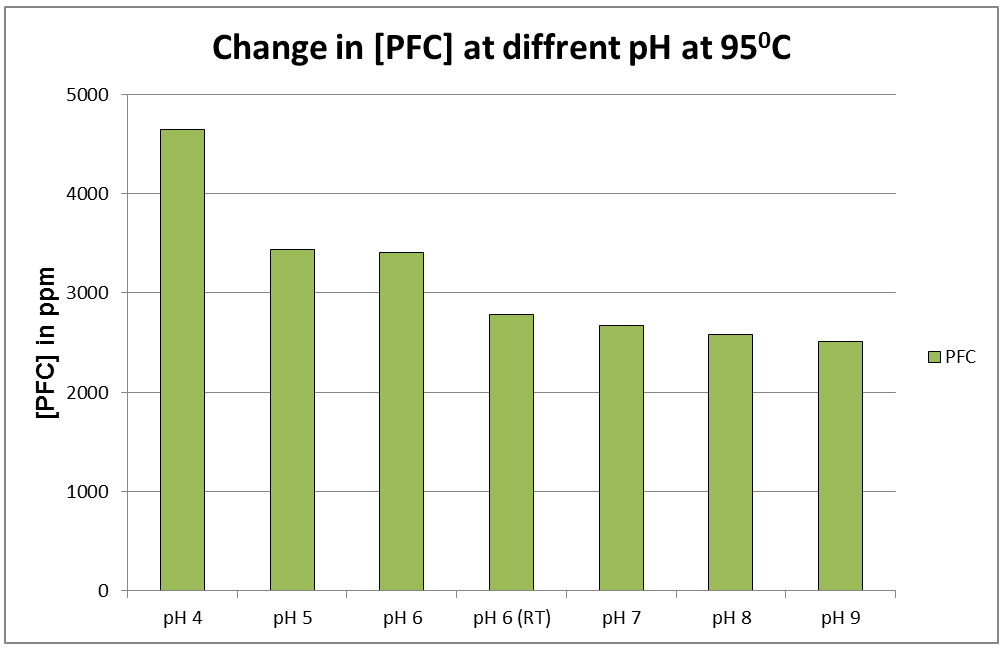

Figure 133. Concentration of PFC at various pH ranges

8.3.2 Compatibility Tests at Different Temperatures:

The visual examination of the precipitation test bottles shown in Figure 134 to Figure 136 confirms that the yield of precipitation is much higher at high temperature and with high calcium concentration.

Figure 134. 5000ppm [SPPCA] with 1000ppm and 2000ppm [Ca^{2+}] at room temperature

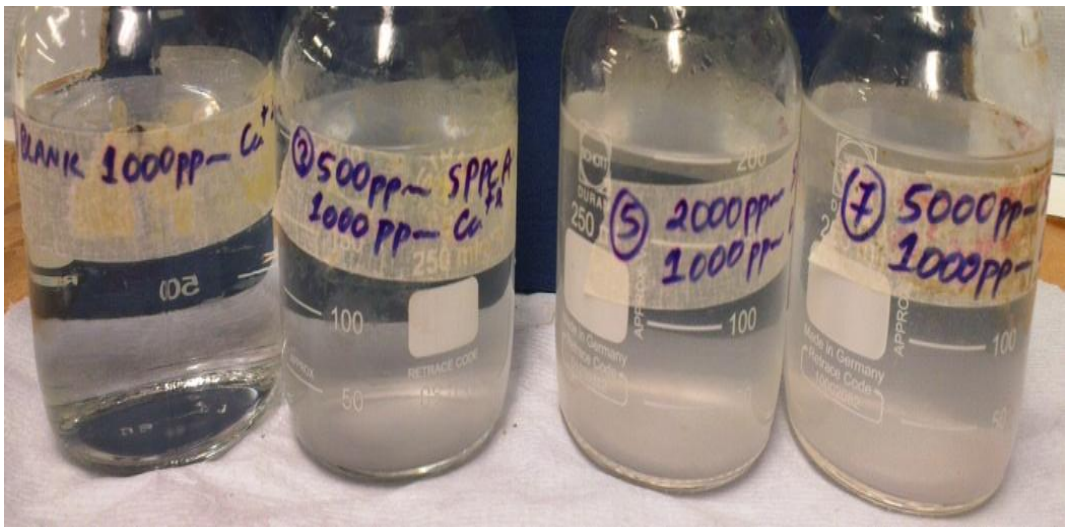

Figure 135. Precipitate formed in different SPPCA concentrations like 0, 500, 2000 and 5000ppm with 1000ppm [Ca2+] at 95oC

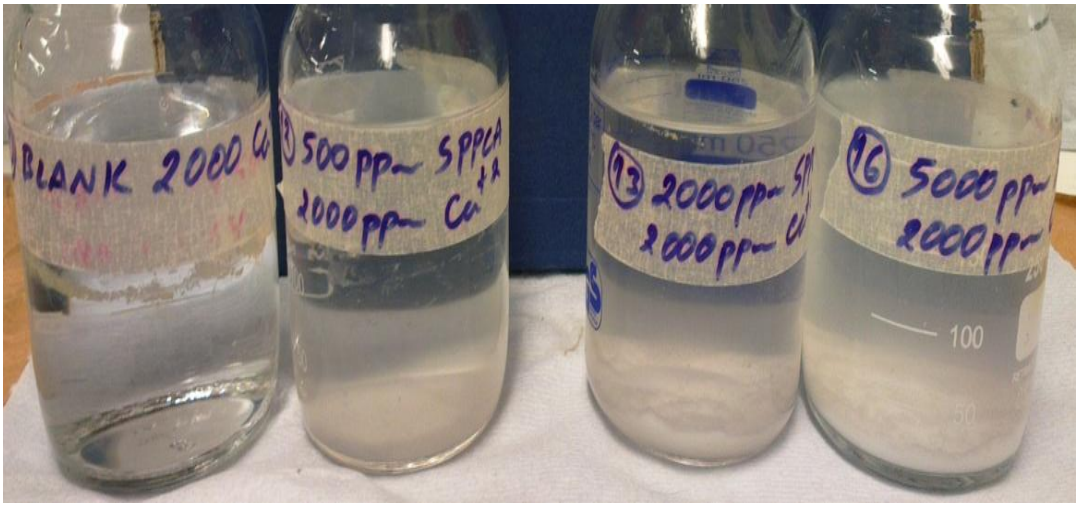

Figure 136. Precipitate formed in different SPPCA concentrations like 0, 500, 2000 and 5000ppm with 2000ppm [Ca^{2+}] at 95^{o}C.

However, Figure 137 shows the results of the SPPCA compatibility tests in FW with 1000 ppm [Ca^{2+}] and Figure 138 shows the results with 2000ppm [Ca^{2+}]. At 95^{o}C, the final concentration of the 5000ppm of SPPCA was 3900ppm measured by ICP. This result shows that at the most extreme conditions tested at [Ca^{2+}] = 2000ppm, [SPPCA] = 5000ppm and 95^{o}C, the SPPCA precipitation readily occurs. From these results, the best conditions for the formation of the precipitate (SPPCA_Ca) are established.

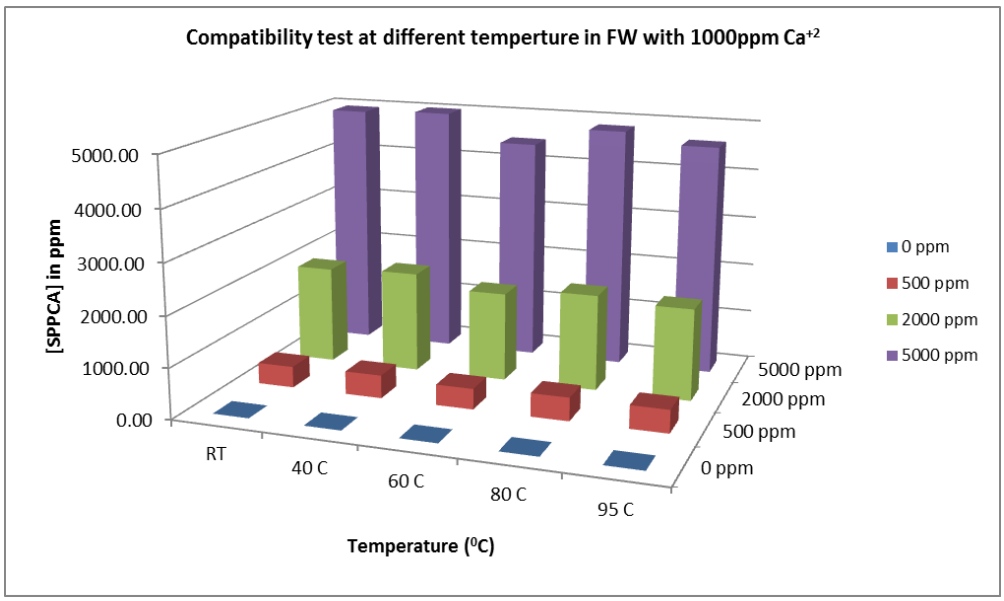

Figure 137. Compatibility test of SPPCA at different temperature in FW with 1000ppm [Ca^{2+}]

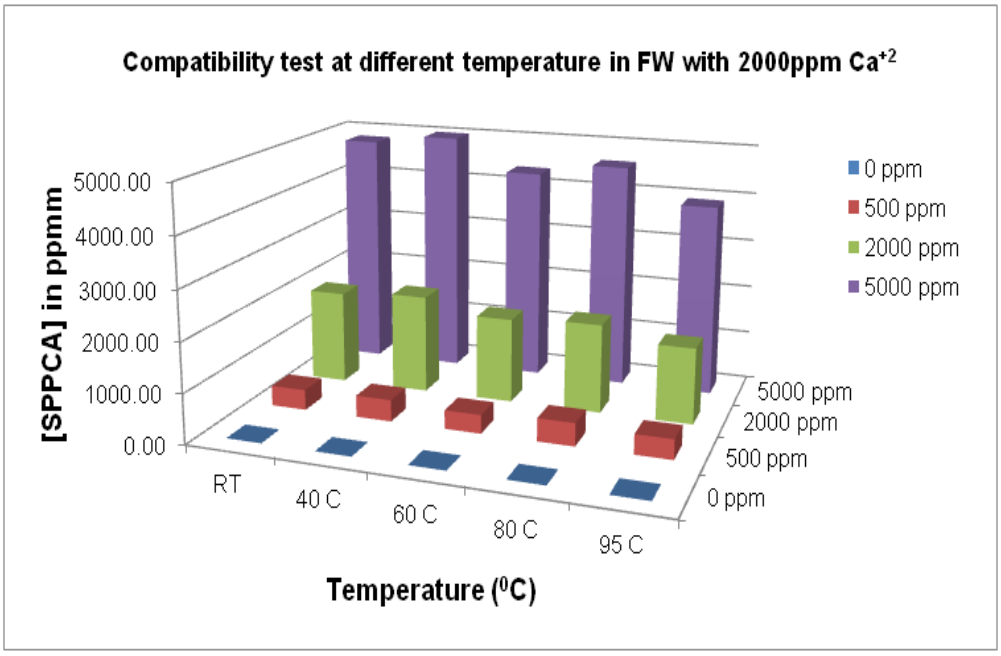

Figure 138. Compatibility test of SPPCA in different temperature in FW with 2000ppm [Ca^{2+}]

From the above compatibility/precipitation tests, results at various temperatures for SPPCA, the molar ratio between calcium and SPPCA in the precipitate was calculated. Figure 139 shows the results establishing the molar ratio of Ca to SPPCA for the system containing 2000ppm of [Ca^{2+}] and 5000ppm of SPPCA at 95^{o}C. The molar *loss* of calcium vs. molar loss of SPPCA results in Figure 139 are strongly correlated

(R^2=0.968) and the stoichiometry of the complex Ca_n_SPPCA is found from the slope of this correlation which gives n ~ 35, i.e. the ratio is ~35 calcium ions to 1 SPPCA molecule. This is in reasonable agreement with previous findings for the stoichiometry of the Ca_PPCA complex where n ~30. Figure 140 shows similar results for the 2000ppm Ca^{+2} and 5000ppm SPPCA results at 80°C. At 80°C, the molar ratio between the [Ca^{2+}] and SPPCA are much much less clear since the precipitate is more soluble at this lower temperature.

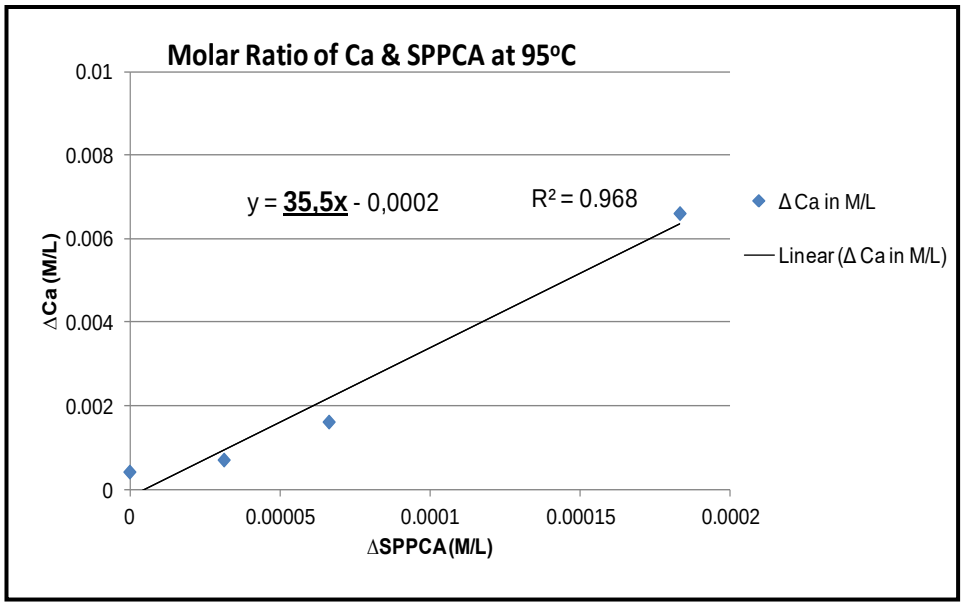

Figure 139. Molar ratio between [Ca^{2+}] = 2000ppm and [SPPCA]=5000ppm at 95°C

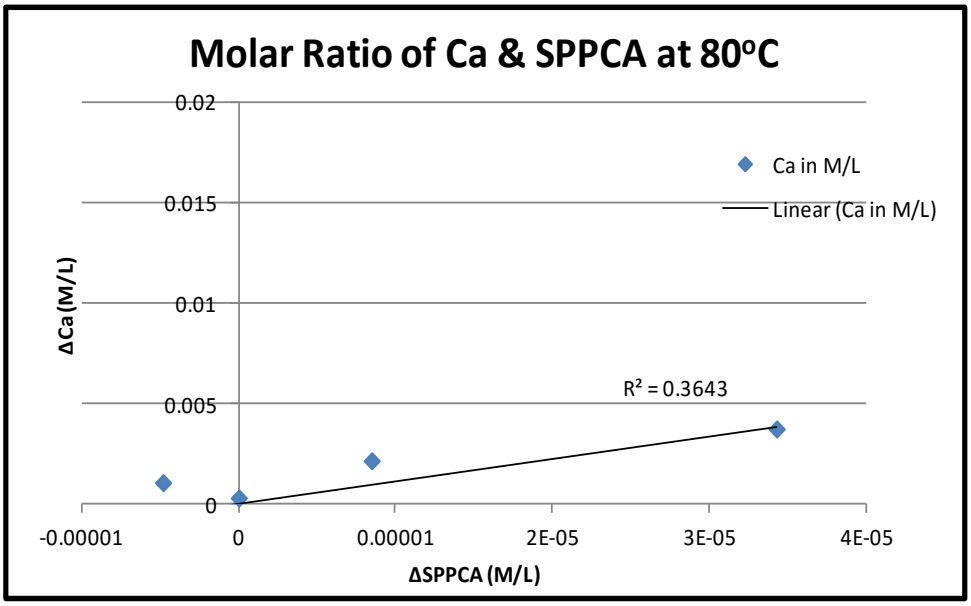

Figure 140. Molar ratio between [Ca^{2+}] = 2000ppm and [SPPCA]=5000ppm at 80^0C

Compatibility/Re-dissolution Test

The objective of the compatibility/re-dissolution tests for both the scale inhibitors, SPPCA and PFC, was to isolate the precipitates formed and study their solubility in different brines. Figure 141 shows the results for the stock solution of 5000ppm, concentration of SPPCA in supernatant and the solubility of the precipitated SPPCA in FW, SW and DW. The precipitated SPPCA at high temperature was formed by the complexation of the scale inhibitor SPPCA and [Ca^{+2}]. Unlike PPCA, the solubility of the precipitate SPPCA_Ca in FW and SW are very close, 760ppm and 780ppm, respectively. The solubility of the precipitated SPPCA in DW is little higher than FW and SW which is about ~900ppm, and this behaviour is expected because the DW is salt free. The calcium concentration for each of the brine was also obtained, and the results are presented in Figure 142.

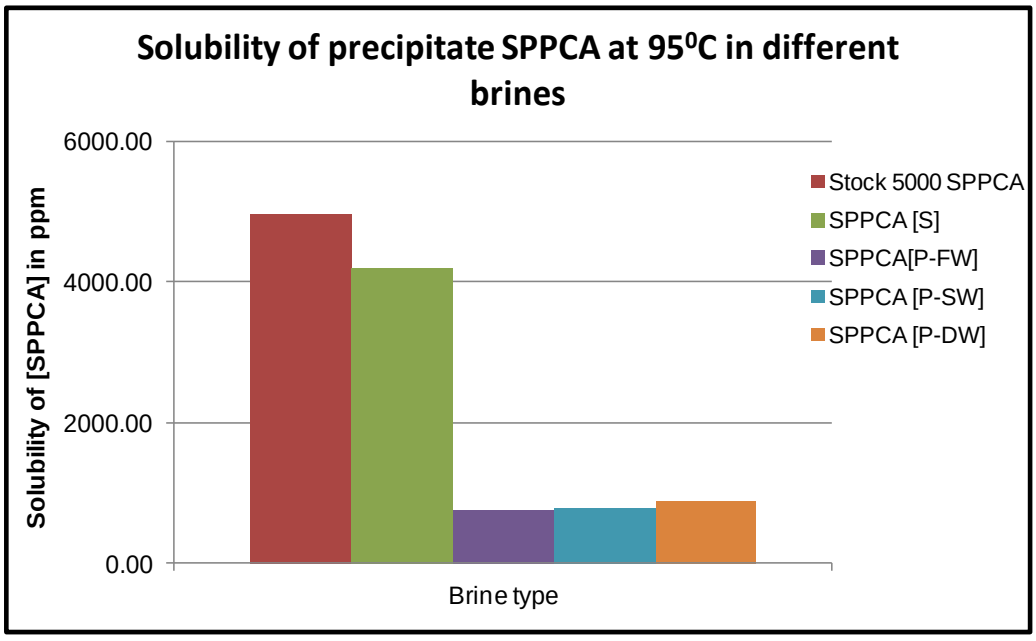

Figure 141. Solubility of precipitated SPPCA at 95^{o}C in different brines (FW, SW and DW)

Initially the concentration of [Ca^{2+}] in FW was 2000ppm; in SW the [Ca^{+2}] is 428ppm, and DW is calcium free. After the re-dissolution test, the final concentrations of [Ca^{2+}] by ICP are, in FW 2200ppm, in SW 650ppm and in DW ~240ppm. Thus, from ICP analysis, the results for calcium concentration are consistent in all the cases. The extra calcium appearing in the re-dissolution stage came from the SI_Ca precipitated

complex. Excess [Ca^{2+}] of about 200-250ppm appeared in all the brines and this is especially noticeable in DW since it was originally calcium free.

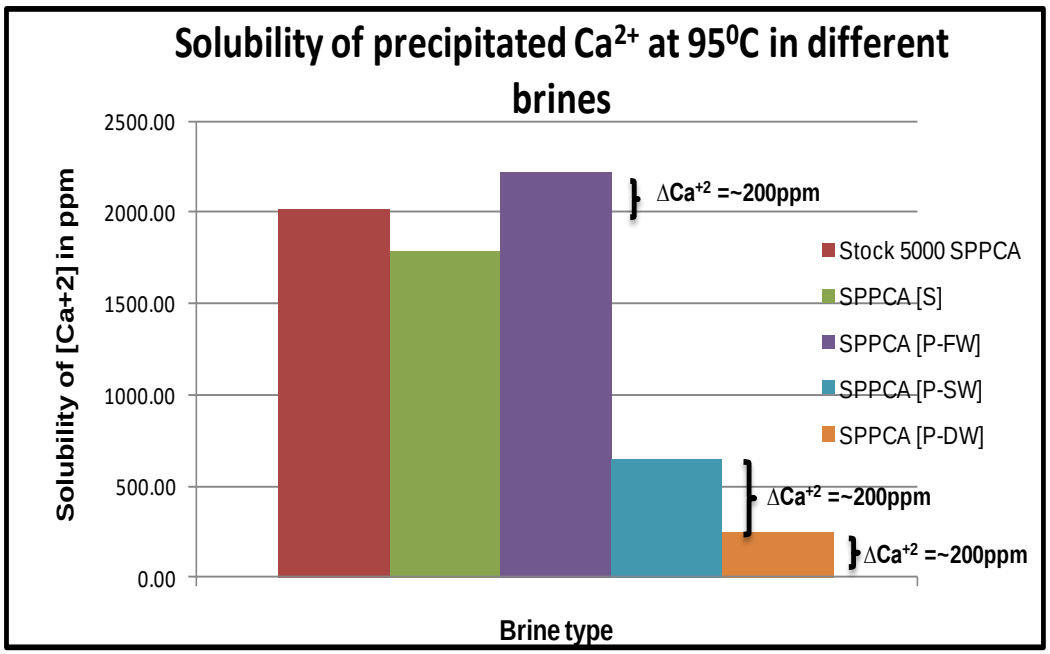

Figure 142. Solubility of precipitated [Ca^{2+}] from SPPCA_Ca complex at 95^{o}C in different brines (FW, SW and DW)

Like SPPCA, the compatibility/re-dissolution test was performed for the PFC scale inhibitor, but instead of 95^{o}C, the test was carried out at room temperature. After re-dissolving the precipitate in different brines (FW, SW and DW), each brine solution was adjusted to pH 2, so that all the precipitates were re-dissolved back into solution. The results for compatibility/re-dissolution test for the PFC are shown in Figure 143. The results for PFC are quite similar to the results for the SPPCA, except that the concentration of the re-dissolved precipitated PFC was (x2) higher than the concentration of the precipitated SPPCA. In Figure 143, it is clear that the concentration of the precipitated PFC in FW, SW is ~1600ppm and in DW ~1700ppm approximately. This behaviour is due to the adjustment of PFC to pH 2, making the precipitate more soluble in the brines.

The [Ca^{+2}] for each brine case was also monitored by ICP as shown in Figure 144. As in the SPPCA case, the additional calcium comes from the precipitated SI_Ca complex and is about 110ppm in each case for the PFC case.

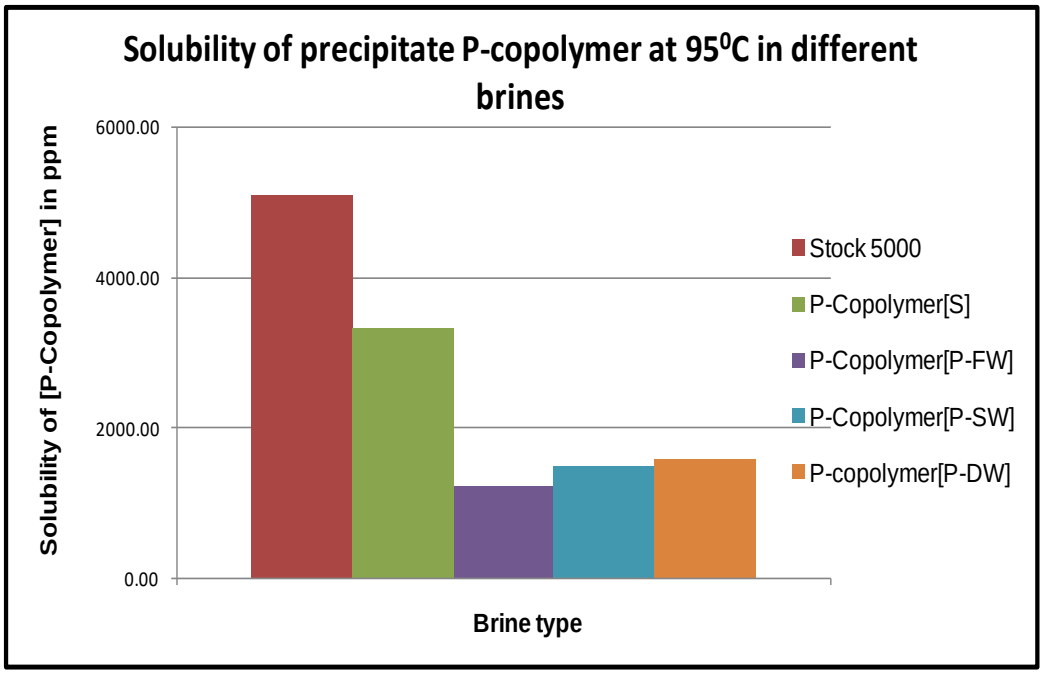

Figure 143. Re-dissolution of precipitated PFC at RT in different brines (FW, SW and DW)

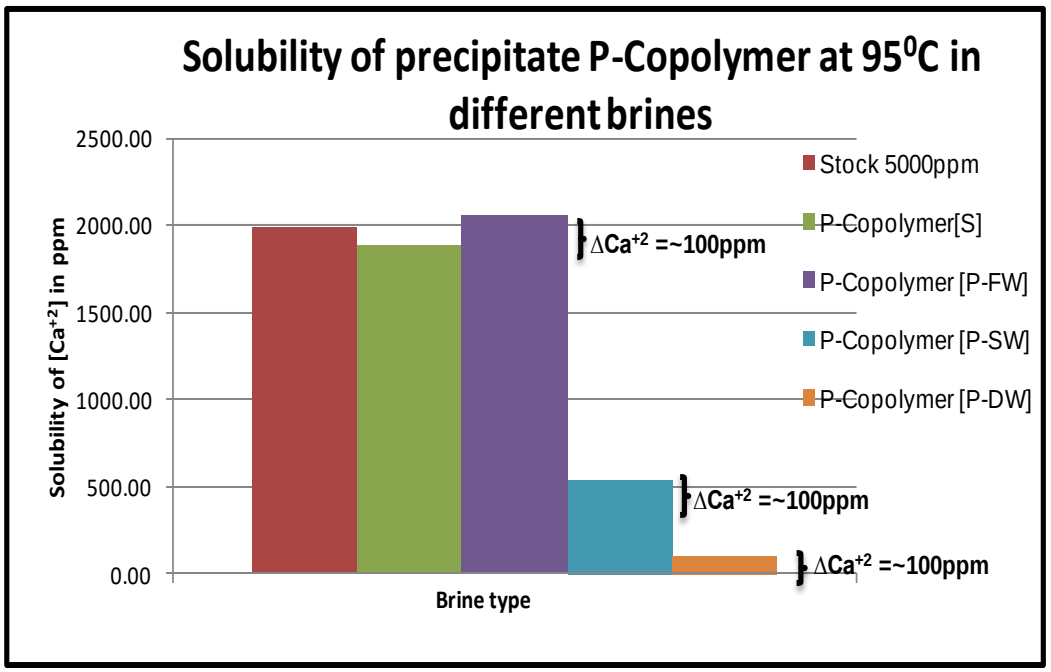

Figure 144. Re-dissolution of precipitated Ca from PFC_Ca complex at RT in different brines (FW, SW and DW)

8.3.3 Molecular Weight Distribution Results – SPPCA and PFC

The MWD results for SPPCA and PFC were obtained from GPC as Mw, Mn and PDI. The results for the two scale inhibitors were discussed on the PMAA based standards. All samples were prepared and submitted for analysis in duplicate, in order to obtain more consistent results (or at least to establish whether there was any sample to sample variation). The values of Mn, Mw and PDI for the SPPCA inhibitor samples are shown in Table 15 and they are very reproducible. In Figure 145, the lowest Mw material (3600g/mol) present in the supernatant of SPPCA as compared to the Mw of the precipitated SPPCA in each of the three brines viz., SPPCA-FW (7200g/mol), SPPCA-SW (8700g/mol) and SPPCA-DW (8700g/mol).

This confirms that during precipitation reaction in stage 1 the high Mw precipitates first, leaving behind the lower Mw material in the solution called supernatant. Thus, like PPCA, the SPPCA precipitate containing the high Mw material compared to the supernatant, which contains lower Mw material. The stock contains both, the high and the low MW species. This is clearly shown in the GPC chromatograms for all the SPPCA samples as shown in the Figure 145. These results for SPPCA are very similar to the results for PPCA.

Table 15. Average molecular weight (Mw), Number Average Molecular Weight (Mn) and Polydispersity (PDI) values of SPPCA based on PMAA standards

Code	Samples	M_n g/mol^{-1}	M_w g/mol^{-1}	PDI
1	Stock 10000ppm	1000	4700	4.63
2	Stock 10000ppm	1000	4600	4.72
3	Stock 5000ppm	1200	4200	3.57
4	Stock 5000ppm	1100	4600	4.13
5	SPN-FW	1000	3600	3.65
6	SPN-FW	1000	3600	3.62
7	SPPCA-Ca-FW	1600	7200	4.46
8	SPPCA-Ca-FW	1300	6900	5.83
9	SPPCA-Ca-SW	2300	8700	3.74
10	SPPCA-Ca-SW	2500	8400	3.30

11	SPPCA-Ca-DW	2200	8700	3.95
12	SPPCA-Ca-DW	2200	9000	4.19

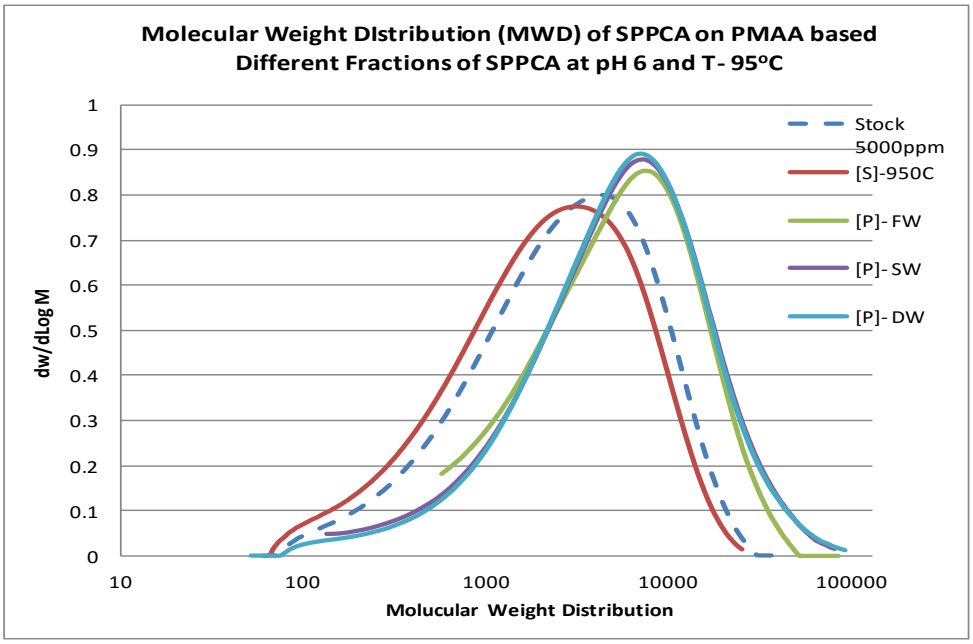

Figure 145. Comparison of the Mw of the stock SPPCA, supernatant and precipitate in FW, SW and DW

Similarly, the various fractions of PFC were obtained from the compatibility and the re-dissolution tests. To fully re-dissolve these samples, the pH of each brine was reduced to pH 2. The Mn, Mw and PDI results for each fraction of the PFC are shown in Table 16. Comparing the average Mw results of the stock samples of the two SIs, PFC and SPPCA, shows that the SPPCA inhibitor contains higher Mw material.

Various precipitates of PFC re-dissolved in different brines showed higher Mw than the supernatant. This result supports the earlier finding that the molecules with a higher molar mass precipitate more readily with Ca^{+2} to form a complex and molecules with low Mw remain dissolved in the solution. Therefore, again the supernatant is enriched with lower Mw material. The difference between the Mw of supernatant and precipitate compared to stock can be clearly seen in Figure 146 which presents the chromatograms of each PFC sample by GPC analysis. The average Mw of the supernatant (~2200g/mol) of PFC is similar to but a little below that of the stocks (~2500g/mol).

Table 16. Average Molecular Weight (Mw), Number Average Molecular Weight (Mn) and Polydispersity (PDI) values of PFC on PMAA standards

Code	Samples	M_n g/mol^{-1}	M_w g/mol^{-1}	PDI
1	Stock 10000ppm	340	2600	7.47
2	Stock 10000ppm	340	2600	7.48
3	Stock 5000ppm	400	2500	6.21
4	Stock 5000ppm	410	2500	5.98
5	SPN-FW	390	2200	5.79
6	SPN-FW	360	2100	5.97
7	PFC-FW	1300	6400	5.15
8	PFC-FW	1100	5200	4.19
9	PFC-SW	1200	5300	4.49
10	PFC-SW	1300	5600	4.22
11	PFC-DW	600	6200	9.94
12	PFC-DW	750	6100	8.06

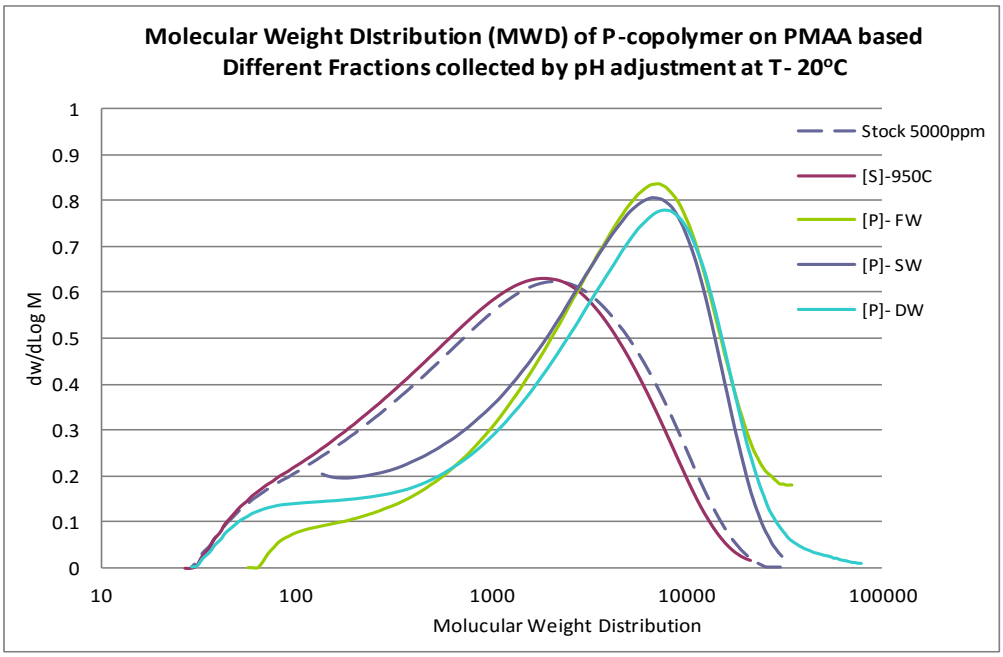

Figure 146. Comparison of the Mw of the stock PFC, supernatant, precipitate in FW, in SW and in DW

8.3.4 Inhibition Efficiency Results– SPPCA and PFC

As discussed previously, one of the aims in studying SPPCA and PFC molecular weights, polydispersity of stock solutions, supernatants and precipitates re-dissolved in different brines, was to help us to understand the performance of these solutions in inhibiting barite scales. After establishing the MWDs of all the various fractions of the SI, we now consider the consequences of these MWD results in terms of the IE for each fraction of both SPPCA and PFC.

Figure 147 shows the IE of SPPCA against barium sulphate scales. It shows that, like PPCA, the precipitated SPPCA is more efficient at inhibiting barite scale than the stock solution of SPPCA and the supernatant. We believe that this result is directly connected with the high Mw material (7200g/mol) present in the precipitated SPPCA. The precipitated SPPCA is efficient at inhibiting barite both in the short term (2 hours) and in the long term (22 hours). However, the supernatant contains more of the lower molar mass (Mw = 3600g/mol) molecules and therefore shows lower IE at all the concentrations tested. Figure 145 shows the chromatogram of the Mw of the stock solution, supernatant and precipitated SPPCA_Ca in FW. This figure clearly shows a displacement curve of precipitated SPPCA which contains a large number of molecules with a high Mw. This makes precipitated SPPCA more effective at inhibiting the barite scales. In addition, the precipitated SPPCA has a 10ppm MIC whereas the MIC for stock SPPCA is ~20ppm.

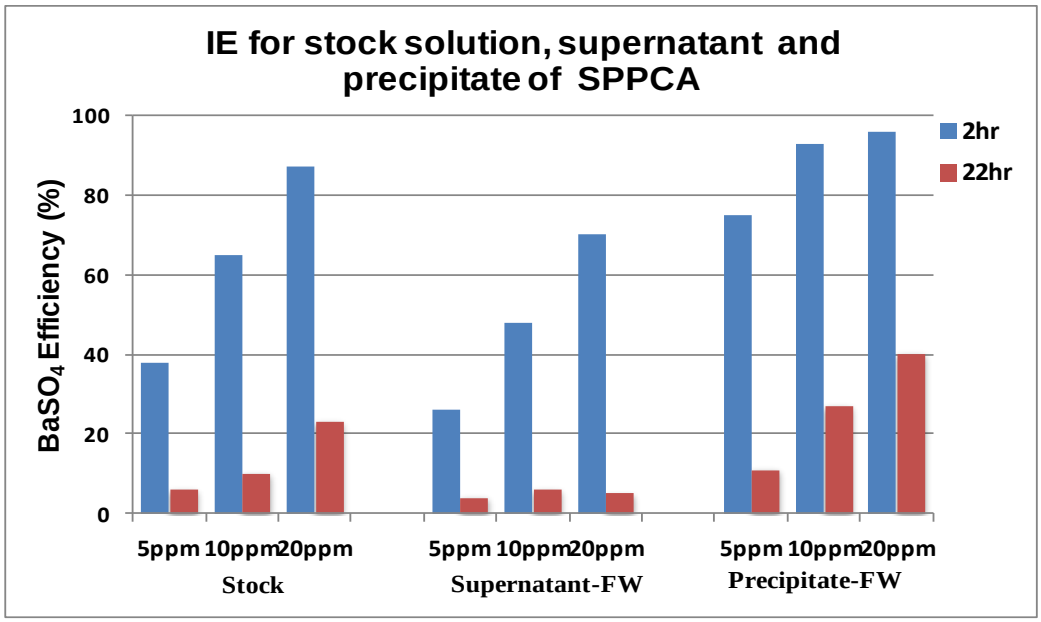

Figure 147. IE test of stock, supernatant and precipitate of SPPCA obtained from compatibility/re-dissolution tests performed at 95^{o}C.

The results for the IE of the PFC samples are presented in Figure 148. Since these results were contrary to expectation, the whole sequence of tests was repeated and the repeat results are presented in Figure 149. Results in Figure 148 and Figure 149 are almost identical, confirming that this result, although unexpected, is entirely repeatable, unlike PPCA and SPPCA, the IE performance of supernatant and precipitated PFC showed completely different behaviour. In this case, the supernatant is highly efficient in inhibiting barite scale, possibly a little better than *both* the stock solution and the precipitated PFC. However, the precipitated PFC shows a comparatively poor IE. An important observation here is that the IE performance at 22 hours shows that all the fractions showed similar IE.

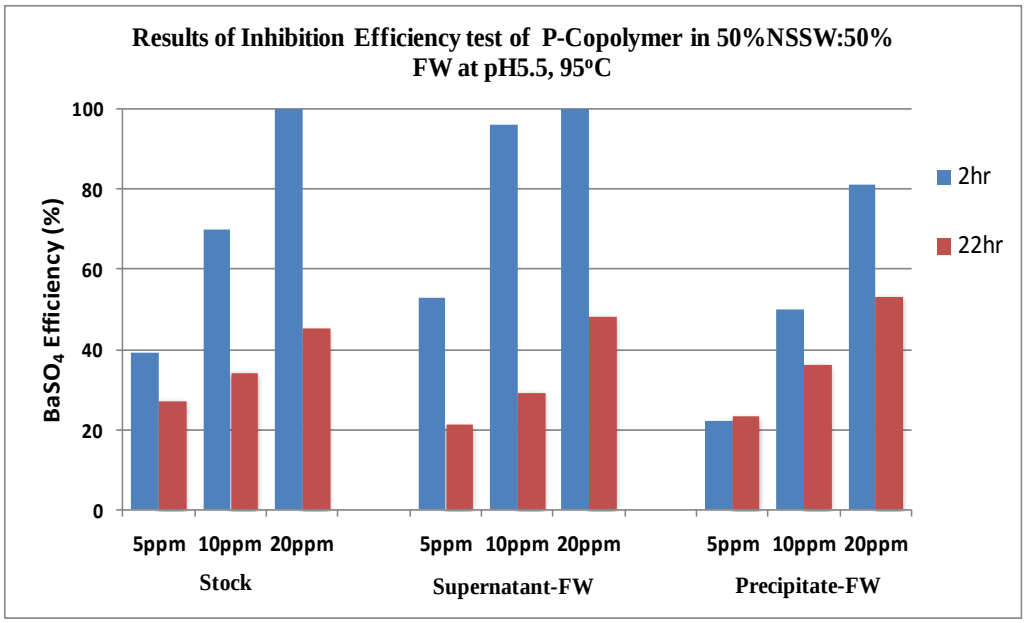

Figure 148. IE test of stock, supernatant and precipitate of PFC obtained from compatibility/re-dissolution test performed at 95°C

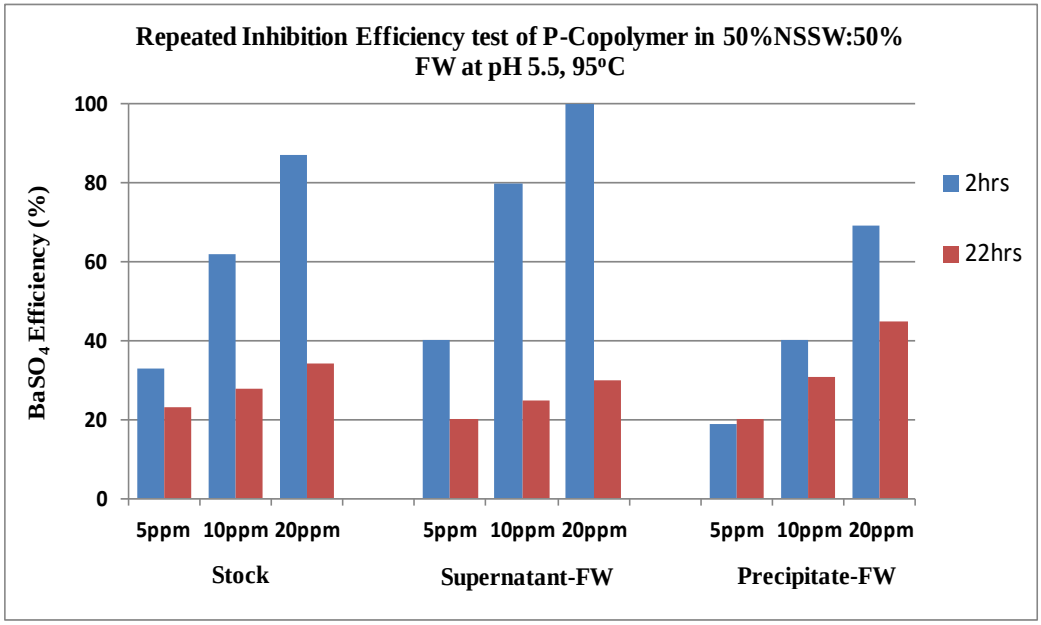

Figure 149. Repeat IE test results of PFC at 95°C

The above experiment was repeated twice in order to avoid any doubt about the results obtained. Referring back to the MWD chromatograms in Figure 146 indicates that, like the PPCA, the precipitated PFC clearly shows the presence of additional high Mw material (Mw ~ 6400g/mol). However, the Mw of the stock and the supernatant in Figure 146 are really quite similar. The stock has Mw ~ 2500g/mol and supernatant has Mw ~ 2200g/mol. Therefore, it appears that high Mw material in this case actually *suppresses* the barite IE in the precipitated PFC. A possible explanation for this rather

unexpected observation may be found in the paper by Graham and Sorbie (1994); two results from this paper are reproduced in Figure 150 below.

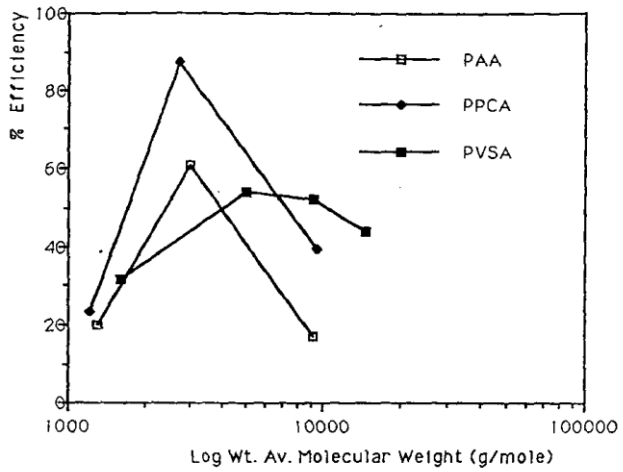

FIGURE 20 - Barium sulphate inhibition efficiency for molecular weight series of PAA, PPCA and PVS at pH 7.0 and T=70°C. Sampled at t=30minutes; effectively nucleation inhibition.

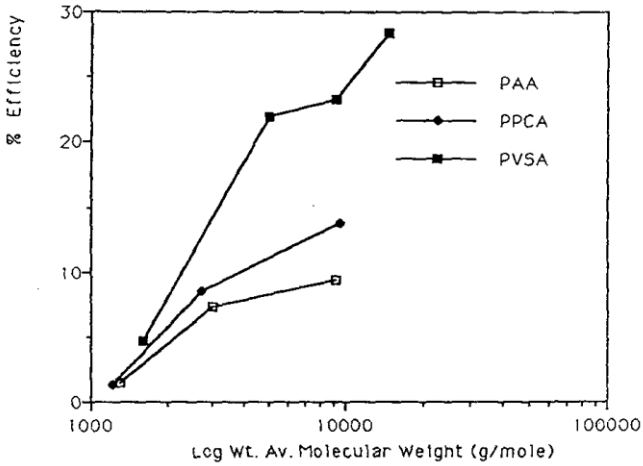

FIGURE 21 - Barium sulphate inhibition efficiency for molecular weight series of PAA, PPCA and PVS at pH 7.0 and T=70°C. Sampled at t=24hours; effectively self nucleated crystal growth retardation.

50/27

Figure 150. Barite IE of high Mw material of 3 polymeric scale inhibitors (PAA, PPCA, PVSA) showing performance at 1/2 hour for nucleation inhibition and at 24 hours for self nucleated crystal growth retardation (Source: Graham and Sorbie, 1994).

Graham and Sorbie (1994) studied the effect of Mw on the IE of some polymeric scale inhibitors. In particular, it was shown that the Mw of the various species had a

significant effect on the efficiency of a particular inhibitor, but that this effect was different for early time (nucleation) inhibition and later time (crystal growth) inhibition. Results in Figure 150 shows that for the early stages of inhibition, a low/medium MW polyelectrolyte gives maximum efficiency, and indeed as the polymer's MW increases with nucleation IE decreases. However, for longer residence times (crystal growth), successively increasing the MW leads to improved inhibition efficiencies i.e. better crystal growth retardation.

The IE results for the PFC presented above may be explained by the earlier findings of Graham and Sorbie (1994). That is, the IE of the precipitated PFC which is rich in very high Mw components is poor for the 2 hour test since this may still be in the nucleation inhibition regime and the very high Mw material is "above optimal" (see Graham and Sorbie, 1994). However, the IE's at 24 hours stay about the same (or little increase) because of the enhanced concentration of higher Mw species in the precipitate. However, more work is required in order to confirm (or refute) this conjectured mechanistic view of the PFC observed behaviour.

8.3.5 MWD Study by Methanol Separation- SPPCA and PPCA

All the polymeric MW work reported until now, the phase separation to obtain precipitated (higher Mw) polymer was carried out by using the actual "precipitation squeeze mechanism". By this we mean that the polymer was precipitated using the same chemistry as is used in a precipitation squeeze i.e. the formation of a sparingly soluble Ca_SI complex. However, the phase separation of a dilute polymer can be also achieved either by adding a poorer solvent to the solution or by changing the temperature or pH.

The alternative method we have used to study the phase separation of PPCA and SPPCA is by adding methanol (MeOH) to the polymeric solution. This process is also known as liquid-liquid extraction where the polymer initially is dissolved in one solvent and is extracted continuously from this solution by addition of another solvent which is fully or partially miscible with the first solvent (Young and Lovell, 2011).

Methodology for Methanol Separation:

In this experiment, the separation of supernatant and precipitated SI is achieved by the addition of methanol (MeOH) to the aqueous polymer solution. This type of experiment allows us to study the MWD of the pure precipitate obtained. Increasing amounts of methanol were added to the solution with 5000ppm of SPPCA and 2000ppm of [Ca^{+2}]. The precipitate obtained after filtration will be redissolved in different brines (FW, SW and DW). Methanol is added to the stock solution of SI in different *successive* amounts in order to vary the solubility parameter of the initial aqueous solution. Thus, is possible to obtain precipitates of pure polymeric SI with different MWs. This precipitate is different from the compatibility/precipitation test precipitate, which is formed at high temperature by complexation with calcium ions.

Experimental Procedure

In the experiment, we used 1L glass bottles containing 250ml of 5000ppm SPPCA solution in FW. Firstly, 20% of methanol (50ml) was added to the polymer solution and after one hour the precipitate obtained was separated by filtration using 5µm PTFE filter papers. The precipitate obtained from this first extract was then dissolved back in the three brines viz., FW, SW and DW using 250ml volumes of each brine., for each precipitate (refer to Figure 151). The supernatant obtained from this first filtration then had another 20% of methanol (50ml) added to it (i.e. to give a total concentration of methanol 40%) in a second extract. The second of the same polymer solution was extracted through filtration. This second precipitate obtained was again dissolved back into the 3 brines, for each precipitate (refer to Figure 151). The process was again repeated, for adding another 20% of methanol (50ml) (i.e. to give a total concentration of methanol 60%) in a third extract, and re-dissolves the precipitate back in the three brines. Thus, in this series of methanol precipitations three successive extracts (i.e. polymer precipitation stages at 20%, 40% and 60% methanol) were performed on the same original SPPCA aqueous solution.

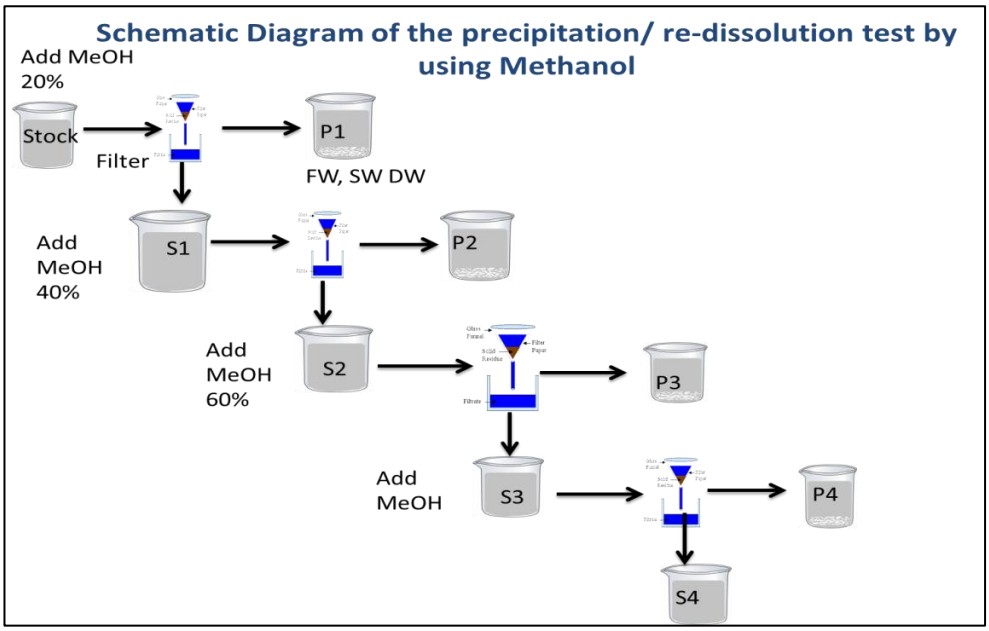

Figure 151. Schematic diagram of the solubility/re-dissolution test of SPPCA using methanol at RT and pH 6

The ICP results for the re-dissolution of the precipitate formed after the methanol separations or extractions are presented in Figure 152 and Figure 153. In Figure 152, the re-dissolution of the precipitated PPCA appears to be maximum (approximately 1800ppm) for the polymeric precipitate from the first 20% addition of methanol, the second addition to 40% methanol makes another ~1000ppm precipitate and the final 60% methanol makes a further ~500ppm precipitate. After the first precipitation, the concentration of the polymer in the supernatant left is ~3000ppm, which was successively precipitating on addition of methanol.

SPPCA is comparatively rather more soluble than PPCA because of the presence of the sulphonate groups along its backbone and the successive re-precipitation results for SPPCA are shown in Figure 153. The first addition of 20% methanol to the SPPCA, makes it precipitate by less than 300ppm (approx.). The addition of 40% methanol separates around 1200ppm of SPPCA, whereas the addition of 60% methanol separates out 600ppm (approx.) from the polymer solution. Comparatively, the concentration of the polymer in the supernatant, which is mostly the low MW material, stays very high after precipitation. This means, the first precipitation is the slice of highest Mw material, the second precipitation contains less higher Mw material and the third sliced contains lower Mw material, and so on.

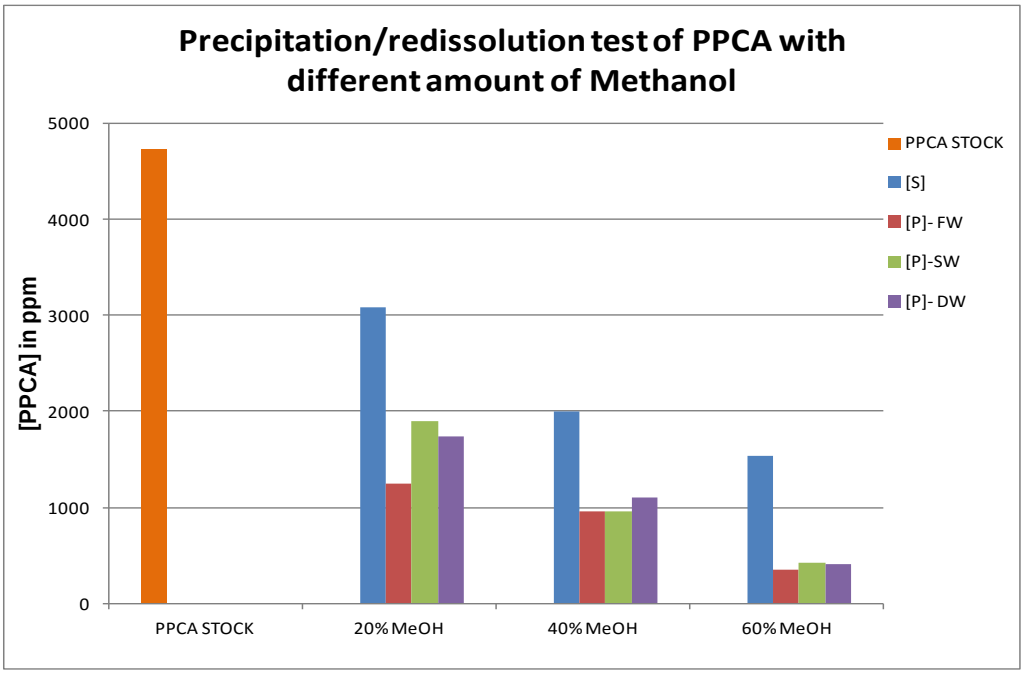

Figure 152: The final concentration of PPCA after the re-dissolution of the precipitate in different brine

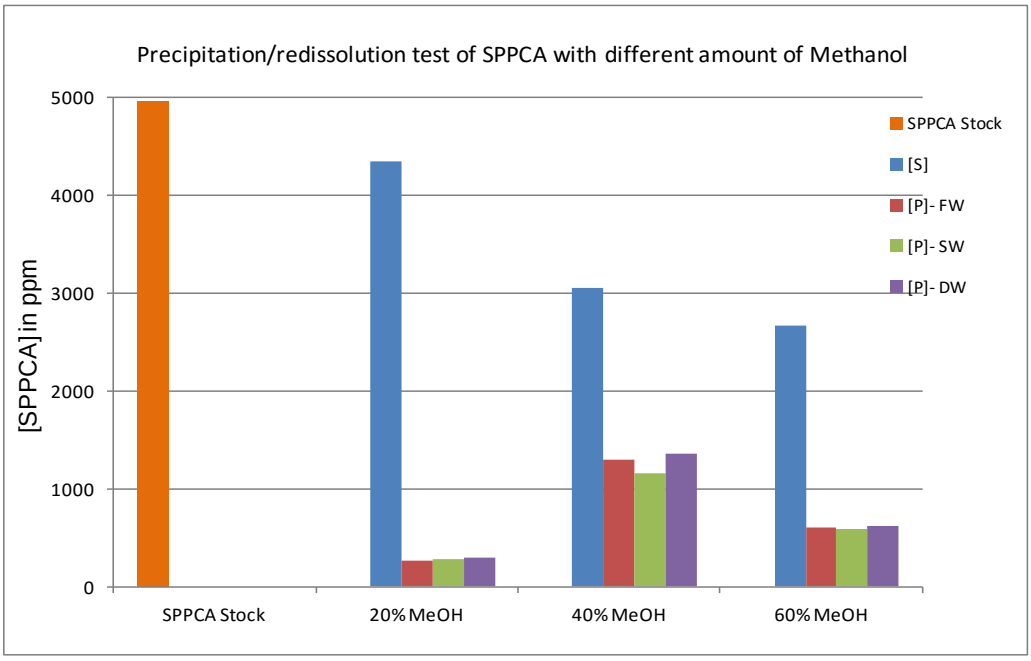

Figure 153. The final concentration of SPPCA after the re-dissolution of the precipitate in different brine

8.3.6 Molecular Weight Distribution Chromatograms by methanol method:

In both the cases (PPCA in Figure 154 and SPPCA in Figure 155), the stock solution MWD is clearly shown in two repeats (brown and blue overlain). The 20% methanol addition produced the very highest Mw material which is shown in the 3 GPC results on the right of the figure in FW (dark green), SW (orange/brown) and DW (light green). The 40% and 60% methanol additions then go on to precipitate lower and lower Mw SPPCA species.

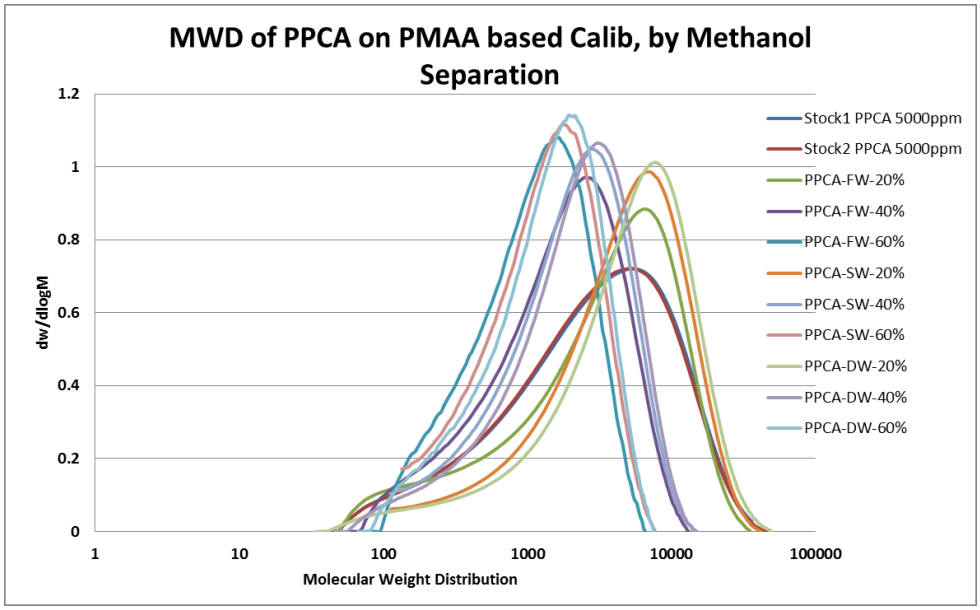

Figure 154. MWD of PPCA on PMAA standards by methanol separation.

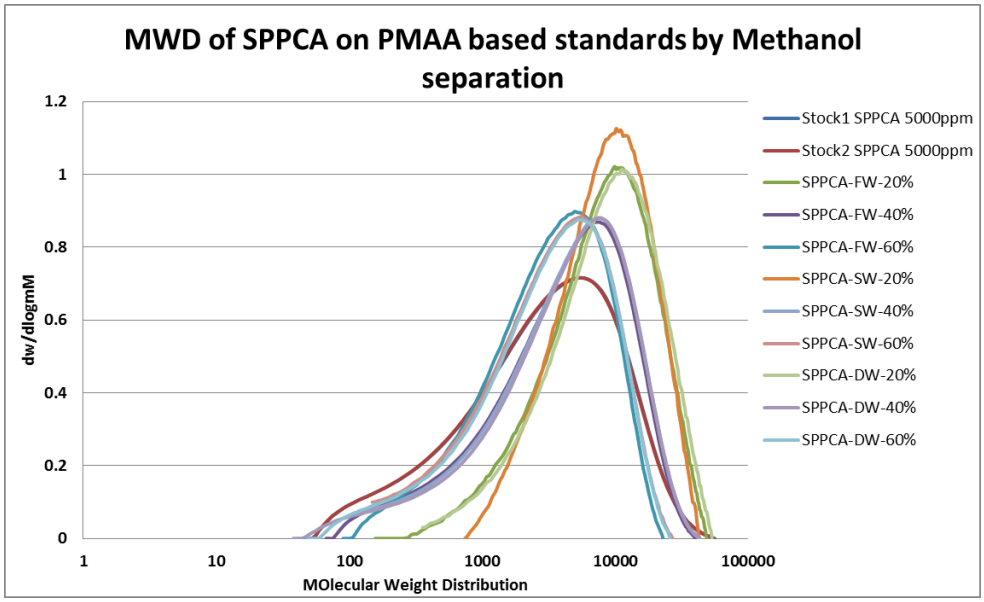

Figure 155. MWD of SPPCA on PMAA standards by methanol separation.

The above GPC chromatograms clearly show that the first addition of 20% methanol separates the highest Mw material of the scale inhibitor leaving behind the lower Mw material in a dispersed phase in a solution. The addition of another 20% methanol in the same solution (making 40% methanol in total) leads to the precipitation of a further amount of less higher Mw material from the solution. The even lower Mw material still left behind in solution at this point. The addition of another 20% methanol (making 60% methanol in total) helps to precipitate even lower Mw material, which is actually quite soluble in the original solution. Therefore, each addition of methanol precipitates lower and lower Mw material. The visual observation of the amount of precipitate formed by each addition of methanol is also shown below.

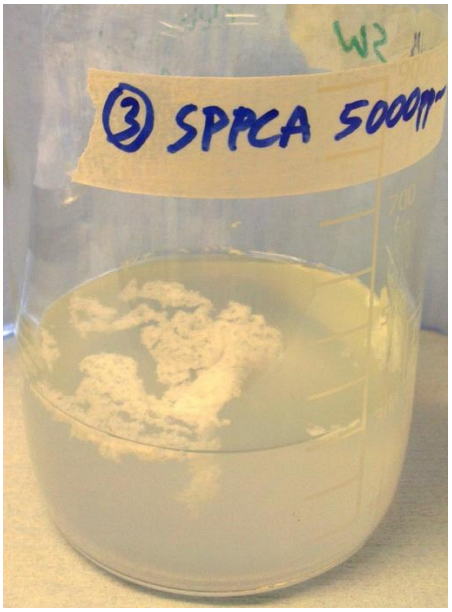

Figure 156: SPPCA_Ca complex precipitate formed by addition of 20% MeOH

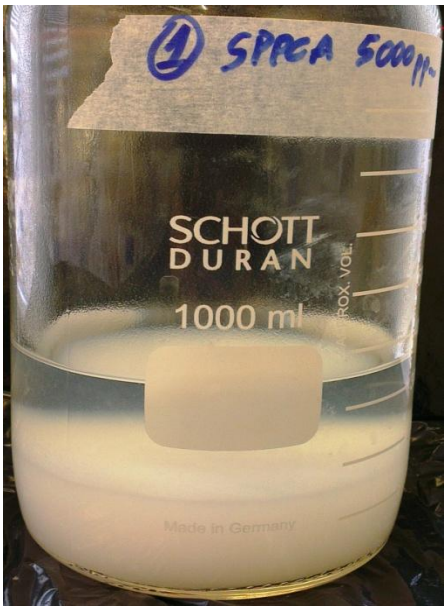

Figure 157: SPPCA_Ca complex precipitate formed by addition of 40% MeOH

Figure 158: SPPCA_Ca complex precipitate formed by addition of 60% MeOH

8.3.7 IE Results for the fractions obtained by Methanol Separation- SPPCA and PPCA

We now compare the polymeric precipitates by static IE tests for the two methods of formation; i.e. where the precipitate is formed at high temperatures by complexation with calcium ions or it is precipitated using methanol separation at room temperature. The common feature in both of these processes is that the precipitate formed first is significantly enriched in the higher Mw material.

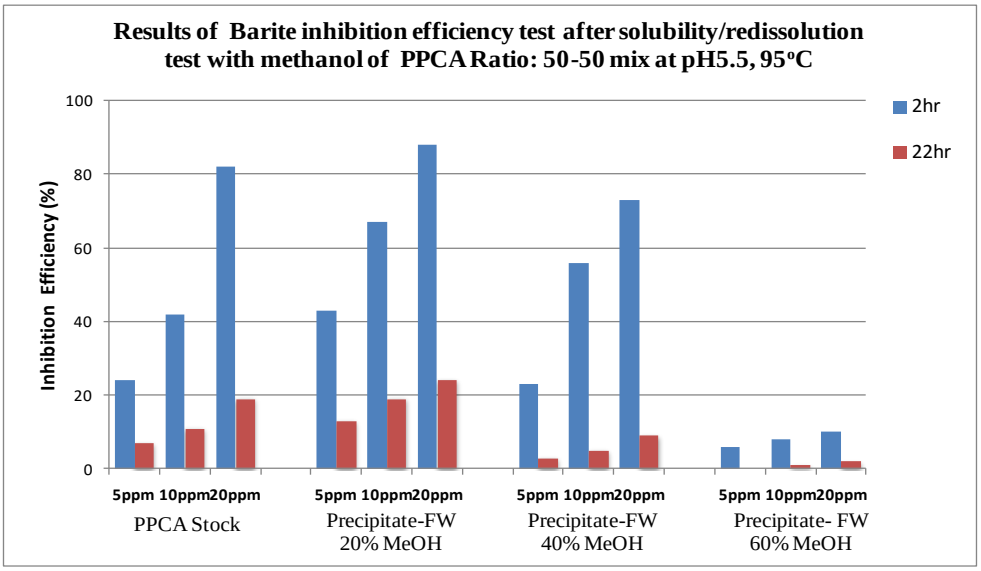

Figure 159: The IE of PPCA's stock, precipitate formed after the addition of 20%, 40% and 60% methanol (MeOH)

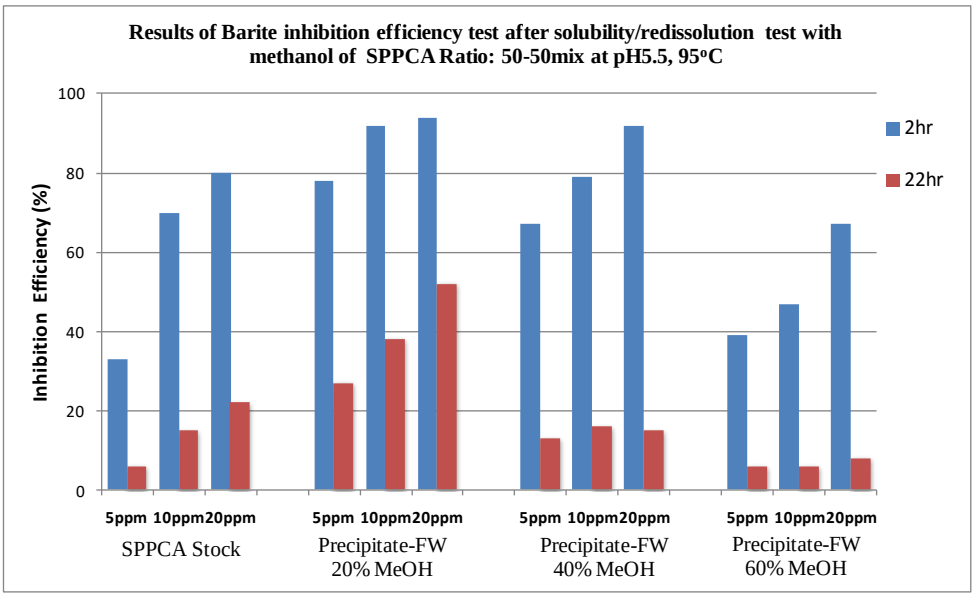

Figure 160: The IE of SPPCA's stock, precipitate formed after the addition of 20%, 40% and 60% methanol (MeOH)

These results were also confirmed using static IE tests for each polymeric precipitate formed by the addition of methanol. Figure 159 shows the IE of PPCA and Figure 160 shows the IE of SPPCA. For PPCA (Figure 159), most of the high Mw material drops out after the first addition of 20% methanol and this fraction shows the maximum efficiency in inhibiting barite scales. The later PPCA precipitation samples (for 40% and 60% methanol) successively dropped in level of IE. Very similar qualitative results are seen for the IE of successively methanol precipitated SPPCA samples; the first

precipitation with 20% methanol shows an MIC level of ~10ppm. In the successive methanol additions (40% and 60%) lower Mw material is gradually precipitated. However, this latter sample must still contain some slightly higher Mw material since the IE of these successive precipitates compared reasonably well to the stock SPPCA. This behaviour for the SPPCA can be broadly expected based on the GPC results for this SI in Figure 160.

8.4 Summary and Conclusions

1. ***General:*** From the results in this section, it is basically proved that the mechanisms (of polymer precipitation, dissolution, IE etc.) derived from our earlier detailed studies on PPCA also apply to the two additional polymeric scale inhibitors studied in this work, i.e. SPPCA and PFC. Our continued conjecture is that these mechanisms will apply to *all* polymeric scale inhibitors and future research should focus on confirming or refuting this view.

2. ***Stoichiometry of Ca_n_SPPCA*:** In the precipitating system, the molar losses of SPPCA (ΔSPPCA) and Ca (ΔCa) correlate extremely well at higher temperatures, e.g. 95°C. The slope of this correlation gives us the stoichiometry of the *Ca_n_SPPCA* complex; i.e. the value of n. It is found that the molar equivalents of Ca:SPPCA in the precipitated complex are in the ratio ~35:1; i.e. n ~35. This value is reasonably close to that for the normal PPCA (where n ~30) However, decreasing the temperature from 95 to 80°C, makes the ΔSPPCA vs. ΔCa correlation much weaker due to solubilisation of the complex and therefore the value of n is much harder to determine.

3. ***Compatibility of SI vs. pH and T*:** both the polymeric scale inhibitors SPPCA and PFC were tested for the compatibility over a range of pH values and temperatures (T). At 95°C, with 5000ppm SI and 2000ppm calcium in FW, the amounts of precipitate formed at pH 6 to pH 9 are very similar. Therefore, like PPCA, higher pH values of pH > 6, do not significantly further affect the precipitation of the SI. The precipitates for both polymeric SIs can be re-dissolved at low pH since this protonates the inhibitor, lowers the amount of Ca-binding that is possible and hence solubilises the precipitate. Like PPCA, more

precipitated calcium complex of both SPPCA and PFC appears at higher temperatures and this gradually solubilises as the temperature is lowered.

4. ***Solubility of Ca_SI precipitate in various brines (FW, SW, DW)*:** The solubility of the Ca/SI complex, originally precipitated from NFFW at 95^{o}C, with initial 5000ppm SI with 2000ppm [Ca^{2+}], has been measured in three brines, viz. FW, SW and DW. The solubility of the precipitated SPPCA at 95^{o}C is very similar in FW and SW (~780ppm) and a little higher in DW (~900ppm). The solubility trend of the precipitated PFC at 95^{o}C is very similar to that of the precipitated SPPCA, except that the concentration of the redissolved precipitated PFC is rather higher than that of the precipitated SPPCA. In FW and SW, the precipitated PFC solubilities were ~1600ppm and in DW the solubility was ~1700ppm. The [Ca^{2+}] was also measured in these solubility experiments in all brines (FW, SW, DW) and this was consistent with the re-dissolution of a Ca/SI complex.

5. ***MWD of Supernatant, Stock and Precipitate*:** The MWD results for the stock SPPCA polymer showed a wide range of MW species in this product, with M_w = 4200, M_n = 1200, PDI = (M_w/M_n = 3.56, and for PFC M_w=2500, M_n=400, and PDI=6.21. We emphasize that these MW figures are *not* accurate *absolute* numerical values but are based on polymeric PMAA standards through a calibration curve (possible error ~25 – 50%). However, they give us qualitatively correct *changes* in Mw and MWD which allows us to interpret the various processes, such as IE, dissolution, analytical results, precipitation etc., in our experiments.

6. ***Comparing MWD of Stock with Supernatant and Precipitate:*** Like PPCA, the MWD results for SPPCA and PFC clearly indicate that both of the precipitated SI/Ca complexes preferentially contain higher MW species leaving the supernatant depleted in high MW components. However, the GPC chromatograms actually shows that supernatant of both the SI, contain quite similar MW material with their respective stocks.

7. ***IE of the SI Fractions (Stock, Supernatant and Precipitate):*** The barite IE of both SIs (SPPCA and PFC) has been determined for stock solutions, precipitate

and supernatant samples. The supernatant sample for each polymer was taken from the first SI/Ca complex precipitation step (in S1) and also for the precipitated SI complex re-dissolved in 3 different brines, i.e. FW, SW and DW. Like PPCA, the supernatant of SPPCA shows very low IE and the precipitated material has a higher IE than the original stock SPPCA. This is explained by the fact that the supernatant is mainly made up of the lower MW components of the SPPCA and the precipitate contains mainly higher MW species. The general effect of this is that the IE of the polymer solubilised from the Ca_SPPCA precipitate is higher than that of the stock SPPCA. In a squeeze return, this effect would overall be quite beneficial since the IE increases (at a given ppm active concentration of SPPCA) in the longer tail of a return curve from a precipitation squeeze; for PPCA and SPPCA.

However, the corresponding IE results for the PFC are rather different to those for SPPCA and PPCA. Results in Figure 148 rather surprisingly show that the 2 hour IE results for the precipitated sample are *poorer* than those for both the supernatant and the stock. This result was unexpected and was immediately repeated and found to be exactly reproducible (see Figure 149). However, it was noted that the 22 hour IE results were quite similar for all samples (Stock, Supernatant and Precipitate). This may be due to the fact that the 2 hour IE relies significantly on nucleation inhibition and it has been shown that there is an optimum Mw size for this process, i.e. when polymers are too big, they are less good at nucleation inhibition (Graham and Sorbie, 1994). However, this conjecture should be confirmed or refuted by further experimental research.

8. ***MWD study by Methanol Separation Process***: As an alternative to precipitation by forming a Polymer/Ca complex (the conventional precipitation squeeze mechanism), we have also produced different MW fractions of the polymeric precipitates by making the brine a poorer solvent by adding methanol (or various other alcohols). The successive initial addition of 20% MeOH precipitated the highest MW material, the next 40% MeOH precipitated the next lower MW material and the further addition of 60% MeOH precipitated even lower MW material. These results were confirmed by measuring the GPC chromatograms (i.e. determining the MWDs) and from the IE test results. When this successive MeOH precipitation method is applied to PPCA and SPPCA completely

consistent results are found with those using conventional (Ca complex) precipitation. That is the first precipitate (highest Mw) has the best IE performance, the next fraction (next highest Mw) has the next best IE etc. This has not yet been applied to the PFC to see if its' behaviour differs in this respect, as found above.

CHAPTER 9- **CONCLUSIONS AND RECOMMENDATIONS**

In this final Chapter, the main findings are summarized without further detailed discussion, since this has already been presented in the previous chapters. A number of areas for future work are also suggested. A general introduction to the thesis, a literature review contexting the main topic of the thesis and a summary of the experimental techniques used are presented in Chapters 1, 2 and 3, respectively.

9.1 Conclusions

This study presents an extensive examination of the *phase separation* of PPCA, which is an industry standard polymeric scale inhibitor. It is widely applied in precipitation squeeze treatments in the field to prevent both carbonate and sulphate scales. The precipitation mechanism helps to improve the squeeze lifetime. The structure of the single phase and two phase (precipitate + supernatant) envelopes has first been reconstructed in agreement with previous work. We then describe several novel contributions to the study of the PPCA_Ca system under the headings below.

Phase Envelope of PPCA

In this chapter, the PPCA/brine Phase Envelope has been mapped out and characterised and it has been shown that a number of factors govern the phase behaviour of PPCA, such as [SI] and [Ca^{2+}], temperature and pH as well as the MW. In fact, these factors are interconnected and it has been shown that increased precipitation of PPCA has been observed with increase in temperature, pH, [SI] and [Ca^{2+}] (Farooqui and Sorbie, 2013). The stoichiometry of the PPCA_Ca complex has also been established and the molar equivalents of Ca:PPCA are in the ratio ~30:1. This is true in both the precipitation (T increasing) and dissolution (T decreasing) cycles which, although very similar, are not quite identical possibly due to kinetic factors. The precipitated and supernatant PPCA fractions have been analysed by both ICP (for P) and Hyamine (for polymeric content)

and for their IE against barite scale. The observations indicate that the PPCA "precipitate" is rich in the higher MW polymer components and the supernatant is corresponding depleted of these components. In the earlier stages of the study, the explanation of the various properties of the PPCA_Ca precipitate and supernatant was thought to be due to MW effects, but later experimental measurements (Chapter 6) confirmed this.

Solubility of the PPCA_Ca Precipitate Complex

A detailed study of the solubility of the PPCA_Ca complex was presented in this chapter. It was shown that the solubility of the precipitated PPCA_Ca complex becomes lower as it is exposed to successive fresh supernatant brine. This solubility behaviour is very unlike that expected from a "solubility product" model. The reason for this is again related to the MWs of the various components of the PPCA. These results clearly point to a "stripping" model of polymer/Ca complex dissolution where the lower MW species are preferentially dissolved into the supernatant brine until some equilibrium is reached. As a consequence of this mechanism, the original precipitate became enriched in (less soluble) higher MW species (Farooqui et al., 2015).

Molecular Weight Distribution of PPCA

By working with colleagues at the University of Warwick, we were able to measure the MWD of the stock solution and various fractions (precipitate and supernatant) of the PPCA system. The MWD results are presented in this chapter and they have given us some very significant insights into the precipitation/dissolution mechanisms which are occurring in polymer precipitation squeeze processes. The MWD results clearly indicate that the precipitated PPCA_Ca complex preferentially contains higher MW species leaving the supernatant depleted in high MW components. The supernatant shows very low IE and the precipitated material has a higher IE than the original stock PPCA. Hence, the low IE and the low polymer content (by Hyamine) are as expected (Farooqui et al., 2014).

The detailed MWD of the precipitate is affected by changing the precipitation temperature. At higher temperature, more higher MW material is entrained in the precipitated PPCA_Ca complex. The corollary is that, at lower precipitation temperatures, more higher MW material is entrained into the supernatant. Thus, poorer

IE of supernatant and better IE of the precipitate is seen for all experiments; but, these IE results become closer precipitation temperature is lowered. That is, the IE result for the supernatant improves and the precipitate decreases at lower precipitation temperatures (Farooqui and Sorbie, 2014).

Dynamic Sand-pack Precipitation Flood of PPCA

It is a logical extension of the PPCA/brine phase behavior results to carry out corresponding PPCA precipitation sand pack floods where this phase behavior is well established. The precipitation regions in the dynamic sand pack floods agree well with the static phase behavior of PPCA. In addition, the core flood [SI] vs. PV effluent results show good qualitative agreement with the associated theory which has been developed in FAST. For example, the range of characteristic behaviour observed in the shut-in periods was as expected from theory. That is, following a shut-in, the effluent concentration rose quite sharply and then subsequently fell off in the following post flush period. The initial rise in [SI] was due to the system coming closer to precipitation equilibrium when the flow stopped.

In the later post flushes, the return profile at slower rates gave an effluent inhibitor concentration which was higher since we are closer to dissolution equilibrium, and this non-equilibrium behaviour is as expected. All of the observed features in these floods were in good accord with the precipitation retention mechanism.

Other Polymeric Scale Inhibitors

The vast majority of the work presented in this thesis is on the polymeric scale inhibitor, PPCA. However, 2 other polymeric scale inhibitors SPPCA and PFC were also studied in a more limited way. These examples were examined to determine if they also exhibited the same mechanisms of polymer precipitation, dissolution, IE etc. established for the earlier detailed studies of PPCA. The conjecture was that these mechanisms will apply to all polymeric scale inhibitors.

Like PPCA, the MWD results for SPPCA and PFC clearly indicate that both of the precipitated SI_Ca complexes preferentially contain higher MW species leaving the supernatant depleted in high MW components. This explains the barite IE result which

shows a very similar effect for both PPCA and SPPCA. The supernatant of SPPCA shows very low IE and the precipitated material has a higher IE than the original stock SPPCA. In a squeeze return, this effect would overall be quite beneficial since the IE increases (at a given ppm active concentration of SPPCA) in the longer tail of a return curve from a precipitation squeeze; for PPCA and SPPCA (Farooqui et al., 2014, 2015).

However, the corresponding IE results for the PFC are rather different to those for SPPCA and PPCA. Surprisingly, our studies showed that the 2 hour IE results for the precipitated sample are *poorer* than those for both the supernatant and the stock. However, it was noted that the 22 hour IE results were quite similar for all samples (stock, supernatant and precipitate). This may be due to the fact that the 2 hour IE relies significantly on nucleation inhibition and it has been shown that there is an optimum Mw size for this process, i.e. when polymers are too big, they are less good at nucleation inhibition (Graham and Sorbie, 1994). However, further work is required on the PFC inhibitor in order to fully explain our preliminary findings.

Field Application and Significance of Results

All of the main conclusions on PPCA summarized in this final chapter on phase separation, IE, SI assay (by ICP and Hyamine) will clearly have an effect on field applications of these polymeric scale inhibitors. For example, the fact that the precipitated PPCA_Ca complex is greatly enriched in higher MW PPCA species will lead to an improved performance relative to that expected from an ICP concentration level as based on the Stock PPCA solution. The work presented in this thesis explains and confirms our hypotheses by directly measuring the MWDs of all the PPCA fractions (stock, precipitate and supernatant).

The results from this work on polymer adsorption/precipitation processes are also being used to test out recent models of coupled adsorption/precipitation and IE. In the work presented here, we have focused on the solubility of the PPCA_Ca complex which would appear in a precipitation squeeze. The initial observations on the solubility of this species appeared to be quite counter intuitive and were not anticipated. However, by being able to carry out MWD experiments on the various PPCA species which appeared in the process, a fairly complete understanding is being generated. This led to our proposal of the "stripping" model of dissolution described above and discussed further elsewhere (Farooqui and Sorbie, 2014). Once a mathematical description of this

model has been developed, it will be incorporated into future field squeeze design model for adsorption/precipitation (Γ/Π) processes for polymers.

9.2 Recommendations for Future Work

Although precipitation squeeze treatments for polymeric scale inhibitors have been the main focus of this work, there is still a need to explore issues which require further research. Some of these are listed below, as follows:

1. The empirical mathematical model following below is in the development stage by using the produced data of this research work.

Mathematical Model of MWD: For our later purposes, related to how we may be able to model the PPCA (and other polymeric) precipitation processes, we have examined some analytical matches to this stock PPCA MWD. After some study, an analytical match, G (M), to the MWD shown in Figure 161 was found which has the following mathematical form:

$$G(M) = \zeta\left(1+\alpha_1.M+\alpha_2.M^2\right).\left(M-M_{\min}\right).\left(M_{\max}-M\right).Exp\left(-\alpha_3\left[\frac{M-\overline{M}}{\alpha_4}\right]^{\alpha_5}\right) \qquad (4)$$

Where the parameters, $\alpha_1 - \alpha_5$ are fitting constants, $M_{\min}$ and $M_{\max}$ are the minimum and maximum MWs (where, $G(M_{\min}) = G(M_{\max}) = 0$) and ζ is a normalisation factor. Note that Figure 161 (a) and (b) show the MW axis being plotted as either log M or as linear in M, respectively.

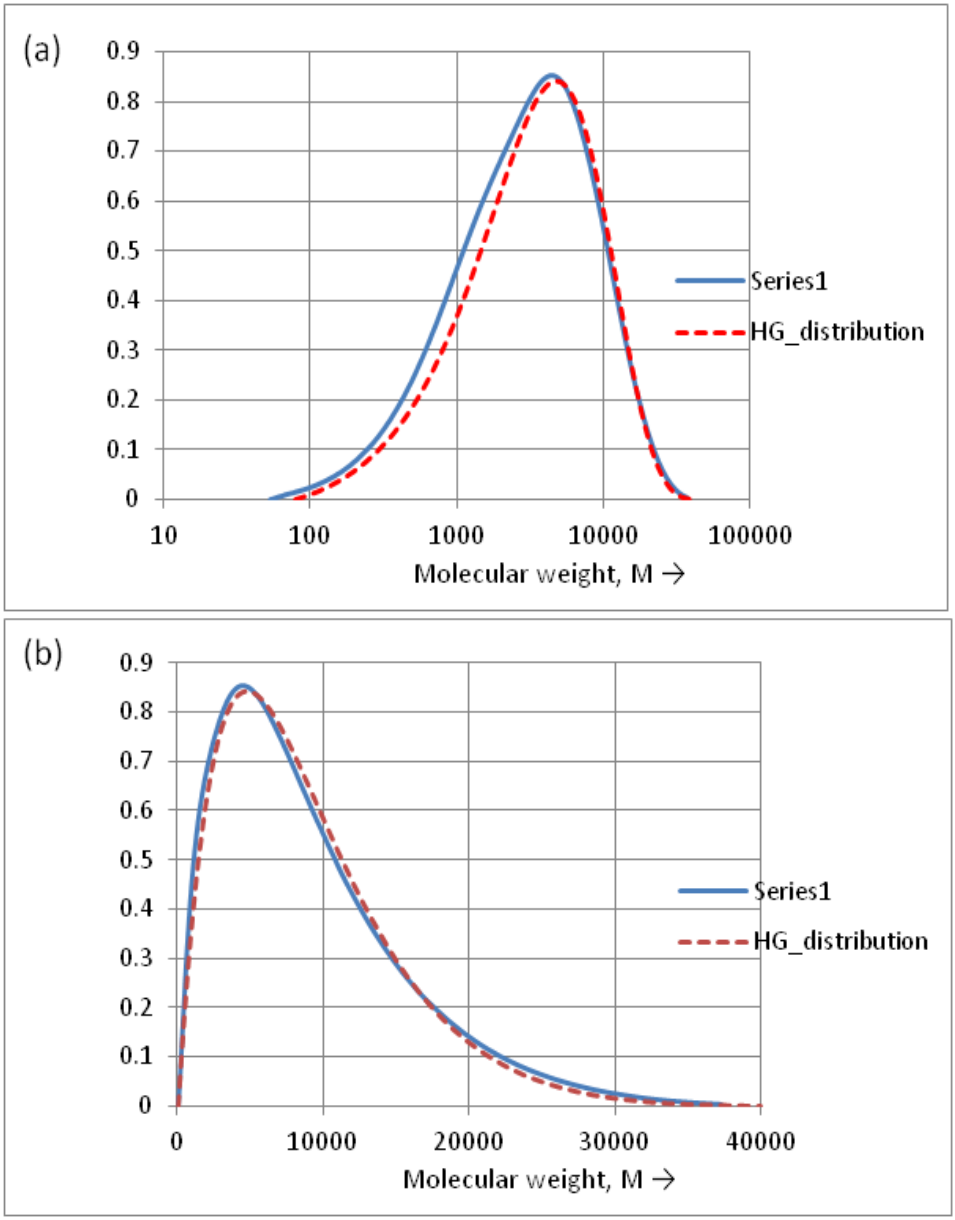

Figure 161: Mathematical matches to the MWD of the stock PPCA solution (Sample 1) where the fit is the dashed line and experiment is the solid line. The M axis is plotted as being (a) log M and (b) as linear in M. The form of the mathematical function, G (M), is given in the text.

2. The study of PPCA should be extended to other polymers like VinylSulphonate Acrylic Acid Co-Polymer (VS-CO), PolyVinylSulphonate (PVS), Maleic Acid Ter (MAT)-Polymer, etc. to develop a better understanding of the behaviour of all polymeric scale inhibitors. This will also confirm (or refute) our conjecture in this work that all polymeric scale inhibitors behave in a similar manner.

3. The effects of cations (Ca^{2+} and Mg^{2+}) on inhibition performance of PPCA should be studied in details and this should also be done for other polymeric scale inhibitors in dynamic precipitation pack flood studies.

4. In addition to chemical composition, the behaviour of particulate materials is often dominated by the physical properties of the constituent particles. These can influence a wide range of material properties including, for example, reaction and dissolution rates, rate of complexation or how easily molecules can flow. Some of the most important physical properties to measure are:

- particle size
- particle shape
- surface properties
- mechanical properties
- charge properties
- microstructure.

Depending upon the material of interest, some or all of these could be important and they may even be interrelated: e.g. surface area and particle size.

5. It is recommended to examine the effect of Mg^{2+} in sand-pack studies: To some extent, Mg^{2+} seems to participate in the reaction at high temperatures in the sand pack flood studies (although this may be "entrainment" rather than actual chemical reaction). It is worth examining the role of Mg^{2+} ion in the reaction to establish if it is actually participating in the complexation of Ca and PPCA or is simply "entrained" in the PPCA_Ca precipitated complex.

6. MS vs. GPC analytical studies: The GPC analytical technique was used in this research to understand the polymer performance. It was used to characterise the complete MWD of the PPCA polymer. To extend this work, it is worth examining the characteristics of the individual molecules by mass spectroscopy (MS), which converts them to ions, which are then manipulated by external electric and magnetic fields. This would provide good complementary (to GPC) molecular information on the PPCA_Ca precipitate.

A better understanding of the mechanism of scale inhibition and the chemistry of polymeric scale inhibitors will greatly help in the development of new inhibitors, as well as in the formulation of models for the prediction of

precipitation squeeze lifetimes. It is envisaged that scale inhibitors of the future will be tailor-made depending upon the application, their environmental safety and ease of biodegradation. Indeed, on their biodegradation properties, they may be designed to "self-destruct" at the end of their use cycle.

APPENDIX A: GENERAL EQUIPMENT AND APPARATUS

I. Solution Preparations and Experimental Procedures

II. Inductively Coupled Plasma - Optical Emission Spectroscopy (ICP-OES)

III. Environmental Scanning Electron Microscopy - Energy Dispersive X-Ray (ESEM-EDX)

IV. Ultra Violet Spectrophotometer (UV)

I. General Solution Preparation and Experimental Procedures

1. Brine Preparation

Composition of Nelson Forties Formation Water (NFFW):

Table 17: Composition of Nelson Forties Formation Water (NFFW)

Ion	Concentration {ppm (mg / L)}	Formula Composition	g / L	g / 5L	g / 10L	g / 15L	g / 20L
Na^{+}	31275	NaCl	79.50	397.50	795.00	1192.50	1590.01
Ca^{2+}	2000	CaCl2.6H20	10.93	54.66	109.32	163.98	218.64
Mg^{2+}	739	MgCl2.6H20	6.18	30.90	61.80	92.69	123.59
K^{+}	654	KCl	1.25	6.23	12.47	18.70	24.94
Ba^{2+}	269	BaCl2	0.48	2.39	4.78	7.18	9.57
Sr^{2+}	771	SrCl2	2.35	11.73	23.46	35.19	46.92
SO_4^{2-}	0	Na2SO4	0.00	0.00	0.00	0.00	0
Li^{+}	50	LiCl	0.3055	1.5275	3.055	4.5825	6.11
Actual Cl^{-}	55534						

NB : 50ppm of Li^{+} has been added as a tracer in the NFFW.

Notes:

1. Lithium is used as an inert tracer in the brine. This is to check for evaporation (if any) during heating which would affect the concentration of the elements present in the solution. As an inert tracer, Lithium does not take part in the reaction nether it adsorbs onto any rock mineralogy.
2. All prepared brines are filtered using 0.45μm Whatman filter paper. This is to remove any dirt or other impurities during filtration.
3. No degassing is required.
4. Brine is prepared couple of days before the experiment starts.

Composition of North Sea Sea Water (NSSW):

Table 18: Composition of NSSW

Ion	ppm	Formula Composition	g/l	g/5L	g/10L	g/15L	g/20L
Na^{+}	10890	NaCl	24.08	120.40	240.80	361.21	481.61
Ca^{2+}	428	CaCl2.6H20	2.34	11.70	23.40	35.09	46.79
Mg^{2+}	1368	MgCl2.6H20	11.44	57.20	114.4	171.59	228.79
K^{+}	460	KCl	0.877	4.385	8.77	13.16	17.54
Ba^{2+}	0	BaCl2.2H20	0.00	0.00	0.00	0.00	0.00

Sr^{2+}	0	SrCl2.6H20	0.00	0.00	0.00	0.00	0.00
SO_4^{2-}	2960	Na2SO4	4.38	21.88	43.8	65.63	87.51
Actual Cl^-	19773						

**Note: NSSW is only used in the Inhibitor Efficiency Tests.

2. Preparation for ICP Standards:

The diluent / matrix used, is 1% Na as NaCl. 250ml of each standard will be prepared.

Table 19: Concentrations of each ICP standard

Standard Number	Constituent(s)	Concentration(s)	Dilution Requirements, in 1% Na as in NaCl, using a 250ml Volumetric flask
Low	1%Na as NaCl		N / A
1	PPCA	5ppmact	25ml of Standard 3
2	PPCA	10ppmact	50ml of Standard 3
3	PPCA	50ppmact	25ml of Standard 4
4	PPCA	500ppmact	50ml of Standard 5
5	PPCA	2500ppmact	1.49g of Bellasol S40 (PPCA)
6*	Ca^{2+}, Mg^{2+}, Li^+	50ppm Ca^{2+}, 25ppm Mg^{2+}, 5ppm Li^+	12.5ml of 1000ppm Std Ca^{2+}, 6.25ml of 1000 ppm Std Mg^{2+}, 1.25ml of 1000ppm Std Li^+
7*	Ca^{2+}, Mg^{2+}, Li^+	200ppm Ca^{2+}, 100ppm Mg^{2+}, 20ppm Li^+	50ml of 1000ppm Std Ca2+, 25ml of 1000ppm Std Mg^{2+}, 5ml of 1000ppm Std Li^+

Therefore to prepare 250ml of 2,500ppm active Bellasol S40, (5.95/4)g = 1.49g is required.

3. Preparation for 1% Na as in NaCl Diluent Solution

This diluent is used for all the coupled adsorption precipitation test, compatibility/re-dissolution, solubility experiments except for IE tests. Diluent Solution is used to dilute samples taken for ICP analysis. For all the ICP samples, 1% Na^+ as NaCl is used as a diluents solution because this brine contains the highest amount of Na^+ (~31000ppm) compared to other cations in the brine. However, 1% Na^+ as NaCl would provide the closest matrix match when analysed using ICP. For all the analysis in these experiments, the samples were diluted 10 times so that they would match the calibrated standards.

1% Na^+ (aq) ≡ 1gm in 100ml = 10gm in 1000ml = 10,000mg in 1L = 10,000ppm

Na^+ (aq) ≡ 25.42g of NaCl (s) / 1L H_2O (l) ≡ 127.10g of NaCl (s) / 5L H2O (l)

Dissolve 127.10g of NaCl (s) in 5L of distilled water. Use a 5L Volumetric Flask.

Preparation for Glassware and Apparatus:

a. Apparatus: Fan assisted oven or water-bath, balance and 1000ml, 250ml and 150ml plastic bottles.
b. For pH measurement: pH meter, pH 7and pH 4buffer solutions for calibration.
c. For Scale Inhibitor Dilutions: 5L volumetric flask, 5L plastic container, 1L beaker and funnel.
d. For filtration: filtering equipment's like vacuum pump, conical flasks and tubing and filter papers (0.45μm) and (0.20)
e. For ICP preparation: 250ml volumetric flasks, 10ml and 2.5ml variable and 1ml variable pipettes.

List of Inventories with Suppliers Name:

a. Brine: chemical compound, supplier and grade

CHEMICAL	SUPPLIER	GRADE
Sodium chloride	VWR	Analar
Calcium chloride 6-hydrate	VWR	Analar
Magnesium chloride 6-hydrate	VWR	Analar
Potassium chloride	VWR	Analar
Barium chloride 2-hydrate	VWR	Analar
Strontium chloride 6-hydrate	VWR	Analar
Sodium Sulphate	VWR	Analar

b. Standards: chemical compound, supplier and grade

Calcium 1000ppm Standard	VWR	Spectrosol
Magnesium 1000ppm Standard	VWR	Spectrosol
Lithium 1000ppm Standard	Merck	Spectrosol

c. Mineral: chemical compound, supplier and grade

Sand	VWR	Analar

d. pH adjustment: chemical compound, supplier and grade

HCl	VWR	Analar
NaOH	VWR	Analar

4. Experimental Procedures for Compatibility/ Precipitation test

Experimental Procedure for Coupled Adsorption Precipitation Test:

1. Filter the FW brine through 0.45um filter paper. About 4500 ml will be required for this experiment. This includes 500ml to prepare the 10,000ppm stock solution of PPCA.
2. Prepare a 10,000ppm SI stock solution in the test brine used.
3. Use this stock solution to prepare the serial concentrations of [SI] for the adsorption/precipitation test in the test brine
4. Weigh appropriate amount (10g, 20g and 30g) of Sand into 150ml plastic bottles for adsorption test and no sand for precipitation test.
5. PH adjust to all stock solution (blank & SI/FW samples) to the required value of pH 6. Record the pH values, before and after adjusted – pHo @ 20^{o}C.
6. Measure out the required volume of each stock solution into the appropriate 150ml plastic bottles in duplicate.
7. Transfer into oven at 95^{o}C immediately. Note the time the samples are put in the oven – To
8. After approximately 1 hour, check the bottle lids are tight, to avoid any evaporation.
9. Weigh the filter paper of 0.2 μm pore size filter for filtration for precipitation test.
10. After 24 hours (t = 24), filter the samples under vacuum through the weighed filter paper. Filtration is carried out at the specific temperature of interest in that experiment. For example, samples from these 95˚C experiments are filtered immediately after they are taken out of the oven. Transfer the filtrate into labelled / numbered 150ml plastic bottles.
11. Leave the precipitation test filter paper to dry overnight. Weigh it again and check the difference in the weights and send it for ESEM/EDAX analysis.
12. Measure the pH of the filtrate samples and record the values – pHf @ 20^{o}C
13. If necessary, prepare some diluent solution (see above section).

14. Prior to ICP Analysis, dilute ALL samples in 9ml of 1% Na^+ (aq.) diluent solution. Use 10ml test tubes. The initial stock solutions retained earlier are diluted – to confirm C_o values (initial concentrations), and the filtrate samples are diluted in the same way, to find C_f values (final concentrations after the adsorption process).
15. ALL stocks and samples are analysed by ICP to confirm C_o values, i.e. $[SI]_o$, $[Ca^{2+}]_o$, $[Mg^{2+}]_o$, $[Li^+]_o$ and find C_f values, i.e. $[SI]_f$, $[Ca^{2+}]_f$, $[Mg^{2+}]_f$, $[Li^+]_f$ in order to determine the effect of the adsorption process.
16. The amount of SI retained by the mineral, Γ (in mg SI/ g rock), was calculated using the expression $\Gamma = V(C_o - C_f)/m$ (where C_o and C_f are the initial and final SI concentrations respectively, V is the SI solution volume and m is the mass of substrate).

Experimental Procedure for Compatibility Test

1. Filter the FW brine through 0.45µm filter paper. About 1500ml will be required for this experiment. This includes 500ml to prepare the 10,000ppm stock solution of PPCA.
2. Prepare 10,000ppm Active [SI] stock solution in the test brine used.
3. Use this stock solution to prepare the 5000ppm [SI] for the compatibility test in the test brine
4. pH adjust the stock solution (SI/FW sample) to the required pH, ie. pH6. Record the pH values, before and after adjusted – pH_o @ 20°C.
5. Measure out the required volume of the stock solution into the appropriate 250ml plastic bottles in duplicate.
6. This test is performed at 95°C. Note the time – t_o
7. After approximately 1 hour, check the bottle lids are tight, to avoid any evaporation.
8. After 24 hours (t = 24), take out the supernatant from the bottle without disturbing the precipitate at the bottom.
9. Measure the pH of the supernatant samples and record the values – pHf @ 20°C
10. If necessary, prepare some diluent solution (see Section
11. Preparation for 1% Na as in NaCl Diluent ***Solution***).
12. For this experiment, before ICP dilute the precipitate solution in FW in order that it is of equivalent [SI] to the supernatant SI solution. Calculations based on previous 5000ppm compatibility test results (See below for calculation).

13. First we need to do the ICP for supernatant then the results of that will help to calculate the volume of FW required for the dissolution of the precipitate.
14. Then will do the ICP for precipitate solution- Precipitate + FW analysed using 1ml sample in 9ml 1% Na.

Chemical Preparations for Inhibition Efficiency Test:

1. Buffer solution= 13.6g sodium acetate tri-hydrate and 0.4g acetic acid in 100ml DW. This gives a mixed pH of 5.54

2. Quenching solution (KCl/PVS)= This solution was prepared by dissolving 28.55g of potassium chloride (3000ppm K^+ ions) and 5g of PVS (1000ppm of PVS) scale inhibitor (ST 810) in 5L of distilled water. The solution was then adjusted with 10%HCl and a concentrated NaOH solution to a pH value between 8 and 8.5. This quench solution contains 1,000ppm PVS which has been shown to effectively stabilise (or quench) the sample and thus prevent further precipitation. The potassium is included in this solution to act as an ionisation suppressant for the atomic absorption determination of barium.

3. Barium ICP Standards – Preparation Details

Prepared 10ppm & 25ppm Ba^{2+} Standards:

Prepare 250ml of each concentration

$[Ba^{2+}]$ / ppm	Volume of Ba^{2+} Standard 1,000ppm Solution Required	Volume of KCl / PVS (aq) / ml
10	{(10/1,000)*250}ml = 2.5ml	247.5
25	{(25/1,000)*250}ml = 6.25ml	243.75

Experimental Procedure for Inhibition Efficiency:

1. Prepare the two brines (NSSW and Forties FW) by dissolving the appropriate salts in distilled water.
2. Vacuum filter brines separately through 0.45μm membrane filter paper.
3. From the previous stage, we have initial stock, supernatant and precipitate solutions. Tests were carried out for both the supernatant & precipitate solution with Initial stock.

4. All 3 Stocks-Precipitate, supernatant & Initial 5000ppm Stock get further diluted to 40ppm, 20ppm & 10ppm. Each [SI] is tested in duplicate.

   Note: the [SI] in FW (SI/FW) must be higher than that required for the test by a factor which accounts for the dilution when mixed with the SW.
5. Measure out appropriate volumes of NFFW/SI and NSSW solutions into their separate "Azlon" (polyethylene) bottles in order to get 50:50 mix.
6. Add 1ml (1 ml buffer/100 ml final brine mixture) of buffer solution to each SW and FW bottle, taking extreme care not to introduce impurities and cap all bottles securely. Shake the bottles to ensure full mixing of buffer with SI/FW solution.

   Note 1: The actual pH obtained must be checked prior to testing: For example, for a 50:50% mix, add 1ml of buffer to 100ml FW, and 1ml of buffer to 100ml SW. Record the individual pH values. Add the FW to the SW and record the pH, checking it is of appropriate value, ~pH5.5.

   Note 2: The buffer is added to the SI/FW solution to ensure that if the FW brine was self-scaling at the test pH, then the SI prevents precipitation occurring until it is mixed with the SW. Also, any precipitation formed prior to mixing, could induce further precipitation on contact with FW, creating false results.
7. Place the bottles containing the SW & SI/FW/buffer into a water-bath and the bottles containing the SW/buffer into an oven, both set to the required temperature (95^{o}C), for tests of a 50:50 SW:FW mixing ratio. Leave for ~60 minutes to reach test temperature.
8. After 60 minutes, mix the two brines together. For a 50:50 mixing ratio, add the SW/buffer to the FW/buffer & SI/FW/buffer solutions in waterbath and shake quickly, ensuring maximum mixing is achieved. Start a stopclock (t = 0).

   Note: The water bath should have sufficient polystyrene balls on the surface to keep evaporation to a minimum.
9. The tests are then sampled at the required time, t = 2 and 22 hours.
10. ICP analysis will be for barium.

    1ml in 9ml KCl/PVS for Ba analysis.e. [*10 Ba: 13.45ppm Max]

Table 20: Bottle list – IE Test:

Bottle No.	FW [PPCA] / ppm for supernatant	MIX [PPCA] / ppm (i.e. after mixing with NSSW)
1	0	0

2	0	0
3	10ppm STK	5
4	10ppm STK	5
5	10ppm Supernatant	5
6	10ppm Supernatant	5
7	10ppm Ppt	5
8	10ppm Ppt	5
9	20ppm STK	10
10	20ppm STK	10
11	20ppm Supernatant	10
12	20ppm Supernatant	10
13	20ppm Ppt	10
14	20ppm Ppt	10
15	40ppm STK	20
16	40ppm STK	20
17	40ppm Supernatant	20
18	40ppm Supernatant	20
19	40ppm Ppt	20
20	40ppm Ppt	20

Hyamine Test Procedure Details

Sep-Pak C18 cartridges (design and purpose): This is a single use disposable cartridge containing an octadecylsilane (Si $(CH_3)^2C_{18}H_{37}$) bonded phase packing material. When using the cartridges with aqueous solutions, it is necessary to pre-wet the cartridge with a water miscible solvent such as methanol, then flush with water before use. The C18 cartridge adsorbs neutral/hydrogen bonding species strongly, but does not adsorb charged species. Thus, in order to adsorb, the inhibitor must be in an un-charged state. To achieve this, the pH of the PPCA or MAT inhibitor solution is reduced to pH 1.5–2. The pKa value for a carboxylic acid grouping is ~4.5. Thus, at this low pH of 1.5–2, the inhibitor is effectively in the un-dissociated (uncharged) acid form. On passing through the C18 cartridge under such conditions, the inhibitor is adsorbed and effectively separated from the interfering salts, which are charged and therefore do not adsorb. The inhibitor can then be eluted from the cartridge free from the interfering salts prior to colorimetric analysis.

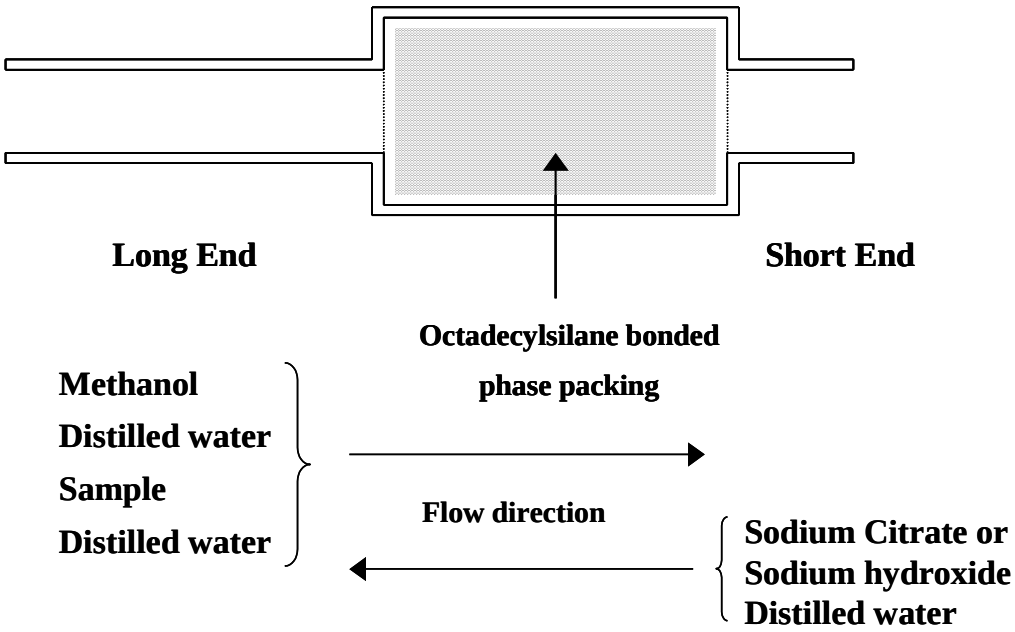

Figure 162 – Sep-Pak C-18 cartridge description

The polyacrylate based species PPCA and MAT can be eluted with a variety of eluents including sodium hydroxide and citrate buffers. The choice of eluent is determined by the analytical method of choice so as to give minimal interference upon colour development/detection. For example, for Hyamine detection, a citrate buffer is the eluent of choice.

Figure 163 shows the calibration curve obtained for PPCA using standards of 0, 0.5, 1, 2, 3, 4, 5, 6, 8 and 10ppm (active). The first point to notice about this calibration curve is that a straight line fit is poor (correlation coefficient, R2 = 0.9767). However, a third degree polynomial gives an almost perfect fit in the range 0.5 - 8.0ppm (R2 = 0.9995).

An examination of the non-linearity of the calibration shows that at values of less than ~ 5ppm (active) the recorded absorbance rises gradually with time up to > 80 minutes, whereas for concentrations greater than 5ppm, the absorbance reduces gradually. Analysis after 40 minutes colour development is seen as a compromise between these two effects. Precision and accuracy data at 2ppm and 5ppm were determined by repeat analysis of standards based on the third order polynomial curve obtained in the range 0.5 - 8ppm from Figure 8.6. The results from such a determination indicate that this analytical technique gives excellent results in laboratory brines.

Precision: The reproducibility of the experimental procedure was as follows:

Sample	A	B
Mean sample value (active conc., ppm)	2.16	4.98
Number of samples analysed	4	4
Standard deviation (ppm)	± 0.0263	± 0.081
Relative error	1.22%	1.63%

Accuracy: By knowing the concentration of the inhibitor in the solution, the following accuracy values were determined:

Known concentration	2ppm	5ppm
Number of samples analysed	4	4
Standard deviation (ppm)	±0.189	±0.0846
Relative error	9.45%	1.69%

However unlike PPCA, other polyacrylates may achieve a straight line fit to their calibration graph in synthetic sea water. This is of no consequence as long as a good fit (R2 ~1) is achieved for the calibration data and successful repeatability is maintained.

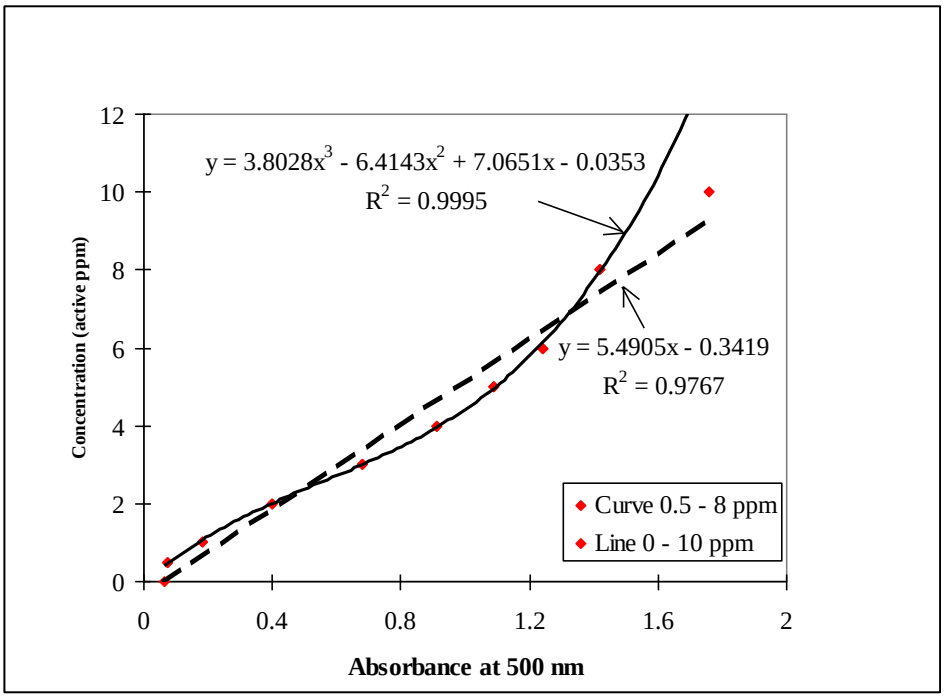

Figure 163: Calibration curve for PPCA in sea water using the Hyamine 1622 method

Special Equipment:

1. UV/visible scanning spectrophotometer (500nm)
2. Razel Syringe Pumps (supplied by Semat Technical (UK) Limited)
3. 50ml volumetric flasks

4. Hyamine 1622 (supplied by VWR)
5. Tri - Sodium Citrate (supplied by VWR)
6. Sep Pak C18 cartridges (supplied by Waters)
7. 5, 10 and 60ml plastipak syringes (supplied by VWR)
8. Optical cells (2 cm path length)
9. 10% hydrochloric acid Analar grade (conc. supplied by VWR)

Method repeatability: Each analytical procedure should be tested thoroughly for its robustness to ensure that excellent repeatability can constantly be achieved. Samples at known concentrations are statistically analysed for their precision and accuracy, the definition of which are outlined below;

Accuracy is the degree of agreement between the measured value and the true value. An absolute true value is seldom known. A more realistic definition of accuracy, then, would assume it to be the agreement between a measured value and the accepted true value.

Precision is defined as the degree of agreement between replicate measurements of the same quantity. It is the repeatability of the result. This is also known as standard deviation. However, good precision does not mean good accuracy, for instance, if there were a systematic error in the analysis. This error would not affect the precision but it does affect the accuracy.

U.V. Spectrophotometer: Always consult the appropriate instruction manual for the specific model. Ensure that the correct program/wavelength has been selected and then place an optical cell of 2cm path length into the spectrophotometer and zero the absorbance on a distilled water sample. The cell should be washed out with some of the sample solution, emptied and re-filled with the sample solution before the absorbance is recorded. Wash out the cell with distilled water in between analysing each sample and ensure the spectrophotometer remains at zero. It is essential that the cell is orientated in the same direction for zeroing and for every analysis.

Other important points to be noted are;

1. Always wipe the transparent faces of the cell with a clean tissue to remove any drops of solution and

2. Check that there are no air bubbles on the inner walls of the cell.

Both these features can lead to erroneous absorbance readings. The spectrophotometers used by FAST are a Philips Spectrophotometer 8730 series, a PYE Unicam SPE-550 or a Camspec M302.

Procedure for C18 Hyamine Analytical Technique:

1. Dilute the inhibitor stock solution down to make 50ml standards at concentrations of 0 - 10ppm active in the appropriate brine i.e. SW, FW, diluent solution.
2. Adjust 50 ml of each standard solution to pH 1.5 - 2.0 by dropwise addition of hydrochloric acid 10% v/v.
3. Attach a 5 ml syringe of methanol to the long end of a Sep-Pak C18 cartridge. Pass the methanol through the cartridge dropwise and discard the expelled solution.
4. Using a syringe, pass 10 ml of distilled water slowly through the cartridge and discard the expelled solution.
5. Using a 60 ml syringe and the Razel syringe pumps, pass inhibitor solution through the cartridge. Collect the fluid in a cup.
6. Wash the cartridge from the same end with 10 ml of distilled water from a syringe, again utilising the Razel syringe pumps. The combined collected fluids from steps 5 & 6 for each of the standard solutions can now be discarded, as the inhibitor should be adsorbed onto the cartridge.
7. Invert the cartridge and attach to the short end, a 10 ml syringe containing 10 ml of a 5% solution of sodium citrate in distilled water.
8. Elute the inhibitor slowly from the C18 cartridge using the 10 ml of sodium citrate solution on the syringe pumps and collect each eluent in a 50 ml volumetric flask.
9. Using the same 10 ml syringe, pass 10 ml of distilled water through the C18 cartridge, again collecting the eluent in the 50 ml volumetric flask.
10. Pipette 10 ml of a 5,000ppm (as supplied) aqueous solution of Hyamine 1622 into the flask and dilute to the mark (50 ml) with distilled water. A 1 minute time interval is suggested for addition of Hyamine to each flask to allow for analysis time on the spectrophotometer.

11. Shake the volumetric flask quickly to ensure that the solutions are mixed and leave to stand for 40 minutes.
12. After 40 minutes, measure the absorbance of each of the standard solutions at 500nm using a spectrophotometer.
13. Construct a calibration graph from the recorded standard solution absorbance values. It is normally a 3rd order curve. Use Microsoft Office Excel 2003 or 2007.

Notes:

i. [SI] should be plotted on the y-axis and UV Absorbance plotted on the x-axis – such that unknown [SI] can be worked out from the equation of the line (i.e. "y" Value). UV Absorbance is a dimensionless quantity (no units).

ii. Ensure the excel chart displays an R^2 value with four decimal places displayed – such that a better assessment of the accuracy of the resultant calibration curve can be made. The excel default setting is for 3 decimal places to be displayed. To change this to four decimal places, select the equation box on the excel chart, right click the mouse, and select "Format Trendline Label" from the menu that appears. The number of decimal places can then be changed to four. This should work successfully in both excel 2003 and 2007 versions.

14. Perform repeat analysis at known concentrations, to determine the repeatability of the method using the previously constructed calibration graph.
15. Repeat the procedure for samples and determine the concentration of chemical in the solution using their recorded absorbance values and the previously constructed calibration graph.

Advantages of this procedure: Each sample analysis takes ~45minutes, although automation using multi-syringe pumps can allow up to 10 samples to be prepared ready for colour development together. This allows for up to 20 determinations to be completed in a full day's work.

7. *Sand Pack Experimental Details*

Experimental Apparatus

In order to carry out sand pack flooding experiments, it is necessary to use sand/crushed rock packed into a glass column, in what is essentially a low pressure chromatography experiment. The glass column acts as a support to hold the sand in place, as shown in the schematic diagram of the sand-pack flooding apparatus in
Figure 164. This apparatus was designed primarily to carry out low pressure flood experiments where transport issues are to be investigated. This is in contrast to a full reservoir core flood apparatus which is designed to tackle high pressure and high temperature core floods. The adsorption column, fittings and tubing were supplied by Anachem. The column is made of glass which 23cm long and has an internal diameter of 1.50cm. The column is placed in a water bath assembly for tests at higher than ambient temperatures.

A wet slurry method was adopted for packing the sand in order to prevent formation of air bubbles in the column and to minimise sagging of sand. The general procedure described below and in FAST GLP/RAs has been followed in this sand-pack experiment (FAST GLP/RA Flooding- sand-pack, 2014).

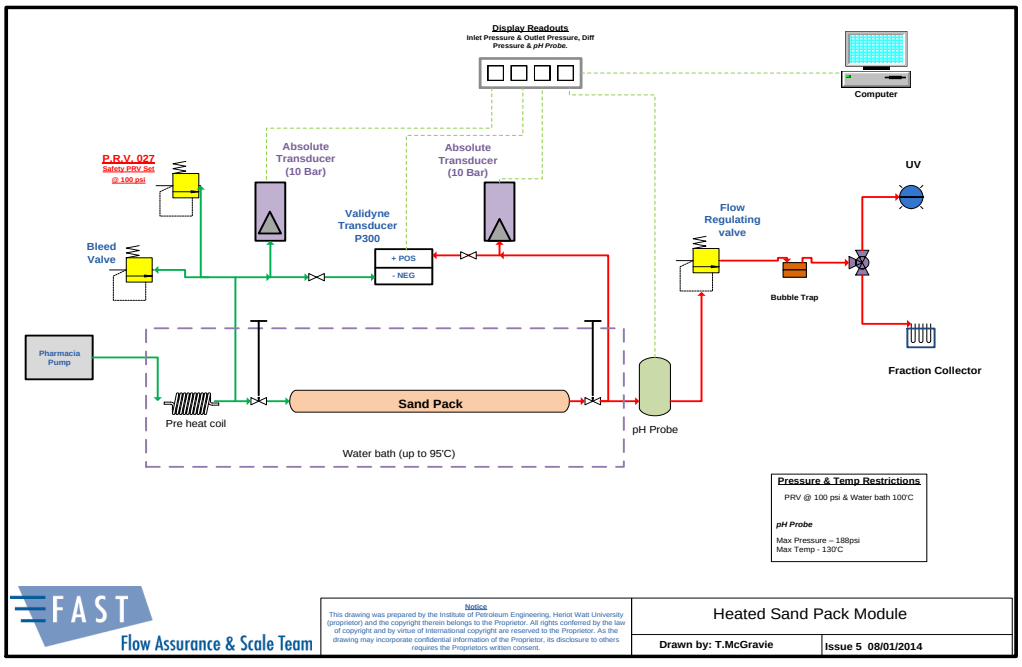

Figure 164: Schematic diagram of the sand-pack rig. (Source: FAST GLP/RA)

Column Packing and System Connection

1. Mix a constant mass of sand with brine for 1 hour to prevent dust formation that may occur during dry mixing. Get rid of any visible dust formation from the mixture.
2. The fixed end piece is fitted first and then the brine solution is introduced to the column to fill about 1/3 of the column length.
3. Open the valve connected to the bottom end fitting to allow the brine solution in the column to flow out slowly to adjust the liquid level as shown in Figure 165.

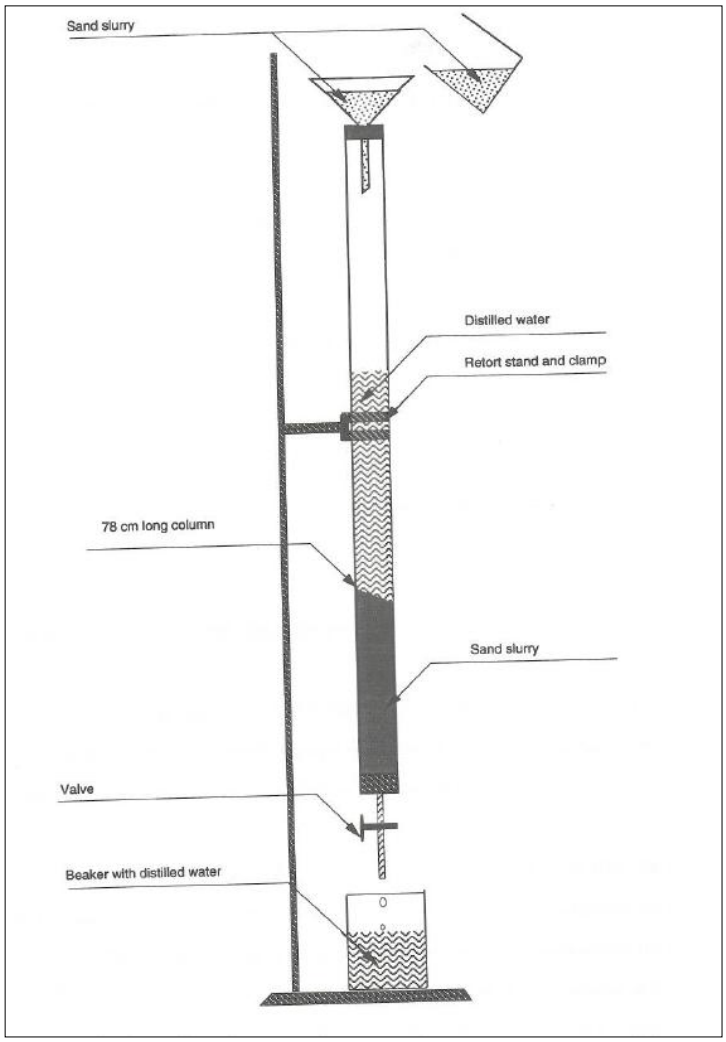

Figure 165: Schematic Diagram of Sand 'Packing' Technique (Source: FAST GLP/RA)

4. Load the column with sand slurry until it is 1 or 2 cm from the desired volume
5. Close the valve and take out the excess solution using a syringe
6. The variable end piece is fitted once the column has been loaded. Tighten "finger" tight.
7. With column in vertical orientation, attach to pump so that injection is from bottom to top of column. Flow with brine at 150ml/hr for at least one hour to

allow sand to settle, removing any voids in the sand bed. Re-tighten variable end piece and measure length of sand bed.

8. The column is connected to the pump and the UV Spectrophotometer.

General Experimental Procedure:

A. Dead Volume Measurement by UV - performed at room temperature

1. Connect two adjustable end pieces with using a short (15cm) glass column. Butt platens, with frits in place and one further frit to fill in any gap between them. Consider the volume occupied by the frits to be the pore space in this system. Perform tracer test in/out with 10ppm iodide in brine to calculate the system's dead volume, as described in following sections or steps A.2 to A.7.

2. The pump must first be flushed with the synthetic brine without any tracer to purge out the previously used brine in the pump.

3. Flush with brine (no tracer) to get the UV/Vis baseline level.

4. Solvent change the pump with the iodide tracer solution to condition the pump with the solvent required for the test.

5. Inject the pack with the iodide tracer solution. Switch on the UV/Vis Spectrophotometer as soon as the pump is started. Use a flow rate (Q) of 150ml/hr.

6. Stop the pump and UV-Vis when the system reaches a plateau. Save the UV file.

7. Solvent change to non-dosed brine. Repeat steps 5-6 for the trace out.

B. Pore Volume and Permeability Measurement

At Room Temperature

1. After loading the column with sand minerals, equilibrate the column with pH adjusted brine (pH determined by experimental conditions) at flow rates of 150 ml/hr until the column shows no sign of further settling and a good, homogeneous sand bed is achieved.
2. Perform Trace In/Out as in Part A. Use 10ppm iodide in brine at 150 ml/hr. It may be desirable to collect 0.5 ml samples via the fraction collector with a 50ppm Li tracer in the brine as well. An estimate of how long the pore volume will take at a specified flow rate can be made by assuming 40% porosity in the

column; allow enough logging time on the spectrophotometer for 5 pore volumes to pass through the column, plus one full dead volume.

3. Change to Non-Tracer Brine for permeability measurement. Flood at five evenly spaced flow rates (10, 20, 30, 40, 50 ml/hr for example) for at least 10 minutes each, recording the differential pressure across the pack at 60 second intervals. These can be used with Darcy's law to calculate the permeability of the pack. Select a range of flow rates that reflect those that will be used in the flood. It may not be possible to get a sufficiently high differential pressure to measure accurately at lower flow rates, so an increase in flow rate may be necessary at this stage (30, 60, 90, 120, 150ml/hr)

At Test Temperature

1. After the pore volume measurement at room temperature, submerge the sand pack column into water bath and raise the bath water temperature to test temperature. Allow at least 1 hour after the water has reached test temperature for the column to completely heat through. Leave outlet valve open to allow for release of pressure (a build-up of pressure may lead to the glass column breaking).
2. Flow brine (no tracer) at 150 ml/hr until steady flow is reached.
3. Repeat steps 2, 3 and 4 for pore volume measurement/permeability measurement above.

C. Main Treatment (MT) and Post Flush (PF)

1. The main Treatment was performed at room temperature- After the pore volume measurement at test temperature; switch off the water bath to cool down to room temperature.
2. Once cooled, take out the sand pack column from the water bath and check for any leaking. Tighten all the fittings. Let the apparatus sit for 24 hours to make sure the inside temperature is at room temperature.
3. If a pH probe is attached in line, calibrate probe and insert into holder
4. Flush with brine (no tracer / pH= experimental pH) at 150 ml/hr for an hour and continue at 20 ml/hr for 5 hours to precondition the sand pack column. The

preconditioning is done at room temperature. The sand pack column is now ready for main treatment.

5. Main treatment: Introduce the prepared treatment brine at 20ml/hr flow rate for up to 5 PV. Differential pressure across the pack was monitored, normally at 1 minute intervals. Samples should also be collected for geochemical data. The pH measurement was also being recorded at 1/minute interval.
6. The flow is stopped after ~5 pore volumes (5PV). Shut-in the sand pack column. The post flushes are then performed at elevated temperatures. During Post flushes we left the outlet valve open to prevent a pressure build up that may break the glass column.
7. Place the sand pack back into the water bath and raise the bath water to test temperature. Leave it overnight, preferably 24 hrs at least, at test temperature. Shut in times may vary, but 24hrs is the standard for laboratory squeeze treatments with FAST. The remainder of the experiment will now take place in the water bath at test temperature.
8. Post-flush treatment: The post-flush treatment was performed at different rates and with different synthetic brine to the main treatment. The post flushes are executed until the effluent concentration drops below minimum inhibitor concentration (MIC), normally 1ppm.
9. Sample Collection:

a. Samples should be collected as for the main treatment; a fine sampling regime is recommended in the early stages of both MT and PF (approximately 1/10 to 1/5 of a pore volume per sample). This may be increased to ½ to 1 pore volume after the first 5 pore volumes of flow.
b. Samples should be analysed for major ions of interest. Different dilutions may be required for different stages; for example, a scale inhibitor may have to be analysed for in undiluted samples as the concentration drops, but other ion concentrations may require dilution at the same stage. Analysis and monitoring of samples, especially from the post flush, in small batches covering 5-10 pore volumes each time is recommended to keep track of changes and update analysis regimes.

II. Inductively Coupled Plasma - Optical Emission Spectroscopy (ICP-OES)

The procedures followed for each of the elements is similar; however different concentrations of calibration standards are employed for the different elements. The measurement time for each element method is 2 seconds, mode 5 is used for single point analysis and primary/secondary slits of 18/81 respectively are used. The exception to this is the PPCA analysis, which uses the Gaussian mode of 2 and primary/secondary slits of 18/15 respectively. In between samples there is a rinse time of 60sec before it returns to analyze the samples. The sampling times allow for sample introduction; 3 minutes to analyze 1 element and 5-6 minutes to analyze four elements.

Experimental Procedure:

1. Clean and start up the ICP. Allow to heat up for 0.5-1 hour with distilled water flowing through the machine. The rinse solution between analyses is 5% Nitric acid and flows for 60sec before moving back to the next sample.
2. Prepare the element calibration standards within the same matrix (normally synthetic SW, FW or 1% NaCl solution) that the samples have been diluted in.
3. After the heat up period, select the method to be used to analyze the samples ensuring that the same method shows in the box at the top of the analysis sheet. This ensures that the correct elements are analyzed.
4. Set up an analysis run to auto-search, auto-attenuate and auto-search again on the highest calibration standard. The next highest standard can now be auto-searched. This process is continued until all of the element containing calibration standards (not standard LOW, which is matrix solution) have been auto-searched. Once the run begins check that the peaks observed are in the middle of the wavelength window and the top standard is the full height of the screen.
5. The machine is now ready to calibrate. Set–up a run to calibrate for the elements in the selected method/matrix.
6. After calibration has been achieved, i.e. a straight line through zero, with an R square number of approximately 1, the ICP is now ready to analyze samples.
7. The samples are placed in the auto-sampler racks. Calibration standards are placed in a rack at the end of the samples. When setting up the analysis run, begin with selecting each of the standards to be analyzed as a sample, and then analyze 10-12

samples before returning to the standards. Repeat these formations until all samples are analyzed, ending with a set of standards.

8. At the bottom of the sample run, add in a description of the run to help with later identification under the specific method. The analysis file is then saved onto the computer.
9. The calculated concentrations, with respect to the previous calibration, are then stored on the computer and printed out.
10. If the results for the calibration standards throughout the run have drifted from their intended concentrations, then the samples can be drift corrected.

Figure 166: ICP-OES - JY 138 Ultrace (Source: FAST GLP/RA)

Table 21: ICP-OES wavelengths and calibration standards used for different elements

Element	Wavelength (nm)	Calibration (Standard)
Barium	233.527	0, 10, 25, 50
Strontium	338.071	0, 10, 25, 50
Calcium	317.933	0, 50, 200
Magnesium	279.806	0, 25, 100
Iron	259.940	0, 10, 40
Lithium	670.784	0, 5, 20
Aluminium	308.215	0, 5, 50, 250
Silicon	212.412 or 250.690	0, 5, 50, 250
Sodium	330.237 <100ppm & 589.592	0, 10, 100, 1000

	>100ppm	
Cobalt	237.86	0, 2, 5
Chromium	205.55	0, 2, 5
Copper	324.754 or 224.700	0, 10, 100
Nickel	221.64	0, 2, 5
Zinc	213.856 or 334.502	0, 10, 100
Molybdenum	202.03	0, 2, 5
Germanium	265.118 or 209.426	0, 10, 100
Boron	249.67	0, 10, 100
Potassium	766.490	0, 20, 100, 1000
Phosphorus - phosphonate	177.440 (0->50ppm) & 214.914 (0, 50, 500,2500)	0, 5, 50, 500, 2500
Phosphorus - PPCA	177.440 (0->50ppm) & 177.441 (0, 50, 500,2500)	0, 5, 50, 500, 2500
Lead	220.353	0, 5, 10
Tin	189.989 or 235.484	0, 10, 100
Tungsten	209.47	0, 2, 5
Sulphur	180.676	0, 5, 10 or 0, 10, 50, 250
Examples of Diluents: NaCl, DW, SW, FW, KCl/PVS, EDTA/KOH, DTPA/KOH, 5% Nitric acid and Acetic acid.		

Examples of Diluents: NaCl, DW, SW, FW, KCl/PVS, EDTA/KOH, DTPA/KOH, 5% Nitric acid and Acetic acid.

III. Environmental Scanning Electron Microscopy - Energy Dispersive X-Ray (ESEM-EDX)

For this study, a Philips XL30 Environmental Scanning Electron Microscope (ESEM), with an Oxford Instruments cryo-stage, and an EDAX energy dispersive x-ray detector (EDX) was used for the analysis. These can be used to image and/or analyze virtually any substance, including wet, oily and out gassing samples that cannot be examined by more conventional SEM's (http://www.pet.hw.ac.uk/cesem/intro.htm). This is presented in Figure 166.

An ESEM is specifically designed to be able to examine micro-structural and ultra-structural details of samples, within a SEM chamber, in their uncoated natural state. An ESEM is able to examine wet, oily and out-gassing samples, without any form of preparation, and is able to maintain specimens within their natural state for prolonged periods within the ESEM viewing chamber. The ESEM works at low vacuum (typically 2 - 6 Torr), and utilizes a chamber gas for imaging, charge suppression and sample humidity.

ESEM is specifically suited to dynamic experimentation of the micron scale and below. ESEM technology allows for dynamic experiments involving fluids, and the possibility of imaging samples undergoing compression and tension. ESEM can therefore be regarded as a micro dynamic experimentation chamber where materials can be examined at a range of pressures, temperatures, under a variety of gases/fluids.

In simpler terms, scanning electron microscopy occurs when an electron beam is scanned across the surface of a sample. As the electrons strike the sample, a variety of signals are generated and it is the detection of these signals that produces an image or the elemental composition of a sample. There are a number of detectors that can be used under a number of different conditions, such as low or high vacuum, cryo-SEM and wet ESEM work. These detectors themselves can be split into categories depending on how they detect the sample signals. For instance, there are secondary electron detectors, solid state backscattered detectors, the environmental secondary electron detector and gaseous secondary electron detectors.

In the XL30 ESEM, the two detectors for high vacuum mode are an Everhardt-Thornley secondary electron detector and a solid state backscattered detector. Both these detectors are permanently within the chamber whereas the various environmental detectors available, all clip into the detector socket at the back of the chamber and are inserted as and when required. A summary of detectors and their suitable detection conditions are presented in Table 22 (Philips XL30 ESEM Instruction manual).

The signals that provide the greatest amount of sample information in SEM are the secondary electrons, backscattered electrons and X-rays. The processes behind these techniques can be detailed as;

(a) Secondary electrons are emitted from the atoms occupying the top surface and are therefore able to produce a readily interpretable image of the surface,
(b) Backscattered electrons are primary beam electrons that are 'reflected' from atoms in the solid,
(c) X Spectrometry or EDX is the interaction of the primary beam with atoms in the sample that causes shell transitions, resulting in the emission of x-rays. The emitted X-rays have an energy, characteristic of the parent element. Detection and measurement of the energy permits elemental analysis (Energy Dispersive X-ray Spectroscopy or EDX). EDX can provide rapid qualitative, or with adequate standards, quantitative analysis of elemental composition with a sampling depth of 1-2 microns. X-rays may also be used to form maps or line profiles, showing the elemental distribution in a sample surface.

Before using ESEM or EDX, always refer to the manufacturers instruction manual (Philips XL30 ESEM Instruction manual) and receive training before commencing work. However, a very general summary of the procedure is as follows;

a. Select the required detector.
b. Load samples into chamber.
c. Select mode – high, low, environmental and the corresponding conditions.
d. Ensure chamber is ready for use.
e. Focus the detector.
f. The SEM is now ready to image/analyse the samples.
g. When the process is finished, release the samples from the chamber.

Figure 167: ESEM - Philips XL30 at Heriot-Watt University (Source: FAST: GLP/RA)

Table 22: ESEM - Summary of detectors and their detection conditions

Detector	Working Mode	Position
Everhardt-Thornley secondary electron	High vacuum	Permanently inside chamber
Backscattered detector	High vacuum	Permanently inside chamber, parked at back
Solid state backscattered detector	High or low vacuum (0.1 – 1.00 Torr)	Stored at back of chamber in a sleeve. To use, remove sleeve and mount under the pole piece.
Environmental secondary electron detector	Environmental 500micron detectors – P ≤ 10 Torr. 300micron detectors for higher P	Primarily SE but incorporates a substantial BSE signal. Detector is cap shaped and fits over the wet mode insert/bullet. Used in conjunction with a hook adaptor which plugs into the GSED (Gaseous SED)

Gaseous secondary electron detectors	Environmental, P ≈ 6 Torr 500micron wet specimens remain hydrated at P ≤ 10 Torr. 1000micron – wider field of view but P ≤ 5 Torr	Fits over end of wet mode bullet/insert and clips into GSED connector at back of chamber
Large field gaseous secondary electron detector (LF-GSED)	Low vacuum (0.1-1.00 Torr). Can be used in a water vapour atmosphere or another gas such as Nitrogen.	Contains a component of BSE. Used in conjunction with low vac/high vac bullet/insert and is plugged into the GSED connector socket at the back of ESEM chamber.
Gaseous backscattered secondary electron detector (GBSED)	Full environmental, P ≤ 10 Torr for 500micron aperture.	3 modes – SE, SE&BSE and BSE. Changes made by using pull-down 'detectors' menu. The detector must be worked at a distance of 10mm due to its size.
Bullet	High or ≤ 1 Torr low vacuum	Screwed into pole piece. It changes pumping regime of lower part of column and forms an attachment point for the various environmental and BSE detectors.
ESEM bullet	Full wet ESEM work. Low vacuum where high conical ESD detector cap is used to minimise the gas path length during EDX analysis.	Screwed into pole piece. It changes pumping regime of lower part of column and forms an attachment point for the various environmental and BSE detectors.

IV. Ultra Violet Spectrophotometer (UV)

For this study, the UV/VIS spectrophotometer is used for the determination of sodium iodide (iodide ion) concentration in brines. The measurement is done during sand pack characterization to measure dead volume and pore volume of the sand pack column. The instruments used for the study is Campsec M302 (Figure 168).

Experimental Procedure:

Sodium Iodide (iodide ion) concentrations are determined by measuring the absorbance of the sample and using a calibration curve equation to determine the concentration. The set up of the spectrophotometer to measure absorbance is detailed below.

1. Switch the instrument on using the power on switch located at the right hand side, towards the rear. Allow 15 minutes for the instrument to stabilize.
2. Set the required wavelength in nanometers (in this case is 230nm).
3. If working in the ultraviolet range (200-400nm) switch on the deuterium lamp using the UV lamp push button switch (after 30 seconds the lamp lights and the LED is illuminated) and allow up to 15 minutes for the lamp output to stabilize.
4. Set the Conc/%T/Abs control to Abs so the read-out appears in absorbance units.
5. To set the absorbance read-out to zero, place a 2 cm cuvette filled with distilled water in the cell holder and close the sample compartment lid. Use either the auto zero push button switch or 100%T control to set the absorbance to 0.

Other important points are;

Always consult the appropriate instruction manual for the specific model (Camspec M302 UV/Vis Spectrophotometer Instruction manual). The cell should be washed out with some of the sample solution, emptied and re-filled with the sample solution before the absorbance is recorded. Wash out the cell with distilled water in between analysing each sample and ensure the spectrophotometer remains at zero. It is essential that the cell is orientated in the same direction for zeroing and for every analysis.

Notes:

1. Always wipe the transparent faces of the cell with a clean tissue to remove any drops of solution,

2. Check that there are no air bubbles on the inner walls of the cell,

3. The single most important aspect of inhibitor residual assay is to ensure that all glassware is cleaned thoroughly prior to use.

These features can lead to erroneous absorbance readings.

Figure 168: UV/Vis Spectrophotometer - Camspec M302 (Source: FAST: GLP/RA)

LIST OF REFERENCES

Adamson, A.W.:"Physical Chemistry of Surfaces", 3rd Edition, John Wiley-Interscience, New York, V. 15(10) p. 698, 1976

Andrei, M., and Malandrino, A.:"Comparative Coreflood Studies for Precipitation and Adsorption Squeeze with PPCA as the Scale Inhibitor", presented in J. Petroleum Science and Technology, V. 21(7&8), 1295-1315, 2003.

Andrei, M., Borgarello, E., and Lockhart, T.P.:"Phase Behaviour of Phosphinopolyacrylate Scales Inhibitor", presented in J. Dispersion Science and Technology, V. 20(1&2), p. 59-81, 1999.

Barthorpe, R.T.:"The Dramatic Effect of Certain Divalent Ions upon Barium Sulphate Inhibition", paper no. 23 NACE Corrosion Conference, Nashville, Tennessee, 27 April-1 May 1992.

Barthorpe, R.T.:"The Dramatic Effect of Certain Divalent Ions upon Barium Sulphate Inhibition", paper no. 23 NACE Corrosion Conference, Nashville, Tennessee, 27 April-1 May 1992.

Bedford, C. T., Burns, P., Fallah, A., Garnham, P. J. and Barbour, W. J.:"A new assay for phosphino carboxylate scale inhibitors at the 5ppm level," presented at the Royal Society of Chemistry Symposium - Chemistry in the Oil Industry, held at Ambleside UK, 12-15 April 1994.

Boak, L.S.:"Investigation of the Adsorption and Barium Sulphate Inhibition Efficiency Properties of Novel Polyethylene Imines with More Conventional Scale Inhibitors", M.Phil. Thesis, submitted to the Department of Petroleum Engineering, Heriot-Watt University, UK, 1996

Boak, L.S., and Sorbie, K.S.:"New Developments on the Analysis of Scale Inhibitors", Paper SPE 130401 presented at the SPE International Conference on Oilfield Scale held in Aberdeen, Scotland 26-27 May 2010.

Boak, L.S., Graham, G.M., and Sorbie, K.S.:"The Influence of Divalent Cations on the Performance of $BaSO_4$ Scale Inhibitor Species", Paper SPE 50771 presented at the SPE

International Symposium on Oilfield Chemistry held in Houston, Texas, USA, 16-19 Feb 1999.

Bonnett, N, Fieler, E.R. and Hen, J.:"Application of a Novel Squeeze Scale Inhibitor in the Beryl Field", SPE 23107, presented at the Offshore Europe Conference held in Aberdeen, 3-6 September, 1991.

Breen, P.J., Diel, B.N., and Downs, H.H.:"Correlation of Scale Inhibitor with Adsorption Thermodynamics and Performance in Inhibition of Barium Sulphate in Low pH Environments", SPE 20688, 65th SPE Annual Technical Conference, New Orleans, LA, 23 – 26 September 1990.

Brown, M.:"Full Scale Attack" Review 30, The BP Technology Magazine, p. 30-32, October- December 1998

Browning, F.H., and Fogler, H.S.:"Precipitation and Dissolution of Calcium Phosphonate for the Enhancement of Squeeze Lifetimes", SPE 25164, proceedings of SPE International Symposium on Oilfield Chemistry, New Orleans, LA, 2 – 5 March 1993.

Camspec M302 UV/Vis Spectrophotometer Instruction Manual

Carlberg, B.L.:"Scale Inhibitor Precipitation Squeeze for Non-Carbonate Reservoirs", SPE 17008, presented at the SPE Production Technology Symposium, Lubbock, TX, 16-17 November 1987.

Carlberg, B.L.:"Precipitation Squeeze Can Control Scale in High Volume Wells", J. Oil Gas, V. 81 (52), US, December 1983.

Carrell, C. D.:'The Occurence, Prevention and Treatment of Sulphate Scale in Shell Expro'; SPE16438, presented at Offshore Europe 87, Aberdeen, September 8-11, 1987.

Chang, K.Y. and Patel, S.:"A Mechanistic Study of PhosphinoCarboxylic Acid for Boiler Deposit Control", p. 48-53 MP/July 1996.

Charleston, J.:"Scale Removal in the Virden, Manitoba Area", SPE 2160, presented at J. Petroleum Technology, V. 22(6), p. 701-704, 1970.

Ciba-Giegy Industrial Chemicals (Now FMC Ltd.), Product Information Bulletin: “Bellasol S40/S45; Analytical procedure for their determination in oilfield brines,” Manchester, January 1990.

Collins, I.R.:“Surface Electrical Properties of Barium Sulphate Modified by Adsorption of Poly alpha, beta Aspartic Acid”, J. Colloid Interface Sci., V. 212(2), p. 535-544, 15 April 1999.

Crabtree, M., Eslinger, D., Fletcher, P., Johnson, A., and King, G.:“Fighting Scales-Removal and Prevention”, Oilfield review, V. 11(3), p. 30 – 45, 1999.

Cushner, M.C., Prybylinski, J.L., and Ruggeri, J.W.:“How Temperature and pH affect the Performance of Barium Sulphate Inhibitors”, paper no. 428, NACE Corrosion 88, St Louise, Missouri, March, 1988.

Davis, K.P., Fidoe, S.D., Otter, G.P., Talbot, R.E., and Veale, M.A.:“Novel Scale Inhibitors Polymers with Enhanced Adsorption Properties”, Paper SPE 80381, presented at the International Symposium on Oilfield Scale, Aberdeen, UK, 29-30 January 2003.

Ebbing D.D., “General Chemistry, Fifth Edition”, Edited by M.S. Wrighton; Published by Houghton Mifflin Company, 1996.

Farooqui, N.M., and Sorbie, K.S.:“Oilfield Scale Inhibitors for Application in Precipitation Squeeze Treatments: Solubility of the PPCA_Ca Complex”, SPE-169792, Aberdeen, UK, 14-15 May 2014.

Farooqui, N.M., and Sorbie, K.S.:“Phase Behaviour of Polyphosphino Carboxylic Acid (PPCA) Scale Inhibitor for Application in Precipitation Squeeze Treatments”, Chemistry in the Oil Industry XlII: Oilfield Chemistry – New Frontiers RSC Conference, Manchester, UK, 4-6 Nov 2013.

Farooqui, N.M., and Sorbie, K.S.:“Study of Ca_PPCA complex of the Polymeric Scale Inhibitor for Precipitation Squeeze Treatment”, Oil Field Chemistry Symposium 2015, Geilo Norway, 22-25 March 2015.

Farooqui, N.M., Sorbie, K.S. Haddleton, D., and Grice, A.:“Polyphosphino Carboxylic Acid (PPCA) Scale Inhibitor for Application in Precipitation Squeeze Treatments: The

Effect of Molecular Weight Distribution", NACE-2014-4100 presented at NACE Corrosion Conference and Expo, San Antonio, TX, 9-13 Mar 2014

Farooqui, N.M., Sorbie, K.S., Boak, L.S.:"Molecular Weight Effects in Polymeric Scale Inhibitor Precipitation Squeeze Treatments", SPE 174214 presented at the SPE European Formation Damage Conference, Budapest Hungary, 3-5 June 2015.

Farooqui, N.M., Sorbie, K.S., Palermo, L., and Lucas, E.:"Polymeric Scale Inhibitor for the Application of Precipitation Squeeze Treatment: The molecular Weight Distribution Effect on the Inhibition Efficiency Performance", IBP1939_14 presented at Rio Oil & Gas Expo and Conference, Rio de Janeiro, Brazil, 15-18 September 2014.

Farooqui, N.M., Sorbie, K.S., Palermo, L., and Lucas, E.:"The Effect of Molecular Weight Distribution on the Inhibition Efficiency Performance of Polymeric Scale Inhibitors during Retention", NACE-2015-5663 presented at NACE Corrosion Conference and Expo, Dallas, TX, 15-19 Mar 2015.

FAST GLP/RA: Flooding- Sandpack Assembly and Flooding 2014.

Frenier, W.W. and Ziauddin, M.:"Formation, Removal, and Inhibition of Inorganic Scale in the Oilfield Environment", Society of Petroleum Engineers, 2008.

Gill, J.S.:"Development of Scale Inhibitors", Paper 229, presented at the NACE CORROSION Conference, 1996.

Graham G.M., Sorbie, K.S. and Littlehales I.:"The Accurate Detection and Assay of Oilfield Scale Inhibitors in Real Field Brines," presented at the conference Water Management Offshore Organised by IBC Ltd, Aberdeen, 6 - 7 October, 1993.

Graham G.M., Sorbie, K.S., Boak, L.S., Taylor, K. and Blilie, L.A.:"Development and Application of Accurate Detection and Assay Techniques for Oilfield Scale Inhibitors in Produced Water Samples," SPE No. 28997, presented at the SPE International Symposium on Oilfield Chemistry, San Antonio, 14-17 February, 1994.

Graham G.M., Sorbie, K.S., and Boak, L.S.:"Development of Accurate Assay Techniques for Poly Vinyl Sulphonate (PVS) and Sulphonated Co-polymer (VS-Co) Oilfield Scale Inhibitors," presented at NIF 6th International Oil Field Chemical Symposium, Geilo, Norway, 19 - 22 March, 1995.

Graham G.M., Sorbie, K.S., Johnston, A. and Boak, L.S.:"Complete Chemical Analysis of Produced Water by Modern Inductively Coupled Plasma Spectroscopy (ICP)," presented at NIF 7th International Oil Field Chemical Symposium, Geilo, Norway, 17 - 20 March, 1996.

Graham, G.M., and Sorbie, K.S.:"The Effect Of Molecular Weight On The Adsorption/Desorption Characteristics Of Polymeric Scale Inhibitors On Silica Sand And In Sandstone Cores", presented in The NACE Annual Conference and Corrosion Show, Baltimore Maryland, 28 Feb – 4 Mar 1994.

Graham, G.M., and Sorbie, K.S.:"Examination of the Change in Returning Molecular Weight Obtained during Inhibitor Squeeze Treatments Using Polyacrylate Based Inhibitors", SPE 29000, presented at SPE International Symposium on Oilfield Chemistry, San Antonio 14-17 February 1995.

Graham, G.M., Boak, L.S., and Sorbie, K.S.:"The Influence of Formation Calcium and Magnesium on the Effectiveness of Generically Different Barium Sulphate Oilfield Scale Inhibitors", SPE 81825, J. SPE Production Facilities, V. 18(1), p.28, 2003.

Graham, G.M., Collins, I.R., Stalker, R., and Littlehales, I.J.:"The Importance of Appropriate Laboratory Procedures for the Determination of Scale Inhibitor Performance", SPE 74697, presented in SPE Oilfield Scale Symposium, Aberdeen, UK 30-31 Jan 2002.

Graham, G.M., Frigo, D.M., McCracken, I.R., Graham, G.C., Davidson, W.J., Kapusta, S., and Shone, P.:"The Influence of Corrosion Inhibitor/Scale Inhibitor Interference on the Selection of Chemical treatments Under Harsh (HP/HT/HS) Reservoir Conditions", SPE 68330, presented at the 3rd SPE International Symposium on Oilfield Scale Aberdeen, UK, 30-31 January 2001.

Graham, G.M., Jordan, M.M., and Sorbie, K.S.:"How Scale Inhibitors Work and How this Affects Test Methodology", Proceedings of the Conference; Solving Oilfield scaling, organised by IBC Technical Services Ltd, Aberdeen, 22-23 Jan 1997.

Graham, G.M., Wattie, I., Mackay, E.J., and Boak, L.S.:"Scale Inhibitor Selection Criteria for Downhole (SQUEEZE) Application in H Chalk Reservoir", SPE 65025 presented at the SPE International Symposium on Oilfield Chemistry, Houston TX, 13-16 Feb 2001.

Graham, G.M.:“A Mechanistic Examination of the Factors Influencing Downhole $BaSO_4$ Oilfield Scale Inhibitors and the Design of New Species”, Doctorate Thesis Submitted to the Department of Petroleum Engineering, Heriot Watt University, 1994

Hardy, J.A.:“Scale control in the South Brae field”, proceeding of conference Advances in Solving Oilfield Problems organised by IBC Technical Services Ltd., Aberdeen, 7-8 October 1992.

Hiemenze, P.C.:“Principles of Colloid and Surface Chemistry”, Marcell Decker Inc., New York, Chapter 12, 1986.

Hills, E.J., Graham, G.M., Langlois, B., Jones, C.:“Molecular Weight and Compositional Controls on the Performance of Polymeric Scale Inhibitors- A mechanistic Interpretation”, presented in 16th International Oil Field Chemistry Symposium, Geilo, Norway, 13-15 March 2005.

Hingston, F.J., Atkinson, R.J., Posner, A.M., and Quirk, J.P.:“Specific Adsorption of Anions”; J. Nature; V. 215(5109), p. 1459-1461, 1967

http://chemwiki.ucdavis.edu/Analytical_Chemistry/Analytical_Chemistry_2.0/12_Chromatographic_and_Electrophoretic_Methods/12B%3A_General_Theory_of_Column_Chromatography

Hunter, R.J. (1988) Zeta Potential In Colloid Science: Principles And Applications, Academic Press, UK

Ibrahim, J., Sorbie, K. S., Boak, L. B.:“Coupled Adsorption/Precipitation Experiments:1 Static Results”, SPE 155109, presented at SPE International Conference held in Aberdeen, UK, May 30-31 2012.

Ibrahim. J.:“Establishing Scale Inhibitor Retation Mechanisms in Pure Adsorption and Coupled Adsorption/Precipitation Treatments” Doctorate Thesis submitted to the Institute of Petroleum Engineering at Heriot Watt University, Nov 2011.

Ile, R.K.:“The Chemistry of Silica”, J. Wiley and Sons, New Your, Chapter 6, 1979.

Inches, I.E., Doueiri, K.E., and Sorbie, K.S.:“Green Inhibitors: Mechanisms in the Control of Barium Sulphate Scale”, NACE 06485, presented at the NACE Corrosion Conference, San Diego, CA, 12-16 March 2006.

Jaafar, M.Z., Vinogradov, J., and Jackson, M.D.:“Measurement of Streaming Potential Coupling Coefficient in Sandstones Saturated with High Salinity NaCl Brine”, Geophysical Research Letters, V. 36 (21), L21306, 2009.

Jordan, M.M., Graham, G.M., Sorbie, K.S., Taylor, K., Hourston, K., Hennessey, S. and Griffin, P.:“The Correct Selection and Application Methods for Adsorption and Precipitation Scale Inhibitors for Squeeze Treatments in North Sea Fields”, SPE 31125 presented at the SPE Formation Damage Symposium, Lafayette L.A., 14-15 Feb 1996.

Jordan, M.M., Sorhaug, E., Marlow, D., and Graham, G.M.:“”Red” vs. “Green” Scale Inhibitors for Extending Squeeze Life- A Case Study from North Sea, Norwegian Sector”, NACE 101037, presented at the NACE International Corrosion Conference and Exposition, 2010.

Jordon, M.M., Sorbie, K.S., Yuan, M.D., Taylor, K., Hourston, K.E., Ramstad, K., and Griffin, P.:“Static and Dynamic Adsorption of Phosphonate and Polymeric Scale Inhibitors onto Reservoir Core from Laboratory Tests to Field Application”, SPE 29002, presented at the SPE International Symposium on Oilfield Chemistry, San Antonio, Texas, 14-17 Feb 1995.

JY Ultrace 138 ICP-OES Instruction Manual

Kahrwad, M., Sorbie, K. S., and Boak, L.S.:“Coulpled Adsorption/Precipitation Of Scale Inhibitors: Experimental Results and Modelling”, SPE 114108 presented at the SPE International Oilfield Scale Conference, Aberdeen, UK, 28-29 May 2008.

Kan, A.T., Varughese, K. and Tomson, M. B.:“Determination of Low Concentrations of Phosphonates in Brines”, SPE 21006, presented at the SPE International Symposium on Oilfield Chemistry, Anaheim, 20-22 February, 1991.

Kelland, M.A.:“Production Chemicals for the Oil and Gas Industry” CRC Press Taylor & Francis Group, 2009.

Lewis, B.G.: “Environmental and Ecological Chemistry – Vol. II - Soil Chemistry UNESCO – EOLSS Sample Chapters”, Northwastern University, Illinois, USA, 2009

Lyo, S.K. and Gomer, R.: “Theory of Chemisorption”, Chapter in Interactions on Metal Surface, Vol 4 in the series of Topic in Applied Physics pp. 41-62, published by Springer Berlin Heidelberg, 1975

MacEwan, K.:“Getting a sense of Scale”, MWV Speciality Chemicals USA, 2013.

Mack, A.R. and Barber, S.A.:“Influence of Temperature and Moisture on Soil Phosphorus: II. Effect Prior to and During Cropping on Soil Phosphorus Avaibility for Millet”, J. Soil Science Society of America; V. 24(6), p. 482-484, 1960

Malandrino, A., Yuan, M.D., Sorbie, K.S. and Jordan, M.M.:“Mechansitic Study and Modelling of Precipitation Scale Inhibitor Squeeze Processes”, paper SPE 29001, presented at the SPE International Symposium on Oilfield Chemistry, San Antonio, TX, Feb 14-17, 1995.

Malvern Master Sizer MS-20 Instruction Manual

Mazzolini, E., Bertrro, L. And Truefitt:“Scale Prediction and Laboratory Evaluation of $BaSO_4$ Scale Inhibitors for Seawater Flood in High Barium Environment”, SPE 20894 presented at Europec 90, Hague, Netherlands, 22-24 October 1990.

McTeir, M. D. K., Ravenscroft, P. D. and Rudkin, C.: “Modified Methods for the Determination of Polyacrylic/Phosphinopolycarboxylic Acid and Polyvinylsulphonic acid Scale Inhibitors in Oilfield Brines,” SPE 25160, presented at the SPE International Symposium on Oilfield Chemistry, New Orleans, LA, 2-5 March, 1993.

Miles, L.:“New Well Treatment Inhibits Scale”, J. Oil and Gasl, V. 8, p. 96-99, June 1970.

NACE Standard TM 0197-97, Laboratory Screening Test to Determine the Ability of Scale Inhibitors to prevent the Precipitation of Barium Sulphate and/or Strontium Sulphate from Solution (for Oil and Gas Production Systems), Item No. 21228, NACE International, 1997.

Nancollas, G.H.:“Oilfield Scale – Physical Chemical Studies of it Formation and Prevention”, Chemicals in the Oil Industry, p.143-164, 1985

Naono, H.:“The Effect of Triophosphate on the Crystallization of Strontium Sulphate”, Bull. Chem. Soc. Japan, 40, p. 1104, 1967

Olsen, S.R. and Watanabe, F.S.:“A Method to Determine a Phosphorus Adsorption Maximum of soils as measured by the Langmuir Isotherm”, J. Soil Science Society of America; V. 21 (2), p. 144-149, 1958

Olson, J.B., Moore, D.C., and Holland-Jones, N.:“A temperature Activated Extended Lifetime Scale Inhibitor Squeeze System”, paper No. 25 presented at the NACE Annual Conference, Nashville, TN, April 27 - May 1, 1992.

Pardue, J.E.:“A New Inhibitor for Scale Squeeze Applications”, SPE 21023, presented in SPE International Symposium on Oilfield Chemistry, Anaheim, CA, 20-22 Feb 1991.

Pardue, J.E.:“Results of Field Test with a New Extended Squeeze Life Scale Inhibitor”, paper no. 35, presented at the NACE Annual Conference and Corrosion Show, Nashville, Tennessee, 27 April – 1 May 1992.

Patent Publication No. US 2012/0032093 A1, “Tagged Scale Inhibitor Compositions and Methods of Inhibiting Scale”, Kemira.

Patent Publication No. US 2003/0073586 A1, “Scale Control Compositions for High Scaling Environments”, National Starch and Chemical Investment Holding Corp.

Patrick, W.H. Jr., and Khalid, R.A.:“Phosphate relaease and Sorption by Soils and Sediments: Effects of Aerobic and Anaerobic Conditions”; J. Science; V. 186(4158), p. 53-55, 1974

Patton, C.C.: Oilfield Water Systems, 2nd Edition, Campbell Petroleum Series, Oklahoma, 1977.

Payne, G.E.:”A History of Downhole Scale Inhibition by Squeeze Treatments on the Murchison Platform”, SPE 16539, presented at the conference Offshore Europe 87, held in Aberdeen, UK, 8-11 September, 1987.

Pennington, J.:“An Overview of Alternative Approaches to the Development of Monitoring Methods for Scale Inhibitors in Oil-Field Produced Waters,” Proceedings of the 3rd International Symposium Chemicals in the Oil Industry, University of Manchester, 19-20 April, 1988.

Philips XL30 ESEM Instruction Manual

Plummer, M.A.:“Preventing Plugging by Insoluble Salts in a Hydrocarbon- Bearing Formation and Associated Producer Wells”, U.S. Patent No. 4,723,603, February 3rd, 1987.

Rabaioli, M.R. and Lockhart, T.P.:“Solubility and Phase Behaviour of Polyacrylate Scale Inhibitors”, J. Petroleum Science and Technology, V. 15, p. 115-126, 1996.

Rabaioli, M.R.; Lockhart, T.P.:“Solubility and Phase Behaviour of Polyacrylate Scale Inhibitors and Their Implications for Precipitation Squeeze Treatment” paper SPE 28998 presented at SPE International Symposium on Oilfield Chemistry held in San Antonio TX, Feb 14-17, 1995.

Schramm, L.L., Mannhardt, K. and Novosad, J.J.:“Electrokinetic Properties of Reservoir Rock Particles”, J. Colloids and Surfaces, V. 55, p. 309 - 331, 1991.

Shaughnessy, C. M. And Kline, W.E.:“EDTA Removes Formation Damage at Prudhoe Bay”, J. of Petroleum Engineering, V. 35(10), p. 1783-1791, October 1983.

Shaw, S.S.:”Investigation into the Mechanisms of Formation and Prevention of Barium Sulphate Oilfield Scale”, Doctorate Thesis submitted to the Department of Petroleum Engineering, Heriot Watt University, 2012

Shaw, S.S., and Sorbie, K.S.:“Synergistic Properties of Phosphonate and Polymeric Scale Inhibitor Blends for Barium Sulphate Scale Inhibition”, Paper SPE 169752-PA, SPE Production and Operations, Vol. 30(01), p.16-25, 2015

Shaw, S.S., and Sorbie, K.S.:“Synergistic Properties of Phosphonate and Polymeric Scale Inhibitor Blends for Barium Sulphate Scale Inhibition”, paper SPE 169752-MS, presented at the SPE International Conference on Oilfield Scale, Aberdeen, UK, 14−15 May 2014.

Shaw, S.S., Sorbie, K.S., and Boak, L.S.:“The Effects of Barium Sulphate Saturation Ratio, Calcium and Magnesium on the Inhibition Efficiency: I Phosphonate Scale Inhibitors”, SPE 130373 SPE International Conference on Oilfield Scale, Aberdeen, UK, 26-27 May 2010a.

Shaw, S.S., Sorbie, K.S., and Boak, L.S.:“The Effects of Barium Sulphate Saturation Ratio, Calcium and Magnesium on the Inhibition Efficiency: II Polymeric Scale Inhibitors”, SPE 130374 SPE International Conference on Oilfield Scale, Aberdeen, UK, 26-27 May 2010b.

Shuler, P.J., and Jenkins, W.H.:“Prevention of Downhole Scale Deposition in Ninian Field”, SPE 19263 Offshore Europe, Aberdeen, 5-8 September 1989.

Singleton, M.A., Collins, J.A., Poynton, N., and Formston, H.J.:“Developments in PhosphonoMethylated PolyAmine (PMPA) Scale Inhibitor Chemistry for Severe $BaSO_4$ Scaling Conditions”, SPE 60216 presented at the Second International Symposium on Oilfield Scale held in Aberdeen, UK, 26-27 January 2000.

Smith, C.F., Nolan III, T.J. and Crenshaw, P.L.:"Removal and Inhibition of Calcium Sulphate Scale in Waterflood Project", J. Petroleum Technology, V. 20(11), p. 1249-1256, 1968.

Sorbie, K. S., Yuan, M. D., Graham, G. M. and Todd, A. C.:“Appropriate Laboratory Evaluation of Oilfield Scale Inhibitors,” presented at Advances in Solving Oilfield Scaling Problems, Organised by IBC Ltd, Aberdeen, 7-8 October 1992.

Sorbie, K.S.:“A General Coupled Kinetic Adsorption/Precipitation Transport Model for Scale Inhibitors Retention in Porous Media: I. Model Formulation”, SPE 130702 presented at the SPE international Conference on Oilfield Scale, Aberdeen, UK, 2010.

Sorbie, K.S.:“A Simple Model of Precipitation Squeeze Treatments”, SPE155111, presented at the International Conference on Oilfield Scale, Aberdeen, UK, 30 - 31 May 2012.

Sorbie, K.S.:“Polymer-Improved Oil Recovery”, Blackie & Son, Glasgow and CRC Press, Boca Raton, FL, 1991.

Sorbie, K.S.:”The Improved Design of Scale Inhibitor Squeeze treatments”, presented at the Water Management Offshore Conference, Organised by IBC Ltd., Aberdeen 22-23 October 1991

Sorbie, K.S., and Gdanski, R.D.:“A Complete Theory of Scale-Inhibitor Transport and Adsorption/Desorption in Squeeze treatment”, SPE 95088, presented at the SPE International Symposium on Oilfield Scale, Aberdeen UK, 11-12 May 2005.

Sorbie, K.S., and Laing, N.:“How Scale Inhibitors Work: Mechanisms of Selected Barium Sulphate Scale Inhibitors Across a Wide Temperature Range”, Paper SPE 87470, presented at the SPE International Symposium on Oilfield Chemistry held in Aberdeen, Scotland, 26-27 May 2004.

Sorbie, K.S., Graham, G.M., and Jordan, M.M.:"How Scale Inhibitors Work and How This Affects Test Methodology"; Paper presented at 4th International Conference and Exhibition on Chemistry in Industry, Manama, Bahrain; 2000.

Sorbie, K.S., Wat, R.M.S., and Todd, A.C.:"Interpretation and Theoretical Modelling of Scale-Inhibitor/ Tracer Corefloods", SPE 20687, SPE Production Engineering, V. 7(3) p. 307-312, August 1992.

Sorbie, K.S., Wat, R.M.S., Todd, A.C., and McClosky, T.:"Derivation of Scale Inhibitor Isotherms for Sandstone Reservoirs", Royal Society of Chemistry Publication– Chemicals in the Oil Industry: Developments and Applications, Edited by P.H. Odgen, 1991.

Stone, M.F.A.:"The Effect of Particle Size on Phosphate Adsorption by Fluvial Sediment"; Master of Arts Dissertation submitted to the Dept. Of Geography, Wilfrid Laurier University, 1987

Taj, S., Papavinasam, S., and Revie, R.W.:"Development of Green Inhibitors for Oil and Gas Applications", Paper NACE 06656, presented at the 61st Annual NACE International Corrosion Conference and Exposition, 2006.

Todd, M.J., Lamont, G., Thortom, A., Gibb, A., Langvik, M., and Sjursaether, K.:"A New Precipitation Squeeze Alternative for Treating Harsh barium Sulphate Scaling in a Highly Naturally Fractured North Sea Carbonate Reservoir", SPE 132901, presented at the Trinidad and Tobago Energy Resources Conference, Port of Spain, Trinidad 27-30 June, 2010.

van der Leeden, M.C., and van Rosmalen, G.M.:"Development of Inhibitors for Barium Sulphate Deposition", proceedings of the 3rd International Symposium on Chemicals in the Oil Industry, p.68-69, 1988.

van der Leeden, M.C., and van Rosmalen, G.M.:"Inhibition of Barium Sulphate Scale Deposition by Polycarboxylates of Various Molecular Structure", SPE 17914, 1988.

van Olphen, H.:"Internal Mututal Flocculation in Clay Suspentions", J. Colloid Science; V. 19(4), p. 313-322, 1964

van Rosmalen, G.M., van der Leeden, and Gouman, J.:“The Influence of Inhibitors on the Growth of Barium Sulphate Crystals in Suspension: Scale Prevention (II)”, J. Kristall und Technik., V. 15(11), p. 1269-1277, 1980.

Vazquez, O., Sorbie, K.S., and Mackay, E.J.:“A General Coupled Kinetic Adsorption/Precipitation Transport Model for Scale Inhibitor Retention in Porous Media: II. Sensivity calculations and Field Predictions”, presented at the SPE Conference on Oilfield Scale, Aberdeen UK, 2010.

Vetter, O.J.:"How Barium Sulphate is Formed: An Interpretation", J. Petroleum Technology; V. 27(12), p. 1515-1524, 1975

Vetter, O.J.:“Oilfield Scale – Can We Handle It”, J. Petroleum Technology, V. 28(12), p. 1402 – 1408, 1976.

Vetter, O.J., and Kandarpa, V.:"Scale Inhibitor Evaluation for Oilfield and Geothermal Operation", Paper SPE7846 presented at the 1979 SPE of AIME International Symposium on Oilfield and Geothermal Chemistry held in Houston, TX, Jan 22-24, 1979.

Vetter, O.J., Kandarpa, V., Schalge, A.L., Stration, M. and Veith, E.:"Test and Evaluation Methodology for Scale Inhibitor Evaluations", Paper SPE16295 presented at the SPE International Symposium on Oilfield Chemistry held in San Antonio, TX, Feb 4-6, 1987.

Vetter, O.J.:"An Evaluation of Scale Inhibitors", J. Petroleum Technology, August 1972.

Wat, R.M.S., Montgomeric, H.T.R., Maclean, A.F., Bland, I.D.:“Squeeze Application using a Polymer Scale Inhibitor, A Case History”, In proceedings of the 4th International Oilfield Chemistry Symposium, 1993

Wat, R.M.S., Sorbie, K.S., Todd, A.C., Yuan, M.D., Chen, P., McLosky, T., and Jiang, P.:“Scale Inhibitor Core Floods in Oilfield Sclae: Its Nature Effect and Prevention”, Progress No. 8, Chapter 1, Department of Petroleum Engineering, Heriot Watt University, Edinburgh, UK, November 1991

Wat, R.M.S., Sorbie, K.S., Todd, A.C., Yuan, M.D., Chen, P., McLosky, T., and Jiang, P.:“Scale Inhibitor Core Floods in Oilfield Sclae: Its Nature Effect and Prevention”,

Progress No. 8, Chapter 1, Department of Petroleum Engineering, Heriot Watt University, Edinburgh, UK, November 1992

Water Analysis Handbook, Hach Company, Loveland Colorado, p.651, 1989.

Weintritt D.J. and Cowan, J.C.:"Unique Characteristics of Barium Sulphate Scale Deposition", J. Petroleum Technology, V. 19(10), pp.1381-1394, 1967.

Williams, E.G., and Saunders, W.M.H.:"Distributuion of Phosphorus in Profiles and Particle size Fractions of Some Scottish Soils", J. Soil Science; V.7(1), p. 90-109, 1956

Williams, J.D.H., Syers, J.K., Shukla, S.S., Haris, R.F., and Armstrong, D.E.: "Levels of Inorganic and Total Phosphorus in Lake Sediments as Related to Other Sediment Parameters", J. Environmental Science and Technology, V. 5(11), p. 1113-1120, 1971

Xiao, J.J.:"Prediction of Barium Sulphate Precipitation in the Presence and Absence of a Polymeric Inhibitor: Phosphino-polycarboxylic Acid", J. Langmuir, V. 17(15), p. 4668-4673, 2001

Xiao, J.J., Kan, A.T., Tomson, M.B., ed., Amjad, Z.:"The Role of Calcium Phosphino-Polycarboxylate Complexation in Inhibiting $BaSO_4$ Precipitation From Here Brine, In: Advances in Crystal Growth Inhibition Technologies", Kluwer Academic/Plenum Publishers, p. 165-186, 2000.

Young, R.J. and Lovell, P.A.:"Introduction to Polymers" Third Edition CRC Press, Taylor and Francis Group, an Informa Business, London, New York, 2011.

Yuan, M. D., Sorbie, K. S.; Todd, A. C., Atkinson, L. M., Riley, H. and Gurden, S.:"The Modelling of Adsorption and Precipitation Scale Inhibitor Squeeze Treatments in North Sea Fields", SPE25165, presented at the SPE International Symposium on Oilfield Chemistry, New Orleans, LA, 3-5 March 1993.

Yuan, M.D., Jamieson, E., and Hammonds, P.:"Investigation of Scaling and Inhibition Mechanisms and the Influencing Factors in Static and Dynamic Inhibition Tests", Paper 98067 presented at the NACE Corrosion Conference, San Diego, 22-27 March 1998.

Yuan, M.D., Sorbie, K.S., and Todd, A.C.:"A New Well Simulator for Modelling Scale Inhibitor Squeeze Treatments in Complex Reservoirs", SPE 21024, presented at the

SPE International Symposium on Oilfield Chemistry, Anaheim, California, 20-22 February 1991